HYBRID DUAL CROSS-LINKED HYDROGELS

INJECTABLE AND 3D-PRINTABLE BIOMATERIALS

KRISTEL BOERE

The printing of this thesis was financially supported by:

Utrecht Institute for Pharmaceutical Sciences (UIPS), Utrecht, the Netherlands
Netherlands society for Biomaterials and Tissue Engineering (NBTE)
Greiner Bio-One

Cover design by Ed van Oosterhout, Leffe Goldstein Lab
Printed by Proefschriftmaken.nl | | Uitgeverij BoxPress

ISBN: 978-90-393-6415-4

This research was supported by Netherlands Institute of Regenerative Medicine (NIRM)

Hybrid dual cross-linked hydrogels

Injectable and 3D-printable biomaterials

Hybride dubbel gecrosslinkte hydrogelen

Injecteerbare en 3D-printbare biomaterialen

(met een samenvatting in het Nederlands)

Proefschrift

ter verkrijging van de graad van doctor aan de Universiteit Utrecht
op gezag van de rector magnificus, prof.dr. G.J. van der Zwaan,
ingevolge het besluit van het college voor promoties in het openbaar
te verdedigen op maandag 16 november 2015 des middags te 2.30 uur

door

Kristel Wilhelmina Maria Boere

geboren op 26 mei 1988 te Raamsdonk

Promotor: Prof. dr. ir. W.E. Hennink

Co-promotor: Dr. ir. T. Vermonden

"If you want a place in the sun,
you've got to put up with a few blisters."

Abigail Van Buren

Table of Contents

CHAPTER 1

GENERAL INTRODUCTION

1.1 Hydrogels for biomedical applications

Hydrogels consist of networks of hydrophilic polymers which absorb and maintain large amounts of water in their three-dimensional structure.[1] As a consequence, hydrogels have found application in products as for example contact lenses, cosmetic implants, hair gels and diapers. Because of their high water content they resemble human tissues and have a good biocompatibility; therefore hydrogels are attractive materials for biomedical applications. Two of the main biomedical applications of hydrogels are in drug delivery and tissue engineering. In drug delivery, pharmaceutically active compounds are loaded in a hydrogel and administered into the body, where the drugs are released in a sustained manner for several days to months.[1,5-8] Therefore, the frequency of drug administration can be decreased and peak concentrations are avoided, thereby reducing potentially harmful side effects. Alternatively, hydrogels are used to specifically deliver its content in the target area. To this end, hydrogels can be formulated into small carrier systems such as nanogels.[9] These nanogels are for example suitable for targeting of antigens to dendritic cells.[10] For tissue regeneration applications, hydrogels can be loaded with cells and administered at the defect site (figure 1.1).[11-14] Growth factors may be added to the hydrogel to enhance the tissue regeneration capability. Differentiation of cells and communication with the surrounding tissue can result in the formation of new functional tissue. This is for example crucial for tissues that do not contain blood vessels, such as articular cartilage, and are therefore not able to regenerate after e.g. traumatic injury, surgical resection or disease.[15] In order to develop a suitable hydrogel material for an aimed biomedical or pharmaceutical application, it must fulfill a number of requirements.[16] Importantly, the hydrogel should induce no or minimal toxicity when applied. Furthermore, in many applications hydrogels should also possess sufficient strength, allowing them to retain at the site of administration and withstand mechanical forces. Preferably, hydrogels should degrade in time, so no additionally surgery is required to remove them once they have fulfilled their task. Another important aspect is to obtain a high control over the hydrogel properties, without batch-to-batch variations. When these properties can be tuned towards a patient specific treatment, these biomaterials can be used in a wide range of biomedical and pharmaceutical applications.

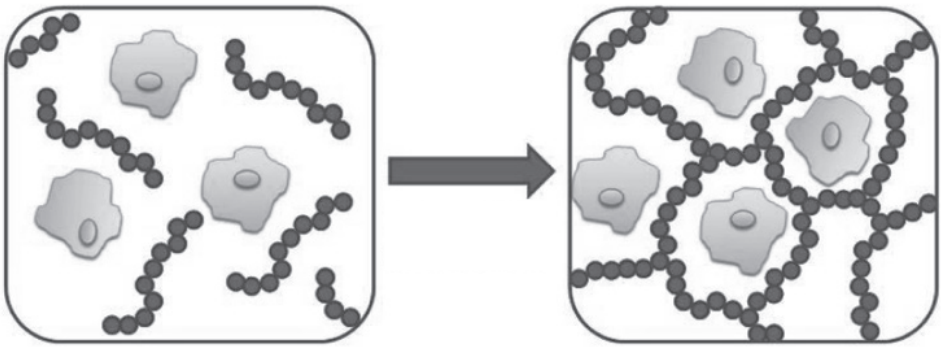

Figure 1.1. Schematic representation of hydrogel formation with cells embedded in the polymer network. Adapted from Ward *et al.*[17] with permission.

1.2 Polymers for hydrogel design

Hydrogels can be designed from a broad variety of polymers, of which many are discussed in more detail in Chapter 2. Two main classes of polymers that can be distinguished are natural and synthetic polymers. Biopolymers, polymers that have a natural origin, are for example polysaccharides, proteins, natural polyesters and nucleic acids.[18,19] Polysaccharides include chondroitin sulfate, hyaluronic acid, cellulose, starch, dextran and alginate. Examples of proteins that can be used for the formation of hydrogels are collagen, gelatin, elastin and silk fibroin. In general, natural polymers have excellent biomimetic characteristics and are often inherently biodegradable, and have therefore high potential for biomedical applications. As main drawbacks, they often display poor mechanical strength, exhibit large batch-to-batch variations and have a notable chance of eliciting an immune response. On the other hand, synthetic hydrophilic polymers such as poly(ethylene glycol) (PEG), poly(*N*-(2-hydroxypropyl)methacrylamide) (pHPMA), poly(2-hydroxyethyl methacrylate) (pHEMA) and polyglycerol have tremendous possibilities in network design with a high control over their final material properties, such as stiffness and permeability for drugs, nutrients etc. However, synthetic biomaterials should be carefully developed to be non-toxic and biodegradable. In many cases, synthetic materials lack intrinsic cellular interactions for successful application in regenerating damaged tissues. A combination of synthetic and natural polymers, referred to as hybrid materials, can synergistically combine the advantageous properties of the individual components.

1.3 Cross-linking strategies

Besides the hydrogel origin (natural or synthetic), another criterion to classify hydrogels is their cross-linking mechanism.[20] Physically cross-linked hydrogels are formed by non-covalent interactions, such as hydrophobic and ionic interactions. On the other hand, in chemically cross-linked hydrogels intermolecular covalent bonds between the polymer chains that form the network are present. Generally, physically cross-linked hydrogels can rapidly form a network, but the resulting hydrogel is mechanically weak, leading to fast erosion or degradation. An important class of physically cross-linked hydrogels consists of stimuli-sensitive polymers.[21-23] By a change in the environment, such as pH or temperature, non-covalent, reversible cross-links are formed. Therefore, these hydrogels are particularly attractive as injectable formulations. In contrast, chemically cross-linked hydrogels generally form relatively rigid, irreversible networks, but often harsh conditions are required for network formation. Physical and chemical cross-linking can also be combined in hydrogel preparation. This dual cross-linking results in an immediate physical network and subsequent mechanical stabilization through the formation of covalent bonds that further cross-link and stabilize hydrogel structure. To find cross-linking conditions that result in quick network formation without inducing toxicity and irreversible alterations in embedded compounds or surrounding tissues is an important scientific challenge with great translational potential. Three promising classes of hydrogels that are developed and investigated in this thesis are temperature responsive, photopolymerizable and chemoselectively cross-linked hydrogels. Other promising methods for hydrogel development are enzymatic cross-linking, double network hydrogels and copper free click chemistry that are further discussed in chapter 2.[24-27] The strategies that are highlighted below hold several favorable characteristics such as ease of polymer manufacturing and hydrogel formation, and compatibility with bioactive molecules.

1.3.1 Temperature responsive hydrogels

Thermosensitive hydrogels undergo a reversible phase transition from liquid to a gel state after a change in temperature (figure 1.2).[28,29] They can be categorized into polymers exhibiting upper critical solution temperature (UCST) or lower critical solution temperature (LCST) behavior. UCST polymers can form a hydrogel at temperatures below this temperature. This class mostly includes biopolymers, such as gelatin that contains triple helix structures, where intermolecular hydrogen bonds are formed at lower temperatures.[18] In contrast, LCST polymers precipitate above this critical temperature. A well-known example of polymers exhibiting LCST behavior is the synthetic polymer poly(*N*-isopropylacrylamide) (pNIPAAm). The phase transition of an aqueous solution of this polymer occurs above 32°C.

NIPAAm contains both a hydrophilic (amide) and hydrophobic (isopropyl) moiety. At temperatures below the LCST, pNIPAAm is soluble in water and forms hydrogen bonds of the amide groups with water molecules, while at the same time water molecules are caged near the isopropyl groups. At higher temperatures the entropy dominates the enthalpy of hydrogen bonding and water molecules disfavor confined hydrogen bonding with NIPAAm, leading to the clustering of hydrophobic groups and release of water molecules. This self-assembly is reversible, since pNIPAAM dissolves again in water once the temperature is below the LCST of 32°C.

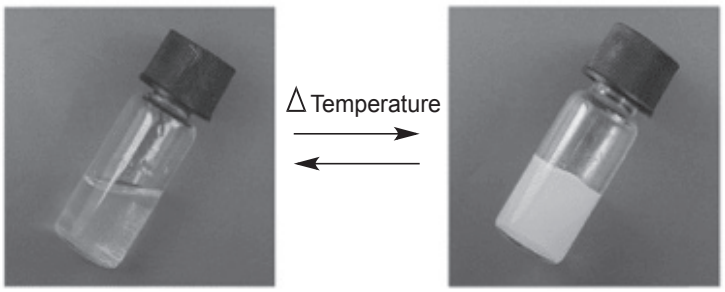

Figure 1.2. Temperature responsive hydrogel formation. Adapted from Lin *et al.*[30] with permission of Royal Society of Chemistry, Copyright © 2008.

1.3.2 Photopolymerizable hydrogels

Photopolymerization occurs upon exposure of the hydrogel building blocks with UV or visible light, and photoinitiators for the formation of covalent networks.[31] After illumination, free radicals are created from the photoinitiator, starting the polymerization of functionalized macromers. For biomedical applications of photopolymerized hydrogels, macromers containing methacrylate or acrylate groups are mostly used. Also biopolymers can be derivatized with these groups making use of functional groups (such as OH, NH_2) present in these molecules to allow UV-induced cross-linking.[32-34] Photopolymerization has several advantages such as fast curing times and temporal control over the polymerization. However, the use of UV light requires additional equipment and the produced radicals can potentially cause cytotoxicity. Although several researchers demonstrated limited toxicity after UV polymerization, it remains a controversial topic.[34-36] Therefore, continuous efforts in further developing suitable illumination equipment and ensuring biocompatibility are necessary for application of photopolymerizable hydrogels in the biomedical field.

1.3.3 Chemoselective cross-linking

Bioorthogonal chemistries[37], also known as chemoselective ligations[38] are efficient chemical reactions that specifically take place at the desired site and have therefore limited effect on native biochemical processes or embedded compounds.[39] One example of a chemoselective reaction is native chemical ligation (NCL).[40] Herein, an *N*-terminal cysteine reacts with a thioester as depicted in figure 1.3A. This reaction generally requires the presence of thiol reactants[41] and has been widely employed for the synthesis of complex peptides and proteins. Recent efforts showed the formation of hydrogels by NCL without the addition of a thiol reactant.[42] Furthermore, a variation of native chemical ligation termed as oxo-ester mediated native chemical ligation was recently introduced that utilizes an activated ester instead of a thioester[43,44] (figure 1.3B) and can be applied for the formation of hydrogels.[45]

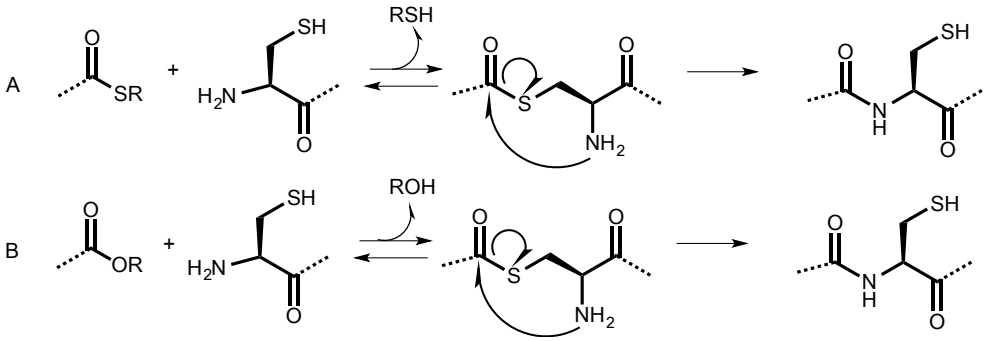

Figure 1.3. Chemoselective cross-linking reactions for hydrogel formation as described in this thesis. A) Native chemical ligation. B) Oxo-ester mediated native chemical ligation.

1.4 Scaffold fabrication

Traditionally, hydrogels were prefabricated by simple mixing of precursors and after cross-linking the formed hydrogels were subsequently used by e.g. implantation in the body.[1] Advances in the field of hydrogels now enable a minimally invasive administration by injection of a liquid formulation.[46] Consequently, no extensive surgerical interventions are required, saving costs and adding to the patients' convenience.[30,47] Alternatively, more complex constructs can be created by the development of new technologies for additive manufacturing, such as bioprinting, yielding hydrogel materials that closely resemble natural tissues.[48]

1.4.1 Injectable materials

Besides that injection offers a minimally invasive surgical procedure, other advantages of injectable hydrogels include the ease of incorporating bioactive compounds by simple mixing them with the hydrogel precursors, and the capability of completely filling irregular defects.[46,49] A major class of injectable hydrogels consists of stimuli-sensitive polymers. Particularly attractive are thermosensitive polymers, since a gel can be spontaneously formed without the need of chemical post-treatment.[50] However, to ensure mechanical stability over a longer time frame, combinations of temperature-induced and chemically cross-linked hydrogels are often investigated.[51,52] Injectable hydrogels that consist of two components with complementary functional groups can form a covalently cross-linked network *in situ*. Gelation kinetics have to be carefully considered to avoid needle obstruction before administration as well as leaching of the hydrogel precursors from the application site shortly after administration. A dual injection syringe, as is depicted in figure 1.4, allows proper mixing of the precursors while chemical cross-linking starts in the needle instead of the syringe, thereby limiting the chance of blockage of the needle or injection of very viscous solutions.[53,54] The presence of thermoresponsive polymers in the formulation ensures immediate stabilization of the hydrogel after injection.

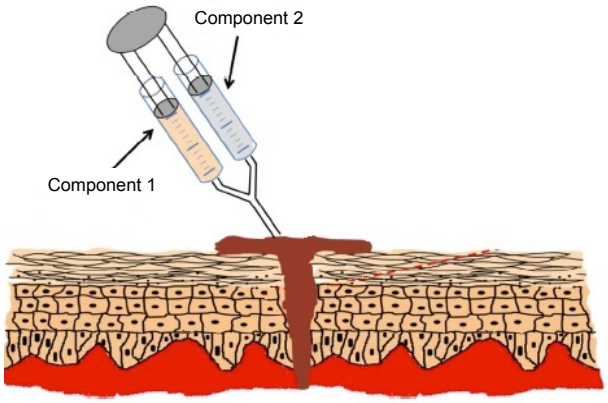

Figure 1.4. Injection of a two component hydrogel. Adapted from Mehdizadeh[54], copyright (2012), with permission from Elsevier.

1.4.2 Additive manufacturing

With the emerging advances in rapid prototyping technologies, more complex scaffolds can be created with properties that cannot not be achieved with simple hydrogel fabrication.[48,55-57] For example, porous constructs allow a rapid diffusion of nutrients and facilitate ingrowth of surrounding tissues. Additionally, tissues with a zonal architecture, such as cartilage that consists of layers with different

cell morphologies and glycosaminoglycan content, can be closely mimicked.[58,59] Biofabrication technologies include electrospinning[60], stereolithography[61] and 3D-printing, which is often referred to as bioprinting or 3D-plotting. [62] Bioprinting allows the layer-by-layer formation of a three-dimensional construct based on a computer-designed model. Materials that can be used for bioprinting are e.g. thermoplastic polymers and viscous polymer solutions. Thermoplastic polymers can be melted and subsequently extruded through a needle, after which they solidify on the printing plate.[63] An interesting thermoplastic polymer for bioprinting is the polyester poly-ε-caprolactone (PCL) since it has a relatively low melting temperature of 60°C and is degradable.[64] Chemical functionalities on this polyester can be introduced to for example tune degradation times or promote cell adhesion.[65,66] On the other hand, aqueous polymer solutions can form dimensionally stable scaffolds after deposition through subsequent cross-linking into a hydrogel.[48] Quick network stabilization must be ensured to obtain constructs with high shape fidelity. Moreover, multi-material constructs can be created as is depicted in figure 1.5, where alternating layers of a thermoplastic polymer and a hydrogel are deposited.[67,68] A thermoplastic polymer is introduced in these constructs as a mechanical support material, whereas the hydrogel forms a suitable environment for encapsulated cells. These hybrid reinforced constructs give therefore rise to remarkable material properties that could not be accomplished with only a single material.

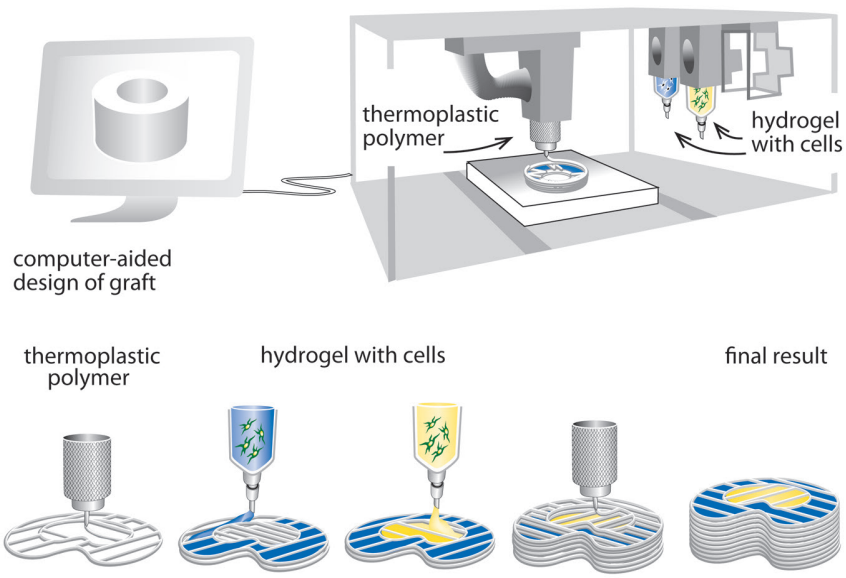

Figure 1.5. 3D-printing of hydrogel-thermoplastic constructs. Adapted from Schuurman *et al.*[67] © IOP Publishing. Reproduced with permission. All rights reserved.

1.5 Aim and outline of thesis

The work described in this thesis was part of the Netherlands Institute of Regenerative Medicine (NIRM) research program. NIRM aims to find innovative approaches to improve existing and create novel regenerative medicine treatments, involving both stem cell research and biomaterial development.[69] The aim of this thesis was to develop new hydrogel-based materials for biomedical applications. Herein the challenges of finding suitable gelation kinetics and cross-linking chemistries for hydrogel formation were addressed. Main emphasis in this thesis was given to the evaluation of chemoselective chemistries, namely native chemical ligation and oxo-ester mediated native chemical ligation, in combination with thermoresponsive polymers to yield building blocks suitable as injectable hydrogel materials. Additionally, novel hydrogel-thermoplastic constructs were fabricated to address the often poor mechanical strength of hydrogels and the challenges to fabricate hydrogels for bioprinting. Hybrid 3D-printed constructs with covalent grafting at the material interface were assessed for the fabrication of mechanically robust materials. We hypothesized that covalent bonds between the hydrogel and thermoplastic material could further enhance the mechanical stability of the construct. Furthermore, hyaluronic acid, gelatin and peptides were introduced in these materials to enhance their cytocompatibility and cellular proliferation performance.

Chapter 2 provides a literature overview of hydrogels for biomedical applications studied in the past 50 years and recent insights and technologies that have the potential to create new hydrogel materials for the future. **Chapter 3** describes the development of a novel hydrogel that is both physically cross-linked by thermogelation and chemically cross-linked by native chemical ligation. This hydrogel is shown to be attractive for the covalent functionalization with collagen mimicking peptides. In **Chapter 4** thermogelling hydrogels chemoselectively cross-linked by native chemical ligation (NCL) are compared with oxo-ester mediated native chemical ligation (OMNCL) for gelation kinetics, cell viability and protein compatibility. Additionally, the versatility of these hydrogels regarding mechanical properties and degradation rates is assessed. **Chapter 5** describes the formation of a hybrid three-dimensionally printed hydrogel-thermoplastic construct. Covalent photopolymerization at the hydrogel-thermoplastic interface is investigated to increase mechanical resistance against shear forces. Chrondrocytes are embedded in gelatin-based hydrogel-thermoplastic materials to assess their differentiation both *in vitro* and *in vivo*. **Chapter 6** presents the ability to fabricate 3D-printed constructs of temperature sensitive and OMNCL cross-linked hydrogels. Hydrogel collapse after extrusion is circumvented by partially cross-linking the hydrogel precursors before plotting. The flow properties of the polymer solutions are investigated by rheology

simulate what can happen during the 3D-printing process. Moreover, covalent grafting these hydrogels to a thermoplastic construct is studied for the development of mechanically enhanced constructs. Finally, **Chapter 7** gives a summarizing discussion of the work described in this thesis, together with some possible future optimizations and perspectives.

1.6 References

1. S. J. Buwalda, K. W. M. Boere, P. J. Dijkstra, J. Feijen, T. Vermonden and W. E. Hennink, *J. Controlled Release*, 2014, **190**, 254-273.
2. J. Kopeček and J. Yang, *Polym. Int.*, 2007, **56**, 1078-1098.
3. N. A. Peppas, P. Bures, W. Leobandung and H. Ichikawa, *Eur. J. Pharm. Biopharm.*, 2000, **50**, 27-46.
4. N. A. Peppas, J. Z. Hilt, A. Khademhosseini and R. Langer, *Adv. Mater.*, 2006, **18**, 1345-1360.
5. T. R. Hoare and D. S. Kohane, *Polymer*, 2008, **49**, 1993-2007.
6. O. Pillai and R. Panchagnula, *Curr. Opin. Chem. Biol.*, 2001, **5**, 447-451.
7. R. Censi, P. Di Martino, T. Vermonden and W. E. Hennink, *J. Controlled Release*, 2012, **161**, 680-692.
8. T. Vermonden, R. Censi and W. E. Hennink, *Chem. Rev.*, 2012, **112**, 2853-2888.
9. A. V. Kabanov and S. V. Vinogradov, *Angew. Chem. Int. Ed.*, 2009, **48**, 5418-5429.
10. D. Li, N. Kordalivand, M. F. Fransen, F. Ossendorp, K. Raemdonck, T. Vermonden, W. E. Hennink and C. F. van Nostrum, *Adv. Funct. Mater.*, 2015, **25**, 2993-3003.
11. B. V. Slaughter, S. S. Khurshid, O. Z. Fisher, A. Khademhosseini and N. A. Peppas, *Adv Mater*, 2009, **21**, 3307-3329.
12. J. L. Drury and D. J. Mooney, *Biomaterials*, 2003, **24**, 4337-4351.
13. K. Y. Lee and D. J. Mooney, *Chem. Rev.*, 2001, **101**, 1869-1880.
14. A. Khademhosseini, J. P. Vacanti and R. Langer, *Sci. Am.*, 2009, **300**, 64-71.
15. R. Langer and J. P. Vacanti, *Science*, 1993, **260**, 920-926.
16. L. S. Nair and C. T. Laurencin, *Prog. Polym. Sci.*, 2007, **32**, 762-798.
17. M. A. Ward and T. K. Georgiou, *Polymers*, 2011, **3**, 1215-1242.
18. S. Van Vlierberghe, P. Dubruel and E. Schacht, *Biomacromolecules*, 2011, **12**, 1387-1408.
19. J. M. Dang and K. W. Leong, *Adv. Drug Delivery Rev.*, 2006, **58**, 487-499.
20. W. E. Hennink and C. F. van Nostrum, *Adv. Drug Delivery Rev.*, 2002, **54**, 13-36.
21. E. S. Gil and S. M. Hudson, *Prog. Polym. Sci.*, 2004, **29**, 1173-1222.
22. C. de las Heras Alarcón, S. Pennadam and C. Alexander, *Chem. Soc. Rev.*, 2005, **34**, 276-285.
23. B. Jeong and A. Gutowska, *Trends Biotechnol.*, 2002, **20**, 305-311.
24. A. Takahashi, Y. Suzuki, T. Suhara, K. Omichi, A. Shimizu, K. Hasegawa, N. Kokudo, S. Ohta and T. Ito, *Biomacromolecules*, 2013, **14**, 3581-3588.
25. J. Xu, T. M. Filion, F. Prifti and J. Song, *Chem. Asian J.*, 2011, **6**, 2730-2737.
26. R. Jin, L. M. Teixeira, P. Dijkstra, C. van Blitterswijk, M. Karperien and J. Feijen, *Biomaterials*, 2010, **31**, 3103-3113.
27. J. P. Gong, Y. Katsuyama, T. Kurokawa and Y. Osada, *Adv. Mater.*, 2003, **15**, 1155-1158.
28. L. Klouda and A. G. Mikos, *Eur. J. Pharm. Biopharm.*, 2008, **68**, 34-45.
29. B. Jeong, S. W. Kim and Y. H. Bae, *Adv. Drug Delivery Rev.*, 2002, **54**, 37-51.
30. L. Yu and J. Ding, *Chem. Soc. Rev.*, 2008, **37**, 1473-1481.
31. K. T. Nguyen and J. L. West, *Biomaterials*, 2002, **23**, 4307-4314.

32. J. W. Nichol, S. T. Koshy, H. Bae, C. M. Hwang, S. Yamanlar and A. Khademhosseini, *Biomaterials*, 2010, **31**, 5536-5544.
33. P. A. Levett, F. P. Melchels, K. Schrobback, D. W. Hutmacher, J. Malda and T. J. Klein, *Acta Biomater.*, 2014, **10**, 214-223.
34. B. Baroli, *J. Chem. Technol. Biotechnol.*, 2006, **81**, 491-499.
35. N. E. Fedorovich, M. H. Oudshoorn, D. van Geemen, W. E. Hennink, J. Alblas and W. J. Dhert, *Biomaterials*, 2009, **30**, 344-353.
36. I. Mironi-Harpaz, D. Y. Wang, S. Venkatraman and D. Seliktar, *Acta Biomater.*, 2012, **8**, 1838-1848.
37. E. M. Sletten and C. R. Bertozzi, *Angew. Chem. Int. Ed.*, 2009, **48**, 6974-6998.
38. T. K. Tiefenbrunn and P. E. Dawson, *Peptide Science*, 2010, **94**, 95-106.
39. Y. Jiang, J. Chen, C. Deng, E. J. Suuronen and Z. Zhong, *Biomaterials*, 2014, **35**, 4969-4985.
40. P. E. Dawson, T. W. Muir, I. Clark-Lewis and S. B. H. Kent, *Science*, 1994, **266**, 776-779.
41. E. C. B. Johnson and S. B. H. Kent, *J. Am. Chem. Soc.*, 2006, **128**, 6640-6646.
42. B.-H. Hu, J. Su and P. B. Messersmith, *Biomacromolecules*, 2009, **10**, 2194-2200.
43. Q. Wan, J. Chen, Y. Yuan and S. J. Danishefsky, *J. Am. Chem. Soc.*, 2008, **130**, 15814-15816.
44. Y. Yuan, J. Chen, Q. Wan, R. M. Wilson and S. J. Danishefsky, *Peptide Science*, 2010, **94**, 373-384.
45. I. Strehin, D. Gourevitch, Y. Zhang, E. Heber-Katz and P. B. Messersmith, *Biomaterials Sci.*, 2013, **1**, 603-613.
46. J. D. Kretlow, L. Klouda and A. G. Mikos, *Adv. Drug Delivery Rev.*, 2007, **59**, 263-273.
47. S. R. Van Tomme, G. Storm and W. E. Hennink, *Int. J. Pharm.*, 2008, **355**, 1-18.
48. J. Malda, J. Visser, F. P. Melchels, T. Jüngst, W. E. Hennink, W. J. A. Dhert, J. Groll and D. W. Hutmacher, *Adv. Mater.*, 2013, **25**, 5011-5028.
49. K. H. Bae, L. S. Wang and M. Kurisawa, *J. Mater. Chem. B*, 2013, **1**, 5371-5388.
50. E. Ruel-Gariepy and J.-C. Leroux, *Eur. J. Pharm. Biopharm.*, 2004, **58**, 409-426.
51. R. Censi, P. J. Fieten, P. di Martino, W. E. Hennink and T. Vermonden, *Macromolecules*, 2010, **43**, 5771-5778.
52. A. K. Ekenseair, K. W. M. Boere, S. N. Tzouanas, T. N. Vo, F. K. Kasper and A. G. Mikos, *Biomacromolecules*, 2012, **13**, 1908-1915.
53. K. M. Park, K. S. Ko, Y. K. Joung, H. Shin and K. D. Park, *J. Mater. Chem.*, 2011, **21**, 13180-13187.
54. M. Mehdizadeh, H. Weng, D. Gyawali, L. Tang and J. Yang, *Biomaterials*, 2012, **33**, 7972-7983.
55. F. P. W. Melchels, M. A. N. Domingos, T. J. Klein, J. Malda, P. J. Bartolo and D. W. Hutmacher, *Prog. Polym. Sci.*, 2012, **37**, 1079-1104.
56. J.-P. Kruth, M.-C. Leu and T. Nakagawa, *CIRP Annals-Manufacturing Technology*, 1998, **47**, 525-540.
57. T. Billiet, M. Vandenhaute, J. Schelfhout, S. Van Vlierberghe and P. Dubruel, *Biomaterials*, 2012, **33**, 6020-6041.
58. B. Sharma and J. H. Elisseeff, *Ann. Biomed. Eng.*, 2004, **32**, 148-159.
59. T. J. Klein, J. Malda, R. L. Sah and D. W. Hutmacher, *Tissue Eng., Part B*, 2009, **15**, 143-157.
60. T. J. Sill and H. A. von Recum, *Biomaterials*, 2008, **29**, 1989-2006.
61. F. P. Melchels, J. Feijen and D. W. Grijpma, *Biomaterials*, 2010, **31**, 6121-6130.
62. B. Derby, *J. Mater. Chem.*, 2008, **18**, 5717-5721.
63. M. E. Hoque, W. Y. San, F. Wei, S. Li, M.-H. Huang, M. Vert and D. W. Hutmacher, *Tissue Eng., Part A*, 2009, **15**, 3013-3024.
64. M. A. Woodruff and D. W. Hutmacher, *Prog. Polym. Sci.*, 2010, **35**, 1217-1256.

65. H. Seyednejad, A. H. Ghassemi, C. F. van Nostrum, T. Vermonden and W. E. Hennink, *J. Controlled Release*, 2011, **152**, 168-176.
66. H. Seyednejad, T. Vermonden, N. E. Fedorovich, R. van Eijk, M. J. van Steenbergen, W. J. A. Dhert, C. F. van Nostrum and W. E. Hennink, *Biomacromolecules*, 2009, **10**, 3048-3054.
67. W. Schuurman, V. Khristov, M. W. Pot, P. R. v. Weeren, W. J. A. Dhert and J. Malda, *Biofabrication*, 2011, **3**, 021001.
68. J. Visser, B. Peters, T. J. Burger, J. Boomstra, W. J. A. Dhert, F. P. W. Melchels and J. Malda, *Biofabrication*, 2013, **5**, 035007.
69. http://www.nirmresearch.nl, (accessed June 25, 2015).

CHAPTER 2

HYDROGELS IN A HISTORICAL PERSPECTIVE: FROM SIMPLE NETWORKS TO SMART MATERIALS

S. J. Buwalda*, K. W. M. Boere*, P. J. Dijkstra, J. Feijen, T. Vermonden and W. E. Hennink, *J. Controlled Release*, 2014, **190**, 254-273.
*Both authors contributed equally

Abstract

Over the past decades, significant progress has been made in the field of hydrogels as functional biomaterials. Biomedical application of hydrogels was initially hindered by the toxicity of crosslinking agents and limitations of hydrogel formation under physiological conditions. Emerging knowledge in polymer chemistry and increased understanding of biological processes resulted in the design of versatile materials and minimally invasive therapies. Hydrogel matrices comprise a wide range of natural and synthetic polymers held together by a variety of physical or chemical crosslinks. With their capacity to embed pharmaceutical agents in their hydrophilic crosslinked network, hydrogels form promising materials for controlled drug release and tissue engineering. Despite all their beneficial properties, there are still several challenges to overcome for clinical translation. In this review, we provide a historical overview of the developments in hydrogel research from simple networks to smart materials.

Graphical abstract

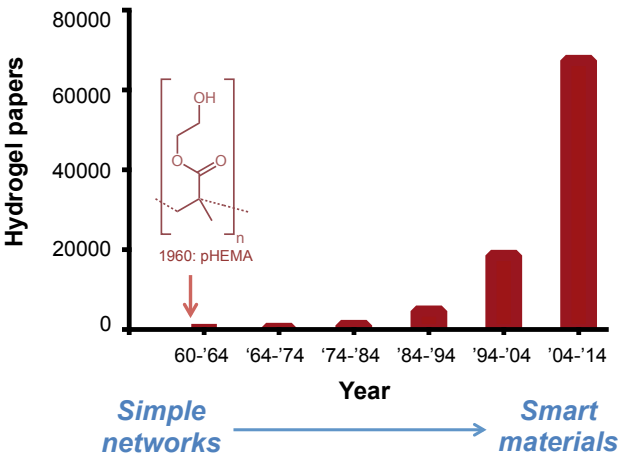

2.1 Introduction

Hydrogels are three-dimensional polymer networks that are able to retain a large amount of water in their swollen state.[1] Hydrogels may be classified as natural, synthetic or hybrid, depending on the source of the constituting polymers. Hydrogels can be chemically crosslinked by covalent bonds, physically crosslinked by non-covalent interactions or crosslinked by a combination of both. The interactions responsible for the water sorption include capillary, osmotic and hydration forces, which are counterbalanced by the forces exerted by the crosslinked polymer chains in resisting expansion.[2] The equilibrium swollen state depends on the magnitudes of these opposing effects, and determines to a large extent some important properties of the hydrogel, including internal transport and diffusion characteristics, and mechanical strength. Many of these properties are governed not only by the degree of swelling, but also directly by the chemical nature of the polymer network and the network morphology. Due to their high water content, the properties of hydrogels resemble those of biological tissues, resulting in an excellent biocompatibility. Furthermore, their soft and rubbery nature minimizes inflammatory reactions of the surrounding cells.[3] After their discovery in the 1960s by Wichterle and Lim[4] hydrogels were first successfully applied as contact lenses. Later, hydrogels have been frequently used as systems for the controlled delivery of biologically active agents. These hydrogels facilitate the localized and sustained release of a drug, thereby decreasing the number of administrations, preventing damage to the drug and allowing for relatively low doses. In this field, the Journal of Controlled Release has played a major role since its launch in 1984 as a place to publish state-of-the-art research and review articles concerning drug delivery from hydrogels. In this contribution for the 30th Anniversary Issue of the Journal of Controlled Release, we present a historical overview of the major developments in hydrogel research over the last 50 years, starting with the relatively simple, chemically crosslinked networks of the 1960s and concluding with today's 'smart' hydrogels (Figure 2.1). We particularly focus on hydrogels for controlled drug delivery, but we also briefly address hydrogels for other biomedical applications such as tissue engineering. Lastly, we present our view on the future of hydrogel research.

Because of the vastness of this research field, obviously not all contributions of the last 50 years could be included in this historical overview. However, many excellent reviews exist that focus on specific areas in hydrogel research.[5-14]

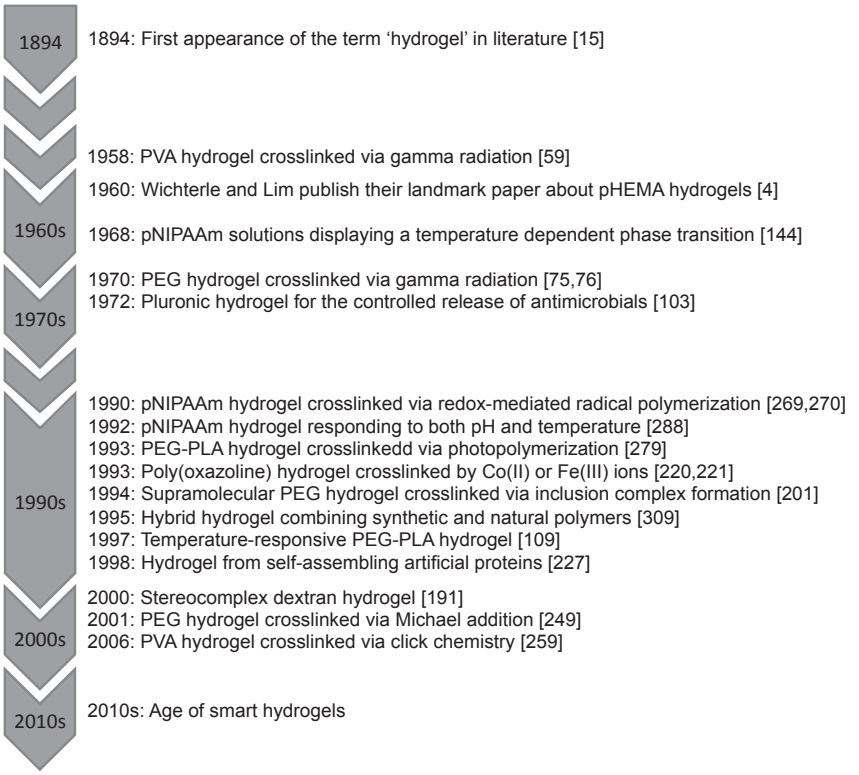

Figure 2.1. Timeline presenting the most important events in the history of hydrogel research.

2.2 First generation hydrogels

Around 1900, the term 'hydrogel' first appeared in scientific literature when it was used to describe a colloidal gel of inorganic salts.[15] In 1960, Wichterle and Lim were the first to report on hydrogels as we know them nowadays, e.g. as water-swollen crosslinked macromolecular networks, in their landmark paper about poly(2-hydroxyethyl methacrylate) (pHEMA) gels for use as soft contact lenses.[4] In the two decades following this discovery, hydrogel research remained essentially focused on relatively simple, chemically crosslinked networks of synthetic polymers with applications mainly in ophthalmic and drug delivery research. The straightforward network structure was also well-suited for fundamental characterization and modeling of various physico-chemical hydrogel properties such as solute diffusivity and crosslink density. Hydrogels were mainly prepared by either polymerization of water-soluble monomers in the presence of a multifunctional crosslinker or by crosslinking of hydrophilic polymers (Figure 2.2). These categories amongst the first generation of hydrogels will be discussed separately hereafter including the most representative examples. The chemical structures of the polymers that were applied

most frequently in hydrogels, pHEMA, poly(vinyl alcohol) (PVA) and poly(ethylene glycol) (PEG), are shown in Figure 2.3.

2.2.1 Hydrogels prepared by polymerization of water-soluble monomers

The hydrogels in this category are prepared by chain-addition reactions, mostly employing vinyl monomers. The mechanism of this type of polymerization has been well established[16] and, in short, consists of an initiating free radical species which adds to a vinyl monomer molecule by opening the π-bond to form a new radical, until the polymerization is terminated at some point by recombination of two radical species or disproportionation. The polymerization of a monomer in the presence of a crosslinking agent in solution has various advantageous aspects over bulk polymerization, such as rapid hydrogel formation under mild conditions and the possibility to obtain pre-defined shapes because the starting materials are in the liquid form.[17]

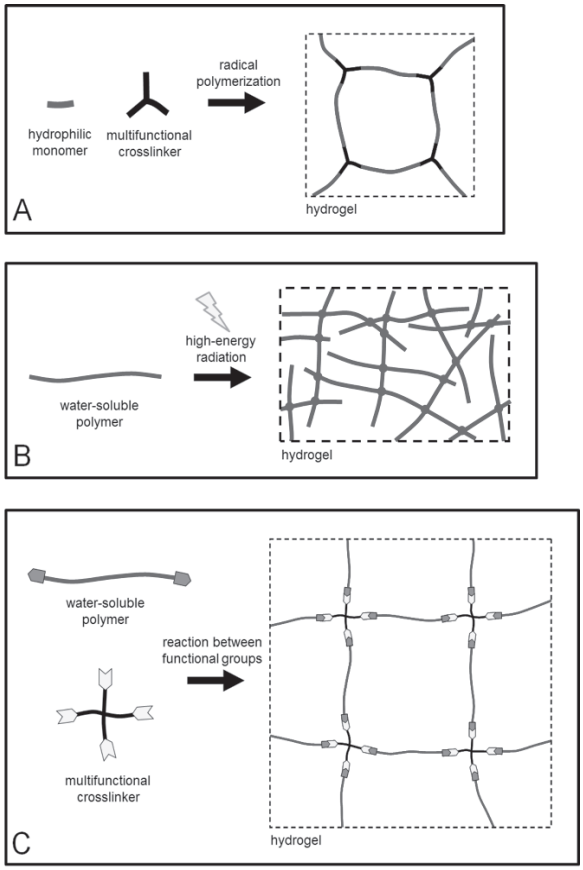

Figure 2.2. Main strategies for the preparation of first generation hydrogels. (A) Polymerization of water-soluble monomers in the presence of a multifunctional crosslinker. (B) Crosslinking of hydrophilic polymers by radiation. (C) Crosslinking of hydrophilic polymers by reaction between complementary groups.

An important hydrogel-forming polymer in terms of production volume in this category is poly(acrylamide) (PAM), which was initially employed mainly in industrial applications such as agricultural gels. In the 1960s, PAM hydrogels were also used for the physical entrapment of cells [18] and enzymes [19], as well as for the covalent attachment of proteins; only recently PAM gels have found widespread biomedical application as soft tissue fillers and augmentation materials.[20] The most extensively studied polymers for application in first generation biomedical hydrogels were the poly(hydroxyalkyl methacrylate)s.

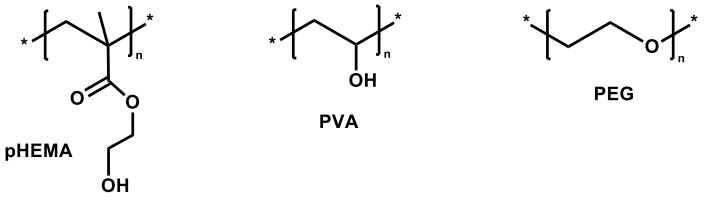

Figure 2.3. Chemical structures of the polymers that were applied most frequently in hydrogels of the first generation.

2.2.1.1 Poly(hydroxyalkyl methacrylate)s

Between 1950 and 1955, Wichterle postulated the fundamental conditions required for synthetic materials in direct contact with living tissues.[21] These included: the absence of extractable impurities; mechanical properties similar to those of the surrounding tissue; sufficient permeability for water-soluble substances such as salts, proteins and oxygen; and resistance to degradation by enzymatic systems. Driven by these requirements, Wichterle and Lim prepared their first hydrogel in 1960 by free radical polymerization of 2-hydroxyethyl methacrylate (HEMA) in aqueous solution with ethylene glycol dimethacrylate (EGDMA) as a crosslinker.[4] These hydrogels found widespread use as soft contact lenses throughout the 1960s, but disadvantages such as insufficient oxygen transport and mechanical fragility sparked research towards improved pHEMA hydrogels.[22] Most notably, from 1970 onwards N-vinylpyrrolidone (NVP) was used to increase the biocompatibility because of its high hydrophilicity, exceeding that of HEMA.[23] NVP was employed as a comonomer together with HEMA [24] or as polymerized PVP grafted onto pHEMA.[25] Both approaches resulted in improved oxygen permeability and wettability of contact lenses, but reports on PVP loss over time [26] led to a preference for copolymerization of HEMA with NVP. Although p(HEMA-co-NVP) contact lenses exhibited several improved properties over pHEMA lenses, the poor copolymerization of methacrylate monomers with NVP due to a large difference in reactivity ratio resulted in hydrogels with an often inconsistent quality in terms of dimensional control, modulus and water content.[27] Therefore, many alternative comonomers were investigated since the late 1970s for

copolymerization with HEMA, including substituted acrylamides,[28] vinyl acetate [29] and substituted methacrylates.[30] Since then significant improvements have been achieved and nowadays materials can be created with various water contents, refractive indices, mechanical properties and oxygen permeabilities. Fifty years after its discovery, pHEMA still remains the basis for many contact lenses.[31,32]

pHEMA hydrogels were also applied in controlled drug delivery applications, as a result of their hydrolytic stability and the possibility to modulate the release properties by introducing co-monomers and varying the crosslink density.[33] Early pHEMA hydrogels possessed a homogeneous network structure and water distribution resulting in optical clarity, which made them suitable for application as contact lenses,[34] as discussed above. The polymerization method in aqueous solution, however, gives rise to a relatively small mesh size, on the scale of nanometers, resulting in limited transport of high-molecular weight compounds.[35] To increase the effective mesh size, in 1972 a freeze-thaw technique was described in which HEMA was polymerized around ice crystals that were subsequently thawed, resulting in macroporous hydrophilic pHEMA membranes.[36] This technique was later expanded for the preparation of pHEMA hydrogels with pore sizes of several micrometers enabling the controlled delivery of macromolecular drugs.[37] Since the 1970s pHEMA based hydrogels have been employed for the controlled release of agents from various drug classes, including anti-arrythmics,[38] contraceptives,[39] antibiotics,[40] ophtalmics,[41] vasoconstrictors,[42] anti-inflammatory drugs[43] and cytostatics.[44] Hydrogels based on pHEMA were also examined in the late 1960s as blood compatible materials [45,46] and as bulk space fillers in reconstructive surgery.[47,48]
Several physical properties of pHEMA hydrogels relevant for the above-mentioned biomedical applications, such as swelling behavior and crosslink density, were studied in detail during this period, most prominently by the group of Peppas.[49] The diffusional characteristics in pHEMA hydrogels of various substances such as oxygen,[50] water[51] and model solutes like NaCl, urea, glucose and lysozyme[52,53] were also investigated.

2.2.2 Hydrogels based on crosslinking of water-soluble synthetic polymers

The second category of first generation hydrogels is constituted by hydrophilic polymers that are covalently crosslinked either by reaction between functional groups or by free radicals. Two polymers have been studied extensively in this category, namely poly(vinyl alcohol) (PVA) and poly(ethylene glycol) (PEG).

2.2.2.1 PVA

PVA, first described in 1924, is a linear synthetic polymer produced by free radical polymerization of vinyl acetate to poly(vinyl acetate) and subsequent hydrolysis of the acetate groups to alcohol groups.[54] The extent of hydrolysis, usually between 85

and 100 %, determines various PVA properties such as crystallinity and aqueous solubility, which are important parameters determining the hydrogel properties. PVA hydrogels have mostly been prepared by chemical crosslinking. Various bi- or multifunctional crosslinkers with groups reactive to the hydroxyl groups of PVA were used for the synthesis of chemical gels, including aldehydes,[55] anhydrides[56] and isocyanates.[57] The models developed by Peppas for determination of the molecular weight between crosslinks, M_c, employing swelling experiments or dynamical mechanical analysis, were applied to PVA hydrogels crosslinked by glutaraldehyde. M_c values typically ranged between 400 and 8000 g/mol depending on the relative amount of crosslinker (Figure 2.4) and the type of experiments performed.[55] The main concern with this crosslinking method is the possible presence of residual crosslinking agents causing adverse effects for biomedical applications.[58] It was demonstrated in the 1960s that irradiation of aqueous PVA solutions by gamma or electron beam radiation also results in the formation of covalently crosslinked hydrogels.[59,60] The formation of free carbon radicals along the backbone and subsequent network formation by recombination of polymer radicals was proposed as the mechanism behind radiation-mediated crosslinking. This crosslink method was considered cleaner and safer than methods involving bifunctional crosslinking agents as mentioned above,[61] with the additional advantage of simultaneous sterilization during hydrogel formation. However, early examples of radiation-crosslinked PVA hydrogels suffered from poor mechanical properties.[62] Reinforcement was achieved by an annealing process, which introduces crystallites in the polymeric network, but as a result the optical clarity of the hydrogel was lost.[63] Physical PVA hydrogels, prepared by repeated freeze-thaw cycles to densify the macromolecular structure, have been reported since the 1970s,[64,65] but the crystallization mechanism behind PVA cryogel formation, as well as their eventual applications such as in tissue engineering, were recognized only in the 1990s.[66]

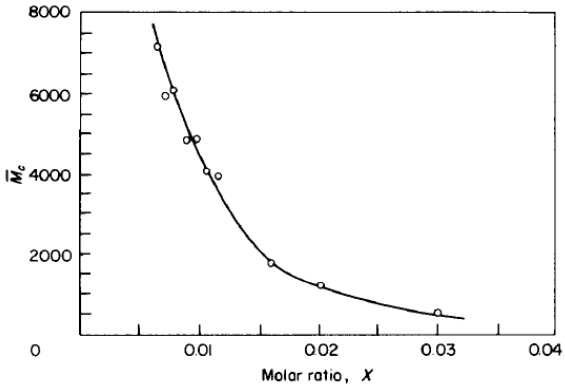

Figure 2.4. Molecular weight between crosslinks M_c versus the molar ratio X glutaraldehyde/PVA repeating unit. Reprinted from,[55] copyright (1980), with permission from Elsevier.

PVA hydrogels were widely studied for use in cardiovascular surgery or other blood-handling procedures, most notably by the group of Sefton. PVA hydrogels were frequently combined with heparin, a natural sulphated glycosaminoglycan, which displays anticoagulant activity by inactivating blood coagulation factors such as thrombin.[67]

PVA based systems were also studied as controlled drug delivery devices, mainly as swelling-controlled hydrogels, which are initially in the dry or glassy state and start to release the drug upon swelling once exposed to biological fluids. PVA hydrogels crosslinked with glutaraldehyde released the model drug theophylline with near zero-order kinetics at a rate that could be controlled by the crosslink density.[68] (Compressed) blends of PVA with other homopolymers such as PVP and PEG were shown to release model drugs of varying size in a controlled manner, and zero-order release was achieved for some formulations.[69,70] The influence of a number of parameters, such as crosslink density and hydrogel morphology, on the diffusion of various model solutes through PVA hydrogels was discussed both theoretically and experimentally in several papers.[68,71,72]

2.2.2.2 PEG

PEG received considerable attention for use in hydrogels during the 1960s and 1970s because of its good biocompatibility and resistance to protein adsorption.[73] Although the terms poly(ethylene glycol) (PEG) and poly(ethylene oxide) (PEO) have been used inconsistently in hydrogel literature, the term PEG refers to polymer chains with lower molecular weights where the hydroxyl end groups still contribute significantly to a glycolic chemical nature, while PEO refers to higher molecular weight polymers where the polyether character dominates.[74] The cutoff is debated but is generally set at 20 kg/mol.[74] For convenience, the term PEG will be used throughout this section.

In the early years of hydrogel research, approaches for the preparation of hydrogels from the highly water-soluble PEG homopolymer mostly concerned covalent crosslinking methods. It was shown that aqueous solutions of PEG can be crosslinked under gamma or electron beam radiation to form a hydrogel.[75,76] The irradiation technique was used by a number of research groups to prepare PEG hydrogels, both from linear and star-shaped PEG.[77-79] Hydrogel formation was also achieved by reaction of PEG end groups with end groups on other PEG macromonomers or low molecular weight crosslinkers. Early examples of specific chemical reactions include free radical polymerization of methacrylate groups[80,81] and reaction between isocyanates and alcohols.[82] More recently, condensation reactions,[83] Michael-type addition,[84] click chemistry,[85] native chemical ligation [86] and enzymatic reactions [87] have also been employed, which will be addressed in a subsequent paragraph of this review (section 2.5.1). Physical crosslinking techniques for PEG homopolymers were described as well, such as the formation of association complexes of PEG with

poly(methacrylic acid),[88] but no applications were reported. Hydrogels based on block and graft copolymers of PEG, such as poly(ethylene glycol)-b-poly(propylene glycol)-b-poly(ethylene glycol) (Pluronics or Poloxamers),[89] started to emerge during the 1960s, but these materials form a class of its own and will be reviewed in section 2.3.1.1.

Early PEG hydrogels were applied mostly as controlled drug delivery systems and as anti-adhesive biomaterials. Graham *et al*. designed hydrogels by crosslinking PEG diisocyanates with hexanetriol for the sustained release of prostaglandin E2,[90] caffeine[91] and morphine.[82] A diffusion controlled release was obtained, which could be tuned by the amount of crosslinker, the PEG M_n and the device geometry (Figure 2.5). Promising clinical data were reported for prostaglandin releasing PEG hydrogels regarding the induction and facilitation of child delivery for patients with an unripe cervix. A contraceptive sponge with the brand name Today, based on crosslinked PEG diisocyanates and containing the spermicide nonoxynolphenol, was commercialized in the beginning of the 1980s and is still on the market today.[92] The same holds for Vigilon, a radiation crosslinked PEG hydrogel supported by a PE net which is sold as a sheet wound covering material, exploiting the biocompatibility and inertness of PEG.[93] These properties also prompted several investigators to study PEG hydrogels as tissue engineering matrices. Examples include photopolymerized hydrogels based on PEG methacrylates for the encapsulation of yeast cells[80] and enzymes.[81]

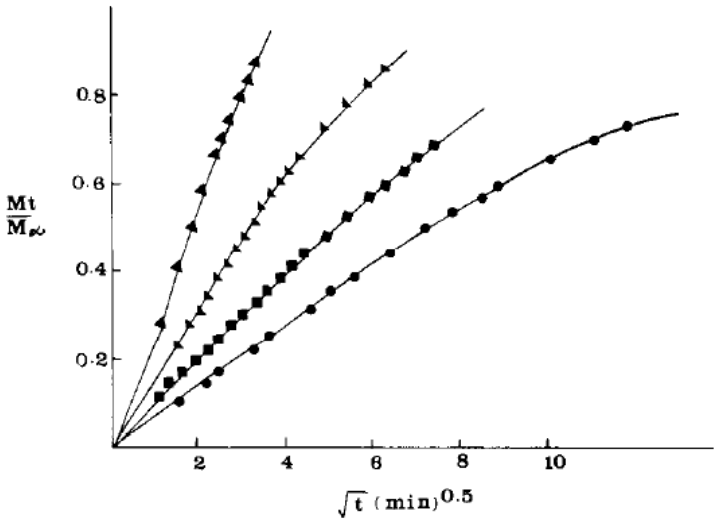

Figure 2.5. Caffeine release from PEG hydrogels with constant length and width but varying thickness. ▲ 1.1 mm; ■ 2.0 mm; ▼ 3.7 mm; ● 5.0 mm. Reprinted from,[91] copyright (1988), with permission from Elsevier.

2.2.3 Hydrogels based on cellulose

Besides entirely synthetic polymers such as pHEMA, PEG and PVA, semi-synthetic derivatives of the natural polymer cellulose also received attention for use in biomedical applications, predominantly for the controlled delivery of drugs. The cellulose ether hydroxypropylmethylcellulose has been widely applied as compressed hydrophilic matrix in which drug release occurred via a combination of diffusion and dissolution of the matrix itself following hydration.[94] The release of a number of drugs with varying hydrophilicity was investigated and near zero-order release was achieved for some water-soluble drugs such as diazepam.[95] Amongst several formulation parameters, varying the polymer concentration was found to be most efficient in controlling the drug release kinetics. [96] More recently, other natural polymers have been investigated as well for use in hydrogels, which will be shortly discussed in section 2.3.5.4.

2.3 Second generation hydrogels

Inspired by the work of Katzir-Katchalsky[97,98] in the 1950s and 1960s on the possibility of transferring chemical energy into mechanical work, in the beginning of the 1970s the hydrogel research focus shifted from relatively simple, water-swollen macromolecular networks to hydrogels capable of responding to a change in environmental conditions such as pH, temperature or concentration of biomolecules. These environmental triggers can be used to evoke specific events, such as gel formation or drug release.

This section focuses mainly on temperature-sensitive hydrogels. Systems sensitive to pH or biomolecules will be addressed only shortly as these are covered extensively by Siegel *et al*.[100]

2.3.1 Temperature-sensitive hydrogels

The most widely studied environmentally responsive systems are temperature-sensitive hydrogels, in which physical entanglements, hydrogen bonding and hydrophobic interactions are the main features that constitute the crosslinks. The temperature dependent balance of these physical interactions governs the thermo-sensitive gelation behavior of the hydrogel. Temperature-sensitive hydrogels are of particular interest because they can be applied as *in situ* forming systems. These are fluids that can be injected into any tissue, organ or body cavity in a minimally invasive manner prior to gelation.[101,102] *In situ* forming hydrogels offer several advantages over systems that have to be formed into their final shape before implantation. To mention, there is no need for surgical procedures, biological components can easily be incorporated by simple mixing and their initially flowing nature ensures proper shape adaptation resulting in a good fit with the surrounding tissue. Poly(ethylene glycol)-polyester block copolymers, poly(N-isopropylacrylamide) (PNIPAAm)

and poly(N-(2-hydroxypropyl)acrylamide) (PHPMAm) are the most extensively investigated polymers in this hydrogel class. Temperature-sensitive hydrogels are applied mainly for the controlled delivery of pharmaceutical agents.

2.3.1.1 Temperature-sensitive hydrogels based on PEG-polyester block copolymers

Aqueous solutions of selected poly(ethylene oxide)-poly(propylene oxide)-poly(ethylene oxide) (PEO-PPO-PEO) triblock copolymers, commercially known as Pluronics (BASF) or Poloxamers (ICI), exhibit a phase transition from the sol to the gel state at low temperatures and from the gel to the sol state at higher temperatures when the concentration is above the critical gel concentration (CGC). Pluronic hydrogels for the controlled release of pharmaceutical agents appeared in the 1970s. Early examples include Pluronic F127 gels for the controlled release of anesthetics[103] and antimicrobials. [104] More recently, the release of ophtalmics,[105] cytostatics[106] and hormones[107] from Pluronic based hydrogels has been studied as well. Significant drawbacks of Pluronic hydrogels are their weak mechanical properties and intrinsic instability, which originate from the weak hydrophobic interactions between the PPO blocks. Moreover, these block copolymers are not biodegradable, which prevents the use of high molecular weight materials since they cannot pass the kidney membranes. These drawbacks prompted several researchers to replace the hydrophobic PPO block for a biodegradable polyester block as a basis for thermo-responsive hydrogels. Both AB-, ABA- and BAB-type copolymers, with A as the PEG block and B the polyester block, were synthesized. Various polyesters have been employed as the hydrophobic block, predominantly poly(lactide) (PLA), poly(glycolic-co-lactic acid) (PLGA) and poly(ε-caprolactone) (PCL) because of their biocompatibility, biodegradability and facile synthesis via the ring opening polymerization of lactide, glycolide or ε-caprolactone. Most thermo-responsive hydrogels are based on PEG and PLA, and emphasis will be placed on these systems in the remainder of this section.

In the late 1990s, the group of Kim synthesized a number of linear AB diblock and ABA triblock copolymers, with A as a hydrophilic PEG block (M_n = 5 kg/mol) and B as a hydrophobic PLA block.[108,109] Diblock copolymers were synthesized by ring opening polymerization of lactide initiated by the hydroxyl group of monomethoxy PEG, while triblock copolymers were prepared by coupling the diblock copolymers with monomethoxy PEG using hexamethylene diisocyanate as chain extender. In comparison with diblock copolymers possessing the same PEG content and PEG molecular weight, triblock copolymers generally yielded hydrogels at lower polymer concentrations (Figure 2.6). The thermo-responsive behavior can be tuned by the hydrophilic/hydrophobic balance, the block length, and the stereoregularity of the PLA block. For PEG-PLLA-PEG triblock copolymers, the CGC decreased from 20 to 12 w/v % upon increase of the PLLA block length from 2 to 5 kg/mol. Release

studies were performed using fluorescein isothiocyanate labeled dextran (M_n 20 kg/mol) as model compound.[110] Zero-order release kinetics were observed for a 35 w/v % PEG-PLLA-PEG hydrogel, which released 40 % of the initial drug load in 12 days. The release rate could be tailored by the initial loading, the molecular weight or hydrophobicity of the drug and the initial polymer concentration.

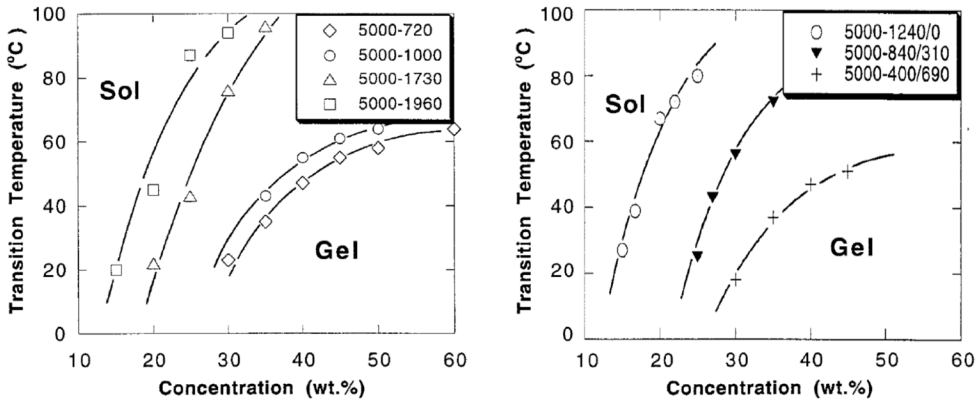

Figure 2.6. Gel-sol transition curves of PEG-PLLA diblock (left) and PEG-PLLA-PEG triblock (right) copolymers. The numbers indicate the molecular weight of each block. Reprinted from,[109] copyright (1999), with permission from John Wiley & Sons, Inc.

Block copolymers with an inverted structure (BAB) were prepared by ring opening polymerization of lactide initiated by the hydroxyl groups of PEG. At room temperature the CGC of triblock copolymers with a PEG M_n of 12.5 kg/mol decreased significantly from 80 to 15 w/v % upon an increase of the PLA block length from 10 to 15 lactyl units, showing a much stronger effect of the PLA block length on the gelation behavior in comparison with ABA-type triblock copolymers.[111] Li *et al*. investigated the degradation behavior of PLA-PEG-PLA triblock copolymers of high molecular weight (total M_n 45 - 75 kg/mol).[112] Degradation was initially very fast with significant weight loss. The PLA/PEG ratio of the remaining material increased rapidly, indicating the release of PEG-rich chains. In the second phase, the degradation rate slowed down because of the high PLA content of the remaining material. The presence of proteinase K strongly accelerated the degradation rate of the hydrogels, showing that the enzyme was able to penetrate into the gel and attack the PLA domains. The PLA/PEG ratio in the residual hydrogel was found to increase as in the case of hydrolytic degradation.

Hydrogels based on alternating multiblock copolymers of PEG and PLA were also reported. The polymers were synthesized by coupling PEG-diols to PLA-diols using succinic anhydride[113,114] or by coupling hydroxyl end functionalized PLA-PEG-PLA triblock copolymers using adipoyl chloride.[115] The PEG/PLLA

multiblock copolymers synthesized by the group of Jeong, having a total M_n of 7 kg/mol, exhibited a CGC of approximately 30 w/v % and underwent a sol-gel-sol transition with increasing temperature.[113] The gelation mechanism was considered by the authors to be governed by micellar aggregation. The transition temperature and gel modulus could be controlled by varying the PLLA block length and PEG molecular weight. The *in situ* gel forming ability of the polymers was demonstrated by subcutaneous injection into rats. The PEG/PLLA multiblock copolymer showed a lower CGC and improved mechanical properties in comparison with an analogous PEG/PDLLA multiblock copolymer,[114] which was attributed to a lower dynamic molecular motion and a higher aggregation tendency of PLLA due to the isotactic localization of the hydrophobic methyl groups.

Besides the linear PEG-PLA copolymers, also a number of star-shaped and branched architectures were explored for the preparation of thermo-responsive hydrogels. Park *et al*. synthesized 3-armed PLA-centered star block copolymers by coupling monocarboxylated PEG to a 3-armed hydroxyl-terminated PLA using dicyclohexylcarbodiimide (DCC) as coupling agent.[116] At a similar PEG block length of 5 kg/mol, an increase in the PLA blocks length led to an expanded gelation window. The 3-armed star block copolymer exhibited a lower CGC in comparison with a PEG-PLA-PEG triblock copolymer possessing the same PEG content. Eight-armed PEG-PLA star block copolymer, prepared by ring opening polymerization of L-lactide using 8-armed PEG with hydroxy end-functional groups as an initiator, represents a star shaped BAB type copolymer.[111] These star block copolymers, with a PEG content of 74 wt %, exhibited approximately the same gelation behavior as PLLA-PEG-PLLA triblock copolymers with a PEG content of 84 wt %. Importantly, the CGC at room temperature decreased from 40 to 15 w/v % when the PLLA block length increased from 10 to 14 lactyl units. Increasing the PEG molecular weight at a constant PLLA block length also resulted in a lower CGC possibly due to enhanced chain entanglements. Recently, highly branched PEG-PLLA copolymers were synthesized by a coupling reaction of 8-armed amine-functionalized PEG and macromonomers having 2 PLLA arms and a N-hydroxysuccinimide activated ester group at the center of the polymer chain.[117] It was reported that 4 out of 8 PEG arms were functionalized with a branched PLA moiety. The copolymers showed thermo-responsive gelation behavior at low concentrations (4 w/v %). The gel-sol transition temperature could be tuned by varying the copolymer concentration and the molecular weight of the PLLA block. Branched block copolymers with a PLLA block length of 12 lactyl units exhibited significantly lower CGCs compared to the 8-armed PEG-PLLA star block copolymers with a similar PEG content and a PLLA block length of 10 lactyl units.[111] This drop in CGC was ascribed to stronger hydrophobic interactions in the branched system, because hydrophobic domains may be formed more easily if only 4 out of 8 arms have to be folded into such a domain instead of 8 out of 8 arms (Figure 2.7).

Recently it was found that 8-armed PEG-PLA star block copolymers, possessing an amide linkage between PEG and PLA, yielded hydrogels with improved mechanical properties and a controlled hydrolytic degradation compared to 8-armed PEG-PLA star block copolymers having an ester linkage between the PEG and PLA blocks.[118,119]

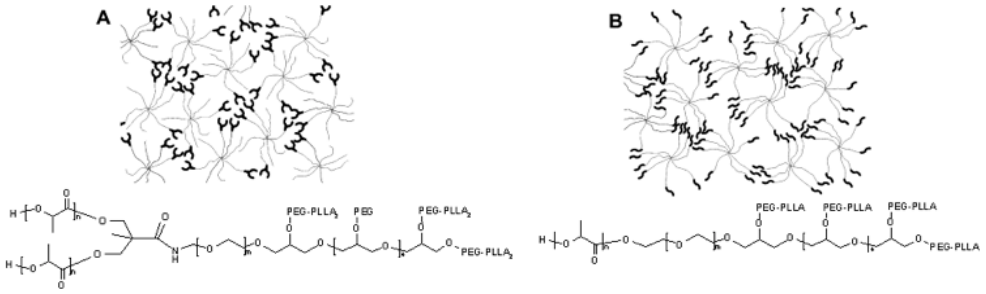

Figure 2.7. Representation of a hydrogel prepared with the highly branched PEG-PLA block copolymer described by Velthoen *et al*. (A)[117] and the 8-armed PEG-PLA star block copolymer described by Hiemstra *et al*. (B).[120] Reprinted from,[117] copyright (2011), with permission from Elsevier.

Hydrogels based on PEG-PLGA-PEG triblock copolymers were introduced in the late 1990s as an alternative for early PEG-PLA based systems. These systems exhibit a sol-to-gel transition at lower temperatures and a gel-to sol transition at higher temperatures. High temperatures, which are potentially harmful for bioactive molecules, can consequently be avoided for the preparation of PEG-PLGA-PEG hydrogels.[121] In PEG-PLGA-PEG systems with a PEG block of < 750 g/mol, the gel window covered the physiological temperature and the CGC and sol-to-gel transition temperature could be tuned by the block length and composition as well as by the addition of additives.[122] The lower sol-to-gel transition was ascribed to growth, packing and interaction of the micelles, while the upper gel-to-sol transition was thought to be due to the collapse of the micellar structure after dehydration of the PEG block.[123,124] After subcutaneous injection of an aqueous solution of PEG-PLGA-PEG (550-2810-550 g/mol) into rats, a transparent hydrogel was formed *in situ* which exhibited good mechanical properties and was stable for 1 month.[125] PEG-PLGA-PEG based hydrogels have been used for the controlled release of various bioactive molecules, including the model drugs ketoprofen and spirolactone,[126] and the growth factor TGF-β1.[127]

BAB-type PLGA-PEG-PLGA triblock copolymers were subsequently introduced as new hydrogel forming materials and commercialized as ReGel.[128] These polymers were synthesized by ring opening polymerization of DL-lactide and glycolide

initiated by PEG, without the need for a possibly toxic coupling agent such as hexamethylene diisocyanate in the case of ABA triblock copolymers. PLGA-PEG-PLGA showed a lower CGC and sol-to-gel transition temperature in comparison with PEG-PLGA-PEG, suggesting a different gelation mechanism for BAB type block copolymers. The temperature-dependent ordered packing of bridged micelles was suggested as the gelation mechanism of concentrated PLGA-PEG-PLGA aqueous solutions.[129] *In vitro* release experiments showed a diffusion-controlled release of paclitaxel from ReGel in the first two weeks, followed by release via a combination of diffusion and hydrogel degradation for 5 weeks.[130] In contrast, paclitaxel release from a Pluronic hydrogel was complete within 1 day (Figure 2.8). *In vivo*, paclitaxel-loaded ReGel showed a higher tumor efficacy and fewer adverse effects than the clinically used formulation of paclitaxel (Taxol). ReGel formulations have also been employed for the controlled release of proteins such as interleukin-2,[131] insulin[132]

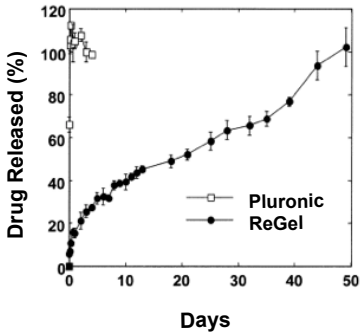

Figure 2.8. *In vitro* release of paclitaxel from PLGA-PEG-PLGA and Pluronic hydrogels. Reprinted from,[130] copyright (2001), with permission from Elsevier.

and testosterone.[133]Bae *et al*. prepared ABA and BAB type block copolymers based on PCL and PEG.[134,135] Copolymers with an appropriate hydrophilic/hydrophobic balance showed both a lower sol-to-gel transition and an upper gel-to-sol transition with increasing temperature, which were ascribed to micellar aggregation through hydrophobic interactions and micellar collapse through increased molecular motion of PCL, respectively. Similar to PL(G)A/PEG based systems, PEG and polyester block lengths as well as block topography were found to influence gelation properties. Solutions of PCL-PEG-PCL exhibited a lower critical gelation temperature and a larger gel window compared with PEG-PCL-PEG, probably due to the possibility of intermicellar PCL bridging leading to more facile aggregation. The release of the model drugs vitamin K, honokiol and albumin from PCL-PEG-PCL hydrogels was governed mainly by diffusion as opposed to matrix degradation because of the high *in vitro* hydrolytic stability of the PCL blocks.[136]

Recently, temperature-responsive gelling systems composed of poly(ε-caprolactone-co-lactide)-b-poly(ethylene glycol)-b-poly(ε-caprolactone-co-lactide) (PCLA-PEG-

PCLA) triblock copolymers were developed.[137,138] It was demonstrated that the molecular weight of PCLA, the caproyl/lactoyl ratio and the nature of the end group had a profound effect on the crystallinity and consequently on the rheological and degradation properties. Good cytocompatibility of an acetyl-capped PCLA-PEG-PCLA hydrogel was proven *in vitro* on erythrocytes and chondrocytes. Moreover, intra-articular biocompatibility *in vivo* was demonstrated using microCT-imaging and histology, as both techniques showed no changes in cartilage quality and/or quantity.[139]

Other examples of hydrophobic blocks in amphiphilic PEG copolymer hydrogels intended for biomedical applications include poly(3-methylglycolide),[140] poly(δ-valerolactone),[141] poly(propylene fumarate)[142] and poly(trimethylene carbonate).[143]

2.3.1.2 Temperature-sensitive hydrogels based on pNIPAAm

Although poly(N-isopropylacrylamide) (pNIPAAm) was first synthesized in the 1950s as a rodent repellent,[144] it did not gain much attention until in 1968 Heskins and Guillet reported about the temperature dependent phase transition of pNIPAAm solutions in water.[145] They ascribed the lower critical solution temperature (LCST) of these solutions to preferred intermolecular hydrogen bond formation between pNIPAAm chains over water-amide hydrogen bond formation due to an entropy effect. Since then, many researchers made attempts to fully elucidate the mechanism of pNIPAAm's thermal behavior.[144,146,147] Using techniques such as light scattering and viscometry, they found a sharp and reversible phase transition of pNIPAAm around 32°C, almost independent of molecular weight and concentration.[148,149] Given the fact that this phase transition occurs between room temperature and body temperature, interest sparked for using pNIPAAm as an injectable material for biomedical applications. However, at high concentrations the phase transition from a hydrated swollen state to a collapsed dehydrated state resulted in a loss of 90% of water.[144] This phenomenon, also known as syneresis, hindered the initial application of pNIPAAm in hydrogel formulations. Therefore, pNIPAAm was copolymerized with a variety of monomers to introduce new functionalities and to prevent syneresis. Copolymerization with a monomer such as dihydroxyethylene-bis-acrylamide and subsequent radical polymerization resulted in the formation of a covalent network besides the thermally induced physical network.[150] Since the 1980s, crosslinked pNIPAAm hydrogels were studied for amongst others the release of vitamin B12, myoglobin[151] and progesterone.[152] However, the release of drugs from these hydrogels was relatively fast, usually within 24 hours. To extend the release time and to enhance the mechanical stability, interpenetrating polymer networks of pNIPAAm were formed.[153] Alternatively, pNIPAAm hydrogels were covalently crosslinked with another polymer with complementary reactive groups. The combination of temperature induced physical crosslinking and chemical crosslinking

will be discussed in section 2.5.3. Additionally, pNIPAAm was copolymerized with hydrophilic or hydrophobic monomers to either increase or decrease its LCST.[154] Despite all these unique properties, pNIPAAm is a non-degradable polymer, therefore limiting its application for drug delivery and tissue engineering purposes.[155] Introduction of biodegradable segments in pNIPAAm resulted in the formation of toxic low-molecular mass pNIPAAm degradation products.[156,157] For this reason, the most attractive approach to form a bioresorbable hydrogel based on pNIPAAm is by manipulating its LCST in time. Hennink and coworkers have developed copolymers of NIPAAm and 2-hydroxyethyl methacrylate monolactate (HEMA-lactate).[158] During incubation in an aqueous solution the lactate ester side groups are hydrolyzed. Due to this hydrolysis, the overall hydrophilicity increased, resulting in an LCST above 37°C and therefore dissolution of the polymer. The LCST could be tuned depending on the length of the lactate side groups and in this way a high control over degradation time was achieved.[159] Later on, HEMA was replaced by N-(2-hydroxypropyl) methacrylamide (HPMA) for its hydrophilicity and low immunogenicity.[160,161] With variations in the formulation a highly tunable degradation rate was obtained.[162] Using a similar hydrolysis-sensitive approach, pNIPAAm has also been copolymerized with dimethyl-γ-butyrolactone acrylate (DBA) that initially resulted in a decrease in LCST with increasing DBA content.[163] In time hydrolysis resulted in an increase of the LCST above 37°C.

2.3.1.3 Other thermoresponsive systems

Thermoresponsive, hydrolytically degradable polymers have also been designed solely based on HPMA-lactate monomers. ABA triblock copolymers with thermosensitive poly(*N*-(2-hydroxypropyl) methacrylamide lactate) A-blocks and a hydrophilic PEG B-block, which can form hydrogels at 37°C have been synthesized by our group (Figure 2.9).[164] Extensive rheological studies showed a high tunability in storage modulus by changing the concentration of the polymers and thermosensitive block length. Diffusion of fluorescein isothiocyanate (FITC)-labeled dextran in these hydrogels was described with a rate depending on polymer design, concentration and temperature.[165]

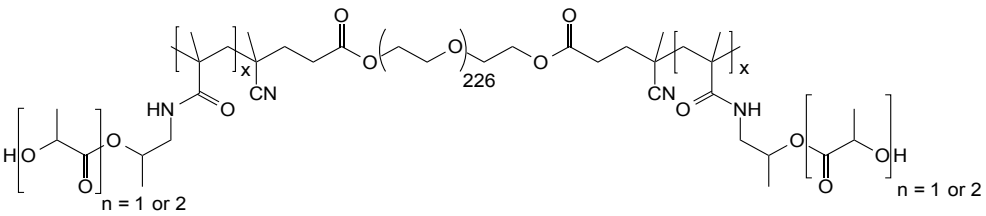

Figure 2.9. Chemical structure of ABA triblock copolymers consisting of a PEG middle block and random outer blocks of HPMA mono and di lactate.

Lutz *et al*. described the synthesis of copolymers of 2-(2-methoxyethoxy)ethyl methacrylate and oligo(ethylene glycol) methacrylate (P(MEO_2MA-co-OEGMA, also abbreviated as pOEGMA).[166] These polymers were synthesized by atom transfer radical polymerization (ATRP) and displayed LCST behavior in water. These systems were particularly of interest since the LCST of these polymers could be precisely tuned depending on the feed ratio of the two monomers.[166] Additionally, these scientists compared these polymers with pNIPAAm and found a similar independence of the LCST on pH and polymer concentration.[167] Moreover, advantages of pOEGMA over pNIPAAm include a smaller difference between phase transition temperature during heating and cooling cycles, a smaller dependence of the LCST on the polymer chain length (Figure 2.10) and a suggested higher biocompatibility.[167] POEGMA based microgels have for example been used for delivery of chemotherapeutic agents.[168]

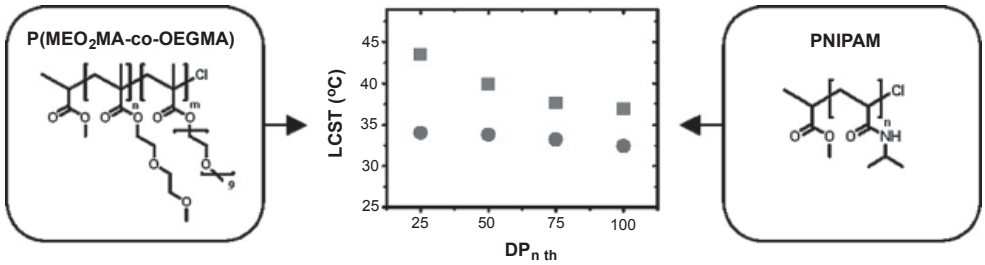

Figure 2.10. Chemical structures of pOEGMA (left) and pNIPAAm (right). The graph in the middle shows the effect on the LCST for different theoretical degree of polymerization (DP_{nth}) for pOEGMA (squares) and pNIPAAm (circles). Reprinted with permission.[167] Copyright (2006) American Chemical Society.

2.3.2 In situ forming hydrogels based on other stimuli

Besides temperature-sensitive hydrogels, the second most used trigger for hydrogel formation is pH. Generally, pH sensitive hydrogels contain either basic or acidic moieties that become ionized at high or low pH, respectively.[169,170] Making use of the variation in pH in different parts of the body, controlled release of the hydrogel content can be established.

Lastly polymers that respond to concentrations of biomolecules have attracted interest as *in situ* forming materials. Biomolecule-sensitive hydrogels can be regarded as perfect mimics of nature, since a conformational change is induced after change in concentration of biomolecules, like the body responds on hormones.[171] The most well-known biomolecule in this category is glucose. Hydrogels were designed containing glucose oxidase, together with pH sensitive moieties. After glucose diffuses into these hydrogels, it is converted to gluconic acid, leading to a decrease in pH and subsequently increase in swelling of the hydrogel due to e.g. protonation of

amine functionalities present in the network.[172,173] Insulin can then be released from the hydrogel, showing the potential of these hydrogels as self-regulating systems. A more detailed overview of pH and biomolecule sensitive hydrogels is given by Siegel *et al*.[100]

2.4 Third generation hydrogels

The temperature- and pH-responsive physical hydrogels discussed in the previous chapter are mainly crosslinked via hydrophobic and ionic interactions, respectively. In the mid-1990s, other physical interactions were recognized and exploited as crosslinking methods that offered the possibility to enhance and finely tune the mechanical, thermal and degradation properties of hydrogels. Many of these interactions also allowed for *in situ* hydrogel formation. This section focuses on stereocomplexation, inclusion complex formation, metal-ligand coordination and peptide interactions as crosslink methods for the preparation of hydrogels.

2.4.1 Stereocomplexed hydrogels

A polymer stereocomplex is defined as a stereoselective interaction between two complementing stereoregular polymers, which interlock and form a new composite with altered physical properties in comparison with the constituting polymers.[174] The first example of stereocomplexation was reported in 1953 by Pauling and Corey for a polypeptide.[175] Stereocomplexation between enantiomeric polylactides was first noticed by Ikada *et al*. in 1987.[176] The complementary polymers PLLA and PDLA are optically active polymers with identical chemical structures but opposite chirality. In the solid state, PLLA forms a left-handed helix, while PDLA forms a right-handed helix. It has been suggested that van der Waals forces between the two helices are the driving force for a dense crystalline packing of the helices in a stereocomplex (Figure 2.11).[177,178] Because stereocomplex crystals are formed at shorter PLA block lengths compared to homopolymer crystals,[179] an operation window exists in which mixing of aqueous solutions of PLLA and PDLA block copolymers results in the formation of a hydrogel through crosslinking by stereocomplexation. From 2000 onwards, stereocomplexation between enantiomeric PLLA and PDLA blocks in amphiphilic copolymers has been employed for the preparation of injectable hydrogels.

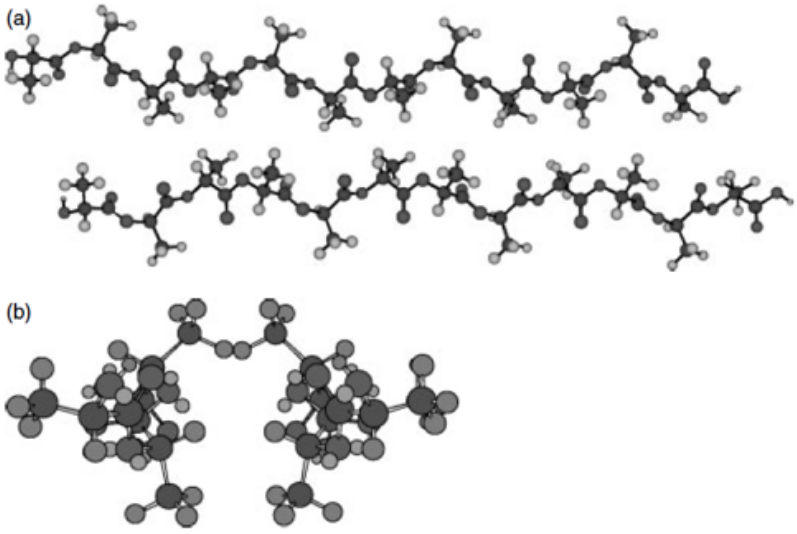

Figure 2.11. A) Projections along the helical axis of a helical conformation of stereocomplexed PLA (upper: PLLA, lower: PDLA). B) Projections perpendicular to the helical axis of a helical conformations of PLLA (left) and: PDLA (right) in stereocomplexed PLA. Reprinted from[177], copyright (2006), with permission from John Wiley & Sons, Inc.

Kimura and coworkers investigated the influence of the architecture of stereocomplexed PEG-PLA block copolymers on the gelation properties.[180,181] Ring opening polymerization of L- or D-lactide initiated by mono- or dihydroxy PEG generated enantiomeric AB diblock and BAB triblock copolymers, respectively, whereas ABA triblock copolymers were obtained by coupling the AB diblock copolymers with hexamethylene diisocyanate. The PEG content of all copolymers in these studies was approximately 50 wt %. Whereas BAB type copolymers may show thermo-reversible gelation, mixing of aqueous solutions of enantiomeric BAB block copolymers afforded systems that exhibit an irreversible sol-gel transition upon temperature increase.

Triblock copolymers with an ABA structure, on the other hand, formed hydrogels at high concentrations showing a reversible gel-sol transition with temperature. Mixed solutions of enantiomeric AB diblock copolymers also yielded hydrogels that exhibit a gel-sol transition upon temperature increase. However, unlike the ABA triblock system, this transition is irreversible.

Grijpma *et al*. and Li *et al*. reported on the synthesis, characterization and stereocomplex mediated gelation of PEG-PLA diblock and PLA-PEG-PLA (BAB) triblock copolymers.[182-185] Thymopentin release from these systems was slower in comparison with the release from single enantiomer hydrogels.[186] When the copolymers were synthesized by ring opening polymerization of L- or D-lactide

initiated by dihydroxy PEG (M_n 4 kg/mol) and zinc lactate as a catalyst for 7 days, hydrogel formation by stereocomplexation was detected for copolymers with PLA blocks of 17 lactyl units but not for copolymers with PLA blocks of 11-13 lactyl units.[187] This was ascribed to racemization of L-lactyl units leading to non-isotactic sequences in the PLLA chains, which prevents the formation of stereocomplexes. Racemization was largely reduced when the reaction time was shortened to 1 day. It appeared that 10 lactyl units per PLA block were sufficient for the formation of stereocomplexed PLA-PEG-PLA hydrogels.

Star-shaped block copolymers of PEG and PLA, showing stereocomplex mediated gelation, were also investigated. It was found that stereocomplexed PEG-$(PLA)_8$ star block copolymers, prepared by ring opening polymerization of L- or D-lactide initiated by 8-armed PEG (M_n 20 kg/mol), gelated faster and formed hydrogels with improved mechanical strength as compared to gels based on stereocomplexed PLA-PEG-PLA triblock copolymers.[111] This was ascribed to a higher number of stereocomplex sites in PEG-$(PLA)_8$.[120] Rheological measurements showed that increasing the average PLA block length from 12 to 14 lactyl units at a polymer concentration of 10 w/v % resulted in an increase in the storage modulus from 0.9 to 7.0 kPa and a decrease in gelation time from 40 minutes to less than 1 minute. It was shown that the release of the relatively small protein lysozyme followed first order kinetics and approximately 90 % was released in 10 days.[188] The relatively large protein immunoglobulin G was released from stereocomplexed hydrogels with nearly zero order kinetics, and up to 50 % was released in 16 days. Replacing the ester linkages between the PEG core and the PLA arms by amide linkages resulted in stereocomplexed hydrogels with improved mechanical properties and controlled degradation at 37 °C in PBS.[189,190]

Nagahama *et al*. prepared enantiomeric 8-armed PEG-PLA-PEG type copolymers by coupling *monocarboxylated* PEG to star-shaped PEG-PLLA or PEG-PDLA diblock copolymers using N,N'-dicyclohexylcarbodiimide as a coupling agent.[191] At low concentrations an aqueous mixture consisting of both enantiomers yielded a sol at room temperature exhibiting an irreversible transition to the gel state upon temperature increase. *In vitro* degradation experiments revealed a faster molecular weight reduction for copolymers in single enantiomer hydrogels compared to mixed enantiomer hydrogels. This suggests that stereocomplex formation has an inhibitory effect on the hydrolysis of the ester groups in the PLA domains.

Also polymers other than PEG have been used in combination with PDLA and PLLA to prepare stereocomplexed hydrogels. Hennink and coworkers synthesized hydrogels from the natural polysaccharide dextran grafted with monodisperse L-lactic acid and D-lactic acid oligomers.[192] Rheological experiments showed that the degree of polymerization (DP) of the lactic acid oligomers must be at least 11 to obtain a hydrogel. Stronger gels were obtained by increasing the DP and degree

of substitution and by decreasing the water content. The degradation time varied from 1 to 7 days, depending on the number, length and polydispersity of the lactate grafts and the initial water content.[193] Protein-loaded hydrogels were prepared by dissolving the proteins in the enantiomeric dextran-lactate solutions prior to mixing. Lysozyme was released in 5 days by diffusion, whereas the release of the larger immunoglobulin G in 8 days was governed by diffusion as well as swelling and degradation of the hydrogel. *In vivo* tests demonstrated that these stereocomplexed hydrogels are biocompatible and effective systems for the local delivery of the cytokine recombinant human interleukin-2.[194,195] In an alternative approach, it was shown that a mixture of crosslinked dextran microspheres substituted with L- or D-oligolactates also resulted in macroscopic hydrogels with high stiffness. Protein release experiments with these systems revealed a continuous lysozyme release during 30 days with full preservation of its enzymatic activity.[196]

Van Nostrum *et al*. reported on stereocomplexed hydrogels prepared from pHPMAm with oligo(lactic acid) side chains of opposite chirality.[197] In comparison with dextran stereocomplexed hydrogels, the degradation time of the pHPMAm stereocomplexed hydrogels was significantly longer, mainly due to the presence of carbonate instead of ester linkages between the oligolactide and the polymer backbone. The degradation time could be tailored from 1 week to 3 months by changing the grafting density and the oligolactide endgroup.

Stereocomplexed hydrogels were also prepared from oligolactide-functionalized pHEMA,[198] Pluronics[199] and 2-methacryroyloxyethyl phosphorylcholine[200] polymers. An extensive recent review concerning stereocomplexes in biomedical applications can be found in reference [201].

2.4.2 Hydrogels crosslinked by other physical interactions

Cyclodextrins (CDs) are cyclic oligosaccharides possessing a hydrophobic cavity that can act as a host for a variety of molecules. The formation of a CD-polypseudorotaxane, where a polymeric guest threads into multiple CD hosts, and subsequent polypseudorotaxane aggregation can lead to the formation of a supramolecular hydrogel (Figure 2.12). This hierarchical self-assembly process was employed for the first time to create a physically crosslinked hydrogel by Li *et al*. in 1994[202]. Disadvantages of early systems, which were based on PEG as guest molecule, included low stability and long gelation times of several hours. Improved hydrogel properties were obtained when aqueous solutions of CDs were mixed with amphiphilic block copolymers such as Pluronics,[203] reverse Pluronics (PPO-PEO-PPO),[204] PCL-PEG-PCL[205] and PEG-PHB-PEG.[206] For example, a 23 wt% hydrogel obtained from a PEG-PHB-PEG amphiphilic triblock copolymer (M_n 13 kg/mol) and α-CD released fluorescein isothiocyanate labeled dextran for over 30 days, in contrast to a similar formulation prepared from high molecular weight PEG (M_n

35 kg/mol) which was only stable for 6 days.[207] CD hydrogels were also prepared with a number of PEG-grafted natural polymers, including dextran,[208] chitosan[209] and heparin.[210] In these cases, the high degree of crosslinking due to the branched polymer architecture resulted in stiff and stable hydrogels. The supramolecular heparin hydrogel described by Zhang *et al*. showed a sustained release of the model protein albumin, which could be tuned by the heparin and α-CD concentration. Interestingly, this supramolecular hydrogel also exhibited a controlled release profile for heparin, and good anticoagulant and blood-compatible properties were reported.[210] A recent development in this field is the preparation of stimuli-responsive polypseudorotaxane hydrogels, including pH-,[211] photo- and dual-responsive[212]

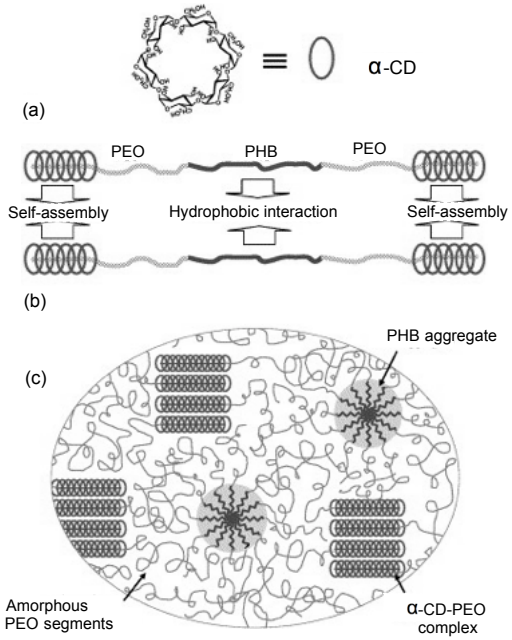

Figure 2.12. The structure of α-CD (a), the schematic illustrations of the proposed structures of α-CD–PEO–PHB–PEO inclusion complex (b), and α-CD–PEO–PHB–PEO supramolecular hydrogel (c). Reprinted from [207], copyright (2006), with permission from Elsevier.

systems. Another widely explored strategy to produce hydrogels is the co-assembly of CDs with hydrophobic groups grafted on polymers. These developments occurred simultaneously with the emergence of the polypseudorotaxane hydrogels described above. Especially the adamantane group has been extensively used a guest molecule for complexation with CD. For example, a thermo-responsive hydrogel was described based on a combination of adamantyl end-functionalized PEG and star-shaped pNIPAAM comprising a β-CD core.[213] Van de Manakker *et al*. prepared hydrogels from a combination of two complementary 8-armed star-shaped PEGs,

either end-functionalized with β-CD or with cholesterol.[214,215] The gel properties could be tuned via the polymer concentration, molar ratio of end groups, molecular weight, architecture of the PEG, temperature and addition of a competitive inclusion complexing agent. Degradation occurred via surface erosion, resulting in near zero-order release of the model proteins lysozyme, albumin and immunoglobulin G.[216] When 8-armed cholesterol-functionalized PEG was combined with free β-CD, hydrogels with improved mechanical properties were obtained.[217] Various other hydrogels based on CD inclusion complexes have been described and reviewed elsewhere.[218-220]

Only a few reports on metallohydrogels, in which the reversible bonds between macromonomers are based on metal-ligand coordination, have been published. The earliest examples were reported by Chujo *et al*., who prepared hydrogels based on bipyridine-functionalized poly(oxazoline) crosslinked by Co(II)[221] or Fe(III)[222] ions. The gels kept their integrity at ambient temperatures for several days, but dissolved rapidly upon temperature increase due to a shift from intermolecular coordination complexes to the entropically favoured intramolecular coordination complexes. Later PEG,[223] Pluronics[224] and PEG-PLA[225] end-functionalized with ligands such as terpyridine or bipyridine were employed as well to prepare hydrogels in the presence of transition metal ions such as Mn(II) and Ni(II). Recently, PEG-based hydrogels were synthesized via coordination between metal ions and bisphosphonate[226] or histidine groups.[227]

The self-assembly of natural building blocks such as peptides into ordered structures, mainly coiled coils or β-sheets, has also been employed for the preparation of hydrogels. Two approaches were used for the design of macromolecules that self-assemble into hydrogels: genetically engineered copolymers and hybrid systems composed of a synthetic polymer and a peptide or protein motif. In the first category, Tirrell *et al*. performed pioneering work on the self-assembly of genetically engineered triblock copolymers prepared from a random coil block flanked by 2 coiled-coil forming blocks.[228] Self-assembly into hydrogels resulted from the balance between oligomerization of the helical ends and swelling of the central water soluble segment. Temperature- and pH-sensitivity could be manipulated by altering the amino acid sequence in the coiled-coil domain.[229] Capello *et al*. prepared protein polymers composed of tandemly arranged silk-like blocks and elastin-like blocks.[230-232] The silk-like blocks form crystallizable hydrogen-bonded β-sheets, providing the hydrogels with thermal and chemical stability, whereas the elastin-like blocks decreased the crystallinity and increased the water solubility of the copolymers. Plasmid DNA delivered from a silk-elastin protein hydrogel showed up to 3 orders of magnitude higher transfection in a murine model of human breast cancer in comparison with

naked DNA.[233] Hydrogels prepared from poly(amino acid) diblock and triblock copolymers were investigated by Deming *et al*.[234] Block copolymers composed of poly(L-lysine) or poly(L-glutamic acid) as hydrophilic block and poly(L-leucine) or poly(L-valine) as the hydrophobic block formed hydrogels at concentrations as low as 0.25 wt %.

The first example of a hybrid hydrogel crosslinked via assembly of coiled coils was reported by the group of Kopecek. They used a HPMA copolymer backbone which was non-covalently crosslinked by a genetically engineered coiled coil protein motif.[235] A non-reversible temperature-induced hydrogel collapse was observed corresponding to the structural transition of the coiled-coil domains from an elongated helix to an unfolded state. It was shown that reversibility of the gel-sol transition can be achieved by crosslinking the HPMA with a pair of oppositely charged peptide grafts.[236] Recently, hydrogels from HPMA polymers with complementary β-sheet peptide grafts were explored for bone tissue engineering.[237] It was demonstrated that the hydrogels provide a support for pre-osteoblast cells and for the template-driven mineralization of hydroxyapatite. Hybrid hydrogels based on PEG coupled to coiled-coil (Figure 2.13)[238] or β-sheet[239] forming peptides were also reported.

A new development is the design of hydrogels capable of translating a specific stimulus, such as enzyme-substrate recognition,[240] into macroscopic motion. The field of self-assembling hybrid hydrogels was extensively reviewed by Kopecek in a recent publication.

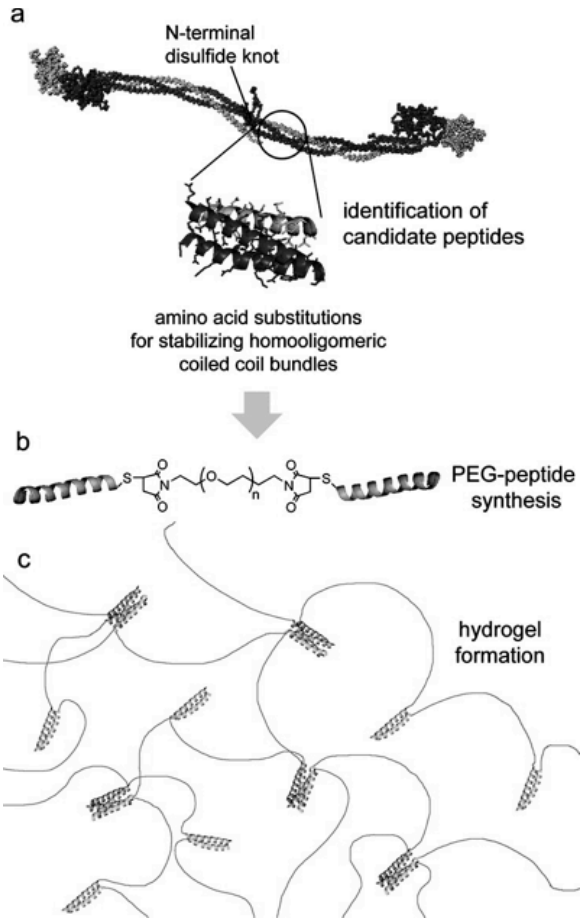

Figure 2.13. Strategy for the preparation of fibrin-inspired coiled-coil biomaterials. Short peptides from the coiled-coil domain of fibrin are identified (a). Substitutions are made to stabilize homo-oligomeric coiled-coil formation, and designed peptides are conjugated to short PEG chains to form triblock peptide-PEG-peptides (b). Triblock copolymers self-assemble in appropriate buffers to produce hydrogels (c). Reprinted with permission from [238]. Copyright (2008) American Chemical Society.

2.5 Smart hydrogels

With the increasing knowledge in organic chemistry, a variety of chemically crosslinked hydrogels has been developed. This section describes the use of smart hydrogels i.e. *in situ* formation of hydrogels through covalent crosslinking between polymers with complementary functional groups that occurs under physiological conditions with minimal toxicity. Additionally, double network hydrogels with a combination of physical, covalent or ionic bonds are described. Further, this section

discusses the design of multi-component hydrogels capable of responding to multiple triggers or forming mechanically strong hydrogels. Altogether, these smart hydrogels allow tailoring properties such as mechanical stability and release kinetics for the desired application.

2.5.1 In situ chemically crosslinkable hydrogels

Hydrogel formation can be catalyzed by enzymes such as horseradish peroxidase,[242] transglutaminase[243,244] and tyrosinase.[244] This class of hydrogels has mostly been applied for tissue engineering and as adhesive materials.[13] However, the use of enzymatic crosslinkable hydrogels is mainly limited by the stability of some enzymes. Hydrogels formed from polymers with complementary functional groups offer a great tunability in hydrogel properties, such as gelation kinetics and mechanical stability.[14,245] In contrast to small-molecule crosslinkers, toxicity of these systems is often limited. Especially polymers that can crosslink under physiological conditions are interesting for drug delivery applications. For example amine and aldehyde-functionalized hyaluronic acid precursors have been synthesized with different degrees of substitution.[246] Mixing of these two precursors in buffer resulted in the formation of a hydrogel. Other examples of chemical crosslinking reactions to form hydrogels include Passerini and Ugi condensation[247,248] and disulfide formation.[249] In 2002, our group published an extensive overview of different chemical crosslinking reactions for the formation of hydrogels.[14] Therefore, this section will focus only on the recent efforts in *in situ* forming hydrogels without the need of catalysts and hydrogel formation by chemoselective crosslinking strategies. Michael addition, a conjugation reaction between nucleophiles such as thiols and electrophilic olefins e.g. (meth) acrylates, has been widely applied for the formation of hydrogels. In 2001 the group of Hubbell described the formation of a hydrogel based on PEG-multiacrylate and PEG dithiol precursors.[250] Albumin was released from these hydrogels with zero-order kinetics and with a rate depending on the polymer concentration. Michael addition is particularly attractive as *in situ* chemical crosslinking method due to its relatively fast kinetics and reaction under physiological conditions without the need for catalysts. For example, PEG-dextran,[251] PEG-oligopeptide[252], PEG-PLA[253] and PEG-hyaluronic acid[254] hydrogels have been prepared using Michael-type addition. Recently, emphasis on controlled crosslinking of hydrogels *in situ* under physiological conditions, without toxic additives has resulted in the use of chemoselective crosslinking strategies for hydrogel formation. Chemoselective crosslinking has the benefit to not interfere with biomolecules such as proteins. The most researched chemoselective crosslinking reaction for hydrogels is click chemistry.[85,255,256] Click chemistry was first introduced by Sharpless and coworkers as new regiospecific linking reactions that give high yields and generally require no purification.[257] Among the different reactions, Cu(I)-catalyzed Huisgen 1,3-dipolar cycloaddition of

terminal alkynes and azides is the most investigated method.[258] Since click reactions can take place under physiological conditions with fast kinetics, it received great attention in pharmaceutical sciences.[256,258,259] The first hydrogel designed by click chemistry was formed based on poly(vinyl alcohol) and described by Hilborn *et al*.[260] Hydrogels crosslinked by click chemistry have for example been used for the release of doxorubicin and benzidamine using hyaluronic acid precursors.[261] However, alkyne-azide cycloadditions generally require the use of toxic catalysts, such as copper, limiting their application in the biomedical field. Recently, hydrogels have been crosslinked by copper-free click chemistry using strain promoted precursors, thereby eliminating the need of (metal-ion) catalysts.[262-264] As is shown in Figure 2.14, covalently crosslinked, degradable hyaluronic acid hydrogels were prepared using azide and cyclooctyne functionalized precursors.

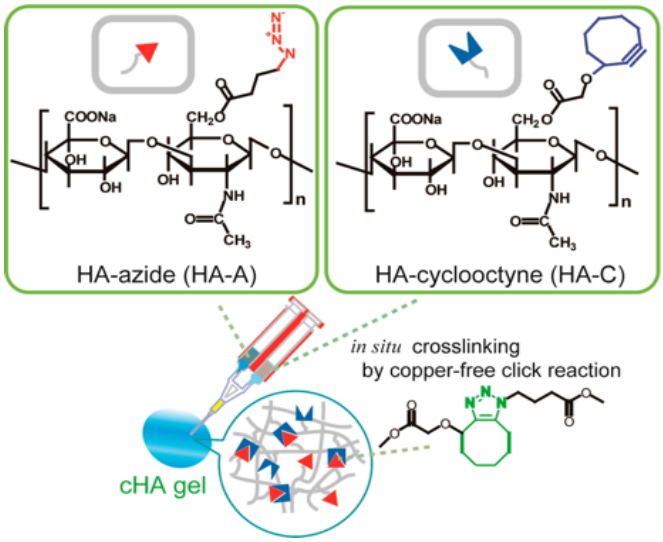

Figure 2.14. *In situ* copper-free click reaction using strain promoted hyaluronic acid precursors. Reprinted with permission from [264]. Copyright (2013) American Chemical Society.

More recently, native chemical ligation has been investigated as an alternative chemoselective crosslinking reaction for the formation of hydrogels.[86,265] In native chemical ligation an N-terminal cysteine and thioester react to form a native peptide bond. This reaction has mostly been applied for the synthesis of peptides and proteins.[266] Cells were successfully incorporated in these hydrogels and were capable of forming new extracellular matrix.[267,268] Using a related reaction mechanism, hydrogels were also formed by oxo-ester mediated native chemical ligation.[269] This reaction has the advantage to increase the reaction kinetics and capture thiol reaction products, resulting in increased cell viability.

2.5.2 Radical polymerization

Macromers containing methacrylate or acrylate moieties can be crosslinked via radical polymerization using potassium persulfate (KPS) and N,N,N′,N′-tetramethylethylenediamine (TEMED) as initiator and catalyst respectively. Hydrogels formed by a redox reaction with TEMED/KPS were first described by Saito *et al*. in 1990.[270,271] Our group prepared dextran-hydroxy-ethyl-methacrylate (dex-HEMA) hydrogels using this redox reaction, where the mechanical properties could be tuned depending on KPS concentration and temperature.[272] Further, controlled release of lysozyme, albumin and IgG from these hydrogels was demonstrated.[273] Similarly, our group described the formation of hydrogels from methacrylated hyaluronic acid.[274] A high control over degree of methacrylation allowed the design of hydrogels with a variety of mechanical properties. Kasper *et al*. reported about the APS/TEMED mediated crosslinking of oligo(poly(ethylene glycol)fumarate) (OPF) hydrogels for the controlled release of plasmid DNA, with a release rate depending on the OPF molecular weight.[275] Recently, hydrogels formed by radical polymerization of poly(*N*-isopropylacrylamide) and *N*,*N*-methylenebisacrylamide have been designed containing bridged nanogels and consequently showing surprisingly high elasticity and mechanical resistance.[276] However, unreacted persulfate and TEMED, including their degradation products, can oxidize and thereby damage encapsulated proteins. Therefore, only after complete removal of these compounds, the hydrogels can be used for biomedical applications.[277]

In a different approach, network formation between (meth)acrylate functionalized polymers can occur in the presence of UV or visible light.[278,279] The photopolymerization reaction is initiated by decomposition of a photoinitiator, resulting in the formation of radicals and subsequent network formation. The formation of a hydrogel through photopolymerization has been first described by Hubbell *et al*. in 1993 and the formed gels released BSA for two months.[280] Later, they described the release of several other proteins and oligonucleotides from these acrylate-modified PEG-oligo-(α-hydroxy acids) hydrogels.[281]

Due to the relative ease of introducing (meth)acrylate functionalities to polymer precursors, recently a variety of natural polymers has been chemically crosslinked after photopolymerization. A multi-component hydrogel consisting of photo-curable gelatin, hyaluronic acid and chondroitin showed capable of facilitating the production of extracellular matrix for cartilage regeneration.[282]

Photo-curing hydrogels have several advantages over other *in situ* forming materials. The network formation is fast and the illumination allows a high spatiotemporal control.[278] Additionally, precise illumination can allow the formation of patterned hydrogels and non-uniform concentration profiles, resulting in different drug release profiles. This was demonstrated by Lu *et al*. with the release of an organic dye from crosslinked poly(2-hydroxyethyl methacrylate) (poly(HEMA)) hydrogels.[283,284] Some

drawbacks of photopolymerization are the need for an external light source, possible reaction with embedded compounds and the potential harmful effects of UV light on stability of embedded cells and proteins. Although several groups have shown the compatibility with e.g. fibroblasts[285], radish peroxidase[286] and stem cells,[287] the use of UV-light in the presence of biomolecules, cells or tissues remains a controversial topic.

2.5.3 Double-network hydrogels

Since the mechanical properties of hydrogels formed from solely physical interactions are usually too weak, this especially hampers their applications where mechanical stability is a requirement, such as in load-bearing tissues.[288] On the other hand, *in situ* chemically crosslinkable hydrogels have generally slow gelation kinetics, possibly resulting in early dissolution of the hydrogel. The first hydrogels responding to more than one trigger were prepared by combining pH and temperature induced gelation. Hoffman *et al*. reported in 1992 about the design of such a hydrogel for the release of amylase.[289] Hydrogels responding to both pH and temperature are generally prepared from copolymers with pH responsive moieties such as *N*,*N*'-diethylaminopropyl methacrylamide or acrylic acid and temperature responsive moieties such as NIPAAm. These hydrogels have been studied e.g. for delivery of insulin,[290,291] coenzyme A[292] and indomethacin.[293] Hydrogels can also be built from combined ionically and covalently crosslinked networks to yield so-called interpenetrating networks, which show tremendous synergistic effects on different properties.[294,295] Importantly, combining physical and chemical crosslinking allows the administration of polymers as liquid formulations that undergo quick gelation due to physical interactions triggered by e.g. temperature and that are subsequently stabilized by chemical reactions. As discussed earlier, the most common post-processing reactions are based on reactions between complementary functional groups or covalent crosslinking by radical polymerization.[14] In combination with thermosensitive polymers, dual gelling hydrogels have for example been designed from thiol and vinyl functionalized pNIPAAm [296] and a combination of hyaluronic acid and pluronic.[297] The gelation kinetics and the resulting properties of the hydrogel are mostly affected by the type of functional groups and the stoichiometry of the two components.[252] P(NIPAAm-co-HEMA) macromers with either alkyne or azide functionalities were *in situ* stabilized by click chemistry.[298] Dual physically and chemically gelling hydrogels have also been formed from thermoresponsive pNIPAAm macromers with epoxy functionalities *in situ* crosslinked with polyamidoamines (PAMAM).[299] As is shown in Figure 2.15, the introduction of this chemical crosslinker significantly increased the swelling of these hydrogels.

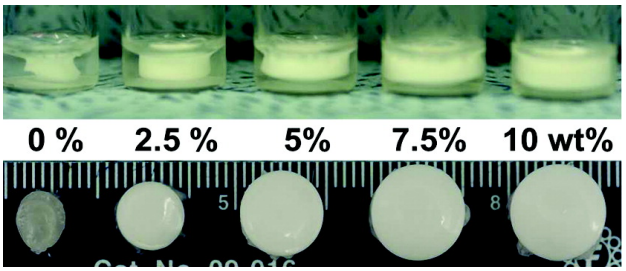

Figure 2.15. Swelling of thermoresponsive, chemically crosslinking hydrogels. Increasing the PAMAM crosslinker content resulted in an increased hydrogel swelling. Reprinted with permission from [299]. Copyright (2012) American Chemical Society.

Furthermore, swelling behavior and compressive mechanical properties of these hydrogels could be tuned depending on the PAMAM crosslinker length, amine/epoxy ratio, preparation time and polymer concentration.[300] Copolymerization with the hydrolysable monomer dimethyl-γ-butyrolactone acrylate (DBA) resulted in the formation of a bioresorbable hydrogel.[301]

In a similar approach, temperature sensitive polymers were combined with supramolecular inclusion complexation between a star-shaped adamantyl-terminated 8-arm PEG and a star-shaped PNIPAAm with a beta-cyclodextrin core (Figure 2.16).[302]

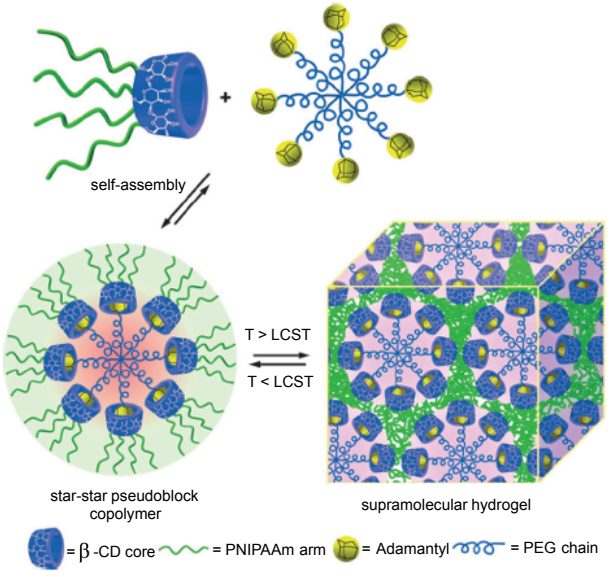

Figure 2.16. Combined inclusion complexation and thermogelation in aqueous solution of a star-star shaped copolymer. Reprinted from [302], copyright (2013), with permission from John Wiley & Sons, Inc.

Vermonden *et al*. reported about the design of a thermoresponsive hydrogel that was initially stabilized by physical crosslinks and further crosslinked after UV irradiation.[303] Release of lysozyme, BSA and IgG from these hydrogels was diffusion-controlled and depended on protein size and hydrogel molecular weight between the crosslinks.[304] The secondary structure and enzymatic activity of lysozyme was not affected during gelation. Interestingly, these hydrogels could also be deposited in defined three-dimensional structures using bioprinting technologies.[305] Additive manufacturing techniques offer the possibility to have high control over the scaffold architecture and the fabrication of multi-layered scaffolds. However, hydrogel-inks for 3D bioprinting need to fulfill many requirements with respect to processing parameters, which was recently reviewed by Malda *et al*.[306]

2.5.4 Combination of natural and synthetic polymers

In order to obtain materials that are both mechanically strong and bioactive, natural and synthetic polymers have been combined.[307,308] Hydrogels based on natural polymers include collagen, chitosan, fibrin, matrigel, agarose, alginate, hyaluronic acid, cellulose and gelatin.[6,309] Initially, non-chemically crosslinked blends of these polymers were formed, showing enhanced cell adhesion and high tunability over mechanical properties.[310-312] More recently, covalently crosslinked hybrid hydrogels consisting of natural and synthetic polymers have been designed by introduction of functional groups in both polymers. Censi *et al*. showed the *in situ* stabilization of thiolated hyaluronic acid and (meth)acrylated thermosensitive polymers by Michael addition reaction.[313] Further, these hydrogels facilitated the diffusion-controlled release of bradikynin. PNIPAAm based polymers with a hydrazide functionality have been *in situ* crosslinked with natural carbohydrate polymers such as hyaluronic acid, carboxymethyl cellulose, dextran and methylcellulose, resulting in the formation of a hydrazone bond.[314] Other examples of natural-synthetic hydrogels include combinations of gelatin methacrylamide and PEG,[315] fibrin and polyurethane[316] and PEG crosslinked with chitosan.[317]

2.5.5 Composite hydrogels

Incorporation of small inorganic molecules such as calcium phosphate and hydroxyapatite in hydrogels can both enhance the mechanical properties of the hydrogel and promote bioactivity e.g. mineralization for bone tissue engineering applications.[318-320] Ceramics-hydrogel composite materials have been studied for drug delivery in tissue engineering, having controlled scaffold porosity and therefore a tailored drug release.[321]

Hybrid and mechanically strong hydrogel constructs can also be formed by alternate deposition of thermoplastic polymer fibers and hydrogels.[322] A hydrogel-electronspun composite showed significantly decreased burst release of BSA from 20 to 7% due to

the incorporation of hydrophobic poly(ε-caprolactone)-based fiber mats.[323] Recently, an alginate hydrogel was reinforced with a 3D Ormocomp framework to protect embedded cells.[324] This hybrid hydrogel construct could increase the cell viability and successfully released dopamine.

Additionally, carbon nanotubes have been suggested to increase the mechanical properties of hydrogels and serve as a structural nanofiber. Single-walled carbon nanotubes were mixed with cyclodextrins to form a reversible gel through π-π interactions.[325] Carbon nanotubes combined with naturally-derived polymers such as gelatin increased the stability of the hydrogel at 37°C without covalent crosslinking.[326] Incorporation of only 2 wt% carbon nanotubes in hyaluronic acid hydrogels and subsequent crosslinking by divinyl sulfone resulted in a 3-fold higher dynamic modulus.[327] Additionally, incorporating pristine multi-walled carbon nanotubes in a polymethacrylic acid hydrogel allowed the triggered release of ^{14}C-sucrose after electrical stimulations.[328]

Incorporating degradable micro- or nanoparticles loaded with a drug in a hydrogel can further extend the possibilities for drug delivery. The drug can be released over a longer time frame, since it first has to leave the particle and subsequently has to diffuse out of the hydrogel matrix.[329] Additionally, these systems can enhance the solubility of hydrophobic drugs in the hydrogel matrix.[330] Finally, microparticles can shield the encapsulated content during hydrogel formation. For example, prednisone acetate has been loaded in poly(*N*-isopropylacrylamide)-*block*-poly(methyl methacrylate) (PNIPAAm-*b*-PMMA) micelles incorporated in a pNIPAAm hydrogel, resulting in a sustained release.[331] In a different hydrogel-microsphere composite, dexamethasone (DX) and vascular epithelial growth factor (VEGF) were either loaded directly in the hydrogel or in microspheres that were encapsulated in this hydrogel, showing a significant effect on the release kinetics.[332] When the drug was encapsulated in the microspheres, a prolonged release was achieved (Figure 2.17).

Composite hydrogels of oligo(poly(ethylene glycol)fumarate) with embedded gelatin microparticles have been developed by the groups of Tabata and Mikos.[333] When these microparticles were loaded with transforming growth factor-β1 (TGF-_1), release kinetics could be tailored from 13 to 170 pg TGF-b1/day for days 1-3 and from 7 to 47 pg TGF-b1/day for days 6-21.[334] In combination with encapsulated mesenchymal stem cells enhanced glycosaminoglycan production and an upregulation of cartilage-relevant genes was achieved *in vivo*, showing the potential of these systems for cartilage regeneration.[335] Additionally, these systems have been used for the simultaneous delivery of insulin-like growth factor-1 (IGF-1) and TGF-_1, either encapsulated in gelatin microparticles or directly in the OPF hydrogel, resulting in a high control over release kinetics.[336]

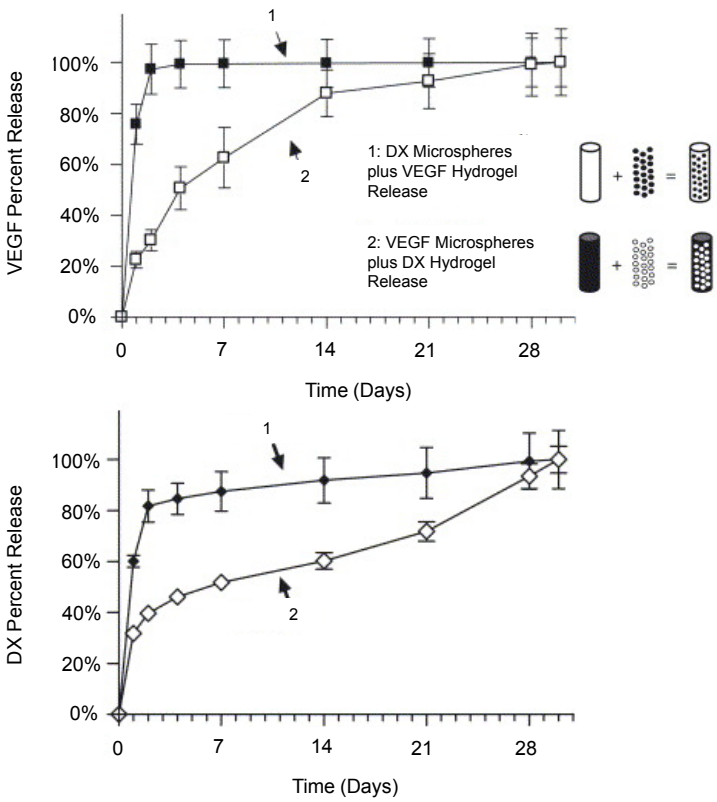

Figure 2.17. Release from microsphere/hydrogel composites prepared with loading DX or VEGF either directly in the hydrogel or embedded in the microspheres. Adapted from [332], copyright (2005), with permission from Elsevier.

2.6 Conclusion and Perspectives

This review describes the progress that has been made in the field of hydrogels for biomedical applications in the past 50 years, starting from the pioneering work of Wichterle and Lim in the 1960s. This historical overview underlines the tremendous development of hydrogels from simple chemically or physically crosslinked networks to complex double network composites. Although not covered in this review, the sophisticated level of these new materials is further reflected in new developments in e.g. shape memory and self-healing hydrogels.

Driven by the need for easy administration and patient convenience an increase in injectable hydrogel formulations has been reported. Stimuli-responsive materials, especially those that quickly respond under mild conditions, form an attractive approach for minimally invasive treatments. The immediate change from a low

viscous solution before injection and quick formation of a strong network *in situ*, requires careful selection of one or more appropriate crosslinkers. Possibilities to modulate release and degradation profiles after hydrogel administration can further improve the clinical translation of these hydrogels.

We further expect that an increasing knowledge in hybrid or composite hydrogel materials will allow controlled release of more sensitive drugs and several drugs from the same hydrogel matrix. Shielding biopharmaceutical drugs in micro- or nanoparticles can help to maintain their distinct three-dimensional structure. Synergistic hybrid materials fulfill many requirements that cannot be achieved with only one type of polymer. However, an increase in material complexity can also limit the chance of commercialization. Although many polymers have been investigated with high potential, an off-the-shelf hydrogel with highly tunable properties that can provide a platform for multiple applications and patient-specific treatment would be the most promising. Realizing the clinical requirements while limiting the complexity of the hydrogel formulation will therefore be the main goal for the coming decades.

References

1. N. A. Peppas and A. R. Khare, *Adv. Drug Delivery Rev.*, 1993, **11**, 1-35.
2. W. E. Roorda, H. E. Bodde, A. G. De Boer and H. E. Junginger, *Pharmaceutisch Weekblad - Scientific Edition*, 1986, **8**, 165-189.
3. J. I. Kroschwitz and H. F. Mark, *Encyclopedia of Polymer Science and Technology*, Wiley-Interscience, Hoboken, New Jersey, USA, 2003.
4. O. Wichterle and D. Lím, *Nature*, 1960, **185**, 117-118.
5. T. Kissel, Y. Li and F. Unger, *Adv. Drug Delivery Rev.*, 2002, **54**, 99-134.
6. A. S. Hoffman, *Adv. Drug Delivery Rev.*, 2002, **54**, 3-12.
7. T. Vermonden, R. Censi and W. E. Hennink, *Chem. Rev.*, 2012, **112**, 2853-2888.
8. R. Censi, P. Di Martino, T. Vermonden and W. E. Hennink, *J. Controlled Release*, 2012, **161**, 680-692.
9. S. R. Van Tomme, G. Storm and W. E. Hennink, *Int. J. Pharm.*, 2008, **355**, 1-18.
10. K. H. Bae, L. S. Wang and M. Kurisawa, *J. Mater. Chem. B*, 2013, **1**, 5371-5388.
11. J. A. Burdick and W. L. Murphy, *Nat. Commun.*, 2012, **3**.
12. S. Saraf, A. Alexander, Ajazuddin, J. Khan and S. Saraf, *J. Controlled Release*, 2013, **172**, 715-729.
13. L. S. Moreira Teixeira, J. Feijen, C. A. van Blitterswijk, P. J. Dijkstra and M. Karperien, *Biomaterials*, 2012, **33**, 1281-1290.
14. W. E. Hennink and C. F. van Nostrum, *Adv. Drug Delivery Rev.*, 2002, **54**, 13-36.
15. J. M. Van Bemmelen, *Z. anorg. Ch.*, 1894, **5**, S. 466.
16. J. Jokl, J. Kopeček and D. Lím, *Journal of Polymer Science Part A-1: Polymer Chemistry*, 1968, **6**, 3041-3048.
17. M. F. Refojo and H. Yasuda, *J. Appl. Polym. Sci.*, 1965, **9**, 2425.
18. A. Freeman and Y. Aharonowitz, *Biotechnol. Bioeng.*, 1981, **23**, 2747-2759.
19. G. P. Hicks and S. J. Updike, *Anal. Chem.*, 1966, **38**, 726-730.

20. H. Orbay, S. Ono, R. Ogawa and H. Hyakusoku, *Plast. Reconstr. Surg.*, 2011, **128**, 325-326.
21. O. Wichterle, *Encycl. Polym. Sci. Techn. Hydrogels 15 (1976) p. 273*.
22. M. Macret and G. Hild, *Polymer*, 1982, **23**, 748-753.
23. Q. Garrett, B. Laycock and R. W. Garrett, *Invest. Ophthalmol. Vis. Sci.*, 2000, **41**, 1687-1695.
24. J. H. O'Driscoll and A. A. Isen, US Pat. 3 700 761, 1972.
25. J. H. O'Driscoll and A. A. Isen, US Pat. 3816571, 1974.
26. B. J. Tighe, in *Hydrogels in Medicine and Pharmacy Volume III: Properties and Applications*, ed. N. A. Peppas, CRC press, Boca Raton, USA, 1987, p. 53.
27. Y.-C. Lai, *J. Polym. Sci., Part A: Polym. Chem.*, 1997, **35**, 1039-1046.
28. K. Dusek, US Patent 3948841, 1976.
29. K. Tanaka, T. Mio and T. Tanaka, US Patent 3813447, 1974.
30. S. Loshaek, US Patent 4028295, 1977.
31. P. C. Nicolson and J. Vogt, *Biomaterials*, 2001, **22**, 3273-3283.
32. J. H. Teichroeb, J. A. Forrest, L. W. Jones, J. Chan and K. Dalton, *J. Colloid Interface Sci.*, 2008, **325**, 157-164.
33. B. D. Ratner and A. S. Hoffman, in *Hydrogels for medical and related applications, ACS Symposium Series 31*, ed. J. D. Andrade, American Chemical Society, Washington, 1976, p. 1.
34. D. G. Pedley, P. J. Skelly and B. J. Tighe, *British Polymer Journal*, 1980, **12**, 99-110.
35. H. R. Oxley, P. H. Corkhill, J. H. Fitton and B. J. Tighe, *Biomaterials*, 1993, **14**, 1064-1072.
36. R. A. Haldon and B. E. Lee, *British Polymer Journal*, 1972, **4**, 491-501.
37. S. M. Murphy, P. J. Skelly and B. J. Tighe, *J. Mater. Chem.*, 1992, **2**, 1007-1013.
38. W. E. Roorda, M. A. De Vries, L. G. J. De Leede, A. G. De Boer, D. D. Breimer and H. E. Junginger, *J. Controlled Release*, 1988, **7**, 45-52.
39. S. Z. Song, J. R. Cardinal, S. H. Kim and S. W. Kim, *J. Pharm. Sci.*, 1981, **70**, 216-219.
40. L. Yean, C. Bunel and J.-P. Vairon, *Die Makromolekulare Chemie*, 1990, **191**, 1119-1129.
41. K. D. Colter, A. T. Bell and M. Shen, *Biomater. Med. Devices Artif. Organs*, 1977, **5**, 1-12.
42. M. B. Huglin and D. J. Sloan, *British Polymer Journal*, 1983, **15**, 165-171.
43. P. Andrade-Vivero, E. Fernandez-Gabriel, C. Alvarez-Lorenzo and A. Concheiro, *J. Pharm. Sci.*, 2007, **96**, 802-813.
44. R. M. Trigo, M. D. Blanco, J. M. Teijon and R. Sastre, *Biomaterials*, 1994, **15**, 1181-1186.
45. E. Brynda, N. A. Cepalova and M. Stol, *J. Biomed. Mater. Res.*, 1984, **18**, 685-694.
46. H. Tanzawa, Y. Mori, N. Harumiya, H. Miyama and M. Hori, *Trans. Am. Soc. Artif. Intern. Organs*, 1973, **19**, 188-194.
47. J. S. Calnan, J. J. Pflug, A. S. Chhabra and N. Raghupati, *Br. J. Plast. Surg.*, 1971, **24**, 113-124.
48. Z. Voldrich, Z. Tomanek, J. Vacik and J. Kopecek, *J. Biomed. Mater. Res.*, 1975, **9**, 675-685.
49. N. A. Peppas, H. J. Moynihan and L. M. Lucht, *J. Biomed. Mater. Res.*, 1985, **19**, 397-411.
50. M. F. Refojo and F. L. Leong, *J. Membr. Sci.*, 1979, **4**, 415-426.
51. M. F. Refojo, *J. Appl. Polym. Sci.*, 1965, **9**, 3417-3426.
52. M. F. Refojo and F.-L. Leong, *Journal of Polymer Science: Polymer Symposia*, 1979, **66**, 227-237.
53. B. D. Ratner and I. F. Miller, *J. Biomed. Mater. Res.*, 1973, **7**, 353-367.
54. M. K. Lindeman, in *Encyclopedia of Polymer Science and Technology*, eds. H. F. Mark and N. G. Gaylord, Interscience, New York, 1971, vol. 14th edition, p. 149.
55. N. A. Peppas and R. E. Benner Jr, *Biomaterials*, 1980, **1**, 158-162.
56. J. Ruiz, A. Mantecón and V. Cádiz, *J. Appl. Polym. Sci.*, 2001, **81**, 1444-1450.

57. V. Giménez, A. Mantecón and V. Cádiz, *J. Polym. Sci., Part A: Polym. Chem.*, 1996, **34**, 925-934.
58. J. E. Gough, C. A. Scotchford and S. Downes, *J. Biomed. Mater. Res.*, 2002, **61**, 121-130.
59. A. Danno, *J. Phys. Soc. Jpn.*, 1958, **13**, 722-727.
60. Y. Ikada, T. Mita, F. Horii, I. Sakurada and M. Hatada, *Radiat. Phys. Chem.*, 1977, **9**, 633-645.
61. J. M. Rosiak and P. Ulański, *Radiat. Phys. Chem.*, 1999, **55**, 139-151.
62. N. A. Peppas and E. W. Merrill, *J. Appl. Polym. Sci.*, 1977, **21**, 1763-1770.
63. N. A. Peppas and E. W. Merrill, *J. Biomed. Mater. Res.*, 1977, **11**, 423-434.
64. N. A. Peppas, *Die Makromolekulare Chemie*, 1975, **176**, 3433-3440.
65. M. M. Kukharchik and N. K. Baramboim, *Vysokomolekul. Soedin.*, 1972, **14B**, 843.
66. V. I. Lozinsky and F. M. Plieva, *Enzyme Microb. Technol.*, 1998, **23**, 227-242.
67. M. F. A. Goosen, M. V. Sefton and M. W. C. Hatton, *Thromb. Res.*, 1980, **20**, 543-554.
68. R. W. Korsmeyer and N. A. Peppas, *J. Membr. Sci.*, 1981, **9**, 211-227.
69. H. B. Hopfenberg, A. Apicella and D. E. Saleeby, *J. Membr. Sci.*, 1981, **8**, 273-282.
70. R. W. Korsmeyer, R. Gurny, E. Doelker, P. Buri and N. A. Peppas, *Int. J. Pharm.*, 1983, **15**, 25-35.
71. K. Burczak, T. Fujisato, M. Hatada and Y. Ikada, *Biomaterials*, 1994, **15**, 231-238.
72. C. T. Reinhart and N. A. Peppas, *J. Membr. Sci.*, 1984, **18**, 227-239.
73. J. Zhu, *Biomaterials*, 2010, **31**, 4639-4656.
74. J. M. Harris, *Poly(ethylene glycol) Chemistry: Biotechnical and Biomedical Applications p. 1-14*, Plenum Press, New York, 1992.
75. P. A. King and J. A. Ward, *J. Polym. Sci., Part A: Polym. Chem.*, 1970, **8**, 253-262.
76. J. W. Stafford, *Die Makromolekulare Chemie*, 1970, **134**, 57-69.
77. J. L. Stringer and N. A. Peppas, *J. Controlled Release*, 1996, **42**, 195-202.
78. P. Kofinas, V. Athanassiou and E. W. Merrill, *Biomaterials*, 1996, **17**, 1547-1550.
79. P. Rempp, P. Lutz, C. Sadron and E. W. Merrill.
80. T. Fujimura and I. Kaetsu, *Zeitschrift fur Naturforschung. Section C: Biosciences*, 1982, **37**, 102-106.
81. A. Tanaka, S. Yasuhara, M. Osumi and S. Fukui, *Eur. J. Biochem.*, 1977, **80**, 193-197.
82. N. B. Graham and M. E. McNeil, *Biomaterials*, 1984, **5**, 27-36.
83. T. Sakai, T. Matsunaga, Y. Yamamoto, C. Ito, R. Yoshida, S. Suzuki, N. Sasaki, M. Shibayama and U. I. Chung, *Macromolecules*, 2008, **41**, 5379-5384.
84. A. Metters and J. Hubbell, *Biomacromolecules*, 2005, **6**, 290-301.
85. M. Malkoch, R. Vestberg, N. Gupta, L. Mespouille, P. Dubois, A. F. Mason, J. L. Hedrick, Q. Liao, C. W. Frank, K. Kingsbury and C. J. Hawker, *Chem. Commun.*, 2006, DOI: 10.1039/B603438A, 2774-2776.
86. B.-H. Hu, J. Su and P. B. Messersmith, *Biomacromolecules*, 2009, **10**, 2194-2200.
87. M. Ehrbar, S. C. Rizzi, R. Hlushchuk, V. Djonov, A. H. Zisch, J. A. Hubbell, F. E. Weber and M. P. Lutolf, *Biomaterials*, 2007, **28**, 3856-3866.
88. K. L. Smith, A. E. Winslow and D. E. Petersen, *Ind. Eng. Chem.*, 1959, **51**, 1361-1364.
89. E. G. Tombropoulos, W. J. Bair and J. F. Park, *Nature*, 1963, **198**, 703-704.
90. M. E. McNeill and N. B. Graham, *J. Controlled Release*, 1984, **1**, 99-117.
91. N. B. Graham, M. Zulfiqar, B. B. MacDonald and M. E. McNeill, *J. Controlled Release*, 1988, **5**, 243-252.
92. D. A. Edelman, S. L. McIntyre and J. Harper, *Am. J. Obstet. Gynecol.*, 1984, **150**, 869-876.
93. S. H. Mandy, *J. Dermatol. Surg. Oncol.*, 1983, **9**, 153-155.
94. H. E. Huber, L. B. Dale and G. L. Christenson, *J. Pharm. Sci.*, 1966, **55**, 974-976.
95. J. L. Ford, M. H. Rubinstein, F. McCaul, J. E. Hogan and P. J. Edgar, *Int. J. Pharm.*, 1987, **40**, 223-234.

96. J. L. Ford, M. H. Rubinstein and J. E. Hogan, *Int. J. Pharm.*, 1985, **24**, 339-350.
97. W. Kuhn, B. Hargitay, A. Katchalsky and H. Eisenberg, *Nature*, 1950, **165**, 514-516.
98. I. Z. Steinberg, A. Oplatka and A. Katchalsky, *Nature*, 1966, **210**, 568-571.
99. J. Kopeček, *J. Polym. Sci., Part A: Polym. Chem.*, 2009, **47**, 5929-5946.
100. R. A. Siegel, *J. Controlled Release*, 2014, **190**, 337-351.
101. E. Ruel-Gariépy and J.-C. Leroux, *Eur. J. Pharm. Biopharm.*, 2004, **58**, 409-426.
102. M. A. Ward and T. K. Georgiou, *Polymers*, 2011, **3**, 1215-1242.
103. P. C. Chen-Chow and S. G. Frank, *Int. J. Pharm.*, 1981, **8**, 89-99.
104. R. M. Nalbandian, R. L. Henry and H. S. Wilks, *J. Biomed. Mater. Res.*, 1972, **6**, 583-590.
105. S. D. Desai and J. Blanchard, *J. Pharm. Sci.*, 1998, **87**, 226-230.
106. W. K. Bae, M. S. Park, J. H. Lee, J. E. Hwang, H. J. Shim, S. H. Cho, D. E. Kim, H. M. Ko, C. S. Cho, I. K. Park and I. J. Chung, *Biomaterials*, 2013, **34**, 1433-1441.
107. M. Katakam, W. R. Ravis and A. K. Banga, *J. Controlled Release*, 1997, **49**, 21-26.
108. S. W. Choi, S. Y. Choi, B. Jeong, S. W. Kim and D. S. Lee, *J. Polym. Sci., Part A: Polym. Chem.*, 1999, **37**, 2207-2218.
109. B. Jeong, D. S. Lee, J. I. Shon, Y. H. Bae and S. W. Kim, *J. Polym. Sci., Part A: Polym. Chem.*, 1999, **37**, 751-760.
110. B. Jeong, Y. H. Bae, D. S. Lee and S. W. Kim, *Nature*, 1997, **388**, 860-862.
111. C. Hiemstra, Z. Zhong, P. J. Dijkstra and J. Feijen, *Macromol. Symp.*, 2005, **224**, 119-131.
112. S. Li, I. Molina, M. Bueno Martinez and M. Vert, *J. Mater. Sci.: Mater. Med.*, 2002, **13**, 81-86.
113. J. Lee, Y. H. Bae, Y. S. Sohn and B. Jeong, *Biomacromolecules*, 2006, **7**, 1729-1734.
114. M. K. Joo, Y. S. Sohn and B. Jeong, *Macromolecules*, 2007, **40**, 5111-5115.
115. F. Li, S. Li and M. Vert, *Macromol. Biosci.*, 2005, **5**, 1125-1131.
116. S. Y. Park, B. R. Han, K. M. Na, D. K. Han and S. C. Kim, *Macromolecules*, 2003, **36**, 4115-4124.
117. I. W. Velthoen, J. Van Beek, P. J. Dijkstra and J. Feijen, *React. Funct. Polym.*, 2011, **71**, 245-253.
118. S. J. Buwalda, P. J. Dijkstra, L. Calucci, C. Forte and J. Feijen, *Biomacromolecules*, 2010, **11**, 224-232.
119. L. Calucci, C. Forte, S. J. Buwalda, P. J. Dijkstra and J. Feijen, *Langmuir*, 2010, **26**, 12890-12896.
120. C. Hiemstra, Z. Zhong, L. Li, P. J. Dijkstra and J. Feijen, *Biomacromolecules*, 2006, **7**, 2790-2795.
121. C. He, S. W. Kim and D. S. Lee, *J. Controlled Release*, 2008, **127**, 189-207.
122. B. Jeong, Y. H. Bae and S. W. Kim, *Macromolecules*, 1999, **32**, 7064-7069.
123. B. Jeong, Y. Han Bae and S. Wan Kim, *Colloids Surf. B. Biointerfaces*, 1999, **16**, 185-193.
124. B. Jeong, Y. K. Choi, Y. H. Bae, G. Zentner and S. W. Kim, *J. Controlled Release*, 1999, **62**, 109-114.
125. B. Jeong, Y. H. Bae and S. W. Kim, *J. Biomed. Mater. Res.*, 2000, **50**, 171-177.
126. B. Jeong, Y. H. Bae and S. W. Kim, *J. Controlled Release*, 2000, **63**, 155-163.
127. P. Y. Lee, Z. Li and L. Huang, *Pharm. Res.*, 2003, **20**, 1995-2000.
128. D. S. Lee, M. S. Shim, S. W. Kim, H. Lee, I. Park and T. Chang, *Macromol. Rapid Commun.*, 2001, **22**, 587-592.
129. M. S. Shim, H. T. Lee, W. S. Shim, I. Park, H. Lee, T. Chang, S. W. Kim and D. S. Lee, *J. Biomed. Mater. Res.*, 2002, **61**, 188-196.
130. G. M. Zentner, R. Rathi, C. Shih, J. C. McRea, M. H. Seo, H. Oh, B. G. Rhee, J. Mestecky, Z. Moldoveanu, M. Morgan and S. Weitman, *J. Controlled Release*, 2001, **72**, 203-215.
131. W. E. Samlowski, J. R. McGregor, M. Jurek, M. Baudys, G. M. Zentner and K. D. Fowers, *J. Immunother.*, 2006, **29**, 524-535.

132. K. Young Jin, S. Choi, K. Jae Joon, M. Lee, K. Kyung Soo and K. Sung Wan, *Pharm. Res.*, 2001, **18**, 548-550.
133. S. Chen and J. Singh, *Int. J. Pharm.*, 2005, **295**, 183-190.
134. M. J. Hwang, J. M. Suh, Y. H. Bae, S. W. Kim and B. Jeong, *Biomacromolecules*, 2005, **6**, 885-890.
135. S. J. Bae, J. M. Suh, Y. S. Sohn, Y. H. Bae, S. W. Kim and B. Jeong, *Macromolecules*, 2005, **38**, 5260-5265.
136. C. Gong, S. Shi, L. Wu, M. Gou, Q. Yin, Q. Guo, P. Dong, F. Zhang, F. Luo, X. Zhao, Y. Wei and Z. Qian, *Acta Biomater.*, 2009, **5**, 3358-3370.
137. A. Petit, B. Müller, R. Meijboom, P. Bruin, F. Van De Manakker, M. Versluijs-Helder, L. G. J. De Leede, A. Doornbos, M. Landin, W. E. Hennink and T. Vermonden, *Biomacromolecules*, 2013, **14**, 3172-3182.
138. A. Petit, B. Müller, P. Bruin, R. Meyboom, M. Piest, L. M. J. Kroon-Batenburg, L. G. J. De Leede, W. E. Hennink and T. Vermonden, *Acta Biomater.*, 2012, **8**, 4260-4267.
139. M. J. Sandker, A. Petit, E. M. Redout, M. Siebelt, B. Müller, P. Bruin, R. Meyboom, T. Vermonden, W. E. Hennink and H. Weinans, *Biomaterials*, 2013, **34**, 8002-8011.
140. Z. Zhong, P. J. Dijkstra, J. Feijen, Y. M. Kwon, Y. H. Bae and S. W. Kim, *Macromol. Chem. Phys.*, 2002, **203**, 1797-1803.
141. M. S. Kim, K. S. Seo, G. Khang, S. H. Cho and H. B. Lee, *J. Polym. Sci., Part A: Polym. Chem.*, 2004, **42**, 5784-5793.
142. E. Behravesh, A. K. Shung, S. Jo and A. G. Mikos, *Biomacromolecules*, 2002, **3**, 153-158.
143. S. Y. Kim, H. J. Kim, K. E. Lee, S. S. Han, Y. S. Sohn and B. Jeong, *Macromolecules*, 2007, **40**, 5519-5525.
144. H. G. Schild, *Prog. Polym. Sci.*, 1992, **17**, 163-249.
145. M. Heskins and J. E. Guillet, *Journal of Macromolecular Science: Part A - Chemistry*, 1968, **2**, 1441-1455.
146. J. Eliassaf, *J. Appl. Polym. Sci.*, 1978, **22**, 873-874.
147. K. Kubota, S. Fujishige and I. Ando, *Polym J*, 1990, **22**, 15-20.
148. S. Fujishige, K. Kubota and I. Ando, *The Journal of Physical Chemistry*, 1989, **93**, 3311-3313.
149. K. C. Tam, X. Y. Wu and R. H. Pelton, *Polymer*, 1992, **33**, 436-438.
150. X. S. Wu, A. S. Hoffman and P. Yager, *J. Polym. Sci., Part A: Polym. Chem.*, 1992, **30**, 2121-2129.
151. A. S. Huffman, A. Afrassiabi and L. C. Dong, *J. Controlled Release*, 1986, **4**, 213-222.
152. L.-C. Dong and A. S. Hoffman, *J. Controlled Release*, 1990, **13**, 21-31.
153. X.-Z. Zhang, D.-Q. Wu and C.-C. Chu, *Biomaterials*, 2004, **25**, 3793-3805.
154. H. Feil, Y. H. Bae, J. Feijen and S. W. Kim, *Macromolecules*, 1993, **26**, 2496-2500.
155. Z. Li and J. Guan, *Expert Opin. Drug Deliv.*, 2011, **8**, 991-1007.
156. C. Zhao, X. Zhuang, P. He, C. Xiao, C. He, J. Sun, X. Chen and X. Jing, *Polymer*, 2009, **50**, 4308-4316.
157. I. Ankareddi, M. M. Bailey, C. S. Brazel, J. F. Rasco and R. D. Hood, *Birth Defects Res. B: Dev. Reprod. Toxicol.*, 2008, **83**, 112-116.
158. D. Neradovic, W. L. J. Hinrichs, J. J. Kettenes-van den Bosch and W. E. Hennink, *Macromol. Rapid Commun.*, 1999, **20**, 577-581.
159. C. J. F. Rijcken, T. F. J. Veldhuis, A. Ramzi, J. D. Meeldijk, C. F. van Nostrum and W. E. Hennink, *Biomacromolecules*, 2005, **6**, 2343-2351.
160. D. Neradovic, C. F. van Nostrum and W. E. Hennink, *Macromolecules*, 2001, **34**, 7589-7591.
161. B. Rihova and K. Kubackova, *Curr. Pharm. Biotechnol.*, 2003, **4**, 311-322.
162. D. Neradovic, O. Soga, C. F. Van Nostrum and W. E. Hennink, *Biomaterials*, 2004, **25**, 2409-2418.

163. Z. Cui, B. H. Lee and B. L. Vernon, *Biomacromolecules*, 2007, **8**, 1280-1286.
164. T. Vermonden, N. A. M. Besseling, M. J. van Steenbergen and W. E. Hennink, *Langmuir*, 2006, **22**, 10180-10184.
165. T. Vermonden, S. S. Jena, D. Barriet, R. Censi, J. van der Gucht, W. E. Hennink and R. A. Siegel, *Macromolecules*, 2009, **43**, 782-789.
166. J.-F. Lutz and A. Hoth, *Macromolecules*, 2005, **39**, 893-896.
167. J.-F. Lutz, Ö. Akdemir and A. Hoth, *J. Am. Chem. Soc.*, 2006, **128**, 13046-13047.
168. T. Zhou, W. Wu and S. Zhou, *Polymer*, 2010, **51**, 3926-3933.
169. Y. Qiu and K. Park, *Adv. Drug Delivery Rev.*, 2012, **64, Supplement**, 49-60.
170. P. Gupta, K. Vermani and S. Garg, *Drug Discov. Today*, 2002, **7**, 569-579.
171. T. Miyata, T. Uragami and K. Nakamae, *Adv. Drug Delivery Rev.*, 2002, **54**, 79-98.
172. K. Ishihara, M. Kobayashi, N. Ishimaru and I. Shinohara, *Polym J*, 1984, **16**, 625-631.
173. C. M. Hassan, F. J. Doyle and N. A. Peppas, *Macromolecules*, 1997, **30**, 6166-6173.
174. J. Slager and A. J. Domb, *Adv. Drug Delivery Rev.*, 2003, **55**, 549-583.
175. L. Pauling and R. B. Corey, *Proceedings of the National Academy of Sciences*, 1953, **39**, 253-256.
176. Y. Ikada, K. Jamshidi, H. Tsuji and S. H. Hyon, *Macromolecules*, 1987, **20**, 904-906.
177. K. Fukushima and Y. Kimura, *Polym. Int.*, 2006, **55**, 626-642.
178. H. Tsuji, *Macromol. Biosci.*, 2005, **5**, 569-597.
179. S. J. de Jong, W. N. E. van Dijk-Wolthuis, J. J. Kettenes-van den Bosch, P. J. W. Schuyl and W. E. Hennink, *Macromolecules*, 1998, **31**, 6397-6402.
180. T. Fujiwara, T. Mukose, T. Yamaoka, H. Yamane, S. Sakurai and Y. Kimura, *Macromol. Biosci.*, 2001, **1**, 204-208.
181. T. Mukose, T. Fujiwara, J. Nakano, I. Taniguchi, M. Miyamoto, Y. Kimura, I. Teraoka and C. W. Lee, *Macromol. Biosci.*, 2004, **4**, 361-367.
182. S. Li and M. Vert, *Macromolecules*, 2003, **36**, 8008-8014.
183. H. Nouailhas, A. El Ghzaoui, S. Li and J. Coudane, *J. Appl. Polym. Sci.*, 2011, **122**, 1599-1606.
184. S. Li, A. El Ghzaoui and E. Dewinck, *Macromol. Symp.*, 2005, **222**, 23-35.
185. D. W. Grijpma and J. Feijen, *J. Controlled Release*, 2001, **72**, 247-249.
186. Y. Zhang, X. Wu, Y. Han, F. Mo, Y. Duan and S. Li, *Int. J. Pharm.*, 2010, **386**, 15-22.
187. H. Nouailhas, F. Li, A. El Ghzaoui, S. Li and J. Coudane, *Polym. Int.*, 2010, **59**, 1077-1083.
188. C. Hiemstra, Z. Zhong, S. R. Van Tomme, M. J. van Steenbergen, J. J. L. Jacobs, W. D. Otter, W. E. Hennink and J. Feijen, *J. Controlled Release*, 2007, **119**, 320-327.
189. S. J. Buwalda, L. Calucci, C. Forte, P. J. Dijkstra and J. Feijen, *Polymer (United Kingdom)*, 2012, **53**, 2809-2817.
190. L. Calucci, C. Forte, S. J. Buwalda and P. J. Dijkstra, *Macromolecules*, 2011, **44**, 7288-7295.
191. K. Nagahama, K. Fujiura, S. Enami, T. Ouchi and Y. Ohya, *J. Polym. Sci., Part A: Polym. Chem.*, 2008, **46**, 6317-6332.
192. S. J. De Jong, S. C. De Smedt, M. W. C. Wahls, J. Demeester, J. J. Kettenes-van Den Bosch and W. E. Hennink, *Macromolecules*, 2000, **33**, 3680-3686.
193. S. J. De Jong, B. Van Eerdenbrugh, C. F. Van Nostrum, J. J. Kettenes-van den Bosch and W. E. Hennink, *J. Controlled Release*, 2001, **71**, 261-275.
194. G. W. Bos, J. J. L. Jacobs, J. W. Koten, S. Van Tomme, T. Veldhuis, C. F. Van Nostrum, W. Den Otter and W. E. Hennink, *Eur. J. Pharm. Sci.*, 2004, **21**, 561-567.
195. G. W. Bos, W. E. Hennink, L. A. Brouwer, W. Den Otter, T. F. J. Veldhuis, C. F. Van Nostrum and M. J. A. Van Luyn, *Biomaterials*, 2005, **26**, 3901-3909.
196. S. R. Van Tomme, A. Mens, C. F. van Nostrum and W. E. Hennink, *Biomacromolecules*, 2008, **9**, 158-165.

197. C. F. Van Nostrum, T. F. J. Veldhuis, G. W. Bos and W. E. Hennink, *Macromolecules*, 2004, **37**, 2113-2118.
198. D. W. Lim, S. H. Choi and T. G. Park, *Macromol. Rapid Commun.*, 2000, **21**, 464-471.
199. H. J. Chung, Y. Lee and T. G. Park, *J. Controlled Release*, 2008, **127**, 22-30.
200. K. Takami, J. Watanabe, M. Takai and K. Ishihara, *J. Biomater. Sci., Polym. Ed.*, 2011, **22**, 77-89.
201. A. Bertin, *Macromol. Chem. Phys.*, 2012, **213**, 2329-2352.
202. J. Li, A. Harada and M. Kamachi, *Polym. J.*, 1994, **26**, 1019-1026.
203. J. Li, X. Ni, Z. Zhou and K. W. Leong, *J. Am. Chem. Soc.*, 2003, **125**, 1788-1795.
204. W. Y. Kuo and H. M. Lai, *Polymer*, 2011, **52**, 3389-3395.
205. S. P. Zhao, L. M. Zhang and D. Ma, *J. Phys. Chem. B*, 2006, **110**, 12225-12229.
206. X. Li, J. Li and K. W. Leong, *Macromolecules*, 2003, **36**, 1209-1214.
207. J. Li, X. Li, X. Ni, X. Wang, H. Li and K. W. Leong, *Biomaterials*, 2006, **27**, 4132-4140.
208. K. M. Huh, T. Ooya, W. K. Lee, S. Sasaki, I. C. Kwon, S. Y. Jeong and N. Yui, *Macromolecules*, 2001, **34**, 8657-8662.
209. K. M. Huh, Y. W. Cho, H. Chung, I. C. Kwon, S. Y. Jeong, T. Ooya, W. K. Lee, S. Sasaki and N. Yui, *Macromol. Biosci.*, 2004, **4**, 92-99.
210. D. Ma, K. Tu and L. M. Zhang, *Biomacromolecules*, 2010, **11**, 2204-2212.
211. Y. Chen, X. H. Pang and C. M. Dong, *Adv. Funct. Mater.*, 2010, **20**, 579-586.
212. L. Zhou, J. Li, Q. Luo, J. Zhu, H. Zou, Y. Gao, L. Wang, J. Xu, Z. Dong and J. Liu, *Soft Matter*, 2013, **9**, 4635-4641.
213. Z. X. Zhang, X. Liu, F. J. Xu, X. J. Loh, E. T. Kang, K. G. Neon and J. Li, *Macromolecules*, 2008, **41**, 5967-5970.
214. F. Van de Manakker, M. Van der Pot, T. Vermonden, C. F. Van Nostrum and W. E. Hennink, *Macromolecules*, 2008, **41**, 1766-1773.
215. F. Van De Manakker, T. Vermonden, N. El Morabit, C. F. Van Nostrum and W. E. Hennink, *Langmuir*, 2008, **24**, 12559-12567.
216. F. D. Van Manakker, K. Braeckmans, N. E. Morabit, S. C. De Smedt, C. F. Van Nostrum and W. E. Hennink, *Adv. Funct. Mater.*, 2009, **19**, 2992-3001.
217. F. Van De Manakker, L. M. J. Kroon-Batenburg, T. Vermonden, C. F. Van Nostrum and W. E. Hennink, *Soft Matter*, 2009, **6**, 187-194.
218. K. L. Liu, Z. Zhang and J. Li, *Soft Matter*, 2011, **7**, 11290-11297.
219. F. Van De Manakker, T. Vermonden, C. F. Van Nostrum and W. E. Hennink, *Biomacromolecules*, 2009, **10**, 3157-3175.
220. J. Zhang and P. X. Ma, *Adv. Drug Delivery Rev.*, 2013, **65**, 1215-1233.
221. Y. Chujo, K. Sada and T. Saegusa, *Macromolecules*, 1993, **26**, 6320-6323.
222. Y. Chujo, K. Sada and T. Saegusa, *Macromolecules*, 1993, **26**, 6315-6319.
223. G. L. Fiore, J. L. Klinkenberg, A. Pfister and C. L. Fraser, *Biomacromolecules*, 2009, **10**, 128-133.
224. M. Chiper, S. Hoeppener, U. S. Schubert, C. A. Fustin and J. F. Gohy, *Macromol. Chem. Phys.*, 2010, **211**, 2323-2330.
225. S. J. Buwalda, P. J. Dijkstra and J. Feijen, *J. Polym. Sci., Part A: Polym. Chem.*, 2012, **50**, 1783-1791.
226. M. R. Nejadnik, X. Yang, T. Mimura, Z. T. Birgani, P. Habibovic, K. Itatani, J. A. Jansen, J. Hilborn, D. Ossipov, A. G. Mikos and S. C. G. Leeuwenburgh, *Macromol. Biosci.*, 2013, **13**, 1308-1313.
227. D. E. Fullenkamp, L. He, D. G. Barrett, W. R. Burghardt and P. B. Messersmith, *Macromolecules*, 2013, **46**, 1167-1174.
228. W. A. Petka, J. L. Harden, K. P. McGrath, D. Wirtz and D. A. Tirrell, *Science*, 1998, **281**, 389-392.
229. C. Xu, V. Breedveld and J. Kopecek, *Biomacromolecules*, 2005, **6**, 1739-1749.

230. A. A. Dinerman, J. Cappello, H. Ghandehari and S. W. Hoag, *Biomaterials*, 2002, **23**, 4203-4210.
231. H. Ghandehari and J. Cappello, *Pharm. Res.*, 1998, **15**, 813-815.
232. M. D. Golinska, M. K. Włodarczyk-Biegun, M. W. T. Werten, M. A. Cohen Stuart, F. A. de Wolf and R. De Vries, *Biomacromolecules*, 2014, DOI: 10.1021/bm401682n, Just accepted: DOI:10.1021/bm401682n.
233. Z. Megeed, M. Haider, D. Li, B. W. O'Malley Jr, J. Cappello and H. Ghandehari, *J. Controlled Release*, 2004, **94**, 433-445.
234. A. P. Nowak, V. Breedveld, L. Pakstis, B. Ozbas, D. J. Pine, D. Pochan and T. J. Deming, *Nature*, 2002, **417**, 424-428.
235. C. Wang, R. J. Stewart and J. Kopecek, *Nature*, 1999, **397**, 417-420.
236. J. Yang, C. Xu, C. Wang and J. Kopecek, *Biomacromolecules*, 2006, **7**, 1187-1195.
237. L. C. Wu, J. Yang and J. Kopeček, *Biomaterials*, 2011, **32**, 5341-5353.
238. P. Jing, J. S. Rudra, A. B. Herr and J. H. Collier, *Biomacromolecules*, 2008, **9**, 2438-2446.
239. I. W. Hamley, G. Cheng and V. Castelletto, *Macromol. Biosci.*, 2011, **11**, 1068-1078.
240. W. Yuan, J. Yang, P. Kopecková and J. Kopecek, *J. Am. Chem. Soc.*, 2008, **130**, 15760-15761.
241. J. i. Kopeček and J. Yang, *Angew. Chem. Int. Ed.*, 2012, **51**, 7396-7417.
242. M. Kurisawa, J. E. Chung, Y. Y. Yang, S. J. Gao and H. Uyama, *Chem. Commun.*, 2005, DOI: 10.1039/B506989K, 4312-4314.
243. B. H. Hu and P. B. Messersmith, *Orthod. Craniofac. Res.*, 2005, **8**, 145-149.
244. T. Chen, H. D. Embree, E. M. Brown, M. M. Taylor and G. F. Payne, *Biomaterials*, 2003, **24**, 2831-2841.
245. D. Y. Ko, U. P. Shinde, B. Yeon and B. Jeong, *Prog. Polym. Sci.*, 2013, **38**, 672-701.
246. P. Bulpitt and D. Aeschlimann, *J. Biomed. Mater. Res.*, 1999, **47**, 152-169.
247. A. E. de Nooy, G. Masci and V. Crescenzi, *Macromolecules*, 1999, **32**, 1318-1320.
248. H. Bu, A.-L. Kjøniksen, K. D. Knudsen and B. Nyström, *Biomacromolecules*, 2004, **5**, 1470-1479.
249. X. Z. Shu, Y. Liu, Y. Luo, M. C. Roberts and G. D. Prestwich, *Biomacromolecules*, 2002, **3**, 1304-1311.
250. D. L. Elbert, A. B. Pratt, M. P. Lutolf, S. Halstenberg and J. A. Hubbell, *J. Controlled Release*, 2001, **76**, 11-25.
251. C. Hiemstra, L. J. van der Aa, Z. Zhong, P. J. Dijkstra and J. Feijen, *Biomacromolecules*, 2007, **8**, 1548-1556.
252. M. P. Lutolf and J. A. Hubbell, *Biomacromolecules*, 2003, **4**, 713-722.
253. S. J. Buwalda, P. J. Dijkstra and J. Feijen, *Macromol. Chem. Phys.*, 2012, **213**, 766-775.
254. R. Jin, L. S. Moreira Teixeira, A. Krouwels, P. J. Dijkstra, C. A. van Blitterswijk, M. Karperien and J. Feijen, *Acta Biomater.*, 2010, **6**, 1968-1977.
255. D. Fournier, R. Hoogenboom and U. S. Schubert, *Chem. Soc. Rev.*, 2007, **36**, 1369-1380.
256. M. van Dijk, D. T. S. Rijkers, R. M. J. Liskamp, C. F. van Nostrum and W. E. Hennink, *Bioconjugate Chem.*, 2009, **20**, 2001-2016.
257. H. C. Kolb, M. G. Finn and K. B. Sharpless, *Angew. Chem. Int. Ed.*, 2001, **40**, 2004-2021.
258. C. D. Hein, X.-M. Liu and D. Wang, *Pharm. Res.*, 2008, **25**, 2216-2230.
259. J. E. Moses and A. D. Moorhouse, *Chem. Soc. Rev.*, 2007, **36**, 1249-1262.
260. D. A. Ossipov and J. Hilborn, *Macromolecules*, 2006, **39**, 1709-1718.
261. V. Crescenzi, L. Cornelio, C. Di Meo, S. Nardecchia and R. Lamanna, *Biomacromolecules*, 2007, **8**, 1844-1850.
262. J. Xu, T. M. Filion, F. Prifti and J. Song, *Chem. Asian J.*, 2011, **6**, 2730-2737.
263. C. R. Becer, R. Hoogenboom and U. S. Schubert, *Angew. Chem. Int. Ed.*, 2009, **48**, 4900-4908.

264. A. Takahashi, Y. Suzuki, T. Suhara, K. Omichi, A. Shimizu, K. Hasegawa, N. Kokudo, S. Ohta and T. Ito, *Biomacromolecules*, 2013, **14**, 3581-3588.
265. J. P. Jung, J. L. Jones, S. A. Cronier and J. H. Collier, *Biomaterials*, 2008, **29**, 2143-2151.
266. P. E. Dawson, T. W. Muir, I. Clark-Lewis and S. B. H. Kent, *Science*, 1994, **266**, 776-779.
267. J. Su, B.-H. Hu, W. L. Lowe Jr, D. B. Kaufman and P. B. Messersmith, *Biomaterials*, 2010, **31**, 308-314.
268. J. P. Jung, A. J. Sprangers, J. R. Byce, J. Su, J. M. Squirrell, P. B. Messersmith, K. W. Eliceiri and B. M. Ogle, *Biomacromolecules*, 2013, **14**, 3102-3111.
269. I. Strehin, D. Gourevitch, Y. Zhang, E. Heber-Katz and P. B. Messersmith, *Biomaterials Sci.*, 2013, **1**, 603-613.
270. K. Otake, H. Inomata, M. Konno and S. Saito, *Macromolecules*, 1990, **23**, 283-289.
271. H. Inomata, S. Goto and S. Saito, *Macromolecules*, 1990, **23**, 4887-4888.
272. J. T. Chung, K. D. F. Vlugt-Wensink, W. E. Hennink and Z. Zhang, *Int. J. Pharm.*, 2005, **288**, 51-61.
273. W. E. Hennink, O. Franssen, W. N. E. van Dijk-Wolthuis and H. Talsma, *J. Controlled Release*, 1997, **48**, 107-114.
274. M. H. M. Oudshoorn, R. Rissmann, J. A. Bouwstra and W. E. Hennink, *Polymer*, 2007, **48**, 1915-1920.
275. F. K. Kasper, S. K. Seidlits, A. Tang, R. S. Crowther, D. H. Carney, M. A. Barry and A. G. Mikos, *J. Controlled Release*, 2005, **104**, 521-539.
276. L.-W. Xia, R. Xie, X.-J. Ju, W. Wang, Q. Chen and L.-Y. Chu, *Nat Commun*, 2013, **4**.
277. C. J. De Groot, M. J. A. Van Luyn, W. N. E. Van Dijk-Wolthuis, J. A. Cadée, J. A. Plantinga, W. D. Otter and W. E. Hennink, *Biomaterials*, 2001, **22**, 1197-1203.
278. B. Baroli, *J. Chem. Technol. Biotechnol.*, 2006, **81**, 491-499.
279. K. T. Nguyen and J. L. West, *Biomaterials*, 2002, **23**, 4307-4314.
280. A. S. Sawhney, C. P. Pathak and J. A. Hubbell, *Macromolecules*, 1993, **26**, 581-587.
281. J. L. West and J. A. Hubbell, *Reactive Polymers*, 1995, **25**, 139-147.
282. P. A. Levett, F. P. W. Melchels, K. Schrobback, D. W. Hutmacher, J. Malda and T. J. Klein, *Acta Biomater.*, 2014, **10**, 214-223.
283. S. Lu, W. F. Ramirez and K. S. Anseth, *J. Pharm. Sci.*, 2000, **89**, 45-51.
284. S. Lu and K. S. Anseth, *J. Controlled Release*, 1999, **57**, 291-300.
285. S. J. Bryant, C. R. Nuttelman and K. S. Anseth, *J. Biomater. Sci., Polym. Ed.*, 2000, **11**, 439-457.
286. L. Pescosolido, S. Miatto, C. Di Meo, C. Cencetti, T. Coviello, F. Alhaique and P. Matricardi, *Eur. Biophys. J.*, 2010, **39**, 903-909.
287. N. E. Fedorovich, M. H. Oudshoorn, D. van Geemen, W. E. Hennink, J. Alblas and W. J. Dhert, *Biomaterials*, 2009, **30**, 344-353.
288. J. L. Drury and D. J. Mooney, *Biomaterials*, 2003, **24**, 4337-4351.
289. D. Liang-chang, Y. Qi and A. S. Hoffman, *J. Controlled Release*, 1992, **19**, 171-177.
290. T. G. Park, *Biomaterials*, 1999, **20**, 517-521.
291. K. Yong-Hee, B. You Han and K. Sung Wan, *J. Controlled Release*, 1994, **28**, 143-152.
292. B.-L. Guo and Q.-Y. Gao, *Carbohydr. Res.*, 2007, **342**, 2416-2422.
293. J. Shi, N. M. Alves and J. F. Mano, *Macromol. Biosci.*, 2006, **6**, 358-363.
294. J.-Y. Sun, X. Zhao, W. R. K. Illeperuma, O. Chaudhuri, K. H. Oh, D. J. Mooney, J. J. Vlassak and Z. Suo, *Nature*, 2012, **489**, 133-136.
295. P. Matricardi, C. Di Meo, T. Coviello, W. E. Hennink and F. Alhaique, *Adv. Drug Delivery Rev.*, 2013, **65**, 1172-1187.
296. Z.-C. Wang, X.-D. Xu, C.-S. Chen, L. Yun, J.-C. Song, X.-Z. Zhang and R.-X. Zhuo, *ACS Appl. Mater. Interfaces*, 2010, **2**, 1009-1018.
297. Y. Lee, H. J. Chung, S. Yeo, C.-H. Ahn, H. Lee, P. B. Messersmith and T. G. Park, *Soft Matter*, 2010, **6**, 977-983.

298. X.-D. Xu, C.-S. Chen, Z.-C. Wang, G.-R. Wang, S.-X. Cheng, X.-Z. Zhang and R.-X. Zhuo, *J. Polym. Sci., Part A: Polym. Chem.*, 2008, **46**, 5263-5277.
299. A. K. Ekenseair, K. W. M. Boere, S. N. Tzouanas, T. N. Vo, F. K. Kasper and A. G. Mikos, *Biomacromolecules*, 2012, **13**, 1908-1915.
300. A. K. Ekenseair, K. W. M. Boere, S. N. Tzouanas, T. N. Vo, F. K. Kasper and A. G. Mikos, *Biomacromolecules*, 2012, **13**, 2821-2830.
301. T. N. Vo, A. K. Ekenseair, F. K. Kasper and A. G. Mikos, *Biomacromolecules*, 2013, DOI: 10.1021/bm401413c.
302. Z.-X. Zhang, K. L. Liu and J. Li, *Angew. Chem. Int. Ed.*, 2013, **52**, 6180-6184.
303. T. Vermonden, N. E. Fedorovich, D. van Geemen, J. Alblas, C. F. van Nostrum, W. J. A. Dhert and W. E. Hennink, *Biomacromolecules*, 2008, **9**, 919-926.
304. R. Censi, T. Vermonden, M. J. van Steenbergen, H. Deschout, K. Braeckmans, S. C. De Smedt, C. F. van Nostrum, P. di Martino and W. E. Hennink, *J. Controlled Release*, 2009, **140**, 230-236.
305. R. Censi, W. Schuurman, J. Malda, G. di Dato, P. E. Burgisser, W. J. A. Dhert, C. F. van Nostrum, P. di Martino, T. Vermonden and W. E. Hennink, *Adv. Funct. Mater.*, 2011, **21**, 1833-1842.
306. J. Malda, J. Visser, F. P. Melchels, T. Jüngst, W. E. Hennink, W. J. A. Dhert, J. Groll and D. W. Hutmacher, *Adv. Mater.*, 2013, **25**, 5011-5028.
307. R. Langer and D. A. Tirrell, *Nature*, 2004, **428**, 487-492.
308. A. Sionkowska, *Prog. Polym. Sci.*, 2011, **36**, 1254-1276.
309. K. Y. Lee and D. J. Mooney, *Chem. Rev.*, 2001, **101**, 1869-1880.
310. M. G. Cascone, B. Sim and D. Sandra, *Biomaterials*, 1995, **16**, 569-574.
311. A. G. A. Coombes, E. Verderio, B. Shaw, X. Li, M. Griffin and S. Downes, *Biomaterials*, 2002, **23**, 2113-2118.
312. M. Santin, S. J. Huang, S. Iannace, L. Ambrosio, L. Nicolais and G. Peluso, *Biomaterials*, 1996, **17**, 1459-1467.
313. R. Censi, P. J. Fieten, P. di Martino, W. E. Hennink and T. Vermonden, *Macromolecules*, 2010, **43**, 5771-5778.
314. M. Patenaude and T. Hoare, *Biomacromolecules*, 2012, **13**, 369-378.
315. M. A. Daniele, A. A. Adams, J. Naciri, S. H. North and F. S. Ligler, *Biomaterials*, 2014, **35**, 1845-1856.
316. Y. Huang, B. Zhang, G. Xu and W. Hao, *Compos. Sci. Technol.*, 2013, **84**, 15-22.
317. H. Tan, H. Luan, Y. Hu and X. Hu, *Macromol. Res.*, 2013, **21**, 392-399.
318. Z. A. C. Schnepp, R. Gonzalez-McQuire and S. Mann, *Adv. Mater.*, 2006, **18**, 1869-1872.
319. S. C. G. Leeuwenburgh, J. A. Jansen and A. G. Mikos, *J. Biomater. Sci., Polym. Ed.*, 2007, **18**, 1547-1564.
320. K. Na, S. w. Kim, B. K. Sun, D. G. Woo, H. N. Yang, H. M. Chung and K. H. Park, *Biomaterials*, 2007, **28**, 2631-2637.
321. W. J. E. M. Habraken, J. G. C. Wolke and J. A. Jansen, *Adv. Drug Delivery Rev.*, 2007, **59**, 234-248.
322. W. Schuurman, V. Khristov, M. W. Pot, P. R. v. Weeren, W. J. A. Dhert and J. Malda, *Biofabrication*, 2011, **3**, 021001.
323. N. Han, J. Johnson, J. J. Lannutti and J. O. Winter, *J. Controlled Release*, 2012, **158**, 165-170.
324. K. S. Kang, S.-I. Lee, J. M. Hong, J. W. Lee, H. Y. Cho, J. H. Son, S. H. Paek and D.-W. Cho, *J. Controlled Release*, 2014, **175**, 10-16.
325. T. Ogoshi, Y. Takashima, H. Yamaguchi and A. Harada, *J. Am. Chem. Soc.*, 2007, **129**, 4878-4879.

326. H. Li, D. Q. Wang, H. L. Chen, B. L. Liu and L. Z. Gao, *Macromol. Biosci.*, 2003, **3**, 720-724.
327. S. Bhattacharyya, S. Guillot, H. Dabboue, J.-F. Tranchant and J.-P. Salvetat, *Biomacromolecules*, 2008, **9**, 505-509.
328. A. Servant, C. Bussy, K. Al-Jamal and K. Kostarelos, *J. Mater. Chem.*, 2013, **1**, 4593-4600.
329. X. Jia and K. L. Kiick, *Macromol. Biosci.*, 2009, **9**, 140-156.
330. M. Gou, X. Li, M. Dai, C. Gong, X. Wang, Y. Xie, H. Deng, L. Chen, X. Zhao, Z. Qian and Y. Wei, *International Journal of Pharmaceutics*, 2008, **359**, 228-233.
331. X.-D. Xu, H. Wei, X.-Z. Zhang, S.-X. Cheng and R.-X. Zhuo, *Journal of Biomedical Materials Research Part A*, 2007, **81A**, 418-426.
332. L. W. Norton, E. Tegnell, S. S. Toporek and W. M. Reichert, *Biomaterials*, 2005, **26**, 3285-3297.
333. S. Young, M. Wong, Y. Tabata and A. G. Mikos, *J. Controlled Release*, 2005, **109**, 256-274.
334. T. A. Holland, Y. Tabata and A. G. Mikos, *J. Controlled Release*, 2003, **91**, 299-313.
335. H. Park, J. S. Temenoff, Y. Tabata, A. I. Caplan and A. G. Mikos, *Biomaterials*, 2007, **28**, 3217-3227.
336. T. A. Holland, Y. Tabata and A. G. Mikos, *J. Controlled Release*, 2005, **101**, 111-125.

CHAPTER 3

THERMORESPONSIVE INJECTABLE HYDROGELS CROSS-LINKED BY NATIVE CHEMICAL LIGATION

K. W. M. Boere, B. G. Soliman, D. T. S. Rijkers, W. E. Hennink and T. Vermonden,
Macromolecules, 2014, **47**, 2430-2438

Abstract

In this study, temperature-induced physical gelation was combined with Native Chemical Ligation (NCL) as a chemical cross-linking mechanism, to yield rapid network formation and mechanically strong hydrogels. To this end, a novel monomer *N*-(2-hydroxypropyl)methacrylamide-cysteine (HPMA-Cys) was synthesized that copolymerizes with *N*-isopropylacrylamide (NIPAAm) to yield thermoresponsive polymers decorated with cysteine functionalities. Triblock copolymers consisting of a poly(ethylene glycol) (PEG) middle block, flanked by random blocks of NIPAAm and HPMA-Cys were successfully synthesized and characterized. Additionally, thioester cross-linkers were synthesized based on PEG and hyaluronic acid, respectively. Upon mixing the thermoresponsive polymer with PEG or hyaluronic acid cross-linker, cysteine and thioester functionalities react under physiological conditions to generate a native peptide bond. An immediate physical network was formed after elevation of the temperature to 37°C due to the self-assembly of the pNIPAAm chains. This network was stabilized in time by covalent cross-linking due to NCL reaction between thioester and cysteine functionalities, resulting in hydrogels with up to ten times higher storage moduli than without chemical cross-links. Finally, a collagen mimicking peptide sequence was successfully ligated to this hydrogel using the same reaction mechanism, showing the potential of this hydrogel for tissue engineering applications.

Graphical abstract

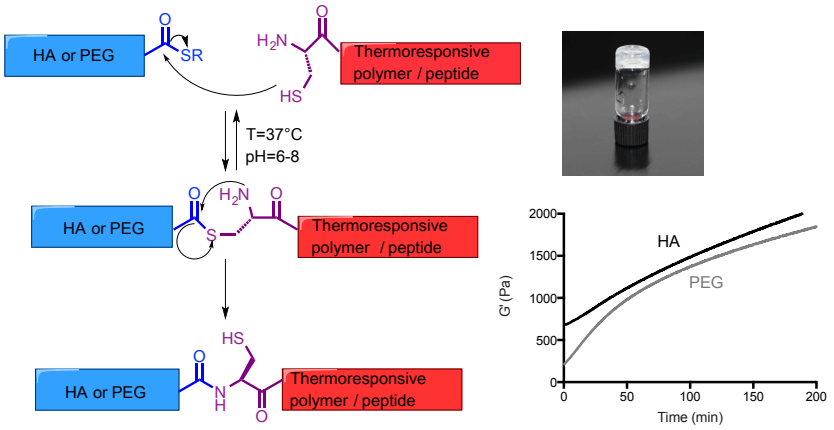

3.1 Introduction

Hydrogels have been extensively studied for drug delivery and tissue engineering applications.[1-5] Their high water content allows the incorporation of cells and/or biomolecules and the exchange of nutrients and metabolites.[6] In particular, *in situ* cross-linkable systems that can be injected as liquid formulations into the body are attractive for minimal invasive treatments.[7-9] Moreover, *in situ* forming hydrogels are able to fill irregularly shaped defect sites, resulting in close contact with the surrounding tissue. Thermosensitive systems are an important class of injectable systems since they can form hydrogels upon temperature changes.[10,11] When thermosensitive polymers pass their lower critical solution temperature (LCST), their polymer chains collapse and aggregate. Although several thermosensitive systems have been investigated, poly(*N*-isopropylacrylamide) (pNIPAAm) based materials are the most studied due to their sharp phase transition at 32°C.[10] However, networks held together by physical interactions only, form mechanically weak scaffolds resulting in fast erosion or degradation before new tissue is formed.[9] Another drawback of solely physical networks is the often-encountered syneresis of the hydrogel, resulting in an incomplete filling of the defect.[12] For these reasons, chemically cross-linkable systems have been developed that allow the formation of covalent bonds *in situ*.[13] Such a dual hardening hydrogel has the advantage of forming an immediate physical network at 37°C, followed by chemical cross-linking *in situ* to enhance the mechanical stability. The addition of thermogelation obviates the often-found problematic slow gelation kinetics of injectable systems due to slow chemical cross-linking. An attractive approach to combine physical and chemical gelation is a two-component system that can be mixed prior to injection. Such systems can be administered as liquid formulations that undergo gelation due to physical forces triggered by e.g. temperature and that are subsequently stabilized by chemical reactions between groups present of the hydrogel building blocks. It has been shown that the mechanical, degradation and swelling characteristics of these two-component hydrogels, can easily be tailored by changing the cross-linking density.[14] However, to develop a biocompatible *in situ* cross-linkable system without adverse side reactions remains a challenge. Frequently studied *in situ* cross-linking reactions, such as radical polymerization induced by UV irradiation[15], Michael addition[16,17], condensation reactions of aldehydes and amines[18], or ring opening of epoxides with amines[19], all have the disadvantage of either forming free radicals or having non-selective reactivity that can cause undesired side reactions with nucleophiles present in biomolecules such as proteins, possibly resulting in toxicity and inflammation.[20] Besides, addition reactions are typically carried out in organic solvents, since water can also react with the cross-linking agents. On the other hand, chemoselective reactions[21] like click chemistry[22-24] generally require

the use of toxic metal catalysts such as Cu^{+}/Cu^{++}. Attempts have been made to eliminate the use of these toxic catalysts for biomedical applications.[25,26] Recently, Hu *et al.*[27] developed an injectable hydrogel using native chemical ligation, a fast and chemoselective cross-linking method. In native chemical ligation, a thioester and an N-terminal cysteine undergo a reversible transthioesterification, whereafter an *N*-to-*S* rearrangement occurs, resulting in the irreversible formation of a native peptide bond.[28] Native chemical ligation has been widely used for the synthesis of peptides and biologically active proteins[29] and its reaction mechanism has been studied in detail.[30] However, only recently NCL has been applied for cross-linking hydrogels.[27] Apart from its chemoselective nature, another attractive feature of native chemical ligation is the possibility to covalently link other functionalities e.g bioactive peptides such as RGD to the polymer network. For tissue engineering, peptide-functionalized hydrogels have shown to promote their adhesion to body tissues as well as to enhance proliferation and differentiation of embedded cells.[31,32] Although native chemical ligation is normally applied using rather toxic catalytic thiols such as 4-mercaptophenylacetic acid (MPAA), or 2-mercaptoethanesulfonate (MESNa)[30], Hu *et al*. succeeded in preparing an injectable hydrogel without using such additives.[27] Furthermore, the group of Messersmith showed the compatibility of these hydrogels with extracellular matrix proteins and stem cells[33] and the use of oxo-ester mediated native chemical ligation, resulting in faster gelation kinetics and thiol capture.[34] However, the application of NCL hydrogels as injectable materials is limited by its relatively slow cross-linking kinetics.

The aim of this study is to develop a dual hardening *in situ* cross-linkable hydrogel formed by temperature-induced physical cross-linking and chemoselective cross-linking by native chemical ligation, without the addition of a catalyst. Combining thermogelation with native chemical ligation allows the formation of an immediate physical network that can be strengthened in time by chemical cross-links. For this aim, a triblock copolymer of pNIPAAm-co-HPMACys-PEG-pNIPAAm-co-HPMACys (PNC) was synthesized containing a newly designed monomer HPMA-Cysteine to introduce cysteine functionalities in a thermosensitive polymer. The methacrylamide group of this monomer allows copolymerization with other (meth) acryl-containing monomers using radical polymerization. As the second component, two different thioester cross-linkers were synthesized: a PEG difunctionalized thioester and a partially functionalized hyaluronic acid (HA) thioester. HA is a natural polysaccharide, present in many tissues in the human body and widely used in hydrogels for biomedical applications due to its favorable biological properties.[35,36] Finally, the PEG thioester was partially functionalized with a peptide using native chemical ligation. As a model peptide, a short discoidin domain receptor-2 (DDR-2) binding peptide (CGPRGQOGVMGFO) was chosen since it was suggested that this sequence positively affects mesenchymal stem cell differentiation, proliferation and

cell adhesion.[37-39] In this paper, we show the use of NCL as a chemoselective cross-linking reaction in combination with thermosensitive polymers as well as for the chemoselective ligation of peptides to hydrogels.

3.2 Materials and Methods

3.2.1 Materials

All commercial chemicals were obtained from Sigma-Aldrich (Zwijndrecht, the Netherlands) and used as received unless indicated otherwise. *N*-(2-Hydroxypropyl) methacrylamide (HPMA) was synthesized by reaction of methacryloyl chloride with 1-aminopropan-2-ol in dichloromethane, essentially according to Ulbrich.[40] Peptide grade dichloromethane (DCM) was obtained from Biosolve (Valkenswaard, the Netherlands). *N,N'*-Dimethyl amino pyridine (DMAP) was purchased from Fluka (Zwijndrecht, the Netherlands). Boc-*S*-acetamidomethyl-L-cysteine (Boc-Cys(Acm)-OH was purchased from Bachem (Bubendorf, Switzerland). PEG10,000-ABCPA macroinitiator was synthesized as described by Neradovic *et al*.[41] Ethylthioglycolate succinic acid (ET-SA) was prepared according to a literature procedure.[27] Tris-(2-carboxyethyl)-phosphine hydrochloride (TCEP) was obtained from Carl Roth (Karlsruhe, Germany). Hyaluronic acid (HA) with a molecular weight of 31 kDa was supplied by Lifecore (Chaska, MN, U.S.A.). 4-(Dimethylamino)pyridinium-4-toluenesulfonate (DPTS) was synthesized according to the method described by Moore *et al*.[42] 2,4,6-Trinitrobenzene sulfonic acid (TNBSA) and 5,5'-dithio-*bis*-(2-nitrobenzoic acid) (DTNB, Ellman's reagent) were obtained from Thermo Fischer Scientific (Rockford, IL, U.S.A.). DDR-2 peptide CGPRGQOGVMGFO (O = hydroxyproline) was supplied by GenScript (Piscataway, NJ, U.S.A). PBS buffer pH 7.4 (8.2 g/L NaCl, 3.1 g/L Na_2HPO_4 12 H_2O, 0.3 g/L NaH_2PO_4 2 H_2O) was purchased from B. Braun (Melsungen, Germany).

3.2.2 Synthesis of Boc-Cys(Acm)-HPMA

In a typical procedure, Boc-Cys(Acm)-OH (4.0 g, 13.7 mmol), HPMA (2.0 g, 13.7 mmol) and DMAP (167 mg, 1.37 mmol) were dissolved in dry DCM (10 mL). To this solution DCC (2.8 g, 13.7 mmol) was added and the reaction mixture was stirred for 16 h under a nitrogen atmosphere at room temperature. Subsequently, the suspension was cooled to 0°C, filtered and the filtrate was concentrated to 5 mL. The product was purified by silica gel chromatography, using DCM/MeOH (9:1 v/v) as eluent. The monomer Boc-Cys(Acm)-HPMA (HPMA-Cys) was obtained as a viscous oil (72% yield).

^{1}H NMR ($CDCl_3$): δ = 6.78 (s, 1H, N*H*), 6.61 (s, 1H, N*H*), 5.74 (s, 1H, H_2C=CH), 5.51 (s, 1H, $CH_2CH(CH_3)O$), 5.34 (s, 1H, H_2C=CH), 5.09 (s, 1H, N*H*), 4.39 (m, 3H, SCH_2NH, SCH_2CH), 3.65 (m, 1H, $CH_2CH(CH_3)$), 3.38 (m, 1H, $CH_2CH(CH_3)$), 2.96 (m, 2H, $CHCH_2S$), 2.02 (s, 3H, $COCH_3$), 1.96 (s, 3H, C=C(CH_3), 1.44 (s, 9H, $(CH_3)_3CO$), 1.28 (d, 3H, $OCHCH_3$) ^{13}C NMR ($CDCl_3$): δ = 170.8 (O-*C*(O)CH, 168.9 CH_3C=O, 155.8 O-*C*(O)-N, 139.7 CH_2=CH, 120.1 CH_2=CH, 80.5 $(CH_3)_3C$, 72.0 $CH_2CH(CH_3)O$, 54.2 SCH_2CH, 43.9 $CH_2CH(CH_3)O$, 41.6 SCH_2NH, 33.5 SCH_2CH, 28.3 $(CH_3)_3C$, 23.2 $CH_3C(O)NH$, 18.7 CH_3C=C, 17.5 $CH_2CH(CH_3)O$. R_t HPLC: 10.2 min.

3.2.3 Synthesis of PEG2000 thioester

In a typical reaction[43], ET-SA (880 mg, 4 mmol), DCC (824 mg, 4 mmol) and DPTS (59 mg, 0.4 mmol) were dissolved in dry DCM (5 mL). To this solution PEG 2000 (2 g, 2 mmol OH functionalities) was added and the obtained reaction mixture was stirred for 16 h at room temperature under a nitrogen atmosphere. Next, solid DCU was removed by filtration and the desired polymer was precipitated in cold diethyl ether. The precipitate was harvested by filtration, dissolved in 10 mL H_2O, dialyzed for two days (Mw cut-off: 2000 Da) against water at 4°C and the solution was subsequently lyophilized. A white powder was obtained in 92% yield, which was characterized by ^{1}H NMR. Degree of substitution (DS), defined as the percentage of hydroxyl groups derivatized by thioester moieties, was determined by ^{1}H NMR from the integral ratio of the methyl protons of the thioester functionalities at 1.3 ppm (I_{TE}) and the PEG protons between 3.2 and 4 ppm (I_{PEG}) using the following equation:

$$DS = \frac{I_{TE}/6}{I_{PEG}/182} \times 100\% \quad (3.1)$$

The degree of substitution (DS) was confirmed by adding two drops of trichloroacetyl isocyanate (TAIC) to the ^{1}H NMR sample. TAIC causes a shift to 4.42 ppm for the CH_2 protons of PEG adjacent to the OH end groups[44]. To calculate the DS, the peak integral at 4.42 ppm was divided by the PEG proton signals between 3.2 and 4.0 ppm.

A second approach to determine the DS was performed by hydrolyzing the PEG thioester in a 0.2 M NaOH solution for two hours under stirring. Quantification of free SH groups was performed using the Ellman's assay.[45]

^{1}H NMR ($CDCl_3$): δ = 4.42 (t, 2H, shift TAIC), 4.14 (q, 2H, CH_3CH_2O), 3.62 (182H, PEG protons), 3.13 (t, 2H, $SC(O)CH_2CH_2$), 2.89 (t, 2H, $SC(O)CH_2CH_2$), 1.21 (t, 3H, CH_3CH_2O).

3.2.4 Synthesis of HA thioester

Hyaluronic acid (Mw 31 kDa) was partially functionalized with ET-SA to introduce thioester functionalities at the primary hydroxyl groups, using EDCI as the coupling agent. In a typical procedure, HA (500 mg, 1.27 mmol primary OH groups), ET-SA (800 mg, 1.82 mmol) and EDCI (500 mg, 2.61 mmol) were dissolved in H_2O (10 mL). The solution was stirred at room temperature for 16 h, while maintaining the pH at 5 with 1N HCl. The HA thioester derivative was purified by dialysis (Mw cut-off: 12-14 kDa) against water for 4 days at 4°C and subsequently lyophilized. The degree of substitution (DS) was determined by hydrolyzing the HA thioester in a 0.2 M NaOH solution for 2 h under stirring and subsequent quantification of formed SH bonds using Ellman's reagent.

^{1}H NMR (D_2O): δ = 4.6-3.3 (protons of hyaluronic acid), 2.86 (s, CHCH_2O) 1.98 (s, CH_3CONH) 1.28 (t, CH_3CH_2O).

3.2.5 Synthesis of PEG-NIP-HPMA-Cys triblock copolymers

In a typical procedure, PEG-ABCPA 10,000 (0.23 g), Boc-Cys(Acm)-HPMA (0.31 g, 0.74 mmol) and NIPAAm (1.0 g 8.85 mmol, feed ratio Boc-Cys(Acm)-HPMA:NIPAAm 7:93) were dissolved in dry acetonitrile (10 mL) in an airtight screw-cap glass vial. The reaction mixture was flushed with nitrogen for 15 min and subsequently stirred for 40 h at 70°C. Next, the polymer was precipitated in cold diethyl ether (100 mL) and the precipitate was filtrated, washed with diethyl ether and dried. The synthesized polymer was obtained in a yield of 77%.

To remove the Boc groups of cysteine, the obtained triblock copolymer was dissolved in TFA/DCM (1:1 v/v, 10 mL) under a nitrogen atmosphere and stirred for two hours. The solvents were evaporated under reduced pressure and the residual solid was dissolved in water (10 mL). The triblock copolymer was purified by dialysis for two days at 4°C against water (Mw cut-off: 12-14 kDa) and lyophilized. To remove the acetamidomethyl (Acm) functionality, 1.0 g of polymer was dissolved in MeOH/H_2O (1:1 v/v, 40 mL) under N_2 atmosphere and 1N HCl (540 μL) was added, followed by the immediate addition of 0.2 M iodine in MeOH/H_2O (1:1 v/v/, 8mL). The obtained brownish mixture was stirred for one hour at room temperature. The excess iodine was quenched by addition of 4 drops of 1M ascorbic acid. The colorless solution was treated with tris-(2-carboxyethyl)-phosphine hydrochloride (TCEP, 500 mg) to reduce possibly formed disulfide bonds between cysteine moieties during 16 h and subsequently dialyzed against water for two days (Mw cut-off: 12-14 kDa). The final deprotected polymer was obtained after lyophilization as a white powder and characterized by GPC and ^{1}H NMR. The cysteine content was quantified by detection of free thiols by Ellman's method[45] and free primary amines were detected by TNBSA assay[46].

3.2.6 Ligation of peptide to PEG thioester

The PEG thioester construct (20 mg, 0.014 mmol thioester functionalities) was dissolved in PBS (400 _L). A 10-fold molar excess of sodium 2-sulfonylethane sulfonate (MESNa, 16 mg, 0.1 mmol) was added as catalyst. In a separate vial, the peptide CGPRGQOGVMGFO (14 or 7 mg for a cysteine : thioester ratio of 1:1 or 0.5:1 mol/mol respectively) was dissolved in PBS (100 μL), in the presence of TCEP (4 mg) to keep SH groups in their reduced form. These molar ratios were chosen to obtain a high degree of substitution (DS) and thereby enable characterization of the reaction products. Both solutions were mixed and allowed to react for 20 h at room temperature. After reaction, the mixture was dialyzed (Mw cut-off: 2000 Da) for two days and the obtained solution was subsequently lyophilized. The ligation product was analyzed by ^{1}H NMR and GPC. The degree of substitution was calculated by NMR from the integrals of the characteristic peptide peaks at δ= 0.8 and 7.2 ppm of valine and phenylalanine respectively. DS was confirmed by making use of the reduced intensity of the signal at δ= 1.2 ppm of the cleaved thioester after NCL reaction.

3.2.7 NMR spectroscopy

The obtained monomers and polymers were characterized on a Varian Mercury Plus 300 spectrometer. For ^{1}H NMR spectra, chemical shifts were referred to the residual solvent peak (δ = 7.26 ppm for $CDCl_3$, 4.79 for D_2O and 2.50 ppm for DMSO-d_6). For ^{13}C NMR spectra, the central line in the chloroform triplet at δ = 77.16 ppm was used as the reference line.

3.2.8 Gel Permeation Chromatography (GPC)

The molecular weights of the polymers were determined by GPC using a Plgel 5 μm MIXED-D column (Polymer Laboratories) with a column temperature of 65°C. DMF containing 10 mM LiCl was used as eluent with an elution rate of 1 mL/min, and the sample concentration was 5 mg/mL. Poly(ethylene glycols) of narrow and defined molecular weights were used as calibration standards. For the samples containing peptide, 10 mM TCEP was added to the GPC samples to keep SH groups in their reduced form.

3.2.9 Determination of Cloud Point

The cloud point (CP) of the polymers was measured with a Shimadzu UV/vis-2450 spectrophotometer. The polymers were dissolved at low and high concentrations of 0.3 wt% and 16 wt% in PBS (pH 7.4), respectively (SI-Figure 3.6). The heating rate was approximately 1°C/min and the absorbance was measured from 4 to 45 °C at 650 nm. The CP was defined as the onset of increasing scattering intensity.[41]

3.2.10 HPLC

Purity of the synthesized Boc-Cys(Acm)-HPMA monomer was analyzed by HPLC using a C18 sunfire column. The monomer was dissolved in H_2O/MeCN (9:1 v/v) at a concentration of 1 mg/mL. A mobile phase gradient, from 100% of eluent A (H_2O/MeCN 9:1 v/v) to 100% of B (MeCN) with a 20 min run time was used. The injection volume of the samples was 5 μL, the flow rate was 1 mL/min and absorbance was measured at λ=210 nm.

3.2.11 Hydrogel formation

Thermosensitive triblock copolymer PEG-NIP-HPMA-Cys (PNC), either protected or deprotected, was dissolved at a concentration of 20 wt% in PBS at 4°C for at least 5 h prior to hydrogel formation. PEG thioesters and HA thioesters were dissolved for 1 h at room temperature at a concentration of 15 wt% in the same solvent. For hydrogel formation, the appropriate thioester solution was added to the PNC solution, shortly mixed with a pipette tip and incubated at 37°C. NCL hydrogels were prepared at a final concentration of 16 wt% PNC and 11 wt% HA thioester or 4 wt% PEG thioester (corresponding to a 1:1 ratio of thioester:cysteine). For vial tilting experiments, hydrogel formation was reported after immobility for at least 15 minutes with vials upside down.

3.2.12 Rheological Characterization

Rheological analysis of hydrogels was performed on an AR-G2 rheometer (TA-Instruments), using a 20 mm steel cone (1°) geometry equipped with a solvent trap. For each measurement 70 μL of sample was used. Temperature sweeps of triblock copolymer solutions/gels were performed from 4 to 50°C at a heating rate of 1 °C / min. Cross-linking of the hydrogels in time was measured *in situ* for 3.5 h at 37°C. A 1% strain (within the linear viscosity region as is shown in SI-Figure 3.5) and a 1 Hz frequency were applied.

3.2.13 Dynamic Mechanical Analysis (DMA)

Elastic modulus measurements were performed on a DMA 2980 Dynamic Mechanical Analyzer (TA-Instruments). Hydrogels were formed from 16 wt% PNC and 4 wt% PEG thioester with or without peptide functionalization. The polymers were incubated at 37°C for 16 h before measuring. Hydrogels of approximately 3 × 4 mm (height × diameter) were placed between the parallel plates and a force ramp was applied at a rate of 0.1 N/min from 0.01 N to 0.1 N at 37°C. A Mann-Whitney-U test was used for comparing Young's moduli between two groups. Raw data were processed in Prism GraphPad Version 6.0 and $p<0.05$ was considered significant. Data are represented as means ± standard deviations.

3.2.14 TNBSA assay

Free primary amine groups of the synthesized triblock copolymer were quantified by reaction with 2,4,6-trinitrobenzene sulfonic acid (TNBSA).[46] Glycine standards were prepared at concentrations ranging from 0 to 0.15 mM in a 0.1 M sodium bicarbonate buffer (pH 8.5). The triblock copolymer was dissolved at a concentration of 0.5 mg/mL in the same buffer. Then, 0.25 mL of 0.01% (w/v) solution of TNBSA in buffer was added to 0.5 mL of polymer solution, and the samples were incubated at 37ºC for 2 h. Subsequently, 0.25 mL of 10% aq SDS and 0.125 mL of 1 N HCl were added to the solution and the absorbance was measured in triplicate at λ = 335 nm using a BMG Spectrostar nano wellplate reader.

3.2.15 Ellman's assay

Ellman's reaction was performed to detect free SH groups.[45] Cysteine hydrochloride monohydrate standards were prepared at concentrations ranging from 0 to 1.5 mM in a 0.1 M sodium phosphate buffer (pH 8.0) supplemented with 1 mM EDTA. The synthesized polymer was dissolved in a concentration of 2.5 mg/mL in the same buffer. The absorbance of the samples containing 50 μL Ellman's reagent (4 mg/mL), 2.5 mL buffer and 250 μL of each sample was measured in triplicate at λ= 412 nm using a BMG Spectrostar nano wellplate reader.

3.3 Results and Discussion

3.3.1 Boc-Cys(Acm)-HPMA synthesis

The monomer Boc-Cys(Acm)-HPMA (Figure 3.1) was synthesized via a DCC-mediated esterification between the hydroxyl functional group of HPMA and the carboxyl functional group of Boc-Cys(Acm)-OH, using DCC as coupling agent and DMAP as catalyst. Boc and Acm protecting groups were carefully chosen to design a monomer that could be copolymerized and subsequently deprotected without affecting the final polymer structure. The monomer was purified by column chromatography over silica gel using DCM/MeOH (9:1 v/v) as eluent and obtained in a yield of 72%. HPLC analysis based on UV detection confirmed a high purity of >96% (R_t= 10.2 min, SI-Figure 3.1). The structure of Boc-Cys(Acm)-HPMA was confirmed by ^{1}H NMR and ^{13}C NMR (SI-Figure 3.2).

3.3.2 Synthesis of triblock copolymer PEG-NIP-HPMA-Cys (PNC)

A thermosensitive ABA triblock copolymer containing HPMA-Cys was synthesized via free radical polymerization using a PEG10,000-ABCPA macroinitiator, and NIPAAm and Boc-Cys(Acm)-HPMA as monomers in a feed molar ratio of 93:7 (Figure 3.1). A triblock copolymer with NIPAAm and Boc-Cys(Acm)-HPMA as the

outer blocks and PEG as the midblock (abbreviated as PNC) was obtained in a yield of 77% with a M_n based on NMR of 64 kDa and a PDI of 2.5.
This triblock copolymer was first treated with TFA/DCM (1:1 v/v) to remove the Boc protecting groups from the NH_2 groups of cysteine. Secondly, the acetamidomethyl (Acm) groups were removed from the SH groups of cysteine by iodine, followed by exposure to TCEP to reduce possibly formed disulfide bonds. Removal of Boc and Acm groups of cysteines resulted in an increase in cloud point of the triblock copolymer from 18°C to 33°C, most likely due to its increased hydrophilicity. The removal of the Boc protecting group was confirmed by ^{1}H NMR by the disappearance of the signal at δ=1.4 ppm. Furthermore, the free NH_2 and SH groups of the cysteine units of the synthesized block copolymer were quantified by the TNBSA and Ellman's assay respectively and found to be lower than the feed (6.2% NH_2 and 5.4% SH compared to a feed of 7.0%). The difference between NH_2 and SH content was within the experimental error of these measurements.[47] As determined by GPC, deprotection resulted in a slight decrease in molecular weight, indicating that disulfide bond formation was negligible. Nonetheless, the molecular weights measured by GPC were higher than those determined by ^{1}H NMR, which can be ascribed to the previously described phenomenon that pNIPAAm based polymers have the tendency to aggregate in DMF.[48] Therefore, M_n of these triblock copolymers was based on NMR, in line with literature.[49] The polymer characteristics are summarized in Table 3.1.

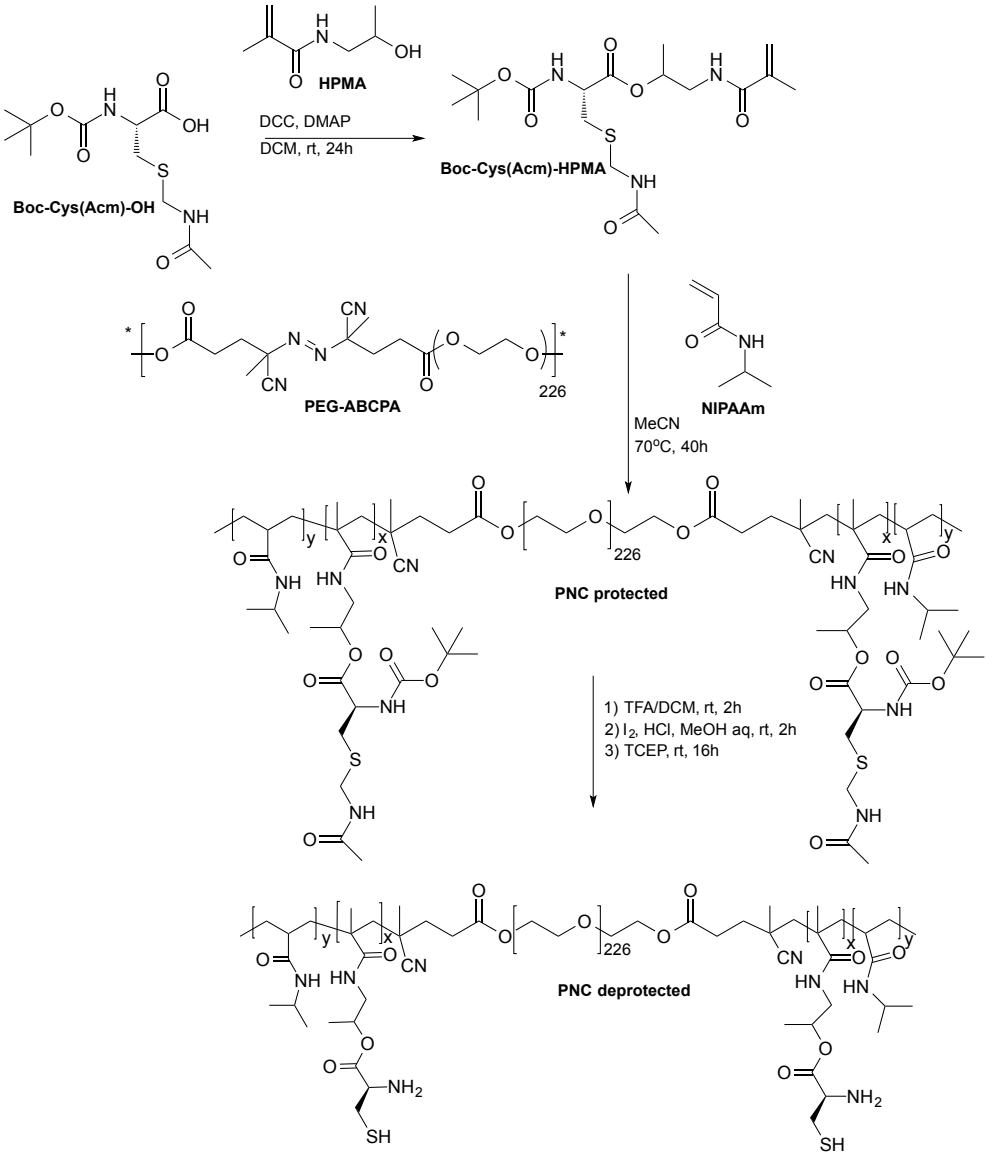

Figure 3.1. Synthesis route of ABA triblock copolymers consisting of a PEG_{10000} B-block and random A-blocks of NIPAAm and HPMA-Cys.

Table 3.1: Polymer characteristics of ABA triblock copolymers synthesized by radical polymerization having a PEG10000 B block and random A blocks of NIPAAm and HPMA-Cys (triblock abbreviated as PNC).

	M_n (kDa)[a]	M_n (kDa)[b]	M_w/M_n [b]	$\%NH_2$ [c]	%SH [d]	Cloud Point (°C) [e]
PNC* (protected)	64	135	2.5	-	-	18
PNC* (deprotected)	58	113	2.6	6.2	5.4	33

[a] Determined by ^{1}H NMR. [b] Determined by GPC. [c] Determined by TNBSA assay, expressed as mol % of A block. [d] Determined by Ellman's assay, expressed as mol % of A block. [e] Determined by light scattering at 650 nm.

* PNC: PEG-NIP-HPMA-Cys triblock, structures shown in figure 3.1.

3.3.3 Synthesis of PEG and HA thioester

Two cross-linkers were synthesized by introduction of thioester functionalities at the hydroxyl groups of polyethylene glycol (PEG) and hyaluronic acid (HA) using ethylthioglycolate succinic acid (ET-SA, SI-Figure 3.3) and DCC or EDCI as coupling agent, respectively (Figure 3.2). A high degree of substitution (DS) is necessary to use PEG as a cross-linker, since only difunctionalized PEG can contribute to network formation. When *N,N'*-dimethyl amino pyridine (DMAP) was used as the catalyst, a maximum DS of 50% was obtained. Therefore, 4-(dimethylamino)pyridinium-4-toluenesulfonate (DPTS) was chosen as catalyst, which has shown to enhance esterification reactions by suppression of the commonly observed side reaction leading to non-reactive *N*-acylurea derivatives[42]. Indeed, using this catalyst the DS of PEG as determined by ^{1}H NMR (shown in SI-Figure 3.4A) was 85%, which was further confirmed by hydrolyzing the thioester and subsequent analysis of free thiol content by Ellman's assay (DS=88%).

Hyaluronic acid was partially functionalized with thioester groups as alternative for the PEG cross-linker. A similar functionalization procedure was followed as for the synthesis of PEG thioester, however the reaction was performed in aqueous solution because of the limited solubility of hyaluronic acid in organic solvents and consequently a water-soluble cardodiimide derivative (EDCI) was selected as the coupling agent. Due to overlap of relevant peaks, the DS of thioester-functionalized HA could not be determined by NMR analysis (spectrum shown in SI-Figure 3.4B). Therefore DS, defined as percentage of disaccharide units of HA derivatized with thioester functionalities, was measured by thioester hydrolysis and subsequent thiol quantification and was found to be 11 %.

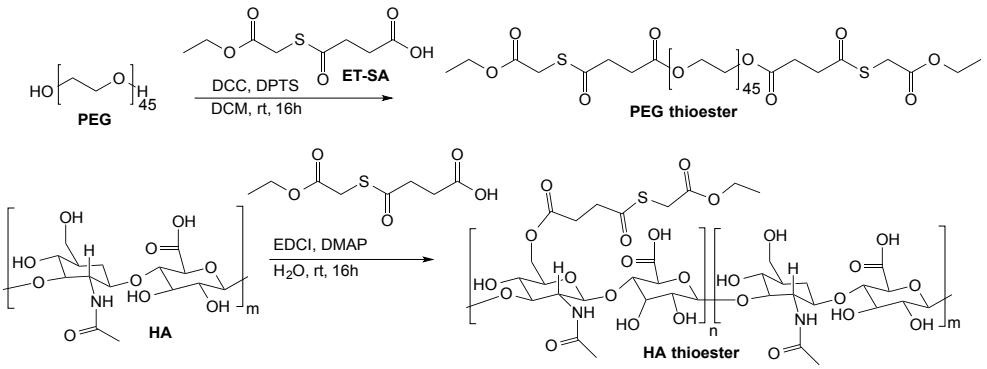

Figure 3.2. Synthesis route of PEG thioester and HA thioester.

3.3.4 Hydrogel characterization

The gelation characteristics of the triblock copolymer PEG-NIP-HPMA-Cys (PNC) were studied by rheology. A temperature sweep experiment showed an increase in storage modulus (G′) and loss modulus (G″) with increasing temperature reflecting the thermosensitive behavior of these polymers in aqueous solution (Figure 3.3). The deprotected triblock formed a hydrogel at higher temperatures than the protected triblock, which was expected from the higher hydrophilicity of the unprotected cysteine moieties, and was in line with the cloud point measurements. A slight decrease of G′ was shown for the protected triblock above 30°C, most likely caused by an increased mobility of the polymers at high temperatures.[50]

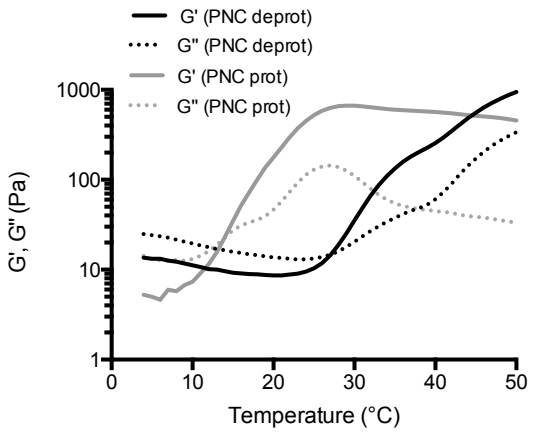

Figure 3.3. Storage (G′) and loss (G″) moduli as a function of temperature for PNC protected (PNC prot) and PNC deprotected (PNC deprot) at a concentration of 16 wt% in PBS.

Hydrogels of PEG-NIP-HPMA-Cys with either PEG thioester or HA thioester were formed by dissolving the individual compounds in PBS and mixing them at room temperature in a concentration of 16 wt% PNC and 4 wt% PEG or 11 wt% HA thioester, achieving a 1:1 functional group molar ratio. Possible gel formation was visually assessed immediately after mixing and after 30 min and 3 h (Figure 3.4). When the solutions were mixed at room temperature, a homogeneous liquid solution was obtained. Incubation of this polymer solution at 37°C for 30 min resulted in the formation of a gel. However, cooling the mixture to room temperature resulted again in a liquid solution which means that at that time point the system was a reversible (physical) gel. Importantly, after 3 h of incubation at 37°C followed by cooling down to room temperature, the hydrogel remained intact, indicating that cross-linking by native chemical ligation indeed had occurred. In principle, hydrogel formation could also be the result of disulfide formation of cysteines in the PNC macromers. However, a 16 wt% PNC solution without thioester cross-linker was still liquid at room temperature after 3 h incubation at 37°C, indicating that the contribution of disulfide bridges to the network formation was negligible. These results demonstrate that an irreversible chemically cross-linked hydrogel after 3 h incubation was only obtained after addition of a thioester cross-linker. The gelation kinetics were followed by rheology measurements during 3.5 h (Figure 3.5A). After mixing the two components, for both the PEG and HA cross-linkers an immediate gelation at 37°C was shown by G' values between 0.2 and 0.7 kPa and tan delta of 0.4. This rapid gel formation is the result of physical interactions between the pNIPAAm chains. In time, cross-linking proceeded through native chemical ligation, resulting in up to 10 times higher G' values than for networks formed by only physical interactions. However, cross-linking after 3.5 h was not completed, but the kinetics could not be further measured accurately due to evaporation of water. Systems containing either HA or PEG thioester cross-linkers showed similar rheological behavior in time (figure 3.5A) in terms of gel formation kinetics as well as G' values. It was shown that immediately after mixing, HA-PNC networks showed higher G' and G'' values. This is most likely caused by the higher thioester functionalities per cross-linker of the HA formulation. On average, the HA cross-linker contained 8 thioester moieties per chain compared to 2 thioester moieties for the PEG cross-linker. Therefore, using the HA cross-linker a strong chemically cross-linked network was obtained rapidly after mixing with PNC. Moreover, the higher viscosity of the HA formulation also contributed to higher initial moduli as compared to the PEG system. To demonstrate again that the cross-linking indeed proceeded through native chemical ligation rather than disulfide formation of the cysteine groups, a sample of 16 wt% of deprotected triblock copolymer in PBS was analyzed by rheology without adding a thioester cross-linker (Figure 3.5B). The sample was first heated from 4 to 50°C at a heating rate of 1°C/min and further followed at 37°C during 3 h. During the heating step,

an increase in storage modulus (G') showed the thermosensitive behavior of the polymer, while at 37°C no further increase in G' was detected for 3 h for this sample without cross-linker. This observation proved that in this time frame negligible disulfide formation occurred and the contribution to gel formation in PNC-PEG and PNC-HA samples was the result of cross-linking by NCL.

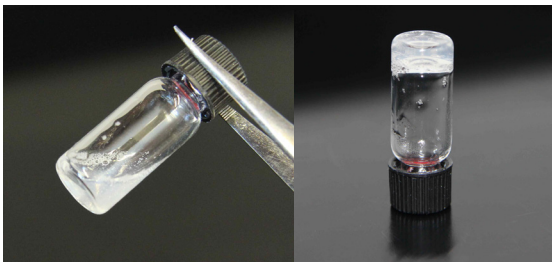

Figure 3.4. Hydrogel formation of 16 wt% PNC and 4 wt% PEG thioester in PBS at 37°C. Left: photo taken at t = 0, right: photo taken at t = 3h. Pictures were taken at room temperature.

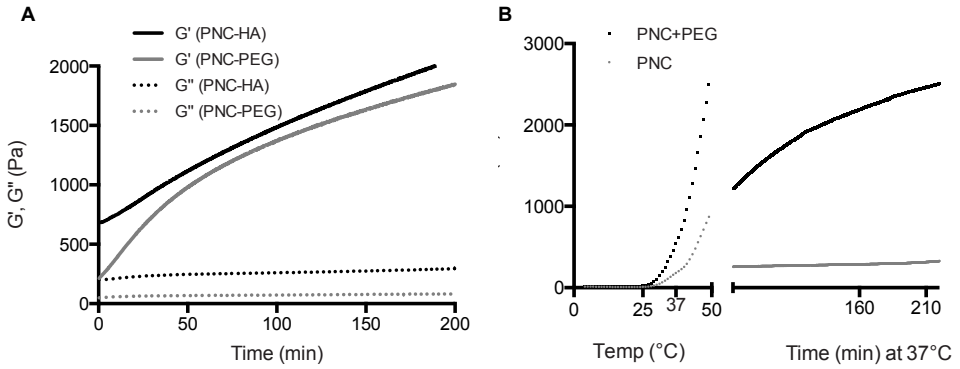

Figure 3.5. A) Storage (G') and loss (G'') moduli as a function of time of a mixture of 4 wt% PEG or 11 wt% HA thioester crosslinker with 16 wt% unprotected PNC at 37°C in PBS. B) Storage (G') modulus of 16 wt% PNC deprotected with and without 4 wt% PEG thioester crosslinker. Samples were heated from 4 to 50°C at 1°C/min, subsequently cooled to 37°C within 1 min and further measured for 3 h at 37°C.

3.3.5 Peptide Ligation

The DDR-2 binding peptide CGPRGQOGVMGFO, known for its beneficial properties in cell differentiation, proliferation and adhesion[37-39] was ligated to part of the available PEG thioester functionalities. An *N*-terminal cysteine was introduced in the peptide sequence to allow ligation via NCL to the thioester functionality of PEG. PEG-peptide conjugates were formed with two different degrees of substitution (DS), using molar feed ratios of 1:1 and 0.5:1 thioester : cysteine peptide using MESNa

as catalyst. These ratios were chosen to enable characterization of covalent ligation of this peptide to PEG thioester. After ligation, the NMR spectrum of the obtained conjugate clearly showed characteristic signals of peptide protons at δ= 0.8 and 7.2 ppm from valine and phenylalanine respectively (Figure 3.6). Furthermore, reduced intensity of the CH_3 signal at δ= 1.2 ppm of the distal CH_3 group of the thioester indicated cleavage of the thioester due to the native chemical ligation reaction. Based on NMR integrals DS was found to be 75 and 27% for molar feed ratios of 1:1 and 0.5:1 thioester : cysteine peptide respectively. The same DS was found based on the decrease in thioester signal at 1.2 ppm as well as integrals of peptide signals. This indicates that the peptide was indeed successfully ligated and non-functionalized peptide was completely removed by dialysis from the reaction mixture. Between 4 and 4.3 ppm, a quartet corresponding to the *O*-CH_2 protons adjacent to the terminal CH_3 (ethyl ester), which partially overlaps with a triplet corresponding to the terminal PEG CH_2 protons is visible in Figure 3.6D. A reduction of the peak integral of the CH_2 quartet at 4.2 ppm indicates that the terminal fragment of PEG thioester is removed after ligation, as is further confirmed by the displayed integral values. In contrast, the NMR spectrum of the reaction product with DS=75% clearly shows that the signals of the CH_2 protons between PEG and the thioester groups are still present after ligation at 2.7 and 2.9 ppm. A slight difference in chemical shift is most

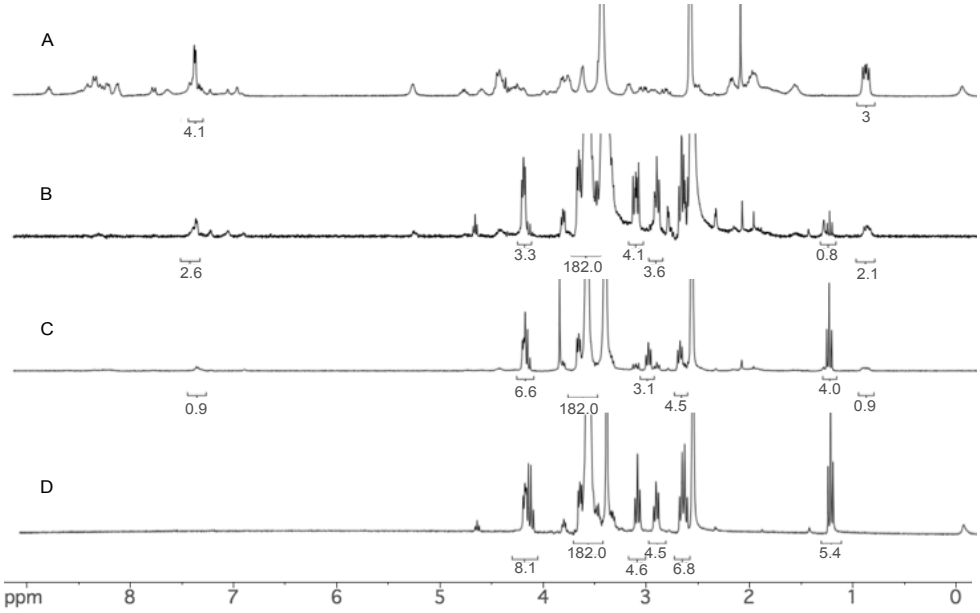

Figure 3.6. ^{1}H NMR spectra of A) peptide, B) reaction product DS = 75%, C) reaction product DS = 27% and D) PEG thioester. The peaks at 0.8 and 7.2 ppm show the peptide signals used to calculate the degree of substitution. The reduced intensity of the peak at 1.2 ppm (triplet of CH_3) demonstrates clearly the cleavage of the thioester ethyl functionality, an indication that the peptide is linked via NCL to the polymer.

likely caused by the peptide coupling. These results confirm the structure of the PEG-peptide conjugate as expected after NCL reaction.

Additional proof of peptide ligation was obtained by GPC analysis (Figure 3.7). After ligation, apart from the non-functionalized PEG-thioester a new peak appeared, showing that the molecular weight of the PEG thioester increased from 2.2-2.4 kDa to 3.8-3.9 kDa. This molecular weight was in good agreement with the theoretical molecular weight of a PEG thioester and one conjugated peptide (2.4 and 1.3 kDa respectively). Furthermore, the peaks at 5.4 and 6.8 kDa showed the presence of difunctionalized PEG-peptide conjugate (2.4 plus 2x1.3 kDa). After NCL reaction thiol functionalities remain that could potentially form disulfide bonds. Although TCEP was added as reducing agent to the GPC samples, a small fraction of disulfide bridged peptide and reaction product was visible at higher molecular weights.

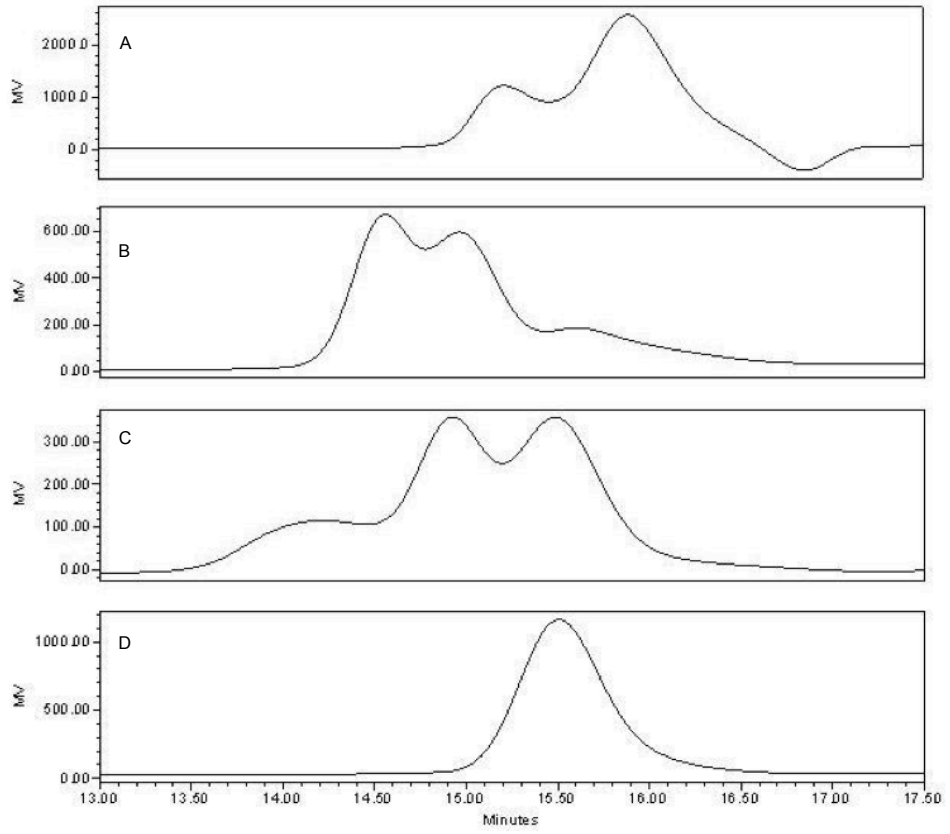

Figure 3.7. GPC chromatograms of A) peptide, B) reaction product DS = 75%, C) reaction product DS = 27% and D) PEG thioester. Displayed values are the peak molecular weights based on RI detection and PEG standards. Ligation resulted in an increase in molecular weight. Disulfide formation was shown for both peptide and the ligated product.

Based on GPC integrals for the product with DS=27%, the reaction product contained approximately 40% non-functionalized PEG thioester and 43% PEG-thioester peptide conjugate. The remaining 17% contained PEG thioester with two peptides ligated and some disulfide product. The same agreement between GPC and NMR was found for the product with DS=75%. These results showed that the PEG thioester was successfully functionalized with peptide with different degrees of substitution. However, it is important to realize that in hydrogel formulations for cell encapsulation experiments, a lower functionalization of peptides to the cross-linker is desired (1-5%) to balance the peptide's biological activity[51] with the cross-linker capacity of the PEG thioester. An alternative approach would be to mix the DS 27% PEG thioester-peptide conjugate with non-functionalized PEG thioester to obtain a degree of functionalization of approximately 5 mol% peptide in the hydrogel. Using this approach, hydrogels were formed from PNC and PEG thioester functionalized with and without peptide conjugate (DS=27%). The Young's moduli of the obtained hydrogels were measured with a dynamic mechanical analyzer (DMA). Incorporation of 25% PEG-peptide conjugate in the hydrogel formulation resulted in a slight reduction in the gel stiffness (from 5.3 ± 0.7 kPa to 4.4 ± 0.8 kPa) that can be explained by the reduced number of available thioester groups for network formation by NCL. A Mann-Whitney-U test showed a non-significant difference between these two groups (P=0.4) and therefore it can be concluded that peptide incorporation had a limited effect on hydrogel formation.

3.4 Conclusion

This study shows that thermoresponsive polymers that can undergo NCL reaction allow the immediate formation of a physical network that is strengthened in time due to the formation of covalent bonds between the hydrogel constituents. Both thioester cross-linkers based on hyaluronic acid and PEG contributed to the formation of a mechanically enhanced hydrogel. Control experiments proved that network formation proceeded through NCL rather than disulfide formation. This hydrogel is particularly attractive for biomedical and pharmaceutical applications, because of the rapid network formation, further chemoselective chemical cross-linking of this network by NCL under mild reaction conditions, and the ability to covalently link a variety of peptides and other bioactive moieties.

Acknowledgements
This research was supported by the Netherlands Institute of Regenerative Medicine (NIRM).

Supporting Information

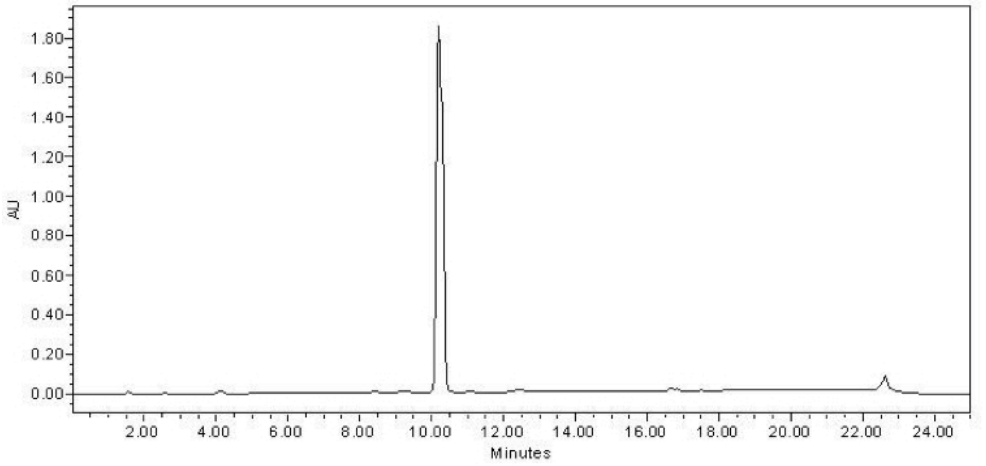

SI-Figure 3.1. HPLC chromatogram of Boc-Cys(Acm)-HPMA using UV detection. R_t Boc-Cys(Acm)-HPMA= 10.2 min.

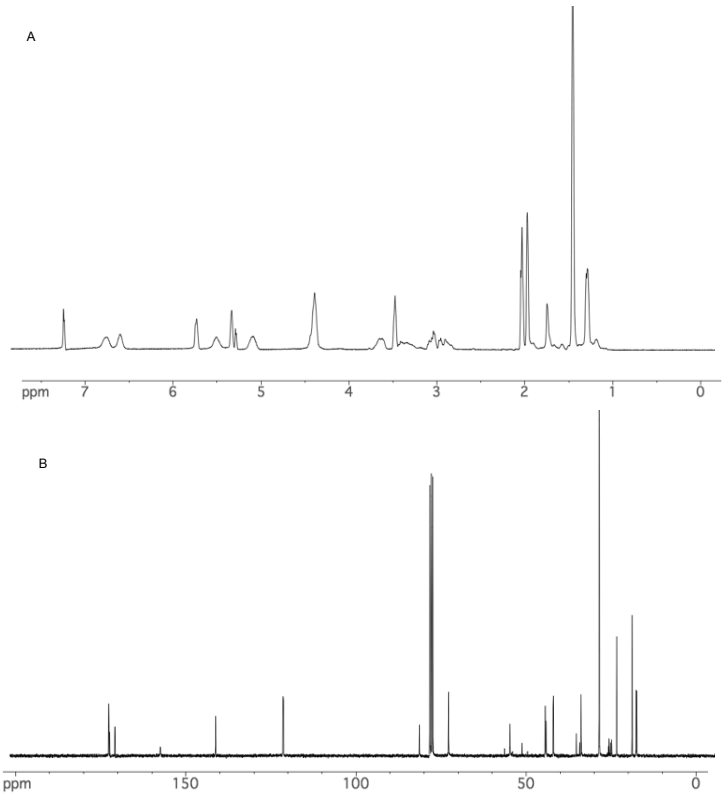

SI-Figure 3.2. A) ^{1}H NMR spectrum of Boc-Cys(Acm)-HPMA in $CDCl_3$. Residual solvent peaks are shown at δ = 3.5 and 5.3 ppm (MeOH and CH_2Cl_2 respectively). B) ^{13}C NMR spectrum of Boc-cys(Acm)-HPMA in $CDCl_3$.

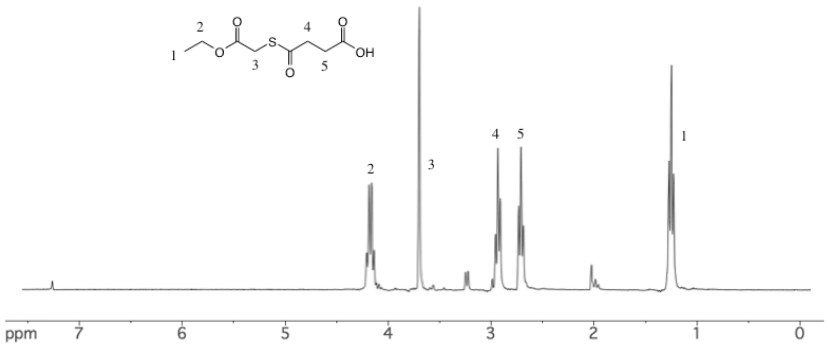

SI-Figure 3.3. ^{1}H NMR spectrum of ET-SA in $CDCl_3$.

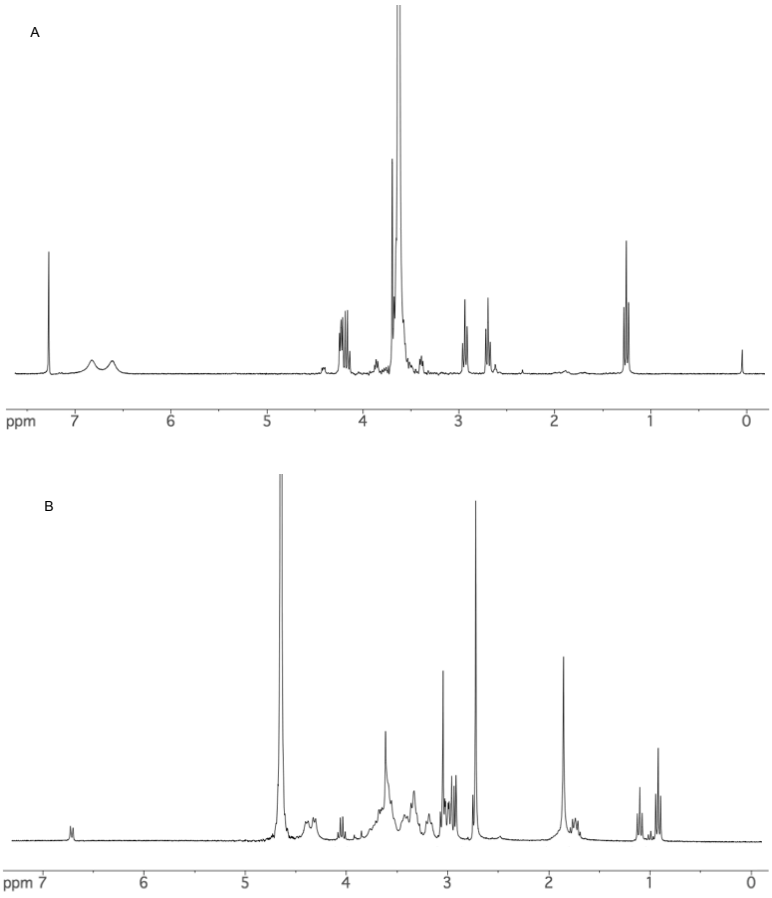

SI-Figure 3.4. A) ^{1}H NMR spectrum of PEG2000 thioester in $CDCl_3$ + TAIC. The peak at δ = 3.5-3.8 ppm shows the PEG CH_2 protons. The peak at δ = 1.3 ppm shows the distal CH_3 group. Unreacted PEG hydroxyl groups were quantified by a reaction with TAIC, which caused a shift of the CH_2 protons of PEG adjacent to the OH end groups to 4.4 ppm. B) ^{1}H NMR spectrum of HA thioester in D_2O.

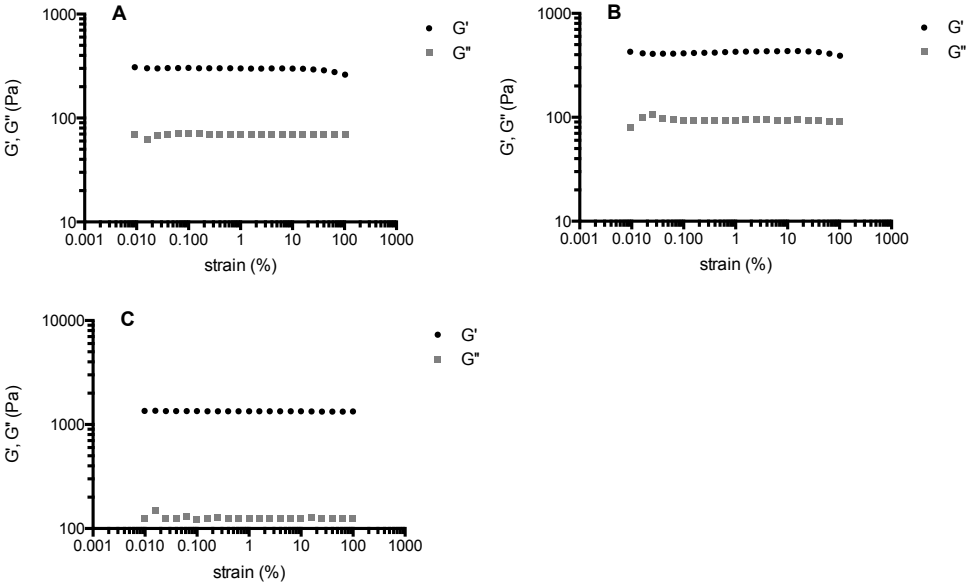

SI-Figure 3.5. Strain sweep at 37°C of PNC and PNC-PEG to determine the linear viscosity region. A) PNC, 16 wt%; B) PNC 16wt% + PEG 4 wt%, immediately after mixing; C) PNC 16wt% + PEG 4 wt%, after 2 h. Further rheology experiments were performed at a strain of 1%.

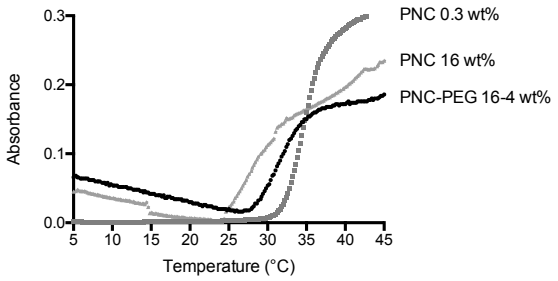

SI-Figure 3.6. Light absorbance at 650 nm as a function of temperature for cloud point determination in PBS: 0.3 wt% PNC; 16 wt% PNC and 16 wt% PNC + 4 wt% PEG thioester 2 h after mixing.

References

1. R. Censi, P. Di Martino, T. Vermonden and W. E. Hennink, *J. Controlled Release*, 2012, **161**, 680-692.
2. T. Vermonden, R. Censi and W. E. Hennink, *Chem. Rev.*, 2012, **112**, 2853-2888.
3. A. S. Hoffman, *Adv. Drug Delivery Rev.*, 2002, **54**, 3-12.
4. K. Y. Lee and D. J. Mooney, *Chem. Rev.*, 2001, **101**, 1869-1880.
5. N. A. Peppas, J. Z. Hilt, A. Khademhosseini and R. Langer, *Adv. Mater.*, 2006, **18**, 1345-1360.
6. D. Seliktar, *Science*, 2012, **336**, 1124-1128.
7. S. Van Tomme, G. Storm and W. E. Hennink, *Int. J. Pharm.*, 2008, **355**, 1-18.
8. D. Y. Ko, U. P. Shinde, B. Yeon and B. Jeong, *Prog. Polym. Sci.*, 2013, **38**, 672-701.
9. K. H. Bae, L.-S. Wang and M. Kurisawa, *J. Mater. Chem. B*, 2013, **1**, 5371-5388.
10. L. Klouda and A. G. Mikos, *Eur. J. Pharm. Biopharm.*, 2008, **68**, 34-45.
11. H. Moon, D. Y. Ko, M. Park, M. Joo and B. Jeong, *Chem. Soc. Rev.*, 2012, **41**, 4860-4883.
12. M. Teodorescu, I. Negru, P. O. Stanescu, C. Drăghici, A. Lungu and A. Sârbu, *React. Funct. Polym.*, 2010, **70**, 790-797.
13. W. E. Hennink and C. F. van Nostrum, *Adv. Drug Delivery Rev.*, 2002, **54**, 13-36.
14. A. E. Ekenseair, K. W. M. Boere, S. Tzouanas, T. Vo, F. Kasper and A. G. Mikos, *Biomacromolecules*, 2012, **13**, 2821-2830.
15. T. Vermonden, N. E. Fedorovich, D. van Geemen, J. Alblas, C. F. van Nostrum, W. J. A. Dhert and W. E. Hennink, *Biomacromolecules*, 2008, **9**, 919-926.
16. R. Censi, P. J. Fieten, P. Di Martino, W. E. Hennink and T. Vermonden, *Macromolecules*, 2010, **43**, 5771-5778.
17. R. Jin, L. Moreira Teixeira, A. Krouwels, P. Dijkstra, C. van Blitterswijk, M. Karperien and J. Feijen, *Acta Biomater.*, 2010, **6**, 1968-1977.
18. R. Zhang, M. Xue, J. Yang and T. Tan, *J. Appl. Polym. Sci.*, 2012, **125**, 1116-1126.
19. A. E. Ekenseair, K. W. M. Boere, S. Tzouanas, T. Vo, F. Kasper and A. G. Mikos, *Biomacromolecules*, 2012, **13**, 1908-1915.
20. Y. Tanabe, K. Yasuda, C. Azuma, H. Taniguro, S. Onodera, A. Suzuki, Y. Chen, J. Gong and Y. Osada, *J Mater Sci: Mater Med*, 2008, **19**, 1379-1387.
21. C. Hackenberger and D. Schwarzer, *Angew. Chem. Int. Ed.*, 2008, **47**, 10030-10074.
22. M. Malkoch, R. Vestberg, N. Gupta, L. Mespouille, P. Dubois, A. Mason, J. Hedrick, Q. Liao, C. Frank, K. Kingsbury and C. Hawker, *Chem. Commun.*, 2006, DOI: 10.1039/b603438a, 2774-2776.
23. D. A. Ossipov and J. Hilborn, *Macromolecules*, 2006, **39**, 1709-1718.
24. M. van Dijk, D. T. S. Rijkers, R. M. J. Liskamp, C. F. van Nostrum and W. E. Hennink, *Bioconjugate Chem.*, 2009, **20**, 2001-2016.
25. N. Agard, J. Prescher and C. Bertozzi, *J. Am. Chem. Soc.*, 2004, **126**, 15046-15047.
26. C. Becer, R. Hoogenboom and U. Schubert, *Angew. Chem. Int. Ed.*, 2009, **48**, 4900-4908.
27. B.-H. Hu, J. Su and P. B. Messersmith, *Biomacromolecules*, 2009, **10**, 2194-2200.
28. P. E. Dawson, T. W. Muir, I. Clark-Lewis and S. B. H. Kent, *Science*, 1994, **266**, 776-779.
29. P. Dawson and S. Kent, *Annu. Rev. Biochem*, 2000, **69**, 923-960.
30. E. Johnson and S. Kent, *J. Am. Chem. Soc.*, 2006, **128**, 6640-6646.
31. J. Collier and T. Segura, *Biomaterials*, 2011, **32**, 4198-4204.
32. E. Jabbari, *Curr. Opin. Biotechnol.*, 2011, **22**, 655-660.
33. J. P. Jung, A. J. Sprangers, J. R. Byce, J. Su, J. M. Squirrell, P. B. Messersmith, K. W. Eliceiri and B. M. Ogle, *Biomacromolecules*, 2013, **14**, 3102-3111.
34. I. Strehin, D. Gourevitch, Y. Zhang, E. Heber-Katz and P. B. Messersmith, *Biomaterials Science*, 2013, **1**, 603-613.

35. J. Burdick and G. Prestwich, *Adv. Mater.*, 2011, **23**, 41-56.
36. G. D. Prestwich, *J. Controlled Release*, 2011, **155**, 193-199.
37. H. Xu, D. Bihan, F. Chang, P. H. Huang, R. W. Farndale and B. Leitinger, *PLOS ONE*, 2012, **7**, e52209.
38. B. Leitinger, *Annu. Rev. Cell Dev. Biol.*, 2011, **27**, 265-290.
39. A. D. Konitsiotis, N. Raynal, D. Bihan, E. Hohenester, R. W. Farndale and B. Leitinger, *J. Biol. Chem.*, 2008, **283**, 6861-6868.
40. K. Ulbrich, V. Šubr, J. Strohalm, D. Plocová, M. Jelínková and B. Říhová, *J. Controlled Release*, 2000, **64**, 63-79.
41. D. Neradovic, C. F. van Nostrum and W. E. Hennink, *Macromolecules*, 2001, **34**, 7589-7591.
42. J. S. Moore and S. I. Stupp, *Macromolecules*, 1990, **23**, 65-70.
43. J. M. Harris, *J. Macromol. Sci., Rev. Macromol. Chem. Phys.*, 1985, **25**, 325-373.
44. V. W. Goodlett, *Analytical Chemistry*, 1965, **37**, 431-432.
45. G. L. Ellman, *Arch. Biochem. Biophys.*, 1959, **82**, 70-77.
46. A. F. S. A. Habeeb, *Anal. Biochem.*, 1966, **14**, 328-336.
47. C. Riener, G. Kada and H. Gruber, *Anal Bioanal Chem*, 2002, **373**, 266-276.
48. D. W. Smithenry, M.-S. Kang and V. K. Gupta, *Macromolecules*, 2001, **34**, 8503-8511.
49. A. J. de Graaf, K. W. M. Boere, J. Kemmink, R. G. Fokkink, C. F. van Nostrum, D. T. S. Rijkers, J. van der Gucht, H. Wienk, M. Baldus, E. Mastrobattista, T. Vermonden and W. E. Hennink, *Langmuir*, 2011, **27**, 9843-9848.
50. T. Vermonden, N. A. M. Besseling, M. J. van Steenbergen and W. E. Hennink, *Langmuir*, 2006, **22**, 10180-10184.
51. J. Su, B.-H. Hu, W. L. Lowe Jr, D. B. Kaufman and P. B. Messersmith, *Biomaterials*, 2010, **31**, 308-314.

CHAPTER 4

THERMOGELLING AND CHEMOSELECTIVELY CROSS-LINKED HYDROGELS WITH CONTROLLED MECHANICAL PROPERTIES AND DEGRADATION BEHAVIOR

K. W. M. Boere, J. van den Dikkenberg, Y. Gao, J. Visser, W. E. Hennink, T. Vermonden, *Biomacromolecules*, 2015, **16**, 2840-2851

Abstract

Chemoselectively cross-linked hydrogels have recently gained increasing attention for the development of novel, injectable biomaterials given their limited side reactions. In this study, we compared the properties of hydrogels obtained by native chemical ligation (NCL) and its recently described variation termed oxo-ester mediated native chemical ligation (OMNCL) in combination with temperature-induced physical gelation. Triblock copolymers consisting of cysteine functionalities, thermoresponsive *N*-isopropyl acrylamide (NIPAAm) units and degradable moieties were mixed with functionalized poly(ethylene glycol) (PEG) cross-linkers. Thioester or *N*-hydroxysuccinimide (NHS) functionalities attached to PEG reacted with cysteine residues of the triblock copolymers via either an NCL or OMNCL pathway. The combined physical and chemical cross-linking resulted in rapid network formation and mechanically strong hydrogels. Stiffness of the hydrogels was highest for thermogels that were covalently linked via OMNCL. Specifically, the storage modulus after 4 hours reached a value of 26 kPa, which was over a 100 times higher than hydrogels formed by solely thermal physical interactions. Endothelial cells showed high cell viability of 98 ± 2 % in the presence of OMNCL cross-linked hydrogels after 16 hours of incubation, in contrast to a low cell viability (13 ± 7 %) for hydrogels obtained by NCL cross-linking. Lysozyme was loaded in the gels and after 2 days more than 90% was released, indicating that the cross-linking reaction was indeed chemoselective as the protein was not covalently grafted to the hydrogel network. Moreover, the degradation rates of these hydrogels under physiological conditions could be tailored from 12 days up to 6 months by incorporation of a monomer containing a hydrolysable lactone ring in the thermosensitive triblock copolymer. These results demonstrate a high tunability of mechanical properties and degradation rates of these *in situ* forming hydrogels that could be used for a variety of biomedical applications.

Graphical abstract

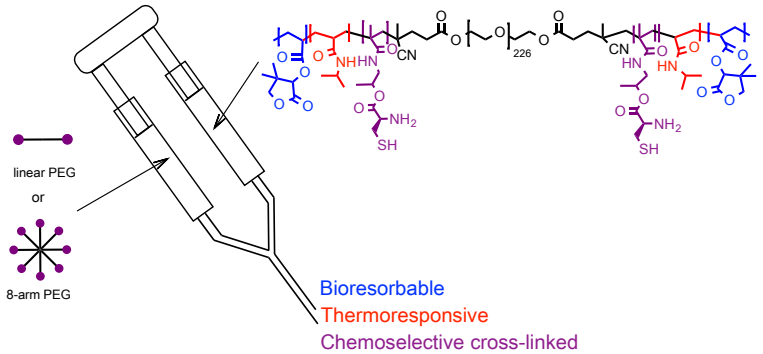

4.1 Introduction

In situ forming hydrogels are an attractive class of biomaterials due to their capability of completely filling irregular tissue defects, using a minimally invasive treatment.[1-6] Particularly interesting are hydrogels that can be formed by both physical and chemical cross-linking, because physical cross-linking induces a quick stabilization of the network after injection, while chemical cross-linking ensures the formation of a mechanically stable network.[7-9] One of the most studied physically gelling hydrogels for biomedical applications is based on temperature sensitive poly(*N*-isopropyl acrylamide) (pNIPAAm), because of its lower critical solution temperature (LCST) of 32°C.[10] However, solely physically formed hydrogels are often mechanically weak, resulting in fast degradation or erosion. On the other hand, solely chemically formed hydrogels either cross-link too quickly, which leads to obstruction in the needle, or too slowly, resulting in leaching away of the polymer precursors from the application site. A dual gelation mechanism therefore combines the advantageous properties of both methods, providing an easy injection and strong network formation.

Although there is a wide variety of chemical cross-linking mechanisms available[11], especially chemoselective reactions such as copper free click chemistry[12], Diels-Alder[13, 14] and native chemical ligation (NCL)[15] recently attracted great interest for application in drug delivery and tissue engineering. The chemoselective nature of these reactions results in efficient cross-linking between the hydrogel components without ligation to other biomolecules. NCL has been widely employed for peptide synthesis[15], but is relatively unexplored in the field of biomaterials. It involves a reaction between an *N*-terminal cysteine and a thioester and proceeds via a reversible transthioesterification to an irreversible rearrangement that results in the formation of an amide bond. Groll et al. reported the synthesis of cysteine functionalized polymers for peptide conjugation by NCL.[16, 17] Hydrogels formed by native chemical ligation without using a catalyst were first reported by the group of Messersmith.[18] Recently, we showed the formation of thermoresponsive hydrogels cross-linked by NCL.[19] The thermoresponsive component was composed of an ABA triblock copolymer having a poly(ethylene glycol) (PEG) B block and A blocks consisting of randomly distributed *N*-isopropylacrylamide (NIPAAm) and *N*-(2-hydroxypropyl) methacrylamide-cysteine (HPMA-cysteine) monomers. Chemical cross-linking was accomplished after mixing this triblock copolymer with hyaluronic acid (HA) or PEG functionalized with thioester groups. The mild reaction conditions and possibility to further functionalize the hydrogel with peptides showed its attractiveness for biomedical applications.

Although these hydrogels were formed in a controlled manner, after cross-linking a thiol byproduct, ethyl thioglycolate, was released, which belongs to a group of compounds recently reported to be cytotoxic.[20] Strehin et al. proposed to use a

variant of native chemical ligation, namely oxo-ester mediated native chemical ligation (OMNCL), thereby eliminating the release of thiol byproducts.[21] Moreover, they showed the chemoselectivity of the OMNCL mechanism by quantitative NMR analysis and the cytocompatibility of the obtained hydrogels both *in vitro* and *in vivo*. In contrast to NCL, OMNCL utilizes an ester instead of a thioester as reactive compound.[22] OMNCL has been first described by the group of Danishefsky as a simplification of native chemical ligation. They showed that the resulting ligation reactions had faster kinetics and higher yields, especially when the ligation took place at sterically hindered sites, yet still showing a high selectivity as proven in competitive experiments.[22] The chemoselectivity of OMNCL for cysteines over other amino acids was further proven in a microarray study.[23]

An ideal hydrogel for biomedical applications should have tunable mechanical properties and degradation rates for use in multiple applications. For tissue engineering purposes, the mechanical properties of the hydrogel should ideally match the stiffness of the target tissue.[24, 25] Controlling and tuning the hydrogel stiffness has been reported in literature to have a significant effect on the performance of cells in terms of cell migration and differentiation.[26] In addition, the hydrogels should degrade in the same time frame as new tissue formation occurs. Although materials based on pNIPAAm homopolymers are widely used in tissue engineering applications, they are not resorbable. Several studies have shown the bioresorbability of NIPAAm based polymers after copolymerization of NIPAAm with hydrolysable monomers, such as *N*-(2-hydroxypropyl)methacrylamide lactate[27] and dimethyl-γ-butyrolactone acrylate (DBA).[28] After hydrolysis, the LCST of the polymers increases in time, resulting in dissolution of the polymers when an LCST of 37°C is reached.

Copolymers of NIPAAm and DBA have been first reported by the group of Vernon.[28] An attractive feature of these copolymers is that degradation could be tuned by the incorporation of DBA and degradation under physiological conditions occurred without releasing low molecular weight degradation products. Further, a good biocompatibility of the obtained hydrogels was reported.[29] In addition, Mikos et al., described the formation of a physically and chemically gelling hydrogel that was bioresorbable after introduction of these DBA groups[30] and its application for bone regeneration[31].

In this work, we further explored the opportunities of our previously developed thermoresponsive hydrogels cross-linked by native chemical ligation, involving the recent knowledge of oxo-ester mediated native chemical ligation. The aim of this study was to compare the properties of thermoresponsive, *in situ* forming hydrogels cross-linked by native chemical ligation and oxo-ester mediated native chemical ligation regarding their gelation kinetics, cell viability and protein compatibility, thereby providing for the first time an in depth comparison of these chemoselectively cross-linked hydrogels. Finally, we present the ability to tune mechanical properties

and degradation rates of our hydrogels by changing the polymer composition, towards controlling the eventual properties of these injectable hydrogels for the desired application.

4.2 Materials and Methods

4.2.1 Materials

All materials were obtained from Sigma-Aldrich (Zwijndrecht, the Netherlands) and used as received unless otherwise noted. *N*-(2-hydroxypropyl)methacrylamide-Boc-*S*-acetamidomethyl-L-cysteine (HPMA-Boc-Cys(Acm)) was synthesized according to a previously published procedure.[19] PEG 20,000 8-arm with a tripentaerythritol core was obtained from JenKem Technology USA (Plano, Tx, USA). PEG 10,000-(4,4´-azobis(4-cyanopentanoic acid) (ABCPA) macroinitiator and ethylthioglycolate succinic acid (ET-SA) were synthesized following established procedures.[18, 32] Tris(2-carboxyethyl)phosphine hydrochloride (TCEP) was obtained from Carl Roth (Karlsruhe, Germany). Peptide grade dichloromethane (DCM) was purchased from Biosolve (Valkenswaard, the Netherlands). *N*,*N*'-Dimethylaminopyridine (DMAP) was obtained from Fluka (Zwijndrecht, the Netherlands). 4-(Dimethylamino)pyridinium-4-toluene-sulfonate (DPTS) was prepared according to a reported procedure.[33] MTS (3-(4,5-dimethylthiazol-2-yl)-5-(3-carboxymethoxyphenyl)-2-(4-sulfophenyl)-2H-tetrazolium) and Celltiter 96 kit #G3580 were purchased from Promega (Madison, WI, USA). DMEM cell culture medium (#D6429) containing 4.5 g/L glucose and 10% FBS was obtained from Sigma-Aldrich. Antibiotic-antimyotic solution containing penicillin-streptomycin and anti-mycotics was obtained from Sigma-Aldrich (Zwijndrecht, the Netherlands). T175 cell culture flasks, well plates and petri dishes were obtained from Greiner Bio-One, Alphen a/d Rijn, the Netherlands. PBS buffer pH 7.4 (8.2 g/L NaCl, 3.1 g/L $Na_2HPO_4{\cdot}12H_2O$, 0.3 g/L $NaH_2PO_4{\cdot}2H_2O$) was purchased from B. Braun (Melsungen, Germany).

4.2.2 Synthesis of PNCD Triblock Copolymers

ABA triblock copolymers (abbreviated as PNCD) were synthesized consisting of a poly(ethylene glycol) 10 kDa B block, following previously published procedures[19]. The A blocks consisted of *N*-isopropylacrylamide (NIPAAm), *N*-(2-hydroxypropyl) methacrylamide-cysteine (HPMA-Cys) and dimethyl-γ-butyrolactone acrylate (DBA). Five different polymers were synthesized by varying the DBA feed (0, 2.5, 5, 7.5 and 10 mol% of total monomer content). The feed ratio of HPMA-Boc-Cys(Acm) was kept at 7 mol% of the total monomer feed. In short, PEG-ABCPA 10,000 Da, HPMA-Boc-Cys(Acm), NIPAAm and DBA (total approximately 3 g, monomer:PEG

ratio 322:1) were dissolved in 40 mL dry acetonitrile under N_2 atmosphere and polymerized for 40 h at 70 °C under stirring. After cooling the mixture to room temperature, the formed polymers were precipitated in cold diethyl ether and collected as a white solid after filtration. Boc protecting groups of cysteine were removed by dissolving the polymer in DCM/TFA (1:1 v/v, 40 mL) and stirring for 2 hours at room temperature. Subsequently, the solution was concentrated under reduced pressure to 10 mL and the polymers were precipitated in diethyl ether. A white solid was obtained and further dried under vacuum at room temperature. Acm protecting groups were removed by dissolving the polymer in MeOH/H_2O (1:1 v/v, 100 mL) under a nitrogen atmosphere, and addition of 1 mL 1 M HCl and 16 mL 0.2 M iodine in MeOH/H_2O (1:1 v/v). The brownish mixture was stirred for 1 h at room temperature, followed by addition of a few drops of 1 M ascorbic acid to quench the excess of iodine. TCEP (1 g) was added to the obtained colorless solution to reduce disulfide bonds. The mixture was stirred for 16 h, dialyzed against water for 3 days at 4 °C (M_w cutoff: 12-14 kDa) and the polymers were obtained after lyophilization. The polymers were characterized by ^{1}H NMR and GPC. Additionally, primary amine and thiol groups of cysteine were quantified by TNBSA and Ellman's assay respectively, following reported procedures[34, 35].^{1}H NMR ($CDCl_3$): δ = 5.45 and 5.32 (d, DBA), 3.97 (s, NIPAAm), 3.80 (t, terminal CH_2 PEG), 3.62 (m, CH_2 PEG backbone), 1.42 (s, Boc HPMA-Cys), 1.11 (s, NIPAAm).

4.2.3 Synthesis of linear and 8-arm PEG thioester cross-linkers

Linear PEG 2,000 Da and 8-arm PEG 20,000 Da with thioester functionalities (abbreviated as PEG linear thioester and PEG 8-arm thioester respectively) were synthesized following literature procedures.[18, 19] Briefly, 6 g linear PEG 2,000 or 15 g 8-arm PEG 20,000 (corresponding to 6 mmol OH groups) was added to a solution of ET-SA (2.6 g, 12 mmol), DCC (2.5g, 12 mmol) and DPTS (177 mg, 1.2 mmol) in dry DCM (100 mL) and the mixture was stirred for 16 h at room temperature. Dicyclohexylurea (DCU) was removed by filtration and the formed polymer was precipitated in cold diethyl ether. PEG thioester was obtained after filtration, further dried under vacuum and characterized by ^{1}H NMR. Additionally, two drops of trichloroacetyl isocyanate (TAIC) were added to the ^{1}H NMR sample to confirm the calculated DS, since TAIC induces a shift of the CH_2 protons of PEG adjacent to the OH end groups to 4.42 ppm.[36, 37] Yield: 92% for PEG linear, 90% for PEG 8-arm,^{1}H NMR ($CDCl_3$): δ = 4.42 (2H, TAIC shift CH_2OH), 4.24 (2H, t, terminal PEG CH_2), 4.14 (q, 2H, CH_3CH_2O), (3.62 (PEG backbone), 3.13 (t, 2H, SC(O)-CH_2CH_2), 2.89 (t, 2H, $SC(O)CH_2CH_2$), 1.21 (t, 3H, CH_3CH_2O).

4.2.4 Synthesis of linear and 8-arm PEG NHS cross-linkers

Linear and 8-arm PEG were functionalized with NHS groups in a two-step synthesis according to a literature procedure.[21] First, the terminal OH groups of PEG were converted into COOH groups by a reaction with glutaric anhydride. In detail, 10 g 8-arm PEG 20,000 (4 mmol OH) or 10 g linear PEG 2,000 (10 mmol OH) was dissolved in 20 mL chloroform. A 5-fold molar excess of glutaric anhydride and pyridine relative to the OH end groups of PEG were added to the PEG solution. The mixture was brought under nitrogen atmosphere and refluxed for 24 hours at 80 °C. The solution was cooled to room temperature, 100 mL of methanol was added and the formed polymer was precipitated in cold diethyl ether. The product was collected after filtration and further dried under vacuum.

In a subsequent reaction, NHS functionalities were introduced on the glutaric acid groups. Glutaric acid terminated PEG (10 g) was dissolved in 30 mL of DMSO together with a 10-fold molar excess of NHS and EDC relative to the COOH groups of PEG and stirred for 1 h at room temperature. Then, 200 mL of methanol was added and the product was precipitated in cold diethyl ether. The precipitate was harvested by filtration and the methanol washing, precipitation and filtration procedure was repeated twice. A white powder was collected and further dried under vacuum. The polymer was characterized by ^{1}H NMR to calculate the degree of substitution (DS). DS was confirmed after addition of TAIC as described in section 4.2.3. Yield: 85% for PEG linear, 88% for PEG 8-arm, NMR ($CDCl_3$): δ = 4.42 (2H, TAIC shift CH_2OH) 4.24 (2H, t, terminal PEG CH_2), 3.62 (PEG backbone), 2.84 (4H, m, $2CH_2$ NHS), 2.71 (2H, t, NOC(O)CH_2), 2.49 (2H, t, NOC(O)$CH_2CH_2CH_2$), 2.06 (2H, p, NOC(O)CH_2CH_2).

4.2.5 Polymer characterization

The obtained polymers were characterized by gel permeation chromatography (GPC) and NMR spectroscopy. The molecular weights were determined by GPC using a PLgel 5μm MIXED-D column (Polymer Laboratories). The column temperature was set to 65 °C and DMF containing 10 mM LiCl was used as eluent. The elution rate was set to 1 mL/min and the sample concentration was 5 mg/mL. Calibration was performed using poly(ethylene glycol) standards of narrow and defined molecular weights (PSS Polymer Standards Service GmbH, Mainz, Germany).

The polymers were also characterized with ^{1}H NMR spectroscopy on an Agilent 400 MHz spectrometer. Chemical shifts were referred to the residual solvent peak (δ= 7.26 ppm for $CDCl_3$ and 4.79 ppm for D_2O). Number average molecular weight (M_n) determination by ^{1}H NMR was based on the integral ratio of the PEG mid block (904 protons) to monomer proton content.

4.2.6 Differential Scanning Calorimetry (DSC)

The lower critical solution temperature (LCST) of the obtained deprotected PEG-NIP-HPMACys-DBA (PNC(D)) triblock polymers was measured using a Discovery DSC (TA Instruments, New Castle, DE, USA). PNC(D) was allowed to dissolve for 4 hours at 4 °C in a concentration of 10 wt% in PBS before measuring. Ten μL was transferred into an aluminum sample pan and the pan was hermetically capped. Thermograms were recorded in triplicate from 0 to 70 °C, using a heating rate of 5 °C/min. The LCST was determined as the onset temperature in the thermogram.

4.2.7 Rheological characterization

Rheological analysis of the hydrogels was performed on a Discovery HR-2 rheometer (TA Instruments, New Castle, DE, USA), using a 20 mm steel cone (1°) geometry equipped with a solvent trap. Temperature sweeps were performed from 4 to 50 °C at a heating rate of 1 °C/min. Time sweeps were performed for 4 h at 37 °C. For all measurements a frequency of 1 Hz and a strain of 1% was applied. This strain and frequency were previously determined to be within the linear viscoelastic region of these polymer solutions and hydrogels.[19]

4.2.8 Hydrogel preparation

Cylindrically shaped hydrogels of 100 μL were prepared in plastic molds with a diameter of 4 mm. Separate solutions of PNC(D) and PEG cross-linker were prepared in volumes of 75 μL and 25 μL PBS, respectively. PNC(D) polymers were dissolved at 4 °C for 3 hours, while PEG cross-linkers were dissolved for 30 min at 4 °C to limit premature hydrolysis. Upon complete dissolution, the PEG cross-linker solution was added to the PNCD solution, shortly mixed and transferred into the mold using a positive displacement pipette. The molds were capped and placed at 37 °C for 3 hours to allow physical and chemical cross-linking.

4.2.9 Dynamic mechanical analysis

Hydrogels were prepared as described in section 4.2.8. The Young's modulus of the obtained hydrogels was determined on a Q800 DMA (TA Instruments, New Castle, DE, USA) in triplicate after 3 or 24 hours cross-linking at 37 °C. Additionally, 24 h cross-linked hydrogels were incubated for 3 h in PBS or PBS containing 20 mM TCEP to reduce possibly formed disulfide bonds and were subsequently measured by DMA. A compression of 0.01 N/min till 0.1 N was applied to the hydrogels at room temperature. The Young's modulus was determined from the linear region of the stress-strain curve between 10 and 15% strain.

4.2.10 GPC analysis of lysozyme ligation to the hydrogel components

To study the selectivity of the chemical cross-linking reactions, the possible ligation of lysozyme to the hydrogel components was analyzed by GPC. PEG 8-arm thioester, PEG 8-arm NHS and PNC were dissolved in a concentration of 10 mg/mL in PBS, either with or without 10 mg/mL lysozyme. After 5 hours of incubation at room temperature, the molecular weights the polymers and proteins present in the mixtures were measured by GPC using a Superdex 75 column and PBS as solvent. Analysis was performed by RI detection and UV detection at 210 and 280 nm. A flow of 0.5 mL/min and a run time of 60 min were applied.

4.2.11 Lysozyme ligation to dual cross-linked hydrogels

Possible protein ligation to PNC-PEG 8-arm thioester and PNC-PEG 8-arm NHS hydrogels was studied using lysozyme as a model protein by measuring the amount of non-grafted protein by release experiments. In detail, stock solutions of 22 wt% PNC, 33 wt% PEG cross-linker and 50 mg/mL lysozyme were prepared. PEG cross-linker (80 μL) and lysozyme (40 μL) were added to PNC (280 μL), mixed and 3 samples of 100 μL were transferred into a cylindrical glass vial (diameter of 5 mm). The final solutions consisted of 15 wt% PNC, 7.5 wt% PEG cross-linker and 0.004 wt% lysozyme. The hydrogels were allowed to form for 16 hours at 37 °C, after which 0.9 mL of PBS buffer pH 7.4 was added on top of the gels. In time, samples of 0.15 mL were taken and replaced by 0.15 mL fresh PBS buffer. The concentration of lysozyme in the different release samples was determined with Acquity UPLC using a BEH C18 1.7 μm, 2.1 x 50 mm column. As eluent a gradient from 0 to 100% of eluent A was used, where eluent A was H_2O/acetonitrile/TFA 95/5/0.1% and eluent B was 100/0.1% acetonitrile/TFA. The injection volumes were 5 μL, the flow rate was set at 0.25 mL/min and detection was done at 210 nm.

4.2.12 Cell viability assays

An MTS assay was performed to assess cytocompatibility of the hydrogels described in this study. C166 mouse endothelial cell line was chosen as a representative of healthy tissue. The cells were seeded on a 96 well plate with 6,000 cells per well and 100 μL DMEM medium including antibiotics was added. Two different experiments were performed. First, hydrogels of 50 mg wet weight consisting of 7.5 wt% PNC and 3.8 wt% PEG cross-linker, were allowed to form for 3 hours as described in section 4.2.8 and were subsequently introduced in the medium on the cell layer. After 16 hours of incubation at 37 °C, the hydrogels were removed and the medium was washed for four times to remove reaction products that could interfere with the MTS assay. In the second experiment, 50 mg prefabricated hydrogels were added to 100 μL medium without cells and incubated for 2 hours. Then, 50 μL of this medium was added to the cell layer and further incubated for 16 hours. In this leachables

assay, the influence of soluble products that are released from the hydrogels on the cell viability was tested. Again, the medium was washed for four times with PBS and subsequently replaced with 100 μL medium. Then, 20 μL MTS reagent was added and further incubated for approximately 2 hours to develop the color. After mixing, absorption was measured at 490 nm on a Biochrom EZ microplate reader. Metabolic activity of the cells was normalized to a negative control (medium, 100% value) and compared to a positive control (medium + 100 μM SDS, 0% value). Brightfield microscopy pictures were taken using a Keyence BZ-9000E microscope before adding MTS to analyze the cell shape with a 20x Nikon objective.
Since a potential application of the hydrogels of this study is e.g. for cartilage tissue engineering[25] a Live/Dead viability assay (calcein AM/ethidium homodimer, Life Sciences, USA) was performed on chondrocytes following previously reported procedures.[38, 39] In short, equine chondrocytes were harvested from full thickness cartilage. Chondrocytes were encapsulated in the hydrogels at a concentration of 5×10^6 cells/mL. Hydrogels containing cells were allowed to form for 3 hours before addition of DMEM medium. Viability was visualized after 7 days of culture using a light microscope (Olympus, BX51, USA) with excitation/emission filters set at 488/530 nm and 530/580 nm to detect living (green) cells and dead (red) cells respectively.

4.2.13 Swelling and degradation study

Hydrogels of 100 μL were prepared as described in section 4.2.8. Three different groups were analyzed in this study, containing 15 wt% PNC(D) and 7.5 wt% PEG 8-arm NHS, 7.5 wt% PNC(D) and 3.8 wt% PEG 8-arm NHS or 15 wt% PNC(D) and 3 wt% PEG linear NHS, all corresponding to a 1:1 molar ratio of functional groups. After incubation of the polymer solutions at 37 °C for 3 hours, the formed hydrogels (4.3 mm diameter, 5.0 mm height) were pushed out from the mold and transferred into a 2 mL glass vial. The hydrogel weight was recorded and 1 mL PBS containing 0.02% NaN_3 was added. At regular time intervals, excess of buffer was removed, the weight of the hydrogels was measured and 1 ml of fresh PBS was added. Measurements were performed twice a week during the first 5 weeks and then once a week until complete degradation or until 6 months. The swelling ratio is defined as the weight at a certain time point (W_t) divided by the initial hydrogel weight (W_0) (Swelling ratio = W_t/W_0). After measuring, 1 mL of fresh buffer was added and the hydrogels were further incubated at 37 °C. Finally, solutions after full degradation were lyophilized, redissolved in D_2O and analyzed by ^1H NMR.

4.3 Results and Discussion

4.3.1 Polymer synthesis and characterization

ABA triblock copolymers consisting of a hydrophilic poly(ethylene glycol) (PEG) B block were synthesized by free radical polymerization. The A block consisted of three different monomers: (1) *N*-isopropylacrylamide (NIPAAm) to render thermoresponsive polymers, (2) *N*-(2-hydroxypropyl)methacrylamide-cysteine (HPMA-Cys) to allow chemoselective cross-linking and (3) dimethyl-γ-butyrolactone acrylate (DBA) to obtain gels with tunable degradation rates. The polymer structure is shown in figure 4.1. After polymerization, the protecting groups present on the amine and thiol groups of cysteine were removed by TFA and iodine treatment, respectively, as described previously.[19] The successful deprotection was confirmed by ^{1}H NMR, TNBSA and Ellman's assays following established procedures.[19] The average molar incorporation of cysteine was 6%, corresponding to an average of 21 cysteine moieties per polymer chain, which was only slightly lower than the feed percentage of 7% for this monomer. As reported in table 4.1, the molar ratios of the three monomers in the obtained polymer as calculated by ^{1}H NMR were in close agreement with the feed ratios. The synthesized polymers are abbreviated as PNC, PNCD2.5, PNCD5, PNCD7.5 and PNCD10 for a molar content of DBA of 0, 2.5, 5, 7.5 and 10 %, respectively. The number average molecular weights measured by GPC were in line with the values calculated from ^{1}H NMR analysis whereas GPC measurements showed polydispersities ranging from 2.1 to 2.4, which is often found for free radical polymerization of multi block copolymers.[40] Based on ^{1}H NMR and GPC, PEG 10 kDa B blocks were flanked by A blocks of an average molecular weight of 21 kDa. The polymers were synthesized in a high yield of 88 % and obtained in a yield of 53 % after full deprotection.

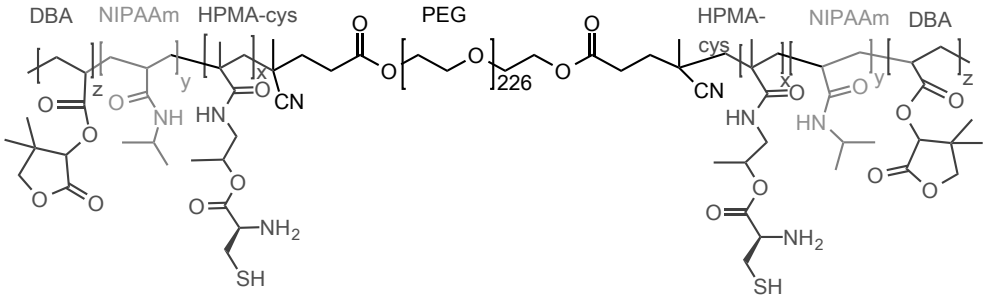

Figure 4.1. Chemical structure of PNCD polymers, consisting of a 10 kDa PEG mid block, flanked by random monomers of HPMA-cys, NIPAAm and DBA.

Table 4.1. Polymer characteristics of ABA triblock copolymers synthesized by radical polymerization having a PEG10000 B block and random A blocks of NIPAAm, HPMA-Cys and DBA (triblock abbreviated as PNCD).

	% Cys		% NIPAAm		% DBA		M_n (kDa)[a]	M_n (kDa)[b]	M_w/M_n [b]
	Feed	NMR	Feed	NMR	Feed	NMR			
PNC	7.0	6.2	93.0	93.8	0	0	20-10-20	43.0	2.36
PNCD 2.5	7.0	6.9	90.5	90.8	2.5	2.3	23-10-23	53.9	2.16
PNCD 5	7.0	5.7	88.0	89.0	5.0	5.3	20-10-20	52.4	2.17
PNCD 7.5	7.0	5.9	85.5	86.1	7.5	8.0	19-10-19	53.2	2.19
PNCD 10	7.0	5.9	83.0	83.8	10.0	10.3	21-10-21	53.0	2.15

[a] Determined by ^{1}H NMR. [b] Determined by GPC.

* PNCD: PEG-NIP-HPMACys-DBA triblock, structure shown in figure 1.

Poly(ethylene glycol) (PEG) cross-linkers either based on a linear PEG having a molecular weight of 2,000 Da or an 8-arm PEG of 20,000 Da with thioester or NHS terminal reactive groups were synthesized. The polymer structures and corresponding ^{1}H NMR spectra are shown in figure 2. Calculations of the degree of substitution (DS) for PEG thioester cross-linkers were based on the integral of the terminal CH_3 group at 1.21 ppm, while for NHS functionalized PEG calculations were performed using the peak at 2.84 ppm, which corresponds to the 2 CH_2 groups of the NHS ring. DS was confirmed by quantifying the unreacted PEG OH groups after addition of trichloroacetyl isocyanate (TAIC) to the NMR sample. PEG linear cross-linkers were synthesized with a high DS of 88 and 90% for thioester and NHS functionalities respectively. Also, 8-arm PEG cross-linkers were obtained with a high DS of 92% for PEG-thioester and 94% for PEG-NHS, respectively.

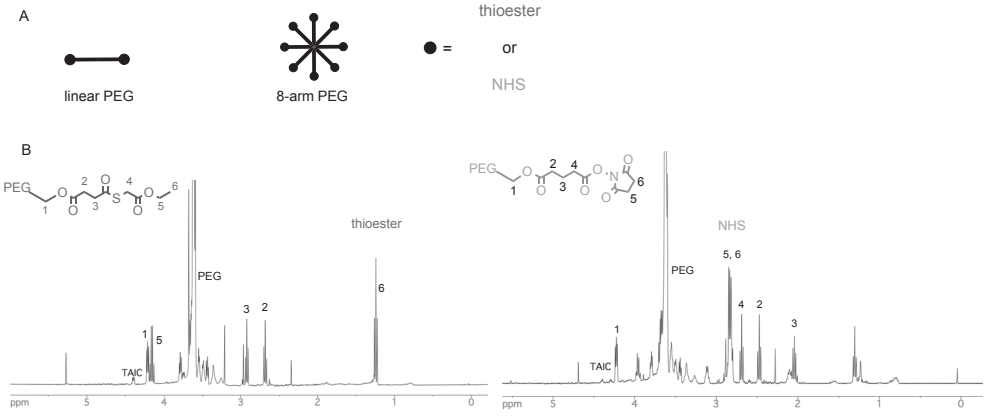

Figure 4.2. A) Schematic display of the cross-linkers used in this study, synthesized from a linear PEG 2,000 or 8-arm PEG 20,000 with either thioester or NHS functionalities. B) ^{1}H NMR of 8-arm PEG thioester and NHS cross-linkers in $CDCl_3$. Peak 6 of PEG thioester at 1.21 ppm and Peak 5,6 of PEG NHS at 2.84 ppm indicate peaks that were used to calculate the degree of substitution for thioester and NHS groups respectively.

4.3.2 Gel formation and mechanical properties

The PNCD polymers were dissolved in PBS at 4 ºC and the thermoresponsive properties of the obtained polymer solutions were measured both by rheology and DSC (figure 4.3). Rheological analysis showed that with increasing temperature, a sudden increase in storage modulus (G') as well as a crossover of G' and G'' (SI-figure 4.1A) was observed, which indicates the phase transition from a liquid solution to a physically cross-linked network. By increasing the DBA content in the polymers, this phase transition occurred at lower temperatures as a result of an increase in hydrophobicity of the polymers. DSC results confirmed that the LCST values of the obtained polymers decreased with increasing DBA content in the polymer. Noteworthy, a linear relationship was obtained between the molar percentage of DBA in the polymers and their LCST (figure 4.3B), which is in line with literature.[28]

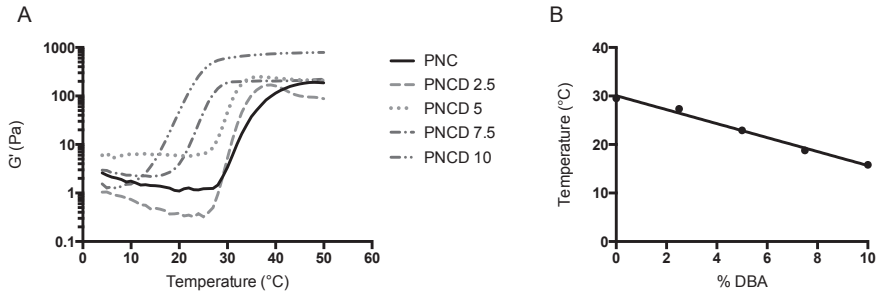

Figure 4.3. Effect of DBA content in thermosensitive PNCD polymers on A) gelation temperature as measured by rheology in 20 wt% concentration and B) LCST as measured by DSC in 10 wt% concentration.

Physically and chemically cross-linked hydrogels were prepared by mixing an aqueous solution of thermoresponsive cysteine functionalized PNCD polymers with a solution of (thio)ester functionalized PEG cross-linkers at 37 °C. The mechanism of chemical cross-linking is shown in figure 4.4.

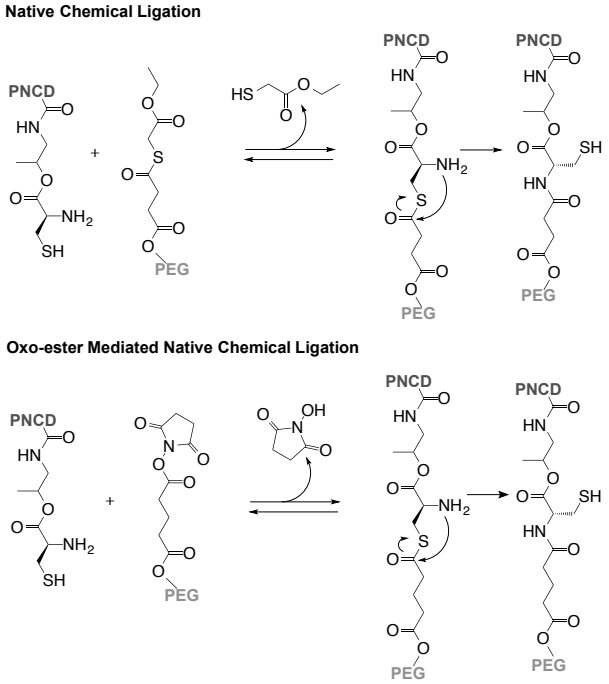

Figure 4.4. Native chemical ligation (NCL) and oxo-ester mediated native chemical ligation (OMNCL) cross-linking mechanisms between cysteine functionalities of PNCD and thioester or oxo-ester functionalities of PEG cross-linkers.

An immediate network formation was visualized at 37 °C by a lack of flow when tilting the vial upside down, as expected from the thermosensitive nature of the polymers. The gelation kinetics and mechanical properties were further analyzed by rheology at 37 °C. Again, an immediately formed physically cross-linked network was obtained characterized by a higher storage modulus than loss modulus (SI-figure 4.1B). In time, the storage modulus increased further, indicating the formation of a more densely cross-linked network due to additional chemical cross-linking. This resulted in 8 to 120 fold higher G' values after 4 hours compared to solely thermal physically cross-linked PNC hydrogels. As depicted in figure 4.5A and B, when changing from a PEG linear to a PEG 8-arm cross-linker, the storage moduli after 3 hours of network formation increased from 1.8 kPa to 8.8 kPa for thioester functionalized PEG and from 4.7 to 24.3 kPa for NHS functionalized PEG. As expected, the increase in number of functional groups per cross-linker was associated

with a 5-fold increase in mechanical strength. Similarly, replacing thioester groups by NHS groups resulted in approximately a 2.5 fold increase in storage moduli. The higher mechanical strength of the OMNCL cross-linked hydrogels is most likely a result of the higher reaction efficiency, in line with previous studies. [21] Furthermore, increasing the total polymer concentration resulted in an increase in mechanical strength (figure 4.5C), again in line with literature.[41]

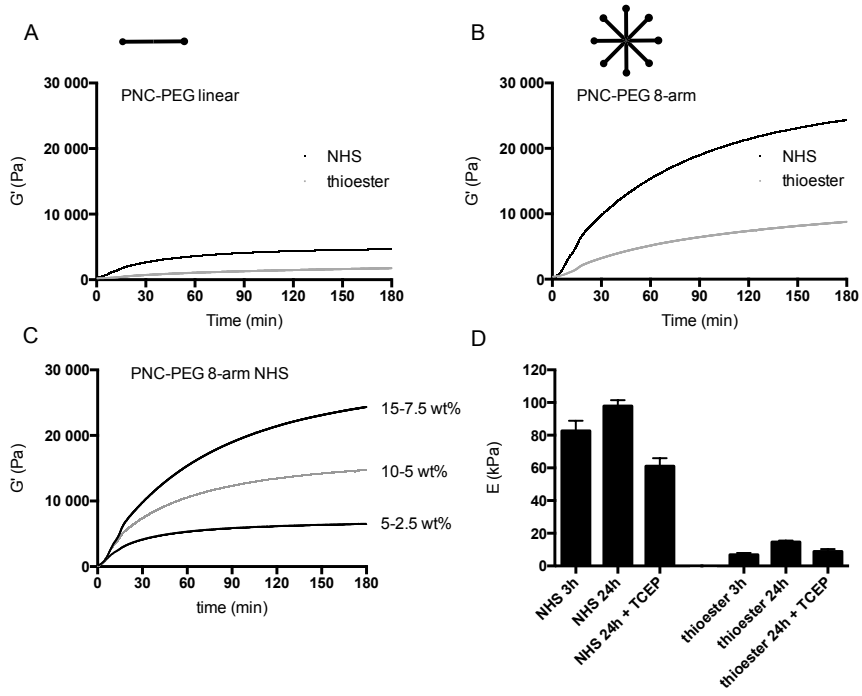

Figure 4.5. A) Storage modulus (G') as a function of time for hydrogels containing linear PEG cross-linker: 15 wt% PNC + 3 wt% PEG linear. B) G' as a function of time for hydrogels containing 8-arm PEG cross-linker: 15 wt% PNC + 7.5 wt% PEG 8-arm. C) G' for three different polymer concentrations of PNC-PEG 8-arm NHS: 15-7.5 wt%, 10-5 wt% and 5-2.5 wt%. D) Young's modulus as measured by DMA: 15 wt% PNC + 7.5 wt% PEG 8-arm after different times of gelation and after incubation in either PBS or PBS containing 20 mM TCEP. Data are shown as mean ± standard deviation (n=3).

Additionally, the mechanical properties of the obtained hydrogels after 3 or 24 hours of hydrogel formation were measured by compression measurements. As shown in figure 4.5D, stiffer hydrogels were obtained using NHS functionalized PEG compared to thioester functionalized PEG, similar to the data obtained with oscillatory shear rheological measurements. The reported Young's modulus showed a further increase in mechanical strength in time. This could be ascribed to the

formation of additional cross-links by disulfide bonds that form with slower kinetics than (oxo-ester mediated) native chemical ligation.[21] After NCL or OMNCL, an amide bond is formed and a free thiol remains available for additional cross-linking, which could further stabilize the hydrogel structure. The formation of these additional disulfide bonds was demonstrated by incubating 24 h cross-linked PNC – PEG 8-arm hydrogels in either PBS or PBS containing 20 mM TCEP to reduce disulfide bonds, following previously reported procedures.[18] After 3 hours of incubation, the stiffness of the hydrogels was measured with dynamic mechanical analysis (DMA). As expected, the Young's modulus of hydrogels that were incubated in 20 mM TCEP decreased from 98 ± 4 kPa to 61 ± 5 kPa for PNC-PEG NHS hydrogels and from 11 ± 1 kPa to 9 ± 1 kPa for PNC-PEG thioester hydrogels as a result of the reduction of disulfide bonds (figure 4.5D).

Additionally, we investigated the influence of a non-stoichiometric ratio of cysteine:thioester functional groups on the gel formation. Interestingly, changing this ratio did not have a significant effect on the mechanical properties in case of the formulations using an 8-arm PEG cross-linker (figure 4.6). In contrast, changing the cysteine:thioester ratio from 1:1 to 1:0.5 for the linear PEG cross-linkers led to a 25% lower storage modulus after 4 hours, while changing the ratio to 1:2 resulted in a 51% lower G'. An excess of thioester functionalities blocks the cysteine groups that are available, resulting in dangling chains that form a dead end. On the contrary, a shortage of thioester groups results in a less tightly cross-linked network. As the PEG 8-arm thioester has 8 functionalities per chain, not all thioester groups need to react before a cross-link is formed. Similar results were obtained for fully cross-linked hydrogels that were measured after 24 h by DMA (figure 4.6C), showing that a non-stoichiometric ratio in case of linear PEG cross-linkers not only influenced the gelation kinetics, but also the final mechanical properties. While a shortage of thioester groups had a considerable effect on the gel formation kinetics, an excess of thioester groups also led to lower final moduli of the hydrogel as a result of the dangling chain ends. In case of the 8-arm cross-linker, only small differences in the final moduli were found. Therefore, besides increasing the overall mechanical properties, hydrogels with 8-arm cross-linkers have the advantage to be less susceptible to a non-stoichiometric ratio of functional groups.

Taken altogether, with limited changes in the overall polymer concentration, the mechanical strength of the hydrogels significantly increased by using an 8-arm PEG cross-linker and using NHS functionalities instead of thioester groups.

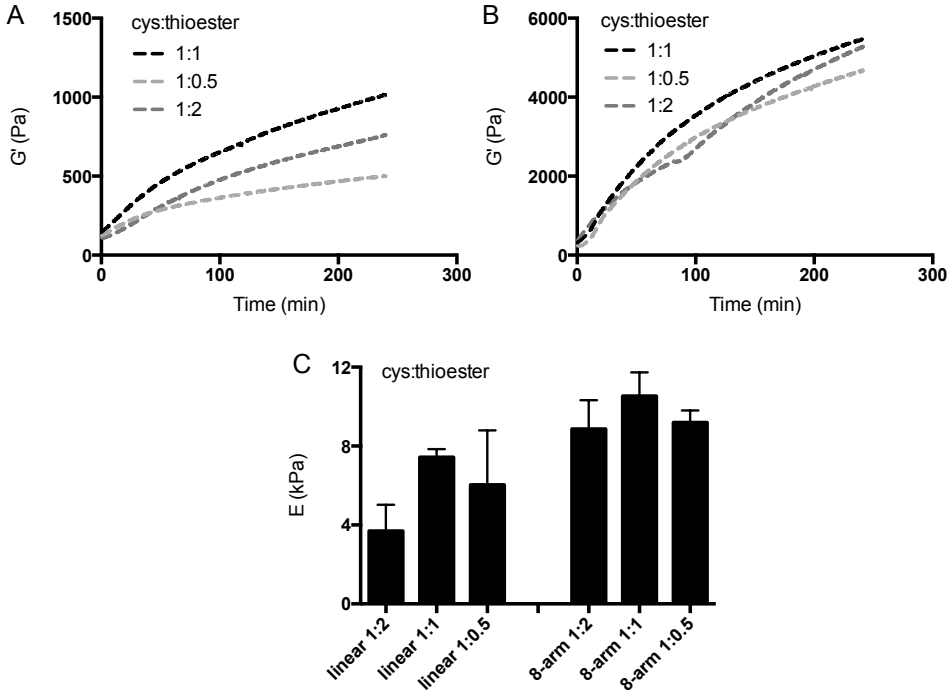

Figure 4.6. Effect of changing cysteine:thioester ratio on mechanical properties as measured by rheology for A) linear PEG cross-linkers and B) 8-arm PEG cross-linkers. C) Young's modulus as measured by DMA for different cysteine:thioester ratios after 24 hours of gel formation. Data are shown as mean ± standard deviation (n=3).

4.3.3 Protein compatibility

Injectable hydrogels for biomedical applications require in many cases the incorporation of proteins e.g. in drug delivery or growth factors for tissue engineering purposes.[42,43] Therefore, it is of utmost importance to use cross-linkers with functional groups that do not interfere with the protein structure and still allow release of the incorporated active proteins.[44] Lysozyme was used as a model protein since its size (molecular weight =14 kDa, hydrodynamic diameter = 4.1 nm [45]) and positive charge at physiological pH (isoelectric point = 11.35 [46]), are similar to many growth factors.[47] We first studied the potential ligation of lysozyme to the individual hydrogel components under physiological conditions by GPC. The molar ratio of NH_2 of lysozyme to NHS or thioester functionalities of PEG in the mixtures was 1:1, while the molar ratio of NH_2 of lysozyme to SH of PNC was 2:1. Figure 4.7 shows the GPC chromatograms with UV detection after at least 4 hours incubation of the hydrogel building blocks with lysozyme. Native lysozyme displays a peak at 32 minutes, and no shift was found for lysozyme mixed with either PNC or PEG thioester. Therefore, it can be concluded that mixing lysozyme with PNC or PEG

thioester did not cause any significant ligation between the functional groups of the protein and the polymers. This was expected since all 8 cysteines present in lysozyme are paired in disulfide bridges.[48] In contrast, lysozyme mixed with PEG NHS showed much shorter retention times of only 16 minutes, indicating that approximately 90% of lysozyme was conjugated to the PEG NHS functionalized cross-linkers, resulting in the formation of a higher molecular weight product. This result is not surprising as it is well known that NHS groups can react with amino groups of e.g. lysine moieties that are present in proteins.[49,50]

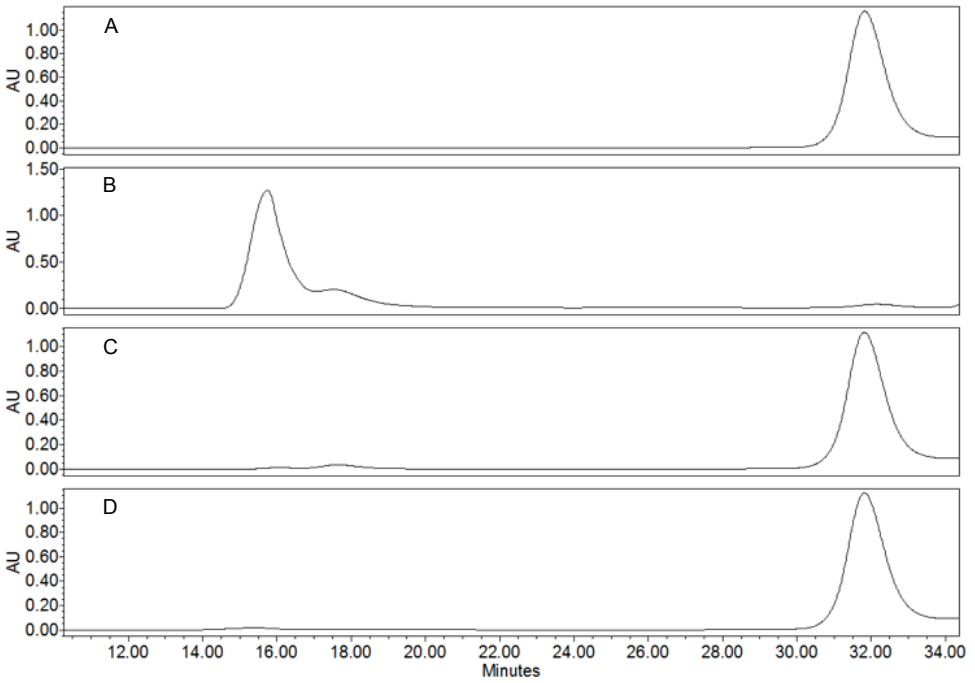

Figure 4.7. GPC chromatograms of lysozyme incubated with different hydrogel components: PNC, PEG NHS or PEG thioester in PBS buffer as measured at 210 nm. A) Lysozyme; B) Lysozyme + PEG NHS; C) Lysozyme + PEG thioester; D) Lysozyme + PNC.

In the experiments reported above, we only studied the potential reaction of lysozyme with the individual hydrogel components. However, during hydrogel preparation thiol side groups of thermosensitive polymers are present that compete with the amines of lysozyme for reaction with the NHS esters. In the hydrogels, the molar ratio of NH_2 of lysozyme was 1:20 to NHS and SH groups. As has been previously reported in literature, in a competitive reaction between amines and cysteines, NHS-activated carboxylic acids preferentially react with the thiol functionality of cysteine.[21,22] Because of the high molar access of SH over NH_2 groups and their higher reactivity, the probability of reaction of lysozyme with PEG NHS is likely low. To investigate

this, a protein release study was performed to study whether lysozyme reacted with the hydrogel components during hydrogel formation. These network-grafted protein molecules are immobile and therefore unable to release in the surrounding medium. The purpose of this release study was to compare the extent of lysozyme release from the PNC-PEG thioester and PNC-PEG NHS hydrogels and to correlate this with the potential grafting of lysozyme to the hydrogel building blocks. Figure 4.8 shows the release of lysozyme from two hydrogel formulations, using either thioester or NHS functionalized PEG 8-arm cross-linkers. As anticipated, the extent of grafting was low and more than 90% of the loaded lysozyme was released from both gels after 2 days, at which time a plateau in release was obtained. This indeed confirms that the reaction between NHS and cysteine is preferred over a reaction between NHS and amino groups of lysine residues of lysozyme.

The amount of lysozyme that was incorporated in the hydrogels was based on literature procedures.[51] It must be noted that when more lysozyme will be loaded in the hydrogel, this will likely increase the potential of a side reaction of lysozyme with the NHS groups, which could have an effect on swelling, volume transition temperature and degradation. In addition, the presence of native proteins may have some effect on the hydrogel properties after injection of the hydrogel precursors *in vivo*. On the contrary, in some applications such as growth factor incorporation, covalent attachment of a protein to the hydrogel can induce beneficial cell differentiation, migration or proliferation, so grafting as such is not necessarily unfavorable.[43,52,53]

In line with the mechanical characteristics, hydrogels containing NHS groups released lysozyme over a slightly longer time frame than hydrogels containing thioester groups. Fast release of lysozyme from the hydrogels was expected as lysozyme is a relatively small protein and this finding is in line with previous studies.[51] When longer release times are needed, this could potentially be accomplished by increasing polymer concentrations, increasing the number of functional groups per polymer chain or by incorporating lysozyme in microparticles that are embedded in the hydrogel.[41,54]

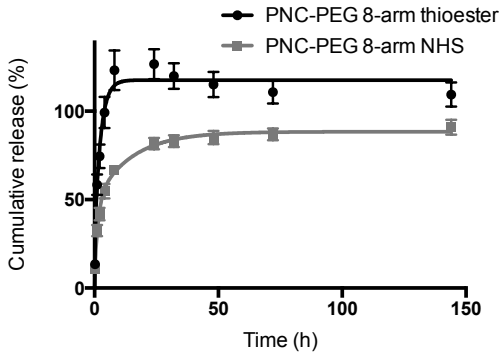

Figure 4.8. Cumulative release of lysozyme from PNC-PEG 8-arm thioester or PNC-PEG 8-arm NHS hydrogels. Hydrogel concentrations were 15 wt% PNC + 7.5 wt% 8-arm PEG. Data are shown as mean ± standard deviation (n=3).

4.3.4 Cell viability

Cell survival in the presence of chemoselectively cross-linked PNC-PEG 8-arm NHS or PNC-PEG 8-arm thioester hydrogels was assessed using two different cell viability assays. Equine chondrocytes were encapsulated in the hydrogels and their viability was studied after 7 days of culture using a live/dead assay (SI-Figure 4.2). Most cells showed simultaneously green cytoplasmic fluorescence and red nuclear fluorescence in the live/dead assay after 7 days. Therefore, it was difficult to draw conclusions about their viability, although overlay pictures might indicate a better cell viability for PNC-PEG 8-arm NHS hydrogels. For this reason, the effect of the hydrogel leachables on the metabolic activity of a mouse endothelial cell line was analyzed with an MTS assay. Also taking into consideration that an MTS assay gives quantitative results, evaluation of the cell viability using this assay was preferred over a live/dead assay. In an MTS assay, a tetrazolium salt is converted to an aqueous soluble formazan product by mitochondrial activity of viable cells, which can be measured colorimetrically.[55]

Two different experimental set-ups were used to evaluate the cell viability. In the first set-up, prefabricated hydrogels, without extraction of possible leachable products, were added to medium containing cells and incubated for 16 hours. After removal of the gels and several washing steps, the metabolic activity was measured. As shown in figure 4.9, cell viability was not affected by the PNC-PEGNHS hydrogels, while addition of the PNC-PEGthioester hydrogels caused a decrease in viability to 13 ± 7 %. Based on literature findings, this decrease in cell viability is most likely caused by the release of ethyl thioglycolate after cross-linking (as schematically shown in figure 4.4).[20] In the second set-up, we further tested this hypothesis using an assay developed to test the cytotoxicity of leachables that are extracted from gels.[56] After incubating

prefabricated hydrogels for two hours in medium, the medium without the gel was added to the cells and further incubated for 16 hours. The MTS results showed a much lower cell viability upon incubation of the extract of PNC-PEGthioester hydrogel as compared to PNC-PEGNHS hydrogel extract. Finally, additional confirmation was obtained after visual analysis of the cell shape (SI-figure 4.3). While the cell shape was hardly affected after contact with the leachables of the PNC-PEGNHS hydrogels, the cells clearly lost their healthy, stretched shape upon incubation with the extract of the PNC-PEGthioester hydrogel. Taken together, PNC-PEGNHS hydrogels have a substantially better cytocompatibility than the PNC-PEGthioester hydrogels, which likely can be ascribed to the reaction product formed (namely ethyl thioglycolate) during the formation of the PNC-PEGthioester hydrogels.

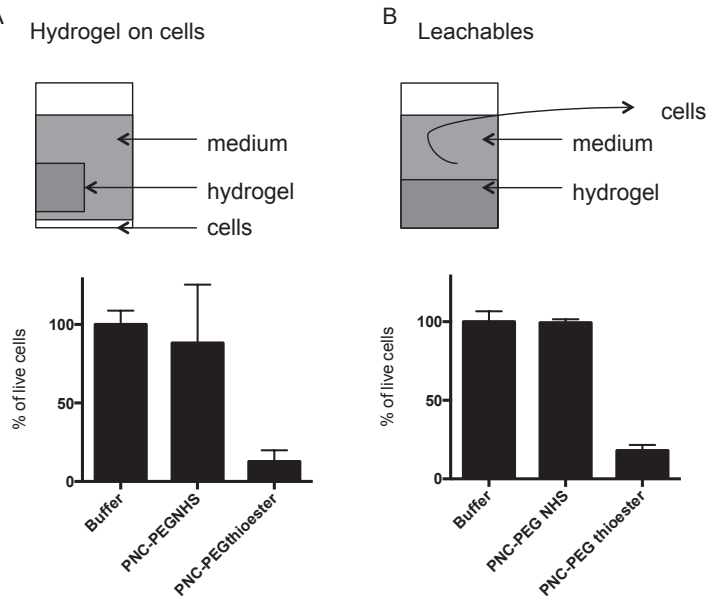

Figure 4.9. Cumulative release of lysozyme from PNC-PEG 8-arm thioester or PNC-PEG 8-arm NHS hydrogels. Hydrogel concentrations were 15 wt% PNC + 7.5 wt% 8-arm PEG. Data are shown as mean ± standard deviation (n=3).

4.3.5 Hydrogel degradation

The degradation of the dual cross-linked hydrogels was assessed under physiological conditions at 37 °C and pH 7.4. Only the NHS-functionalized PEG cross-linkers were included in this study, due to their favorable gelation kinetics, mechanical properties and cytocompatibility. Hydrolysis of the ester bonds present in the hydrogel network can occur at three different positions: 1) hydrolysis of the ester bonds between the PEG mid block and thermosensitive outer blocks; 2) hydrolysis of ester bonds within the chemical cross-links (figure 4.4); 3) hydrolysis of the ester bonds in the lactone

ring of DBA. Hydrolysis of ester bonds at positions 1 and 2 leads to dissolution of the hydrogel, whereas hydrolysis at position 3 increases hydrophilicity and thus the swelling of the hydrogel network. Previous studies have shown that at physiological pH, only the ester bonds in the DBA ring are hydrolyzed and not the ester bond between the ring and the polymer backbone, thereby preventing formation of additional soluble byproducts.[28] Three different hydrogel formulations were tested, exhibiting storage moduli between 5 and 24 kPa after 3 hours of hydrogel formation (SI-Figure 4.4). These formulations were chosen to assess the influence of concentration and the difference between a linear and 8-arm PEG cross-linker on the degradation rates. PNC was mixed with a linear PEG cross-linker in a total polymer concentration of 18 wt% and is further abbreviated as 'linear'. PNC-PEG 8-arm hydrogels were studied at a total polymer concentration of 11 or 22 wt% and abbreviated as '8-arm low' and '8-arm high', respectively. In all cases, a 1:1 molar ratio between NHS and cysteine functionalities was used to obtain efficient cross-linking. A low concentration linear PEG hydrogel formulation was not included in the degradation study, since the mechanical properties were too weak to allow the formation of a stable hydrogel. As expected from our rheology experiments (figure 4.5), hydrogels containing 8-arm PEG cross-linkers and higher polymer concentration formed stronger hydrogels. Degradation studies of the PNC-PEGNHS hydrogels lacking DBA functionalities, showed slow degradation and even after 6 months the hydrogels were still not fully degraded into water soluble products (figure 4.10). Likely, the ester bonds are located in the hydrophobic domains of the hydrogel network, therefore limiting the accessibility of water molecules. Interestingly, '8-arm low' and 'linear' did not show any increase in swelling during the degradation study, while '8-arm high' hydrogels swelled in the first couple of days to two times of their original weight (SI-Figure 4.5). The denser network of this hydrogel formulation was most likely not fully cross-linked when it was placed in buffer. Therefore, an increase in swelling was possible until thermodynamic equilibrium was reached. After 6 months, 'linear', '8-arm low' and '8-arm high' had remaining gel weights of 29%, 12% and 13% respectively. The highest remaining gel weight of 'linear' was probably caused by the shorter PEG chains that are incorporated in the network, thereby reducing the overall hydrophilicity of the polymer network. A similar influence of the molecular weight of the PEG cross-links on the degradation rate has been previously reported by Zustiak et al.[57]

To increase the degradability of the hydrogels, PNCD polymers containing DBA moieties were mixed with PEG-NHS cross-linkers, using the concentrations as described above. As depicted in figure 4.10, the degradation rate accelerated and decreased from more than 6 months for the formulations without DBA moieties, to only 12 to 57 days for formulations containing different amounts of DBA, which is in line with previous studies[28,30]. During hydrolysis, the lactone ring of DBA opens

and yields at pH 7.4 networks with negatively charged carboxylate ions. Hence, the hydrophilicity of the polymer chain increases and the polymers exhibit a charge repulsion between the polymer chains in the hydrogel, which causes an increase in water uptake. As a consequence, the ester groups in the cross-links are more exposed to water and therefore more susceptible for hydrolysis. Indeed, during incubation the hydrogels swell up to 7 times of their original weight, after which they fully dissolve. As was expected from the rheology measurements, the hydrogels of PNCD-PEG 8-arm high were the most stable, as a result of their high cross-link density. We expect that even a larger range of degradation times could be obtained by further varying the DBA content. Figure 4.10D summarizes the degradation times of the different hydrogel formulations and shows a linear relationship between DBA content and time till full dissolution, thereby underlining the ability to control the degradation rates using these polymeric hydrogels.
Solutions after full degradation were lyophilized, redissolved in D_2O and measured by ^1H NMR to analyze the chemical nature of the soluble degradation products. The results showed the formation of a copolymer with completely hydrolyzed DBA lactone ring (SI-figure 4.6), as has also been demonstrated in previous work.[28]

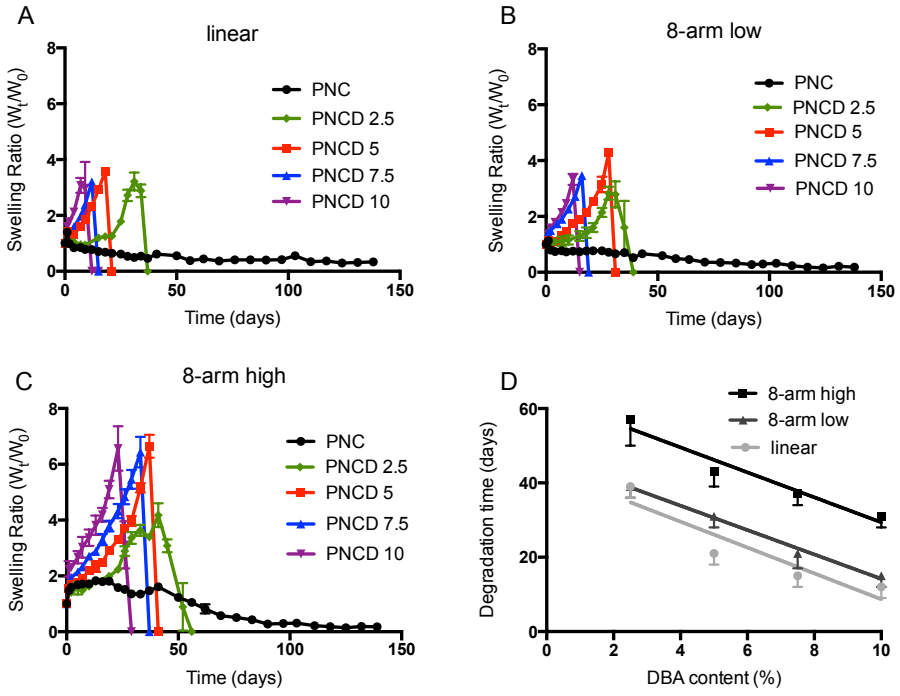

Figure 4.10. Swelling ratio (W_t/W_0) in time of three different hydrogel formulations with 0, 2.5, 5, 7.5 and 10% DBA content. A) 15 wt% PNC(D) + 3 wt% PEG linear. B) 7.5 wt% PNC(D) + 3.8 wt% PEG 8-arm. C) 15 wt% PNC(D) + 7.5 wt% PEG 8-arm. Data are shown as mean ± standard deviation (n=3). D) Effect of DBA content on time till full degradation.

4.4 Conclusion

This study evaluated the mechanical properties, cytocompatibility, protein compatibility and degradation kinetics of chemoselective and thermosensitive dual cross-linked hydrogels. After mixing two liquid precursor solutions, consisting of a thermoresponsive polymer and PEG cross-linker, physically cross-linked hydrogels were immediately formed at 37 °C. Mechanically stable hydrogels were obtained after chemoselective cross-linking of the two hydrogel components by native chemical ligation (NCL) or oxo-ester mediated native chemical ligation (OMNCL). The mechanical properties could be enhanced using OMNCL or 8-arm PEG cross-linkers. Additionally, degradation rates were tuned and controlled after incorporation of hydrolysable DBA groups in the hydrogel network. Although the NCL cross-linked hydrogels showed cytotoxicity to endothelial cells, cell viability was not affected after incubation with OMNCL cross-linked hydrogels. The favorable and controllable properties of the studied OMNCL cross-linked hydrogels are attractive for further evaluation in biomedical applications.

Acknowledgements
This work was supported by a grant from the Dutch government to the Netherlands Institute for Regenerative Medicine (NIRM, grant No. FES0908).

Supporting Information

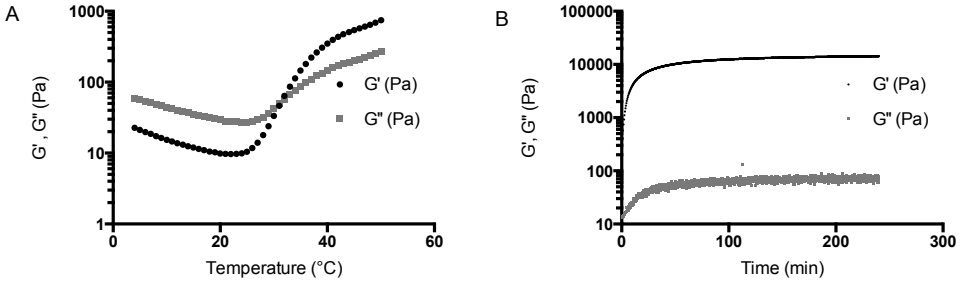

SI-Figure 4.1. A) Storage modulus (G') and loss modulus (G") of hydrogels consisting of 20 wt% PNC as a function of temperature. B) G' and G" of hydrogels containing 7.5 wt% PNC and 3.8 wt% PEG 8-arm NHS as a function of time.

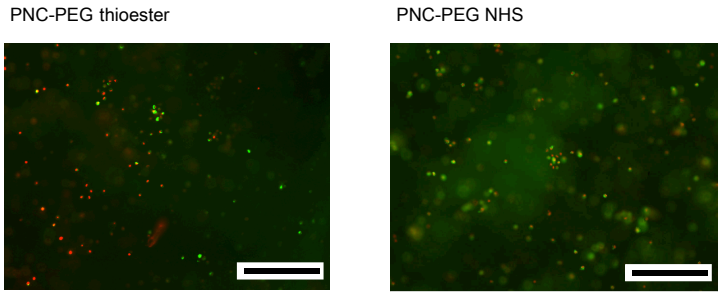

SI-Figure 4.2. Chrondrocyte viability as analyzed by a live/dead assay for PNC-PEG 8-arm thioester and PNC-PEG 8-arm NHS hydrogels (7.5-3.8 wt%) after 7 days, displaying an overlay of green (live) and red (dead) fluorescence. Scale bar represents 200 μm.

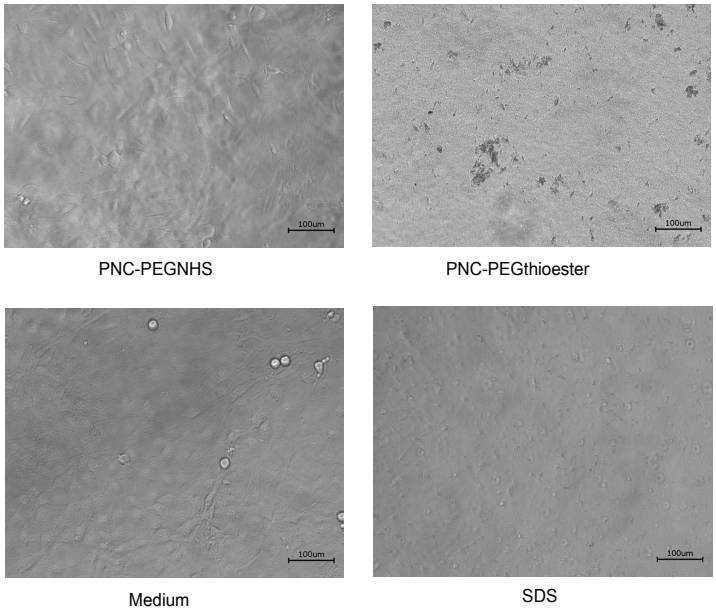

SI-Figure 4.3. Microscopy pictures of C166 mouse endothelial cells after 16 hours of indirect contact with PNC-PEG 8-arm NHS or PNC-PEG 8-arm thioester hydrogels. Medium and PNC-PEGNHS groups show healthy stretched cells and some dividing round cells. PNC-PEG thioester shows necrotic cells and some cell debris. In the SDS condition are cells depicted with solubilized membranes. Scale bar represents 100 μm.

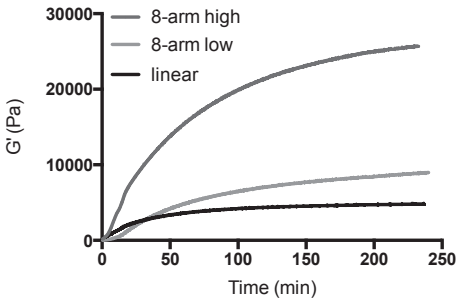

SI-Figure 4.4. Rheology profiles of PNC-PEGNHS hydrogels studied for degradation: 15 wt% PNC + 7.5 wt% PEG 8-arm (8-arm high), 7.5 wt% PNC + 3.8 wt% PEG 8-arm (8-arm low) and 15 wt% + 3 wt% PEG linear (linear).

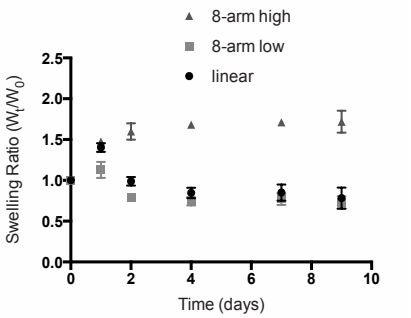

SI-Figure 5. Swelling ratio of PNC-PEG hydrogels during the first 10 days of incubation in PBS. Formulations: 8-arm high (15 wt% PNC + 7.5 wt% PEG 8-arm), 8-arm low (7.5 wt% PNC + 3.8 wt% PEG 8-arm) and linear (15 wt% + 3 wt% PEG linear).

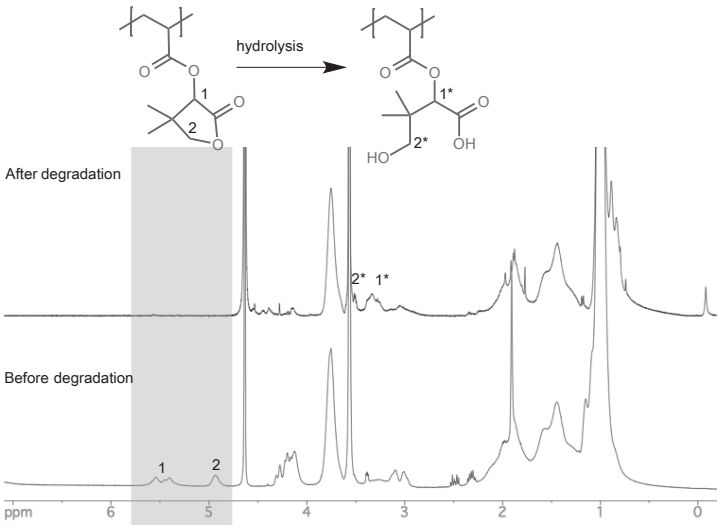

SI-Figure 4.6. ^{1}H NMR of PNCD10 – PEG 8-arm NHS before and after degradation. Grey area shows the peaks of the protons in the DBA ring that disappear after hydrolysis.

References

1. S. J. Buwalda, K. W. M. Boere, P. J. Dijkstra, J. Feijen, T. Vermonden and W. E. Hennink, *J. Controlled Release*, 2014, **190**, 254-273.
2. S. Van Tomme, G. Storm and W. E. Hennink, *Int. J. Pharm.*, 2008, **355**, 1-18.
3. L. Yu and J. Ding, *Chem. Soc. Rev.*, 2008, **37**, 1473-1481.
4. K. H. Bae, L.-S. Wang and M. Kurisawa, *J. Mater. Chem. B*, 2013, **1**, 5371-5388.
5. N. A. Peppas, P. Bures, W. Leobandung and H. Ichikawa, *Eur. J. Pharm. Biopharm.*, 2000, **50**, 27-46.
6. Y. Li, J. Rodrigues and H. Tomas, *Chem. Soc. Rev.*, 2012, **41**, 2193-2221.
7. A. E. Ekenseair, K. W. M. Boere, S. Tzouanas, T. Vo, F. Kasper and A. G. Mikos, *Biomacromolecules*, 2012, **13**, 1908-1915.
8. R. Censi, P. J. Fieten, P. Di Martino, W. E. Hennink and T. Vermonden, *Macromolecules*, 2010, **43**, 5771-5778.
9. W. Xue, S. Champ and M. B. Huglin, *Polymer*, 2001, **42**, 3665-3669.
10. L. Klouda and A. G. Mikos, *Eur. J. Pharm. Biopharm.*, 2008, **68**, 34-45.
11. W. E. Hennink and C. F. van Nostrum, *Adv. Drug Delivery Rev.*, 2002, **54**, 13-36.
12. J. C. Jewett and C. R. Bertozzi, *Chem. Soc. Rev.*, 2010, **39**, 1272-1279.
13. S. Kirchhof, F. P. Brandl, N. Hammer and A. M. Goepferich, *J. Mater. Chem. B*, 2013, **1**, 4855-4864.
14. S. Kirchhof, A. Strasser, H.-J. Wittmann, V. Messmann, N. Hammer, A. M. Goepferich and F. P. Brandl, *J. Mater. Chem. B*, 2015, **3**, 449-457.
15. P. E. Dawson, T. W. Muir, I. Clark-Lewis and S. B. Kent, *Science*, 1994, **266**, 776-779.
16. M. Kuhlmann, O. Reimann, C. P. Hackenberger and J. Groll, *Macromol. Rapid Commun.*, 2015, **36**, 472-476.
17. M. Schmitz, M. Kuhlmann, O. Reimann, C. P. Hackenberger and J. r. Groll, *Biomacromolecules*, 2015, **16**, 1088-1094.
18. B.-H. Hu, J. Su and P. B. Messersmith, *Biomacromolecules*, 2009, **10**, 2194-2200.
19. K. W. M. Boere, B. G. Soliman, D. T. S. Rijkers, W. E. Hennink and T. Vermonden, *Macromolecules*, 2014, **47**, 2430-2438.
20. P. B. Messersmith, J. Su and B.-H. Hu, 2011, US Patent 20110262492A1.
21. I. Strehin, D. Gourevitch, Y. Zhang, E. Heber-Katz and P. B. Messersmith, *Biomaterials Sci.*, 2013, **1**, 603-613.
22. Q. Wan, J. Chen, Y. Yuan and S. J. Danishefsky, *J. Am. Chem. Soc.*, 2008, **130**, 15814-15816.
23. M. J. Weissenborn, R. Castangia, J. W. Wehner, R. Šardzík, T. K. Lindhorst and S. L. Flitsch, *Chem. Commun.*, 2012, **48**, 4444-4446.
24. K. Y. Lee and D. J. Mooney, *Chem. Rev.*, 2001, **101**, 1869-1880.
25. J. L. Drury and D. J. Mooney, *Biomaterials*, 2003, **24**, 4337-4351.
26. D. E. Discher, P. Janmey and Y.-l. Wang, *Science*, 2005, **310**, 1139-1143.
27. D. Neradovic, M. J. van Steenbergen, L. Vansteelant, Y. J. Meijer, C. F. van Nostrum and W. E. Hennink, *Macromolecules*, 2003, **36**, 7491-7498.
28. Z. Cui, B. H. Lee and B. L. Vernon, *Biomacromolecules*, 2007, **8**, 1280-1286.
29. Z. Cui, B. H. Lee, C. Pauken and B. L. Vernon, *J. Biomed. Mater. Res., Part A*, 2011, **98A**, 159-166.
30. T. N. Vo, A. K. Ekenseair, F. K. Kasper and A. G. Mikos, *Biomacromolecules*, 2014, **15**, 132-142.
31. T. N. Vo, A. K. Ekenseair, P. P. Spicer, B. M. Watson, S. N. Tzouanas, T. T. Roh and A. G. Mikos, *J. Controlled Release*, 2015, **205**, 25-34.
32. D. Neradovic, C. F. van Nostrum and W. E. Hennink, *Macromolecules*, 2001, **34**, 7589-7591.

33. J. S. Moore and S. I. Stupp, *Macromolecules*, 1990, **23**, 65-70.
34. A. F. S. A. Habeeb, *Anal. Biochem.*, 1966, **14**, 328-336.
35. G. L. Ellman, *Arch. Biochem. Biophys.*, 1959, **82**, 70-77.
36. V. W. Goodlett, *Anal. Chem.*, 1965, **37**, 431-432.
37. R. De Vos and E. J. Goethals, *Polym. Bull.*, 1986, **15**, 547-549.
38. J. Visser, P. A. Levett, N. C. R. te Moller, J. Besems, K. W. M. Boere, M. H. P. Van Rijen, J. C. de Grauw, W. Dhert, R. van Weeren and J. Malda, *Tissue Eng., Part A*, 2015, **21**, 1195-1206.
39. R. Censi, W. Schuurman, J. Malda, G. Di Dato, P. E. Burgisser, W. J. A. Dhert, C. F. Van Nostrum, P. Di Martino, T. Vermonden and W. E. Hennink, *Adv. Funct. Mater.*, 2011, **21**, 1833-1842.
40. T. Vermonden, N. A. M. Besseling, M. J. van Steenbergen and W. E. Hennink, *Langmuir*, 2006, **22**, 10180-10184.
41. R. Censi, T. Vermonden, H. Deschout, K. Braeckmans, P. di Martino, S. C. De Smedt, C. F. van Nostrum and W. E. Hennink, *Biomacromolecules*, 2010, **11**, 2143-2151.
42. T. Vermonden, R. Censi and W. E. Hennink, *Chem. Rev.*, 2012, **112**, 2853-2888.
43. R. Censi, P. Di Martino, T. Vermonden and W. E. Hennink, *J. Controlled Release*, 2012, **161**, 680-692.
44. N. Hammer, F. P. Brandl, S. Kirchhof, V. Messmann and A. M. Goepferich, *Macromol. Biosci.*, 2015, **15**, 405-413.
45. E. W. Merrill, K. A. Dennison and C. Sung, *Biomaterials*, 1993, **14**, 1117-1126.
46. L. Wetter and H. Deutsch, *J. Biol. Chem.*, 1951, **192**, 237-242.
47. M. L. Macdonald, R. E. Samuel, N. J. Shah, R. F. Padera, Y. M. Beben and P. T. Hammond, *Biomaterials*, 2011, **32**, 1446-1453.
48. R. E. Canfield and A. K. Liu, *J. Biol. Chem.*, 1965, **240**, 1997-2002.
49. S. Kalkhof and A. Sinz, *Anal. Bioanal. Chem.*, 2008, **392**, 305-312.
50. G. W. Anderson, J. E. Zimmerman and F. M. Callahan, *J. Am. Chem. Soc.*, 1964, **86**, 1839-1842.
51. R. Censi, T. Vermonden, M. J. van Steenbergen, H. Deschout, K. Braeckmans, S. C. De Smedt, C. F. van Nostrum, P. Di Martino and W. E. Hennink, *J. Controlled Release*, 2009, **140**, 230-236.
52. B. K. Mann, R. H. Schmedlen and J. L. West, *Biomaterials*, 2001, **22**, 439-444.
53. P. R. Kuhl and L. G. Griffith-Cima, *Nat. Med.*, 1996, **2**, 1022-1027.
54. T. A. Holland, Y. Tabata and A. G. Mikos, *J. Controlled Release*, 2003, **91**, 299-313.
55. G. Malich, B. Markovic and C. Winder, *Toxicology*, 1997, **124**, 179-192.
56. L. Klouda, M. C. Hacker, J. D. Kretlow and A. G. Mikos, *Biomaterials*, 2009, **30**, 4558-4566.
57. S. P. Zustiak and J. B. Leach, *Biomacromolecules*, 2010, **11**, 1348-1357.

CHAPTER 5

COVALENT ATTACHMENT OF A 3D-PRINTED THERMOPLAST TO A GELATIN HYDROGEL FOR MECHANICALLY ENHANCED CARTILAGE CONSTRUCTS

K. W. M. Boere*, J. Visser*, H. Seyednejad, S. Rahimian, D. Gawlitta, M. J. van Steenbergen, W. J. A. Dhert, W. E. Hennink, T. Vermonden and J. Malda,
Acta Biomater., 2014, **10**, 2602-2611.

*Both authors contributed equally

Abstract

Hydrogels can provide a suitable environment for tissue formation by embedded cells, allowing its application in regenerative medicine. However, hydrogels only possess limited mechanical strength and have therefore been reinforced for application in load-bearing conditions. In most approaches the reinforcing component and the hydrogel network have poor interactions and the synergetic effect of both materials on the mechanical properties is not effective. Therefore, in the present study, a thermoplastic polymer blend of poly(hydroxymethylglycolide-co-ε-caprolactone)/poly(ε-caprolactone) (pHMGCL/PCL) was functionalized with methacrylate groups (pMHMGCL/PCL) and covalently grafted to gelatin methacrylamide (gelMA) hydrogel through photopolymerization. The grafting resulted in an at least 5x increased interface-binding strength between the hydrogel and thermoplastic polymer material. GelMA constructs were reinforced with 3D printed pHMGCL/PCL and pMHMGCL/PCL scaffolds and tested in a model for a focal articular cartilage defect. In this model, covalent bonds at the interface of both materials resulted in constructs with an improved resistance to repeated axial and rotational forces. Moreover, chondrocytes embedded within the constructs were able to form cartilage-specific matrix both *in vitro* and *in vivo.* Thus, by grafting the interface of different materials, stronger hybrid cartilage constructs can be engineered.

Graphical abstract

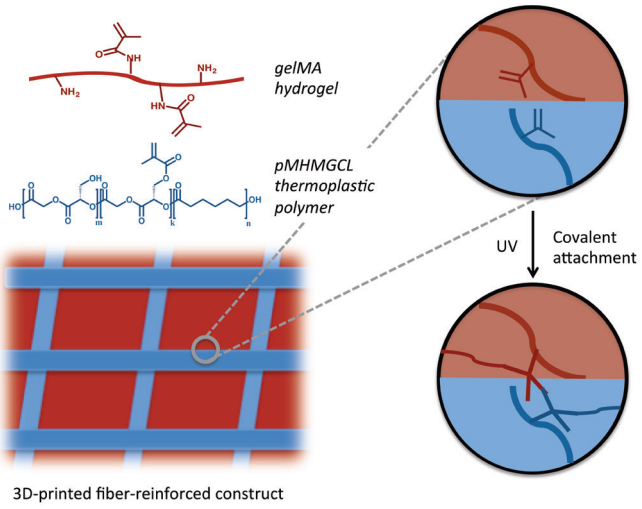

5.1 Introduction

Hydrogels consist of hydrophilic polymer networks that are able to hold large amounts of water in a three-dimensional (3D) structure, while maintaining their shape.[1,2] Thereby they can provide a 3D aqueous environment to embedded cells, analogous to the extracellular matrix of natural tissues.[3,4] For tissue engineering purposes, stem cells,[5,6] tissue specific cells[7] and/or bioactive factors[5,8,9] can be incorporated in the temporary hydrogel scaffold to direct specific tissue regeneration.[3,10] By doing so, hydrogel systems have already been clinically applied for regeneration of a range of tissue types including skin, blood vessels, neural tissues and cartilage.[3,11] Unfortunately, hydrogels have limited mechanical strength due to their high water content,[12,13] which may result in construct failure of the hydrogel under mechanically challenging conditions, as found in the load-bearing bone and cartilage tissues. One approach to overcome this limitation is by stimulation of extracellular matrix formation of the cells prior to implantation, resulting in a stiffer implant.[14] However, this requires long *in vitro* preconditioning periods, limiting clinical translation. The most straightforward approach to directly enhance the stiffness and strength of a hydrogel is by increasing its polymer concentration and crosslinking density.[15,16] Nevertheless, this also impacts the diffusion rates of bioactive factors, nutrients and cell metabolites through the hydrogel, thereby most likely also the regenerative capacities of embedded cells.[1,16,17] Therefore, alternative strategies have been explored to increase the strength of hydrogel constructs, *e.g.* through creation of interpenetrating polymer networks (IPNs)[18-22] or incorporation of solid particles[23-25] and nanofibers/nanotubes.[26-28] Mechanical properties of hydrogels can also be improved by integrating a secondary scaffold material, such as fiber mats,[29-31] randomly organized porous polylactic acid scaffolds[32,33] non-woven meshes[34] or electrospun polymer networks.[35-39] Moreover, with advances in biofabrication techniques, a rigid thermoplastic polymer network can be fabricated layer-by-layer, along with the hydrogel construct[40-45] allowing for a tailored reinforcement of hydrogels. In addition, when mechanical stability is provided by this secondary rigid network, hydrogels with a lower crosslink density can be processed,[41] which is beneficial for the viability and proliferation capacity of embedded cells.[1,16,17,46] Besides, reinforcing the cell-laden hydrogel with a secondary scaffold material may also reduce the often-experienced swelling or shrinking of the hydrogel-based implant that can lead to imperfect filling of the tissue defect.[47] In the present generation of constructs, however, the reinforcing network and the hydrogel show insufficient adhesion, mostly because of their different physicochemical properties,[42,48] which leads to construct disintegration upon application of mechanical stresses. Hence, the introduction of chemical bonds between both components may improve the construct strength to withstand the challenging mechanical conditions in the musculoskeletal system.

Therefore, this study aims to mechanically enhance cartilage implants by grafting a hydrogel to a 3D-fabricated biodegradable thermoplastic polymer network. To achieve this, the polyester poly(hydroxymethylglycolide-co-ε-caprolactone) (pHMGCL)[49] was functionalized with methacryl groups coupled to the hydroxyl side groups of this polymer. In previous studies, we have shown that pHMGCL is more hydrophilic than e.g. poly-ε caprolactone (PCL) due to the presence of the pendant hydroxyl groups,[49] facilitating cell attachment, matrix deposition[50] and resulting in an increased degradation rate.[51] Thereby, pHMGCL is more likely to balance its degradation to the formation of neo-tissue,[52] compared to PCL.[41-43] However, pHMGCL containing more than 20% HMG is an amorphous polymer with a low glass transition temperature (T_g) and therefore has low dimensional stability. PCL, on the other hand, is semi-crystalline, which is beneficial for dimensional stability, but has no reactive groups to allow for example surface grafting. To increase the dimensional stability of pHMGCL, it can be blended with PCL.[53] The blending also improves the physical properties of the material for scaffold fabrication techniques such as electrospinning[54] and 3D fiber deposition (3DF).[50]
In the present study, covalent binding between methacrylated pHMGCL (pMHMGCL) blended with PCL and a methacrylated gelatin hydrogel (gelMA) through photopolymerization was investigated. The interface-binding strength between gelMA and pMHMGCL/PCL was studied and reinforced constructs as fabricated with 3DF were tested with a repetitive loading regime. Finally, the *in vitro* and *in vivo* regenerative capacities of human chondrocytes within these fiber-reinforced constructs were analyzed.

5

5.2 Materials and Methods

5.2.1 Materials

All reagents and solvents were purchased from Sigma-Aldrich (Zwijndrecht, the Netherlands) and used without purification, unless stated otherwise. Benzyl alcohol, acetone, triethylamine (TEA) and dimethyl sulfoxide (DMSO) were obtained from Merck (Darmstadt, Germany). Peptide grade dichloromethane (DCM) and tetrahydrofuran (THF) were obtained from Biosolve (Valkenswaard, the Netherlands). *N,N'*-dimethyl amino pyridine (DMAP) was purchased from Fluka (Zwijndrecht, the Netherlands). Irgacure 2959 was obtained from Ciba Specialty Chemicals Inc (Basel, Switzerland). Type II collagenase was purchased from Worthington Biochemical Corp, (Lakewood, New Jersey). Phosphate-buffered saline (PBS), Dulbecco's Modified Eagle Medium (DMEM), ITS-X, penicillin, streptomycin and Picogreen DNA assay were provided by Invitrogen (Carlsbad, California). Fetal bovine serum (FBS) was purchased from Biowhittaker (Walkersville, Maryland). FGF-2 and

TGF-β2 were obtained from R&D Systems (Minneapolis, Minnesota). Human serum albumin was provided by SeraCare Life Sciences (Milford, Massachusetts). Histoclear II was obtained from BiozymTC, the Netherlands. Buprenorphine (Temgesic) was purchased from Schering-Plough/Merck (USA). Antibody against collagen type II (1:100; II-6B3II) was obtained from Developmental Studies Hybridoma Bank, USA. Polylactic acid (PLA) filament for 3D-printing was obtained from Ultimaker LTD, Geldermalsen, The Netherlands.

5.2.2 Synthesis of poly-ε caprolactone (PCL)

Poly-ε-caprolactone (PCL) was synthesized by ring opening polymerization of ε-caprolactone (CL) using benzyl alcohol (BnOH) and stannous octoate ($SnOct_2$) as initiator and catalyst, respectively, according to a previously described method.[49] The molar ratio of CL/BnOH was 300/1 in the feed. The obtained PCL was characterized by ^{1}H NMR, GPC and DSC.

5.2.3 Synthesis of methacrylated poly(hydroxymethylglycolide-co-ε-caprolactone) (pMHMGCL)

Poly(hydroxymethylglycolide-co-ε-caprolactone) (pHMGCL) was synthesized as described before by ring opening polymerization of 3S-benzyloxymethyl-1,4-dioxane-2,5-dione (benzyl protected hydroxymethyl glycolide (BMG)) and ε-caprolactone in the melt using BnOH and $SnOct_2$ as initiator and catalyst, respectively, followed by removal of the protecting benzyl groups by catalytic hydrogenation.[49] pHMGCL was synthesized by melt polymerization in a 40/60 molar ratio of HMG/CL and the monomer to initiator molar ratio was 300. These random copolymers were further functionalized aiming for derivatization of 50% of the available hydroxyl groups of pHMGCL with methacrylate groups (Figure 5.2). In a typical reaction, pHMGCL (4.2 g, 13.2 mmol OH groups) was dissolved in freshly distilled THF (40 mL), in an aluminum foil covered, dry round-bottom flask. After dissolution, DMAP (39.3 mg, 0.32 mmol) and TEA (897 µL, 6.4 mmol) were added as catalyst and base, a combination that has shown to efficiently functionalize hydroxyl groups with methacryloyl groups [55]. Next, methacrylic anhydride (960 µL, 6.4 mmol, feed ratio methacrylic anhydride/$OH_{polymer}$ = 0.5) was added. To prevent premature crosslinking, hydroquinone monomethyl ether (84 mg, 0.67 mmol) was added and the reaction proceeded overnight under N_2 atmosphere in an ice-cooled flask. After 16 hours, the polymer was purified by three times precipitation in ice-cold water, followed by centrifugation and removal of the supernatant. The precipitate was re-dissolved in DCM and dried using anhydrous Na_2SO_4. The salts were filtered off, DCM was evaporated and the polymer was dried under vacuum at room temperature for several days. The obtained methacrylated pHMGCL (pMHMGCL) was characterized by ^{1}H NMR, DSC, and GPC.

5.2.4 Synthesis and gel preparation of gelatin methacrylamide (gelMA)

GelMA was synthesized by reaction of type A gelatin with methacrylic anhydride at 50 °C for one hour as previously described.[56] GelMA was dissolved in demineralized H_20 at 70°C in a concentration of 10% (w/v). The solution also contained Irgacure 2959 (0.1% w/v), a photoinitiator that has shown to be well compatible with living cells.[57,58] When a clear solution was obtained, the osmolarity of the gel was adjusted to physiologic levels (1x PBS) by adding 50 ul concentrated PBS (disodium hydrogen phosphate 60 g/L, sodium dihydrogen phosphate 6.6 g/L and sodium chloride 164 g/L) to 1 ml of methacrylated gelatin.

5.2.5 Preparation of p(M)HMGCL/PCL blends

PHMGCL or pMHMGCL was dissolved in DCM and mixed with PCL in a 1:1 weight ratio at a concentration of 0.2 g/mL DCM (total volume was 5 ml). The mixture was concentrated by blowing air for 10 minutes and next, the viscous polymer solution (~3 ml) was pipetted on a petri dish. DCM was allowed to evaporate overnight at room temperature and a white solid was obtained, which was subsequently analysed by differential scanning calorimetry (DSC). For sake of readability, the pMHMGCL/PCL blend and pHMGCL/PCL blend are abbreviated as MA+ blend and MA- blend respectively.

5.2.6 Nuclear magnetic resonance (NMR)

^{1}H NMR spectra of the obtained polymers and blends were recorded on a Mercury 300 MHz instrument (Varian Associates Inc., NMR Instruments, Palo Alto, CA). Chemical shifts are recorded in ppm with reference to the solvent peak (δ= 7.26 ppm for $CDCl_3$ in ^{1}H NMR).

5.2.7 Differential scanning calorimetry (DSC)

Thermal properties of polymers and blends were measured using a DSC Q2000 apparatus (TA Instruments, New Castle, DE, USA). Scans of polymer samples (approximately 5 mg, loaded into Tzero aluminum pans (TA Instruments)) were taken from -80 °C to 100 °C with a heating rate of 10 °C/min and a cooling rate of 0.5 °C/min under nitrogen flow of 50 mL/min. The glass transition temperature (T_g) was recorded as the midpoint of heat capacity change in the second heating run. Melting temperature (T_m) and heat of fusion (ΔH_f) were determined from the onset of the endothermic peak position and integration of the endothermic area, respectively. The thermal transitions of PCL, pHMGCL and pMHMGCL are reported for the second heating run; the thermal transitions of the blends for the first heating run.

5.2.8 Gel permeation chromatography (GPC)

Molecular weights (M_w and M_n) of the different polymers were measured by GPC analysis using a 2695 Waters Alliance system and a Waters 2414 refractive index detector. Two PL-gel 5 μm mixed-D columns fitted with a guard column (Polymer Labs, M_w range 0.2-400 kDa) were used. The columns were calibrated with polystyrene standards of known molecular weights using AR grade THF, eluting at 1 mL/min flow rate at 30 °C. The concentration of samples was 5 mg/mL and the injection volume was 50 μL.

5.2.9 Creep-recovery test: interface-grafting strength

To investigate grafting strength between gelMA and the MA+ blend and to compare this with gelMA and the MA- blend, creep-recovery tests were performed with an AR G-2 rheometer (TA-instruments), equipped with a UV light guide connected to a BluePoint lamp 4 (350-450 nm, Hönle UV technology (Munich, Germany) at 37°C. Flat discs (surface area 80 mm^2, thickness 0.1 mm) of MA+ or MA- were prepared as described in section 5.2.5. GelMA solutions were prepared at a concentration of 20% w/v in deionized water containing 0.1 w/v% Irgacure 2959. For each sample, measurements were performed in triplicate. The MA+ and MA- discs were attached with a photosticker (HEMA, Groningen, the Netherlands) to the upper 20 mm diameter plate of the geometry (Figure 5.3a). 100 μL of GelMA solution (20% w/v, also containing 0.1% w/v Irgacure) was pipetted at the bottom plate before lowering the top plate to a gap of 1.0 mm: the level at which gelMA and MA+ or MA- had a standardized surface interface of 100 ± 10 mm^2 (Figure 5.3a). Then, the construct was UV-illuminated for 10 minutes (light intensity of 180 mW/cm^2). Next, the obtained constructs were mechanically deformed at different torque values ranging from 50 to 1500 μNm consisting of 5 minutes creep followed by 5 minutes recovery, while keeping the temperature at 37°C. In the creep step, a constant torque force was exerted on the top MA+/- layer that was connected to the gelMA sheet and the observed strain or deformation of the material was recorded over time. In the recovery step, the applied force was released, allowing the (grafted) materials to recover to their starting position, representing the elastic properties of the material. The percentage of recovery was calculated as follows:

$$\frac{\text{strain}(5\,\text{min}) - \text{strain}(10\text{min})}{\text{strain}(5\text{min})} \times 100\% \quad (5.1)$$

5.2.10 Three-dimensional fiber deposition

Printing of PCL, MA+ and MA- was performed using a Bioscaffolder (SYS+ENG, Salzgitter-Bad, Germany)[41]. Constructs were designed with Rhino 3D software (McNeel, Seattle, WA, USA) and the Standard Tessellation Language (STL) files of these models were translated to the Bioscaffolder through computer-aided

manufacturing (CAM) software (PrimCAM, Einsiedeln, Switzerland). 1) A semi-open hollow cuboid was printed (LxWxH: 12x4x2mm), which was filled with gelMA for measuring construct strength; 2) a dome-shaped scaffold (diameter: 15 mm, height 3 mm, strand spacing 1.5 mm, 27 layers) was fabricated for mechanical testing in a model representing an articular chondral defect; 3) a cylindrical scaffold (diameter: 10 mm, height: 0.9 mm, strand spacing 2 mm, 5 layers) was fabricated as a reinforcing framework to gelMA loaded with chondrocytes for *in vitro* and *in vivo* evaluation. Optimal printing was achieved by melting PCL at 160 °C and MA+ and MA- at 140 °C for extrusion with a 25G metal needle (DL Technology LLC, Haverhill, MA, USA), at a pressure of 0.5 MPa, and a deposition speed of 250 mm/min, producing fibers with a mean thickness of 0.26 mm. Air (20 °C) was blown over the construct to facilitate rapid solidification of the printed fibers. A shape inspired by the femoral condyles of a knee joint was fabricated from PLA with an Ultimaker^{tm} (Ultimaker LTD, Geldermalsen, The Netherlands) filament-extrusion machine. An indentation was included (diameter: 15 mm, depth 1 mm) to mimic a chondral defect. The dome-shaped scaffolds were fabricated to tightly fit in this holder for mechanical testing.

5.2.11 Fabrication of reinforced gelMA constructs

GelMA solution (10% w/v, containing 0.1% w/v Irgacure 2959) was added to the MA+ or MA- framework to create fiber-reinforced constructs. First, a mold was printed from PVA with the Ultimaker^{tm} machine in which the frameworks were placed. Then, the gelMA solution was infused at the periphery of the frameworks using a positive displacement pipet, until all pores were completely filled. The constructs were UV-irradiated for 10 minutes with a UV intensity of 120 mW/cm^2. After photopolymerization, the constructs were taken from the molds and any excess of gelMA at the outside of the constructs was removed.

5.2.12 Integrity of constructs on axial loading

To investigate whether interface grafting of pMHMGCL to gelMA results in a stronger construct, two approaches were used to investigate construct failure.
1) The semi-open cuboids filled with gelMA were UV-irradiated for 10 minutes at 120 mW/cm^2 and placed in unconfined position between the parallel plates (upper plate 6 mm in diameter) using a DMA 2980 Dynamic Mechanical Analyzer (TA Instruments, New Castle, DE, USA). A force ramp of 0-15 N, with incremental steps of 1.5 N/min was applied at the centre of the construct. Construct failure was defined as the force at which gelMA was squeezed out of the MA+ or MA- cuboid. The force and displacement were recorded throughout compression. Measurements were performed in triplicate and the results were analysed using Thermal Advantage (v. 1.1A) and Microsoft® Excel software.

2) Cylindrical dome-shaped scaffolds, consisting of MA+/gelMA or MA-/gelMA were UV irradiated for 10 min (120 mW/cm^2) and were then press-fit in a holder inspired by a knee chondral defect. Because the indentation was 1 mm deep, and the top of the dome was 3 mm in height, the implant raised maximally 2 mm from the defect ridge, matching the curvature of the joint model. In this semi-confined environment the constructs were axially loaded with 20 N (using an AR G-2 rheometer (TA-instruments)) and the change in height of the scaffold was recorded during the compression. Next, 100 creep-recovery cycles were applied onto the construct, each consisting of a 10-second creep step with a torque of 0.01 Nm followed by a 10-second recovery step. The construct was axially compressed for approximately 1 mm, so that the mechanical properties of the PLA holder would not disturb the measurements. The construct strain, resistance to compression and recovery during the creep-recovery cycles were analysed and the constructs were visually inspected after the mechanical loading for signs of structural damage. SI-Figure 5.4 shows the experimental set-up.

5.2.13 Harvest of human chondrocytes

Macroscopically healthy human cartilage from a discarded talus bone was obtained immediately after resection from a 7-years old patient, undergoing an orthopaedic intervention for an ankle disease, according to the institutional code of conduct regarding the use of discarded tissues in the University Medical Center Utrecht. The cartilage was sectioned into small slices under sterile conditions and washed three times with PBS supplemented with penicillin and streptomycin. The full-thickness cartilage was digested overnight using 0.15% type II collagenase at 37 °C and the obtained cell suspension was filtered (100 μm cell strainer) and washed three times with phosphate-buffered saline (disodium hydrogen phosphate 3 g/L, sodium dihydrogen phosphate 0.33 g/L and sodium chloride 8.2 g/L). Cells were then resuspended in chondrocyte expansion medium: DMEM supplemented with 10% heat-inactivated FBS, 100 units/mL penicillin and 100 μg/mL streptomycin, and 10 ng/mL FGF-2 and expanded for 10 days in monolayer cultures (seeding density 5,000 cells/cm^2) for use in passage 2.

5.2.14 In vitro redifferentiation of chondrocytes in a fiber reinforced gelMA construct

Chondrocytes were resuspended in 10% gelMA (also containing Irgacure 0.1% (w/v)) at a concentration of 20x10^6 cells/mL. As a negative control group to histological stainings, a sample of chondrocytes was mortalized through a 2-hour trypsin treatment (0.25% trypsin-EDTA, life technologies Europe, Bleiswijk, the Netherlands) before suspension in the hydrogel. The pores of the printed cylindrical MA+ constructs (described in section 5.2.10) were infused with the cell-laden

gelMA solution and UV-irradiated for 5 minutes. For *in vitro* redifferentiation, these samples (n=4) were cultured for 6 weeks in chondrocyte differentiation medium: DMEM supplemented with 0.2 mM ascorbic acid 2-phosphate, 0.5% human serum albumin, 1x ITS-X, 100 units/mL penicillin and 100 µg/mL streptomycin, and 5 ng/mL TGF-β2, with biweekly medium change.

5.2.15 In vivo redifferentiation of chondrocytes in a fiber reinforced gelMA construct

For *in vivo* redifferentiation, the fiber-reinforced samples (n=4) described in the previous paragraph were pre-cultured for 2 weeks in chondrocyte differentiation medium before subcutaneous implantation. This study was approved by the local Ethics Committee for Animal Experimentation and was in compliance with the Institutional Guidelines on the Use of Laboratory Animals. Four 11-weeks old male athymic rats (Hsd:RH-*Foxn1*^{rnu} Harlan Laboratories B.V., The Netherlands) were anesthetized with 1.5% isoflurane. A dorsal pocket was created on each rat in which the 10-mm diameter cylindrical construct was placed with a forceps. The skin was closed using Vicryl 4.0 sutures. Preoperatively and postoperatively, the animals received 0.05 mg/kg buprenorphine subcutaneously. The rats were housed in groups at the Central Laboratory Animal Institute of Utrecht University. The rats were sacrificed and the samples were harvested 8 weeks after implantation. Scaffold morphology and cellular differentiation was investigated and a quarter of each explant was analysed with ^{1}H NMR to assess degradation of the MA+ component.

5.2.16 Histological, immunohistochemical and biochemical analysis

After the *in vitro* and *in vivo* differentiation experiments, the samples were split and processed for histology, immunohistochemistry and biochemistry. Therefore, one part of the samples was dehydrated through a graded ethanol series, cleared in Histoclear and embedded in paraffin. The samples were sectioned into 5 µm slices and a triple stain of Weigert's hematoxylin, fast green, and Safranin-O was applied to detect tissue formation and deposition of glycosaminoglycans (GAGs).

Immunolocalization of collagen type II involved dewaxing and rehydration through graded alcohol series, washing in PBS/Tween (0.1%), followed by antigen retrieval with 1 mg/mL pronase (30 min) and 10 mg/mL hyaluronidase (30 min). Next, samples were blocked with 0.3% H_2O_2 and 5% BSA (bovine serum albumin) in PBS for 30 minutes and then incubated overnight at 4 °C with antibodies against collagen type II (1:100 from ascites, II-II6B3, Developmental Studies Hybridoma Bank). Then, samples were washed and incubated for 60 minutes with a horseradish peroxidase-conjugated goat anti-mouse antibody. Antibody-binding was visualized using 3,3'diaminobenzidine (DAB) solution for 10 minutes and counterstaining was performed with Mayer's hematoxylin. Isotype control stainings were performed by

using mouse isotype IgG1 monoclonal antibody at concentrations similar to those used for the primary antibodies. All stained sections were examined using a light microscope (Olympus BX51).
For DNA and GAG quantification, a part of the *in vitro* samples was digested overnight in 20 µl papain solution per mg construct (0.01 M cysteine, 250 µg/ml papain, 0.2 M NaH_2PO_4 and 0.01 M EDTA) at 60 °C. Total DNA was quantified using a Quant-iT Picogreen dsDNA kit (Invitrogen) according to the manufacturer's instructions. Total GAG content was determined by photospectrometry at 540 and 595 nm after reaction with 1,9-dimethyl-methylene blue (DMMB, 341088; Sigma) using a microplate reader (Biorad).[59] The ratio of both absorbances was calculated and the GAG content was quantified using chondroitin sulphate C (C4384; Sigma). Concentrations in the papain digest were expressed as GAG/DNA.

5.2.17 Statistics

A Mann-Whitney-U test for independent samples was used for comparing construct failure between the two groups. Raw data were processed in SPSS version 18 (IBM software, USA) and $p<0.05$ was considered significant. All data are represented as means ± standard deviations.

5.3 Results and Discussion

Poly(hydroxymethylglycolide-co-ε-caprolactone) (pHMGCL) was methacrylated (pMHMGCL) and blended with poly-ε caprolactone (PCL) (1:1) to obtain the thermoplastic polymer blends pHMGCL/PCL (abbreviated as MA-) and pMHMGCL/PCL (abbreviated as MA+). In addition, a hydrogel was produced from methacrylated gelatin (gelMA). Figure 5.1 shows an overview of the performed experiments to characterize the polymers and blends and to investigate interface-binding strength between both materials and the cartilage specific matrix production in hydrogel constructs reinforced with a MA+ scaffold.

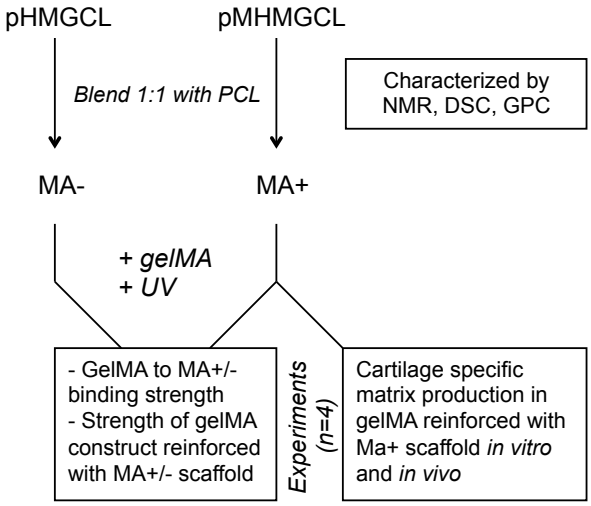

Figure 5.1. Overview of the performed experiments in the present study. Poly(hydroxymethylglycolide-co-ε-caprolactone) pHMGCL, methacrylate-functionalized pHMGCL (pMHMGCL) and their corresponding blends with poly-ε caprolactone (MA- and MA+ respectively) were characterized with NMR, DSC and GPC. Reinforced constructs of MA- and MA+ with methacrylated gelatin (gelMA) were UV-irradiated and the interface-binding strength and strength of the reinforced construct was tested. Constructs of MA+/ gelMA were further tested *in vitro* and *in vivo* for cartilage specific matrix production. All mechanical, *in vitro* and *in vivo* experiments were performed in quadruplicate.

5

5.3.1 Polymer synthesis and characterization

Poly(benzyloxymethylglycolide-co-ε-caprolactone), pBMGCL, was synthesized via ring opening polymerization (ROP) of benzyl protected hydroxymethyl glycolide (BMG) and ε-caprolactone in the melt at 130 °C for 16 hours using benzyl alcohol (BnOH) and stannous octoate ($SnOct_2$) as initiator and catalyst, respectively, and obtained in a high yield (Table 5.1). The synthesized polymer was deprotected to yield poly(hydroxymethylglycolide-co-ε-caprolactone), pHMGCL (Figure 5.2). The molar ratio of HMG/CL was calculated using ^{1}H-NMR by comparing the integrals of peaks belonging to methylene protons of HMG units (3.7-4.0 ppm) and those of CL units (1.3-4.2 ppm) and was found to be very close to the feed ratio, as expected for polymers obtained in high yield (Table 5.1). The thermal properties of pBMGCL and pHMGCL were investigated by DSC and no melting endotherms were detected showing that these polymers were completely amorphous as can be expected for a random copolymer.[60] DSC analysis also showed that removal of the bulky benzyl rings resulted in a decrease in T_g (Table 5.1).

Table 5.1. Overview of the polymer characteristics

	HMG/CL molar ratio*	Degree of methacrylation****	Yield (%)	M_w (kDa)	PDI	T_g (°C)	T_m (°C)	ΔH (J/g)
PCL	N.A	0	87	79.1	2.0	-61	57	71
pBMGCL		0	96	36.6	2.3	-25	-	-
pHMGCL	39/61	0	95	31.9	1.8	-38	-	-
pMHMGCL	39/61	44	74	32.4	2.2	-22	-	-
MA-**						-44	56	40
MA+***						-47	52	37

* HMG/CL ratio based on ^{1}H NMR analysis

** 1:1 pHMGCL/PCL

*** 1:1 pMHMGCL/PCL

**** Measured by ^{1}H NMR

Subsequently, pHMGCL was functionalized with methacrylate groups aimed at a degree of methacrylation of 50% using methacrylic anhydride, 4-dimethylamine (DMAP) and triethylamine (TEA) as the reactant, catalyst and base (Figure 5.2) to yield pMHMGCL.

A degree of methacrylation of 50% was chosen because it allows for sufficient bonding after photopolymerization without losing the beneficial properties of the pendant hydroxyl groups.[49] The structural analysis of the obtained polymer by ^{1}H NMR (SI-Figure 5.1) showed the presence of methacrylate groups at 1.9-2.0 ppm and 5.6- 6.4 ppm (peaks j and i). The degree of substitution (DS) was calculated by comparison of the average integrals of peaks at 1.9-2.0 ppm and those of protons attributed to non-functionalized HMG units (4.0-4.3 ppm) and found to be 44%.

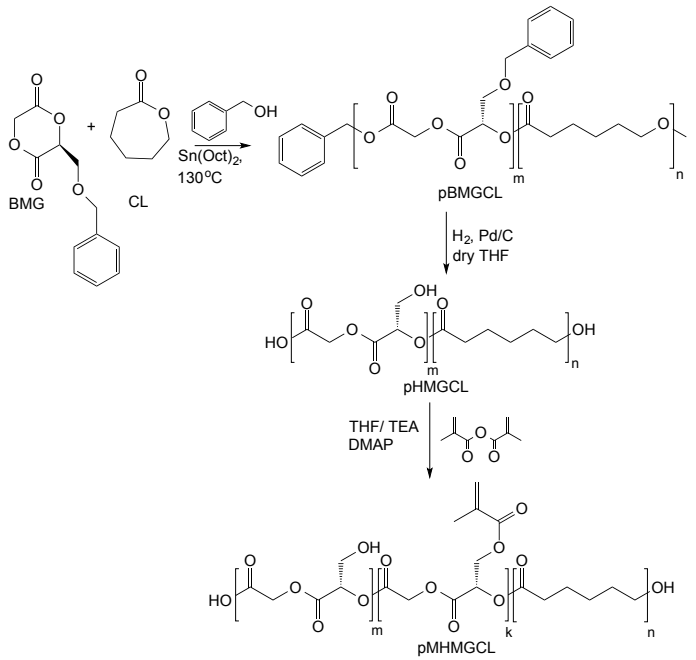

Figure 5.2. Synthesis of poly(benzyloxymethylglycolide-co-ε-caprolactone) pBMGCL, poly(hydroxymethylglycolide-co-ε-caprolactone) pHMGCL, and methacrylate-functionalized pHMGCL (pMHMGCL).

After introduction of the methacrylate groups, the molecular weight of the polymer as determined by GPC showed a very slight increase from 31.9 kDa for pHMGCL to 32.4 kDa for pMHMGCL indicating that neither premature cross-linking nor chain scission had occurred. DSC analysis showed that after methacrylation the T_g increased from -38°C to -22°C, which indicates a lower mobility of pMHMGCL chains with rather bulky methacrylate side groups compared to polymers bearing only hydroxyl groups.

PCL was synthesized via ring opening polymerization following the procedures for the synthesis of pBMGCL. DSC analysis showed a melting temperature of PCL of 57°C and a heat of fusion (ΔH) of 71 J/g, similar to other reported PCLs.[61] GPC analysis showed a molecular weight (M_w) of 79.1 kDa and polydispersity of 2.0.

Since p(M)HMGCL is fully amorphous with a low T_g, it was blended with PCL to introduce crystallinity and allowing the preparation of scaffolds of suitable dimensional stability. DSC thermograms of the blends pMGMGCL and PHMGCL with PCL (MA+ and MA-, blend ratio 1:1) are shown in SI-Figure 5.2. The melting temperatures of MA+ and MA- were slightly lower than that of PCL (Table 5.1). The heat of fusion (ΔH) of the blends was lower compared to PCL (37 and 40 J/g, for MA+ and MA- respectively, compared to 71 J/g for PCL). The reduction in ΔH

is in agreement with the percentage of PCL in the scaffolds, which is in line with previously obtained results of blends from PCL/pHMGCL.[53] Also, a single T_g was found between the T_g of PCL and p(M)HMGCL, showing that p(M)HMGCL and PCL are fully miscible.

5.3.2 Binding strength of MA+ or MA- to gelMA

To determine the binding strength of MA+ or MA- to gelMA, creep recovery experiments were performed. A schematic representation of the experimental set-up is shown in Figure 5.3a. Torque forces ranging from 50 to 1500 μNm were applied to measure the resistance over the interface between MA+ or MA- and GelMA. A torque force up to 300 μNm over the grafted MA+ or MA- with gelMA yielded a strain between 0.5 and 0.8% for both groups and subsequently; after removal of the torque, 95-100% recovery was observed (data not shown). These numbers are similar to creep-recovery tests for gelMA alone (data not shown), reflecting the elastic properties of gelMA. At a torque force of 400 μNm, the MA- / gelMA samples showed a high strain (12-100%) with a negligible recovery of only 0-3% (Figure 5.3b). This indicates complete loosening of the material interface, which was macroscopically confirmed. The high variation in the maximal reported strain is due to the early disintegration of the MA-/gelMA constructs. Importantly, at torque forces of 400-1500 μNm the interface of MA+ with gelMA remained intact as confirmed by a low strain and recovery of 94-99%. When the torque force was further increased, the test samples detached from the machine, but leaving the material interface intact. Therefore it can be concluded that the binding strength between MA+ and gelMA is at least 5 times higher than that between MA- and gelMA. This indicates that upon UV-polymerization, reaction between the two methacrylate-functionalized materials had occurred, resulting in a higher mechanical resistance after applied rotational forces.

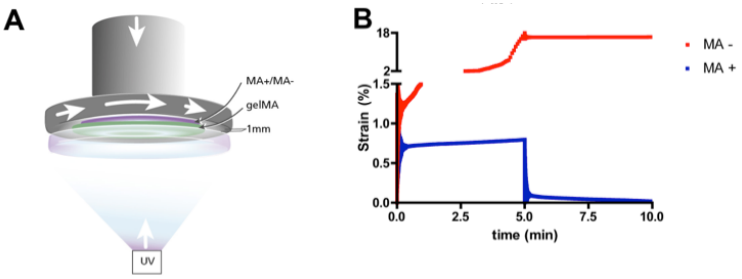

Figure 5.3. A) Samples of 100 μl gelMA hydrogel were placed at the bottom glass plate of a rheometer and sheets of MA- or MA+ were attached to the top metal plate which was lowered onto the gelMA sample with a 1 mm gap. The two components were UV-illuminated through the bottom glass plate. Subsequently, torque forces were exerted over the construct for 5 minutes followed by a recovery period of 5 minutes; B) Strain and recovery as a function of time at a torque force of 400 μNm.

5.3.3 Construct integrity on axial loading

In a second mechanical experiment, the construct integrity of MA+/MA- with gelMA was tested by axial loading (Figure 5.4). The semi-open cuboids printed from MA+ and MA- that were filled with gelMA were loaded with increasing axial compressive forces till construct failure occurred. Construct failure was defined as the moment at which gelMA was pushed out of the thermoplastic cuboid frame, accompanied by an abrupt drop in measured height of the construct as recorded in force-displacement graph (SI-Figure 5.3). Figure 5.4d shows that the MA+ construct with gelMA could withstand a significantly higher ($p<0.05$) axial mechanical force before construct failure occurred (7.7 ± 2.4 N) as compared to the MA- construct (2.7 ± 0.5 N). This experiment confirmed that photopolymerization between MA+ and gelMA had occurred, resulting in a three-fold higher mechanical resistance during axial compression.

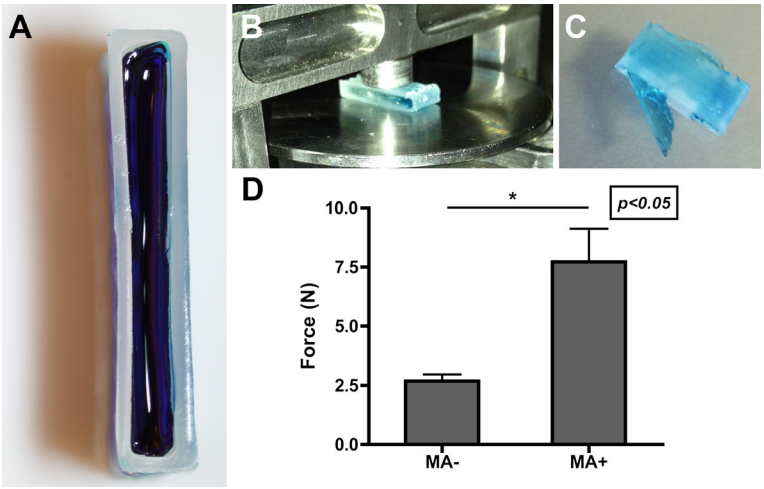

Figure 5.4. A) hollow cuboids (LxWxH: 12x4x2mm) were printed from MA- and MA+ and filled with gelMA (stained blue); B) compression was performed till C) the construct failed as defined by gelMA being squeezed out of the construct; D) force at construct failure.

5.3.4 Mechanical testing of fiber-reinforced constructs in a model mimicking an articular joint

Reinforced constructs were studied in a model resembling an articular cartilage defect (Figure 5.5a). The experimental set-up is shown in SI-Figure 5.4. The constructs were first axially loaded followed by 100 cycles of rotational forces in order to simulate repeated movement of a joint. A typical creep-recovery registration by the rheometer is shown in Figure 5.5b. During these repetitive rotational forces, a significantly higher deformation, as reflected in the percentage strain, was found for MA-/gelMA constructs compared to the MA+/gelMA constructs.

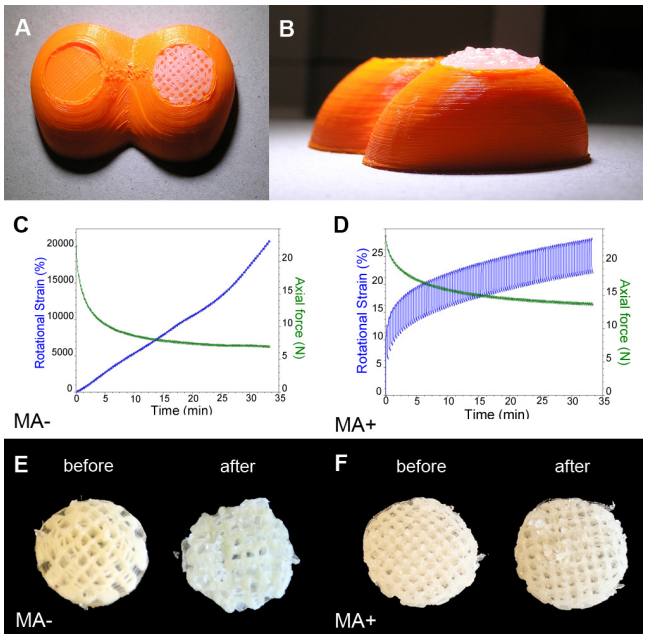

Figure 5.5. A) a model representing the femoral condyles of the human knee was fabricated from poly lactic acid (orange). Fiber reinforced constructs were press-fit in a designed indentation in the condyle (diameter 15 mm, depth 2 mm); B) side view of a femoral condyle model; C) effect of 100 cycles of rotational forces (0.01Nm creep of 10 sec, followed by 10 sec recovery) on the rotational strain and axial force of MA- scaffolds and D) MA+ scaffolds; E) photographs of the MA- scaffolds before and after the applied forces; F) photographs of the MA+ scaffolds before and after the applied forces.

Table 5.2 shows that loading 20 N on the constructs compressed the MA-/gelMA scaffolds to a higher extent than the MA+/gelMA scaffolds (71 ± 4% for MA-/gelMA compared to 43 ± 5% for MA+/gelMA). In addition, after the repetitive rotational forces, the residual loading on the MA-/gelMA scaffolds was only 7.4 ± 0.4 N whereas for the MA+/gelMA scaffolds 14.1 ± 0.5 N of compressive strength remained. The lack of recovery after repeated rotational forces and the low values of residual compressive strength for MA-/gelMA constructs demonstrate the lack of integration of both materials. On macroscopical assessment after the loading regime the shape of the MA+/gelMA constructs appeared to be unchanged, but the MA-/gelMA constructs showed an irreversible structural damage (Figure 5.5c). GelMA without a reinforcing scaffold was tested under the same loading regime and was found to disintegrate completely, showing that reinforcement is necessary to use these constructs in load-bearing applications. It should be noticed that 20 N is only a fraction of a full load-bearing situation in which forces lay typically in the range of 1700-2700 N in an average weight person.[62] Yet in this model gelMA reinforced with

a MA+ scaffold showed a superior mechanical strength, compared to reinforcement with a MA- scaffold and gelMA alone.

Table 5.2. Construct strain following axial compression of 20 N and residual compression strength after 100 cycles of 0.01 Nm creep-recovery.

	Axial compression/strain*	Residual compression strength**
MA-/gelMA	71 ± 4 %	7.4 ± 0.4 N
MA+/gelMA	43 ± 5 %	14.1 ± 0.5 N

* Percentage of construct height compressed after axial loading

** Remaining axial loading after 100 creep-recovery cycles (axial loading at start =20 N)

5.3.5 Chondrogenic differentiation in a fiber-reinforced construct *in vitro*

After six weeks of *in vitro* culture, human chondrocytes in MA+ reinforced gelMA constructs had produced a network of GAGs and collagen type II (Figure 5.6), which are the main cartilage-specific extracellular matrix components [63]. GAGs were deposited and had diffused throughout the whole hydrogel compartment as is indicated by the red staining (Figure 5.6a), compared to the negative control samples. (Figure 5.6b). Also, chondrocytes and GAGs were present at the interface with the MA+ network (Figure 5.6c). The formation of such an interconnected matrix is essential in order to achieve an adequate cartilage-like function of the construct.[14,64] The amount of GAGs that was produced in the constructs after six weeks was found to be 10.5 ± 2.7 mg GAG / mg DNA, which is in line with earlier reports of chondrocytes in GelMA-based scaffolds.[14,64] In addition, immunohistochemistry revealed the presence of a pericellular matrix of cartilage specific collagen type II (Figure 5.6d).

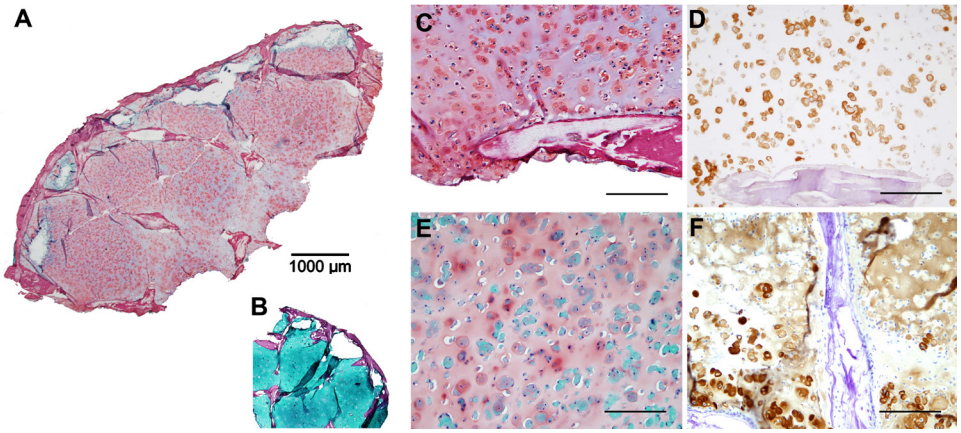

Figure 5.6. Human articular chondrocytes produced cartilage-specific matrix components in MA+ reinforced gelMA constructs after 6 weeks *in vitro* culture as shown by positive safranin-O staining (A, C; red) for glycosaminoglycans (GAGs) produced by chondrocytes in gelMA. The MA+ scaffold architecture is visible in dark red. In negative control samples (B), GelMA stains green and the MA+ stains dark red by the safranin-O triple staining. Staining collagen type II staining is visible in the pericellular matrix of the chondrocytes (D), MA+ scaffold in purple. After 8 weeks *in vivo* with 2 weeks pre-culturing there was production of GAGs (E), although less extensive compared to *in vitro* cultures (C). An interconnected collagen type II network was formed *in vivo (F)*. Scale bar C-F = 200 µm.

5.3.6 Chondrogenic differentiation in a fiber-reinforced construct *in vivo*

The MA+/gelMA constructs were implanted in rats and it was shown that a network of GAGs was present eight weeks after subcutaneous implantation (Figure 5.6e). Here, GAGs were not quantified because normalization to DNA of implanted cells was impossible due to infiltration of host cells and their DNA in the implanted constructs. Collagen type II production was more pronounced *in vivo* compared to *in vitro* results as shown by the extensive network formation reflected by the immunohistochemical stainings (Figure 5.6f). Also, collagen type II was deposited at the interface of the MA+ scaffold, contributing to the integration of neo-tissue with the polyester scaffold. This is important, since the neo-tissue together with the MA+ scaffold will determine the mechanical properties of the construct after the hydrogel component has been degraded [52].

5.3.7 Degradation of pMHMGCL *in vivo*

Degradation of the explanted MA+ component was shown with ^{1}H NMR by the disappearance of HMG units (SI-Figure 5.5), which is in line with previous observations.[51,65] Furthermore, NMR shows a reduction in the methacrylate signals at 5.6 and 6.4 ppm. This is most likely caused by both crosslinking of pMHMGCL

with gelMA and hydrolysis of the ester groups connecting the methacrylate groups of pMHMGCL. Since no photoinitiator was incorporated in the polyester, it was to be expected that not all methacrylate groups in pMHMGCL had photopolymerized. Degradation of these constructs will therefore lead to the formation of methacrylic acid. As is shown before for methacrylated dextran-based hydrogels,[66,67] methacrylic acid does not cause cytotoxicity and therefore does not affect the suitability of these materials for tissue engineering purposes.

5.4 Conclusion

This study showed that a 3D-fabricated pMHMGCL/PCL thermoplastic polymer scaffold could be covalently linked to a chondrocyte-laden gelMA hydrogel. Covalently grafting both materials significantly improved the binding strength between the materials and consequently resulted in an enhanced mechanical integrity of reinforced hydrogel constructs. Embedded chondrocytes showed significant cartilage-specific matrix deposition in these constructs both *in vitro* and *in vivo.* Moreover, since both materials have shown their ability to support matrix formation and both can be applied in additive manufacturing techniques, the current work allows for the fabrication of mechanically enhanced, patient-specific cartilage implants.

Acknowledgements
The authors would like to thank Kim Benders for her assistance in isolating human chondrocytes. Also we would like to thank Marco Raaben for optimizing printing parameters for MA+/MA-, Ben Peters for designing the knee implant model and Jeremy Besems for assisting in the histology analyses. The collagen type II monoclonal antibody (developed by T.F. Linsenmayer) was obtained from the Developmental Studies Hybridoma Bank. Jos Malda was supported by the Dutch Arthritis Association, Kristel Boere and Jetze Visser were supported by Netherlands Institute of Regenerative Medicine (NIRM). Debby Gawlitta was supported by the Dutch Technology Foundation, STW (Veni 11208).

Supporting Information

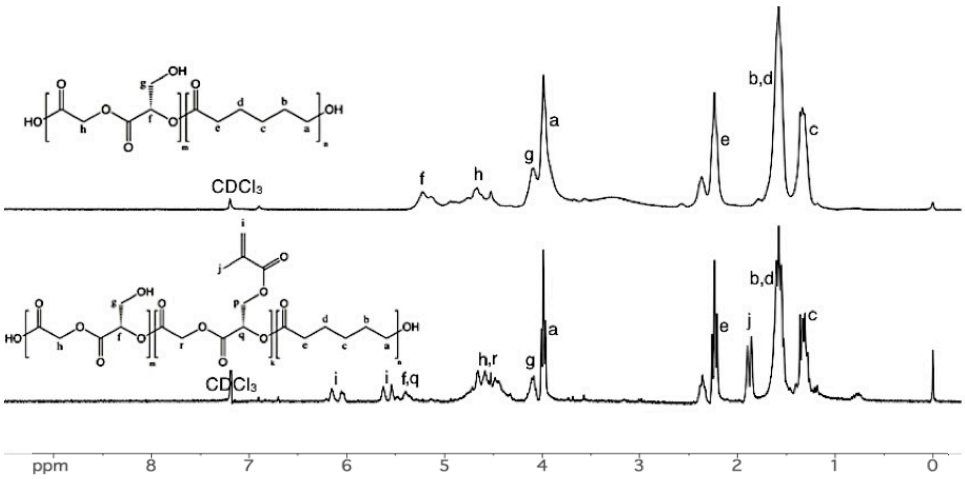

SI-Figure 5.1. ^{1}H NMR spectra of (above) pHMGCL, and (below) pMHMGCL in $CDCl_3$. Methacrylate peaks of pMHMGCL are shown at 1.9-2.0 ppm (peak j) and 5.6-6.4 ppm (peaks i).

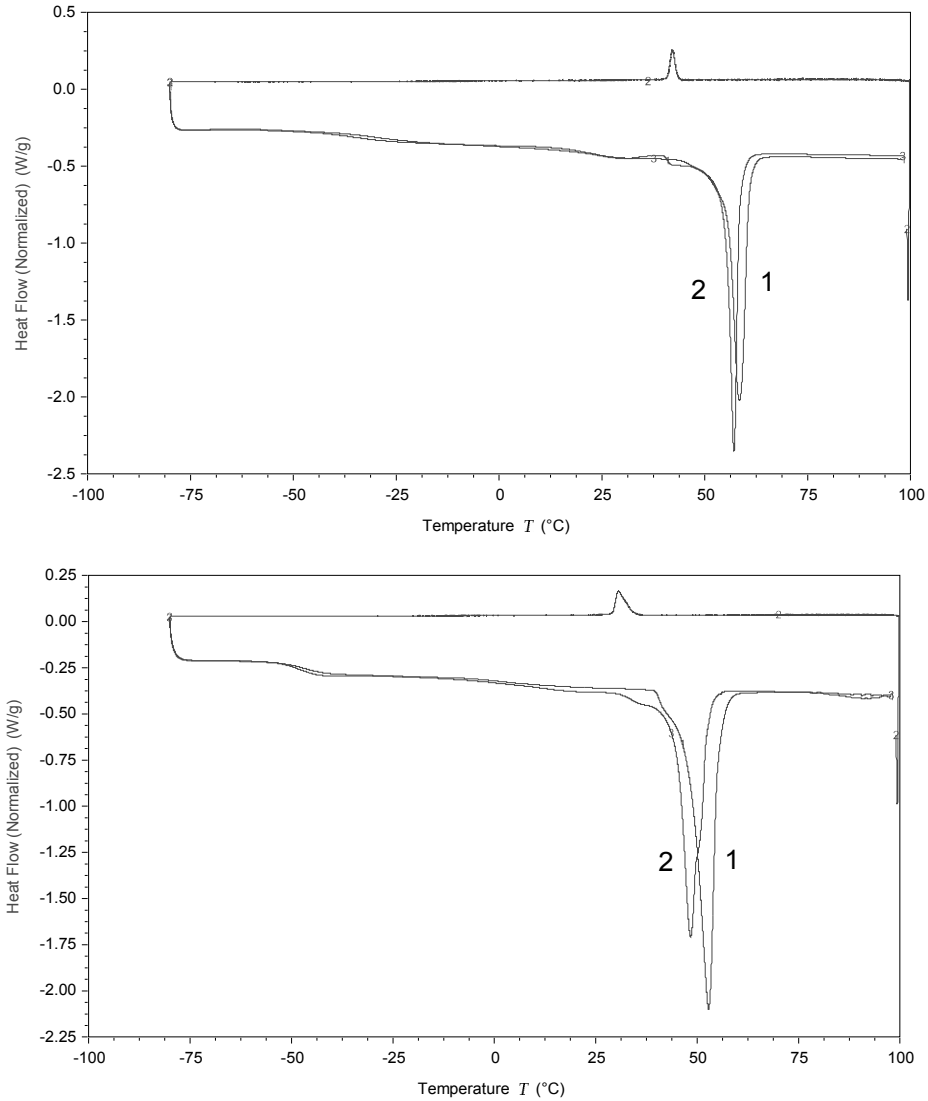

SI-Figure 5.2. DSC thermograms of the blends A) MA- (1:1 PCL:pHMGCL) and B) MA+ (1:1 PCL: pMHMGCL). 1 and 2 show thermograms of the 1st and 2nd heating run respectively.

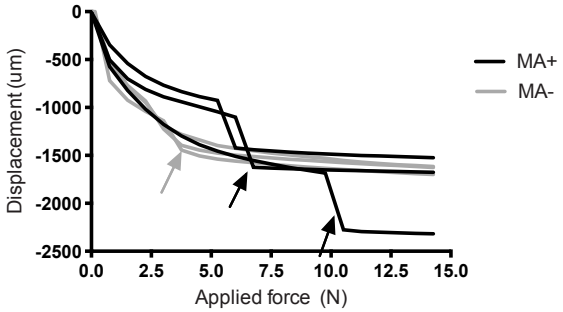

SI-Figure 5.3. Force-displacement graph of rectangle fiber reinforced constructs. A drop in displacement was visible when the hydrogel was squeezed out from the reinforced construct.

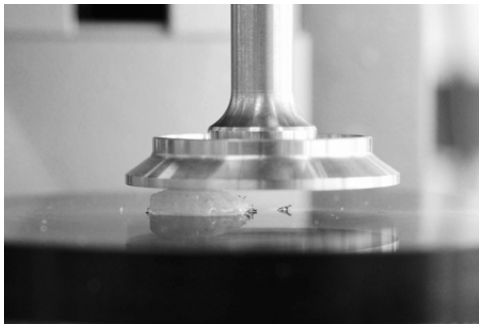

SI-Figure 5.4. Experimental set-up of the mechanical integrity test for constructs used in a knee chondral defect. Mechanical tests were performed with a rheometer, set at an initial axial loading of 20N, followed by 100 creep-recovery cycles of 0.01Nm.

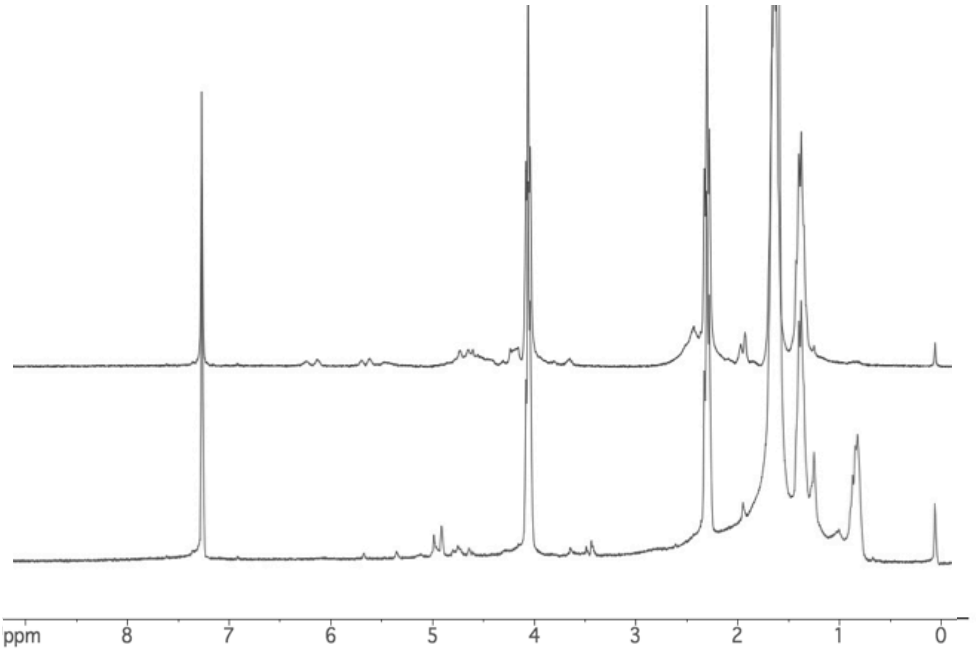

SI-Figure 5.5. ^{1}H NMR spectrum in $CDCl_3$ of MA+ before (above) and after (below) 8 weeks implantation in rats. Degradation was confirmed by the disappearance of the peak at 4.2 ppm (HMG peak).

References

1. D. Seliktar, *Science*, 2012, **336**, 1124-1128.
2. T. Vermonden, R. Censi and W. E. Hennink, *Chem Rev*, 2012, **112**, 2853-2888.
3. N. C. Hunt and L. M. Grover, *Biotechnol Lett*, 2010, **32**, 733-742.
4. A. Abbott, *Nature*, 2003, **424**, 870-872.
5. L. Bian, D. Y. Zhai, E. Tous, R. Rai, R. L. Mauck and J. A. Burdick, *Biomaterials*, 2011, **32**, 6425-6434.
6. K. C. Rustad, V. W. Wong, M. Sorkin, J. P. Glotzbach, M. R. Major, J. Rajadas, M. T. Longaker and G. C. Gurtner, *Biomaterials*, 2012, **33**, 80-90.
7. T. J. Klein, S. C. Rizzi, K. Schrobback, J. C. Reichert, J. E. Jeon, R. W. Crawford and D. W. Hutmacher, *Soft Matter*, 2010, **6**, 5175-5183.
8. W. Lee, V. Lee, S. Polio, P. Keegan, J.-H. Lee, K. Fischer, J.-K. Park and S.-S. Yoo, *Biotechnol Bioeng*, 2010, **105**, 1178-1186.
9. R. Censi, P. Di Martino, T. Vermonden and W. E. Hennink, *J Control Release*, 2012, **161**, 680-692.
10. E. J. Sheehy, T. Vinardell, C. T. Buckley and D. J. Kelly, *Acta Biomater*, 2013, **9**, 5484-5492.
11. K. L. Spiller, S. A. Maher and A. M. Lowman, *Tissue Eng Part B Rev*, 2011, **17**, 281-299.
12. K. S. Anseth, C. N. Bowman and L. Brannon-Peppas, *Biomaterials*, 1996, **17**, 1647-1657.
13. T. Billiet, M. Vandenhaute, J. Schelfhout, S. Van Vlierberghe and P. Dubruel, *Biomaterials*, 2012, **33**, 6020-6041.

14. W. Schuurman, P. A. Levett, M. W. Pot, P. R. van Weeren, W. J. A. Dhert, D. W. Hutmacher, F. Melchels, T. J. Klein and J. Malda, *Macromol Bioscience*, 2013, **13**, 551-561.
15. W. E. Hennink and C. F. van Nostrum, *Adv Drug Deliv Rev*, 2002, **54**, 13-36.
16. J. Malda, J. Visser, F. P. Melchels, T. Jüngst, W. E. Hennink, W. J. A. Dhert, J. Groll and D. W. Hutmacher, *Adv Mater*, 2013, **25**, 5011-5028.
17. S. Khalil and W. Sun, *J Biomech Eng*, 2009, **131**, 111002.
18. H. Shin, B. D. Olsen and A. Khademhosseini, *Biomaterials*, 2012, **33**, 3143-3152.
19. S. Suri and C. E. Schmidt, *Acta Biomater*, 2009, **5**, 2385-2397.
20. D. Myung, W. U. Koh, J. M. Ko, Y. Hu, M. Carrasco, J. Noolandi, C. N. Ta and C. W. Frank, *Polymer*, 2007, **48**, 5376-5387.
21. L. Pescosolido, W. Schuurman, J. Malda, P. Matricardi, F. Alhaique, T. Coviello, P. R. van Weeren, W. J. A. Dhert, W. E. Hennink and T. Vermonden, *Biomacromolecules*, 2011, **12**, 1831-1838.
22. P. Matricardi, C. Di Meo, T. Coviello, W. E. Hennink and F. Alhaique, *Adv Drug Deliv Rev*, 2013, **65**, 1172-1187.
23. R. Krüger and J. Groll, *Biomaterials*, 2012, **33**, 5887-5900.
24. M. K. Shin, S. Kim, I. , S. J. Kim, B. J. Kim, I. So, M. Kozlov, E., J. Oh and R. Baughman, H. , *Appl Phys Lett*, 2008, **93**, 163902.
25. M. Reza Nejadnik, A. G. Mikos, J. A. Jansen and S. C. G. Leeuwenburgh, *J Biomed Mater Res A.*, 2012, **100**, 1316-1323.
26. S. Ryon Shin, H. Bae, J. Min Cha, J. Young Mun, Y.-C. Chen, H. Tekin, H. Shin, S. Farshchi, M. R. Dokmeci, S. Tang and A. Khademhosseini, *ACS nano*, 2012, **6**, 362-372.
27. V. Saez-Martinez, A. Garcia-Gallastegui, C. Vera, B. Olalde, I. Madarieta, I. Obieta and N. Garagorri, *J Appl Polym Sci*, 2011, **120**, 124-132.
28. D. Kai, M. P. Prabhakaran, B. Stahl, M. Eblenkamp, E. Wintermantel and S. Ramakrishna, *Nanotechnology*, 2012, **23**, 95705.
29. J. L. Holloway, A. M. Lowman and G. R. Palmese, *Acta Biomater*, 2010, **6**, 4716-4724.
30. I.-C. Liao, F. Moutos, T. , B. Estes, T. , X. Zhao and F. Guilak, *Adv Funct Mater*, 2013, **23**, 5833-5839.
31. J. Jang, H. Oh, J. Lee, T.-H. Song, Y. Hun Jeong and D.-W. Cho, *Appl Phys Lett*, 2013, **102**, 211914.
32. E. J. Caterson, L. J. Nesti, W. J. Li, K. G. Danielson, T. J. Albert, A. R. Vaccaro and R. S. Tuan, *J Biomed Mater Res*, 2001, **57**, 394-403.
33. J. S. Wayne, C. L. McDowell, K. J. Shields and R. S. Tuan, *Tissue Eng*, 2005, **11**, 953-963.
34. G. A. Ameer, T. A. Mahmood and R. Langer, *J Orthop Res*, 2002, **20**, 16-19.
35. M. Kim, B. Hong, J. Lee, S. E. Kim, S. S. Kang, Y. H. Kim and G. Tae, *Biomacromolecules*, 2012, **13**, 2287-2298.
36. J. Coburn, M. Gibson, P. A. Bandalini, C. Laird, H. Q. Mao, L. Moroni, D. Seliktar and J. Elisseeff, *Smart Struct Syst*, 2011, **7**, 213-222.
37. J. M. Coburn, M. Gibson, S. Monagle, Z. Patterson and J. H. Elisseeff, *Proc Natl Acad Sci U S A*, 2012, **109**, 10012-10017.
38. S. Catros, F. Guillemot, A. Nandakumar, S. Ziane, L. Moroni, P. Habibovic, C. van Blitterswijk, B. Rousseau, O. Chassande, J. Amedee and J. C. Fricain, *Tissue Eng Part C*, 2012, **18**, 62-70.
39. L. A. Bosworth, L.-A. Turner and S. H. Cartmell, *Nanomedicine*, 2013, **9**, 322-335.
40. T. Xu, K. W. Binder, M. Z. Albanna, D. Dice, W. Zhao, J. J. Yoo and A. Atala, *Biofabrication*, 2012, **5**, 015001.
41. W. Schuurman, V. Khristov, M. W. Pot, P. R. van Weeren, W. J. Dhert and J. Malda, *Biofabrication*, 2011, **3**, 021001.

42. H. Lee, S. Ahn, L. J. Bonassar and G. Kim, *Macromol Rapid Commun*, 2013, **34**, 142-149.
43. J. H. Shim, J. S. Lee, J. Y. Kim and D. W. Cho, *J Micromech Microeng*, 2012, **22**, 085014.
44. J. Visser, B. J. Peters, T. J. Burger, J. Boomstra, W. J. A. Dhert, F. P. W. Melchels and J. Malda, *Biofabrication*, 2013, **5**, 035007.
45. J. Kundu, J.-H. Shim, J. Jang, S.-W. Kim and D.-W. Cho, *J Tissue Eng Regen Med*, 2013, DOI: 10.1002/term.1682.
46. C. A. DeForest and K. S. Anseth, *Annu Rev Chem Biomol Eng*, 2012, **3**, 421-444.
47. D. Dado and S. Levenberg, *Semin Cell Dev Biol*, 2009, **20**, 656-664.
48. F. T. Moutos and F. Guilak, *Biorheology*, 2008, **45**, 501-512.
49. H. Seyednejad, T. Vermonden, N. E. Fedorovich, R. van Eijk, M. J. van Steenbergen, W. J. Dhert, C. F. van Nostrum and W. E. Hennink, *Biomacromolecules*, 2009, **10**, 3048-3054.
50. H. Seyednejad, D. Gawlitta, W. J. A. Dhert, C. F. van Nostrum, T. Vermonden and W. E. Hennink, *Acta Biomater*, 2011, **7**, 1999-2006.
51. H. Seyednejad, D. Gawlitta, R. V. Kuiper, A. de Bruin, C. F. van Nostrum, T. Vermonden, W. J. Dhert and W. E. Hennink, *Biomaterials*, 2012, **33**, 4309-4318.
52. D. W. Hutmacher, *Biomaterials*, 2000, **21**, 2529-2543.
53. H. Seyednejad, W. Ji, F. Yang, C. F. van Nostrum, T. Vermonden, J. J. J. P. van den Beucken, W. J. A. Dhert, W. E. Hennink and J. A. Jansen, *Biomacromolecules*, 2012, **13**, 3650-3660.
54. H. Seyednejad, W. Ji, W. Schuurman, W. J. A. Dhert, J. Malda, F. Yang, J. A. Jansen, C. F. van Nostrum, T. Vermonden and W. E. Hennink, *Macromol Bioscience*, 2011, **11**, 1684-1692.
55. R. Censi, T. Vermonden, H. Deschout, K. Braeckmans, P. di Martino, S. C. de Smedt, C. F. van Nostrum and W. E. Hennink, *Biomacromolecules*, 2010, **11**, 2143-2151.
56. A. I. van den Bulcke, B. Bogdanov, N. de Rooze, E. H. Schacht, M. Cornelissen and H. Berghmans, *Biomacromolecules*, 2000, **1**, 31-38.
57. T. Vermonden, N. E. Fedorovich, D. van Geemen, J. Alblas, C. F. van Nostrum, W. J. A. Dhert and W. E. Hennink, *Biomacromolecules*, 2008, **9**, 919-926.
58. N. E. Fedorovich, M. H. Oudshoorn, D. van Geemen, W. E. Hennink, J. Alblas and W. J. A. Dhert, *Biomaterials*, 2009, **30**, 344-353.
59. D. Gawlitta, M. H. P. van Rijen, E. J. M. Schrijver, J. Alblas and W. J. A. Dhert, *Tissue Eng Part A*, 2012, **18**, 1957-1966.
60. C. A. M. Loontjens, T. Vermonden, M. Leemhuis, M. J. van Steenbergen, C. F. van Nostrum and W. E. Hennink, *Macromolecules*, 2007, **40**, 7208-7216.
61. C.-S. Wu, *Polymer*, 2005, **46**, 147-155.
62. I. Kutzner, B. Heinlein, F. Graichen, A. Bender, A. Rohlmann, A. Halder, A. Beier and G. Bergmann, *J Biomech*, 2010, **43**, 2164-2173.
63. J. A. Buckwalter and H. J. Mankin, *J Bone Jt Surg, Am Vol*, 1997, **79-A**, 600-614.
64. P. Levett, F. Melchels, K. Schrobback, D. Hutmacher, J. Malda and T. Klein, *Acta Biomater*, 2014, **10**, 214-223.
65. N. Samadi, C. F. van Nostrum, T. Vermonden, M. Amidi and W. E. Hennink, *Biomacromolecules*, 2013, **14**, 1044-1053.
66. C. J. de Groot, M. J. A. Van Luyn, W. N. E. van Dijk-Wolthuis, J. A. Cadée, J. A. Plantinga, W. den Otter and W. E. Hennink, *Biomaterials*, 2001, **22**, 1197-1203.
67. J. A. Cadée, M. J. A. van Luyn, L. A. Brouwer, J. A. Plantinga, P. B. van Wachem, C. J. de Groot, W. den Otter and W. E. Hennink, *J Biomed Mater Res*, 2000, **50**, 397-404.

CHAPTER 6

3D-PRINTING OF REINFORCED TWO-COMPONENT HYDROGELS

Published in slightly modified form:
K. W. M. Boere, M. M. Blokzijl, J. Visser, J. E. A. Linssen, J. Malda, W. E. Hennink, T. Vermonden, *Journal of Materials Chemistry B*, 2015, DOI: 10.1039/C5TB01645B.

Abstract

Progress in biofabrication technologies is mainly hampered by the limited number of suitable hydrogels that can act as bioinks. Here, we present a new bioink for 3D-printing, capable of forming large, highly defined constructs. Hydrogel formulations consisted of a thermoresponsive polymer mixed with a poly(ethylene glycol) (PEG) or hyaluronic acid (HA) cross-linker with a total polymer concentration of 11.3 and 9.1 wt% respectively. These polymer solutions were partially cross-linked before plotting by a chemoselective reaction called oxo-ester mediated native chemical ligation, yielding printable formulations. Deposition on a heated plate of 37 °C resulted in stabilization of the construct due to the thermosensitive nature of the hydrogel. Subsequently, further chemical cross-linking of the hydrogel precursors proceeded after extrusion to form mechanically stable hydrogels that exhibited a storage modulus of 9 kPa after 3 hours. Flow and elastic properties of the polymer solutions and hydrogels were analyzed under similar conditions as those occurring during the 3D-printing process. These experiments showed the ability to extrude the hydrogels, as well as their rapid recovery after applied shear forces. Hydrogels were printed in grid-like structures, hollow cones and a model representing a femoral condyle, with a porosity of 47.9 ± 2.3%. Furthermore, an *N*-hydroxysuccinimide functionalized thermoplastic poly-ε-caprolactone (PCL) derivative was successfully synthesized and 3D-printed. We demonstrated that covalent grafting of the developed hydrogel to the thermoplastic reinforced network resulted in improved mechanical properties and yielded high construct integrity. Reinforced constructs also containing hyaluronic acid showed high cell viability of chondrocytes, underlining their potential for further use in regenerative medicine applications.

Graphical abstract

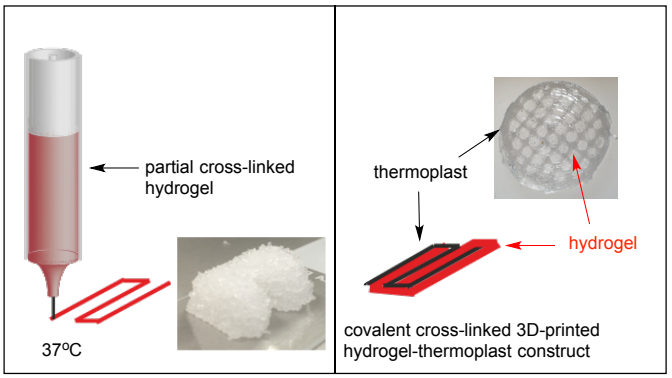

6.1 Introduction

Additive manufacturing is an emerging technique for the fabrication of complex three-dimensional (3D) constructs.[1-3] The manufacturing of constructs containing biological components is termed biofabrication and currently often used in the field of regenerative medicine. Inks for biofabrication are typically based on hydrogels, in which cells or bioactive factors can be encapsulated.[1,4-6] Complex geometries having a porous network can be created based on a computer-designed model, facilitating high diffusion of nutrients and metabolites required for tissue regeneration. Furthermore, a layer-controlled arrangement of different cell-types and biomolecules can be achieved by the incorporation of cells in the printing process. In this way, anatomical structures can be created such as those replicating blood vessel networks[7] or those mimicking the zonal architecture of cartilage.[8] Whilst hydrogels have been widely investigated for biomedical applications[9-11], tuning their properties towards a favorable bioprinting strategy remains a challenge.[1,12]

Many established biofabrication approaches rely on hydrogel formation by temperature-induced physical cross-linking often combined with subsequent chemical cross-linking.[13-15] A drawback of these techniques is that a high polymer concentration is required to stabilize the hydrogel structure for printing multiple layers with high shape fidelity.[14,16] A high polymer content can potentially limit the diffusion of nutrients and metabolites, and can consequently have a negative impact on cell migration and proliferation.[17] Additionally, to stabilize the network, small molecules or UV light are frequently used to induce subsequent covalent cross-linking. Besides the difficulties to control the shape fidelity of the constructs, the effect of these methods on the cytotoxicity of cells is under debate.[9,18]

As alternative for photopolymerization, chemoselective reactions offer exciting opportunities for the formation of biomaterials.[19] Oxo-ester mediated native chemical ligation (OMNCL) has been proposed as a promising reaction because of its high efficiency, mild reaction conditions and high selectivity. [20] This ligation reaction involves conjugation between an activated ester and an *N*-terminal cysteine and has been previously demonstrated to be highly compatible with incorporated cells and bioactive molecules.[21] Recently, we reported thermosensitive OMNCL cross-linked hydrogels that showed tunable degradation rates and mechanical properties.[22] Importantly, solutions of relatively low polymer concentrations of 12 wt% were transferred into mechanically stable hydrogels as a result of the combined physical and chemical cross-linking mechanism.

However, to enable bioprinting of hydrogels with solutions of low polymer concentrations, while still obtaining mechanically strong constructs with high shape fidelity, new biofabrication approaches have to be investigated.[1] Partial pre-crosslinking of the hydrogel precursors is an attractive approach to facilitate a good shape fidelity of printed constructs using low polymer concentrations.[23-25] Rutz

et al.[24] described partial pre-crosslinking of functionalized poly(ethylene glycol) (PEG) cross-linkers with natural polymers, thereby forming a variety of 3D-printed hydrogels with low polymer contents. These bioinks were deposited with a low flow, without collapse and resulting constructs maintained high shape fidelity. However, the obtained hydrogel networks were still relatively soft, which could hamper their potential therapeutic applications under for example load-bearing conditions where the gels are exposed to mechanical forces.

Mechanically strong constructs containing hydrogels with low polymer concentrations can be fabricated using multi-material constructs based on hydrogels that are reinforced with a thermoplastic polymer network.[26-28] Poly-ε-caprolactone (PCL) is a widely used thermoplastic polymer in biofabrication, given its relatively low melt processability (at 60 °C) and mechanical properties.[29] As an alternative for PCL, our group reported the use of a hydroxyl-functionalized variation, poly(hydroxymethylglycolide-co-ε-caprolactone), abbreviated as pHMGCL.[30,31] Compared to PCL, pHMGCL showed increased degradation rates, improved cell adhesion and was shown to be 3D-printed with good shape fidelity.[32] Importantly, methacrylate groups can be introduced to allow covalent grafting of a hydrogel and thermoplastic after photopolymerization.[33] A synergistic effect on the mechanical properties of these hydrogel-thermoplastic constructs was found as a result of covalent grafting at the interface between the hydrogel and thermoplastic, which resulted in a remarkable stabilization and increased mechanical resistance against shear forces.[33]

In this study, the two novel approaches of partial pre-crosslinking and thermoplastic grafting were combined for the fabrication of a mechanically strong 3D-printed construct that was cross-linked by oxo-ester mediated native chemical ligation. Thermoresponsive hydrogels were used to obtain additional network stabilization as a result of physical crosslinking immediately after deposition on a heated plate. Furthermore, these hydrogels were covalently grafted to a strong thermoplastic scaffold for the formation of even more mechanically robust constructs. Covalent cross-linking by OMNCL within the hydrogel as well as between the hydrogel and thermoplastic material was assessed to obtain a mechanically strong and fully integrated construct.

6.2 Materials and Methods

6.2.1 Materials

All chemicals were purchased from Sigma-Aldrich and used as received, unless stated otherwise. Hyaluronic acid (HA, 33 kDa) was obtained from Lifecore (Chaska, Mn, USA). Poly(hydroxymethylglycolide-co-ε-caprolactone (PHMGCL, 8% HMG) was synthesized according to literature procedures.[30] *N*-(2-hydroxypropyl) methacrylamide-Boc-*S*-acetamidomethyl-L-cysteine (Boc-Cys(Acm)-HPMA) was synthesized following a previously published procedure.[34] *N*-(3-Dimethylaminopropyl)-*N*′-ethylcarbodiimide hydrochloride (EDCI) was purchased from Bachem (Bubendorf, Switzerland). PEG 20,000 8-arm with a tripentaerythritol core was obtained from JenKem Technology USA (Plano, Tx, USA). Ethylthioglycolate succinic acid (ET-SA) was synthesized according to a published procedure.[35] PEG 10,000-(4,4′-azobis(4-cyanopentanoic acid (ABCPA) macroinitiator was synthesized following established procedures.[36] Tris(2-carboxyethyl)phosphine hydrochloride (TCEP) was obtained from Carl Roth (Karlsruhe, Germany). 4-(dimethylamino) pyridinium-4-toluene-sulfonate (DPTS) was synthesized following published procedures.[37] Poly(ethylene glycol) standards for GPC analysis were obtained from PSS Polymer Standards Service GmbH (Mainz, Germany). Cell culture flasks, well plates and petri dishes were obtained from Greiner Bio-One, Alphen a/d Rijn, the Netherlands. Red food coloring agent Ponceau 4R, E number 124 was obtained from Queen Fine foods Pty. Ltd. (Alderley Q., Australia). Phosphate buffered saline (PBS) pH 7.4 (8.2 g/L NaCl, 3.1 g/L $Na_2HPO_4{\cdot}12H_2O$, 0.3 g/L $NaH_2PO_4{\cdot}2H_2O$) was purchased from B. Braun (Melsungen, Germany).

6.2.2 Synthesis of PNC triblock copolymer

PEG-NIPAAm-HPMACys triblock copolymer (abbreviated as PNC) consisting of a 10 kDa PEG mid block flanked by random blocks of NIPAAm and HPMACys with a feed ratio of 93:7 mol% of NIPAAm:HPMA-Cys was synthesized as previously reported.[34] Briefly, PEG ABCPA macroinitiator, NIPAAm and HPMA-Boc-Cys(Acm) were dissolved in dry acetonitrile at a PEG:monomer ratio of 1:322, stirred for 48 h at 70 °C under N_2 atmosphere and the polymer was subsequently collected after precipitation in diethyl ether. The Boc and Acm protecting groups on cysteine were removed by TFA and iodine treatment respectively.[34] In detail, 3 g polymer was dissolved in DCM/TFA (1:1 v/v, 40 mL), stirred for 2 h, concentrated under reduced pressure and precipitated in diethyl ether. Next, the polymer was dissolved in MeOH/H_2O (1:1 v/v, 100 mL), followed by the addition of 1 mL 1 M HCl and 16 mL 0.2 M iodine in MeOH/H_2O (1:1 v/v). The mixture was stirred for 1 h at room temperature under N_2 atmosphere, after which the excess of iodine was quenched with a few drops of 1M ascorbic acid. Subsequently, the polymer in 100 mL MeOH/

H_2O was treated with 1 g TCEP for 16 h to reduce disulfide bonds, purified by dialysis and lyophilized. The obtained protected and deprotected PNC polymers were characterized by ^{1}H NMR and deprotected PNC was also characterized by GPC. PNC protected: yield 88%, ^{1}H NMR ($CDCl_3$): 3.97 (s, NIPAAm), 3.80 (t, terminal CH_2 PEG), 3.62 (m, CH_2 PEG backbone), 1.42 (s, Boc HPMA-Cys), 1.11 (s, NIPAAm). PNC deprotected: yield 62%, ^{1}H NMR ($CDCl_3$): 3.97 (s, NIPAAm), 3.80 (t, terminal CH_2 PEG), 3.62 (m, CH_2 PEG backbone), 1.11 (s, NIPAAm). GPC: M_n = 43.0 kDa, M_w/M_n = 2.36.

6.2.3 Synthesis of PEG 8-arm NHS cross-linker

PEG 20,000 8-arm was functionalized with *N*-hydroxysuccinimide (NHS) groups in a two step procedure according to literature procedures.[21] Briefly, PEG 20,000 8-arm (10 g, 4 mmol OH terminal groups), glutaric anhydride (2.27 g, 20 mmol) and pyridine (1.6 mL) were dissolved in 20 mL chloroform and refluxed at 80 °C for 24 hours under N_2 atmosphere. Methanol (100 mL) was added and the polymer was precipitated in 500 mL cold diethyl ether. The product was collected after filtration as a white powder and further dried under vacuum. Then, 10 g glutaric acid terminated PEG was dissolved in 50 mL DMSO together with NHS (4.4 g, 38 mmol) and EDCI (7.3 g, 38 mmol) and stirred for 1 h at room temperature. Subsequently, methanol (100 mL) was added and the product was collected as a white powder after precipitation in diethyl ether and filtration. Yield: 85%, Degree of substitution (DS): 92%, ^{1}H NMR ($CDCl_3$): δ = 4.24 (2H, t, terminal PEG CH_2), 3.62 (PEG backbone), 2.84 (4H, m, 2 CH_2 NHS), 2.71 (2H, t, NOC(O)CH_2), 2.49 (2H, t, NOC(O)$CH_2CH_2CH_2$), 2.06 (2H, p, NOC(O)CH_2CH_2).

6.2.4 Synthesis of HA-NHS cross-linker

Hyaluronic acid (HA) was partially functionalized with *N*-hydroxysuccinimide (NHS) groups following a literature procedure.[38] In short, 1.0 g of hyaluronic acid (33 kDa) was dissolved in 30 mL PBS. NHS (1.6 g, 14 mmol) and EDCI (1.43 g, 7.4 mmol) were added and the mixture was stirred for 2 h at room temperature. Next, the polymer was precipitated in cold ethanol (-20 °C) and centrifuged for 10 minutes at 7,000 min^{-1} at 0 °C. This procedure was repeated twice and the HA-NHS product was collected as a white solid and further dried under vacuum. ^{1}H NMR spectrum was recorded to calculate the degree of substitution (DS), defined as the number of NHS moieties per 100 disaccharide units. Yield: 93%, Degree of substitution (DS): 38%, ^{1}H NMR (D_2O): δ = 4.6-3.3 (protons of HA), 2.79 (CH_2 of NHS), 2.00 (NHC(O)CH_3).

6.2.5 Synthesis of pHMGCL-NHS

Poly(hydroxymethylglycolide-co-ε-caprolactone (pHMGCL) containing 8 mol % HMG groups (3.5 g, 2.2 mmol OH groups) was dissolved in 20 mL chloroform. Glutaric anhydride (1.1 g, 9.6 mmol) and pyridine (0.8 mL) were added and the mixture was refluxed for 24 h at 80 °C. Next, the mixture was cooled to room temperature and the polymer was precipitated in cold methanol (500 mL). The polymer derivatized with glutaric acid groups (pHMGCL-glut) was collected as a white solid after filtration. The obtained pHMGCL-glut (3.4 g) was dissolved in 30 mL chloroform and DCC (2.06 g, 10 mmol), DPTS (147 mg, 0.5 mmol) and NHS (1.15 g, 10 mmol) were added. The mixture was stirred for 3 h at room temperature. Next, dicyclohexyl urea (DCU) was removed by filtration and the obtained polymer was precipitated twice in cold methanol. The product was collected after filtration as a white solid and further dried under vacuum. PHMGCL-NHS was characterized by GPC, ^{1}H NMR and DSC.

Yield: 95%, molar ratio NHS/CL : 8/92, ^{1}H NMR ($CDCl_3$): δ = 1.2–1.4 (m, $CH_2CH_2C\mathit{H}_2CH_2CH_2$), 1.5–1.7 (m, $C(O)CH_2CH_2CH_2CH_2CH_2$), 2.1 (m, $CH_2C\mathit{H}_2CH_2C(O)ON$), 2.3 (t, $C(O)C\mathit{H}_2CH_2CH_2CH_2CH_2$), 2.6-2.8 (m, $C\mathit{H}_2CH_2C\mathit{H}_2C(O)ON$), 2.8 (t, $NC(O)C\mathit{H}_2C\mathit{H}_2$), 4.1 (t, $C(O)CH_2CH_2CH_2CH_2C\mathit{H}_2$), 4.2–4.3 (m, $CH–C\mathit{H}_2$), 4.4–4.8 (m, $OC\mathit{H}_2C(O)$), 5.2–5.5 (m, C*H*).

6.2.6 Polymer characterization

The obtained polymers were characterized by gel permeation chromatography (GPC) and NMR spectroscopy. The molecular weight of PNC was determined by GPC using a PLgel 5μm MIXED-D column (Polymer Laboratories) and a Waters 2414 refractive index detector. The column temperature was set at 65 °C and DMF containing 10 mM LiCl was used as eluent. The elution rate was 1 mL/min and the sample concentration was 5 mg/mL. Calibration was performed using poly(ethylene glycol) standards of narrow and defined molecular weights.

The molecular weights of pHMGCL and PHMGCL-NHS were determined by GPC using a PL-gel 5μm MIXED-D column and a Waters 2414 refractive index detector. AR grade THF was used as eluent with a 1 mL/min flow rate at 30 °C. Polystyrene standards of known molecular weight were used for calibration.

The polymers were further characterized by ^{1}H NMR spectroscopy on an Agilent 400 MHz spectrometer. Chemical shifts are referred to the residual solvent peak (δ= 7.26 ppm for $CDCl_3$ and 4.79 ppm for D_2O).

The thermal properties of the thermoplastic polymers were analyzed by DSC using a TA Instruments DSC Q2000 apparatus. Scans were taken from -80 °C to 100 °C with a heating rate of 10 °C/min and a cooling rate of 0.5 °C/min under a nitrogen flow. The glass transition temperature (T_g) was recorded in the second heating run as the midpoint of heat capacity change. Melting temperature (T_m) and heat of fusion (ΔH_f)

were determined from the onset of endothermic peak and integration of endothermic area in the second heating run, respectively.

6.2.7 Rheological characterization

Rheological analysis of polymer solutions and hydrogels was performed on a Discovery HR-2 rheometer (TA Instruments, New Castle, DE, USA), using a 20 mm steel cone (1°) geometry equipped with a solvent trap. Flow and elastic properties of the polymer solutions and hydrogels were analyzed under similar conditions as during the 3D-printing process. Time sweeps were performed for 30 min at 20 °C, immediately followed by 3 h at 37 °C. Oscillation was performed at a frequency of 1 Hz and a strain of 1%, previously determined to be within the viscoelastic region of these hydrogels.[34]

To evaluate the effect of shear on the hydrogels similar to the shear experienced during printing, 30 min pre-crosslinked hydrogels were subjected to an increasing shear rate of 1 to 1000 s^{-1} at 20 °C under flow conditions. Strain recovery of the 30 min pre-crosslinked hydrogels was tested by applying 4 consecutive times a 3 minute logarithmic increase of strain rate from 0.001 to 1000 s^{-1} at 20 °C under oscillation conditions and the effect of strain on viscosity, and storage and loss modulus was analyzed.

6.2.8 3D-printing of hydrogel

Hydrogels were printed using a 3D Discovery Printer and BioCAD software (RegenHU, Villaz-St-Pierre, Switzerland). A solution of PNC was shortly mixed for 1 minute with a solution of PEG-NHS or HA-NHS, to a total concentration of 7.5-3.8 wt% PNC-PEG or 7.5-1.6 wt% PNC-HA, and transferred into a 3 or 10 mL syringe. The polymeric solutions were allowed to pre-crosslink for 30 min before starting filament deposition. A pressure of 3-4 bar was applied for pneumatic extrusion. Printing head movement speed in the x and y plane (F_{xy}) of 5 mm/s and a layer height of 0.25 mm was used. Nordson EFD (Westlake, Ohio, USA) dispensing SmoothFlow tapered tips with an inner nozzle diameter of 0.25 mm was used that matched with the high solution viscosity. 3D-printing was performed using a heated plate of 37-40 °C. A red food coloring agent, Ponceau 4R, E number 124 was added to the HA-NHS solution in a concentration of 50 μL coloring agent per 1 mL HA solution to obtain additional visual contrast that allowed accurate evaluation of the porosity. Hydrogel porosity of the 3D-printed condyle shape PNC-PEG constructs was estimated after measuring the construct dimensions and weighing the construct, using the following equation:

$$\left(1 - \frac{\text{hydrogel weight (mg)}}{\text{hydrogel volume (mm}^3\text{)}}\right) \times 100\% \quad (6.1)$$

6.2.9 3D-printing of NHS functionalized thermoplastic polymer

Thermoplastic pHMGCL-NHS constructs were printed using a BioScaffolder dispensing system (Sys+Eng, Salzgitter-Bad, Germany). Cylindrical scaffolds (diameter: 15 mm, height: 0.9 mm, strand spacing 1.5 mm, 5 layers) were designed with Rhino 3D software (McNeel, Seattle, WA, USA) and the Standard Tessellation Language (STL) file of this model was translated to g-code and executed on a BioScaffolder with computer-aided manufacturing (CAM) software (PrimCAM, Einsiedeln, Switzerland).[33] PHMGCL-NHS was melted at 140 °C for extrusion through a 25G metal needle (DL Technology LLC, Haverhill, MA, USA). A pressure of 0.4 MPa was applied, followed by screw-driven extrusion at a deposition speed of 250 mm/min. The BioScaffolder was placed within a laminar flow cabinet to ensure rapid solidification of the printed fibers.

6.2.10 Dynamic mechanical analysis

Cylindrically shaped PNC-PEG hydrogels of 7.5-3.8 wt% with a volume of 100 μL were prepared in plastic molds with a diameter of 4 mm. Reinforced pHMGCL-NHS – PNC-PEG materials were prepared after filling the pores of constructs described in section 6.2.9 with PNC-PEG hydrogel. The Young's moduli of these constructs were determined on a Q800 DMA (TA Instruments, New Castle, DE, USA) in triplicate after 3 hours cross-linking at 37 °C. Compression from 0.01 till 0.1 N with a rate of 0.01 N/min was applied to the hydrogels and from 0.01 to 5 N with a rate of 0.5 N/min to the reinforced constructs at room temperature. The Young's modulus was determined from the first linear region of the stress-strain curve.

6.2.11 Creep-recovery test: interface-grafting strength

The effect of grafting of PNC-PEGNHS and pHMGCL-NHS was investigated in creep-recovery tests that were performed using a Discovery HR-2 rheometer (TA-instruments), similarly to previously described methods.[33] Flat discs (surface area 80 mm^2, thickness 0.1 mm) of pHMGCL and pHMGCL-NHS were prepared after dissolving the polymer in chloroform (160 mg/mL) and depositing droplets on a glass petri dish, subsequently allowing the chloroform to evaporate overnight. PEG-NHS and PNC solutions in PBS were prepared at 4 and 15 wt% concentrations, respectively, 4 hours before starting the experiment. Measurements were performed in triplicate. The pHMGCL or pHMGCL-NHS discs were attached with a photosticker (HEMA, Groningen, the Netherlands) to the upper 40 mm diameter plate of the geometry. PEG-NHS (50 μL) was mixed with PNC (50 μL) and pipetted on the bottom plate before lowering the top plate to a gap of 1.0 mm at which the hydrogel and thermoplastic had a narrow surface interface. The construct was allowed to cross-link for 3 hours at 37 °C. Next, the obtained constructs were mechanically deformed at different torque values ranging from 100 to 1000 μNm, using a step-wise increase

of 100 μNm. This deformation consisted of a 1 minute creep followed by 1 minute recovery, while keeping the temperature at 37 °C. In the creep step, a constant torque force was applied on the top thermoplastic layer that was in contact with the hydrogel and the observed strain or deformation of the material was recorded over time. In the recovery step, the applied force was released, and the construct was allowed to recover to the starting position. The torque value at which the deformation resulted in detachment of the hydrogel and thermoplastic was noted as the construct failure.

6.2.12 Live/Dead viability

A Live/Dead viability assay (calcein AM/ethidium homodimer, Life Sciences, USA) was performed on the reinforced pHMGCL-NHS – PNC-PEG and pHMGCL-NHS – PNC-HA constructs, as previously described[14,39] and according to recommendations of the manufacturer. Briefly, chondrocytes were harvested from full thickness cartilage of an equine stifle joint, after consent of the owner of the horses, according to previously published procedures.[39] Chondrocytes were encapsulated in the hydrogels at passage 2 at a concentration of 5×10^6 cells/mL. Hydrogels containing cells were allowed to form for 1.5 h at 37°C before culture medium was added. Viability of the chondorocytes was visualized using a light microscope (Olympus, BX51, USA) with excitation/emission filters set at 488/530 nm and 530/580 nm to detect living (green) cells and dead (red) cells respectively after 1.5 h. Live and dead cells were counted for two samples per group at four locations within the construct. Cell viability was calculated using the following equation:

$$\frac{\text{live cells}}{\text{total cells}}\times 100\% \tag{6.2}$$

6.2.13 Histology

Constructs that were previously analyzed with a live/dead assay were fixed in formalin for histological examination. The samples were dehydrated through a graded ethanol series, cleared in xylene and embedded in paraffin. The samples were subsequently sectioned (5_m) and stained with hematoxylin and eosin (H&E) to visualize cell distribution in the reinforced constructs.

6.2.13 Statistics

Construct failure data from creep-recovery experiments, Young's modulus data from DMA measurements and cell viability data were assessed by a Mann-Whitney-U test, using GraphPad Prism 6 software (La Jolla, Ca, USA). A $p<0.05$ was considered as significant.

6.3 Results and Discussion

6.3.1 Hydrogel components

Polymer structures of the hydrogel building blocks used in this study and the OMNCL mechanism are shown in Figure 6.1. The triblock copolymer PEG-NIPAAm-HPMACys (PNC) was synthesized by radical polymerization and consisted of a PEG 10 kDa midblock, flanked by 20 kDa random blocks of NIPAAm and HPMA-cysteine. NIPAAm was introduced for its thermosensitive characteristics, while cysteine functionalities enable covalent chemical cross-linking.[34] The obtained molar ratio of NIPAAm:cysteine in the PNC polymer was 94:6 according to NMR analysis, which is in good agreement with the feed ratio (93:7). This polymer exhibited a lower critical solution temperature (LCST) of 30 °C in water, hence behaving as a liquid solution at room temperature and forming a physically cross-linked network above its LCST.[34] Poly(ethylene glycol) (PEG) 8-arm and hyaluronic acid (HA) cross-linkers were functionalized with *N*-hydroxysuccinimide (NHS) groups with a degree of substitution (DS) of 92% and 38% respectively as determined by ^{1}H NMR. DS is defined as the percentage of PEG hydroxyl or HA carboxylic acid groups that were converted into NHS moieties. The NHS functionalized polymers were purified by precipitation instead of dialysis, to limit potential premature hydrolysis of the NHS ester bonds.

6.3.2 3D-printing and rheological assessment

A few requirements were listed to achieve optimal 3D-printing based on previous experience and the experiments reported by Rutz *et al*.[24] Firstly, we aimed for a maximal pre-crosslinking time of 30 minutes before starting extrusion, since a long waiting time can have negative effects on cells that can be entrapped in the hydrogel. Secondly, the hydrogel should be deposited as an intact filament with sufficient yield stress and without collapse on the printing plate. Therefore, polymer concentrations of the aqueous solutions were optimized to allow extrusion of gel filaments without filament fracturing or clogging the nozzle while maintaining high shape fidelity. It was found that hydrogel concentrations above 25 wt% were deposited as lose fractions instead of intact filaments, thereby creating structures with low shape fidelity as well as quick nozzle obstruction. In contrast, hydrogels with a total polymer concentration below 8 wt% required pre-crosslinking times of more than 30 minutes before allowing extrusion without a collapse of the construct.

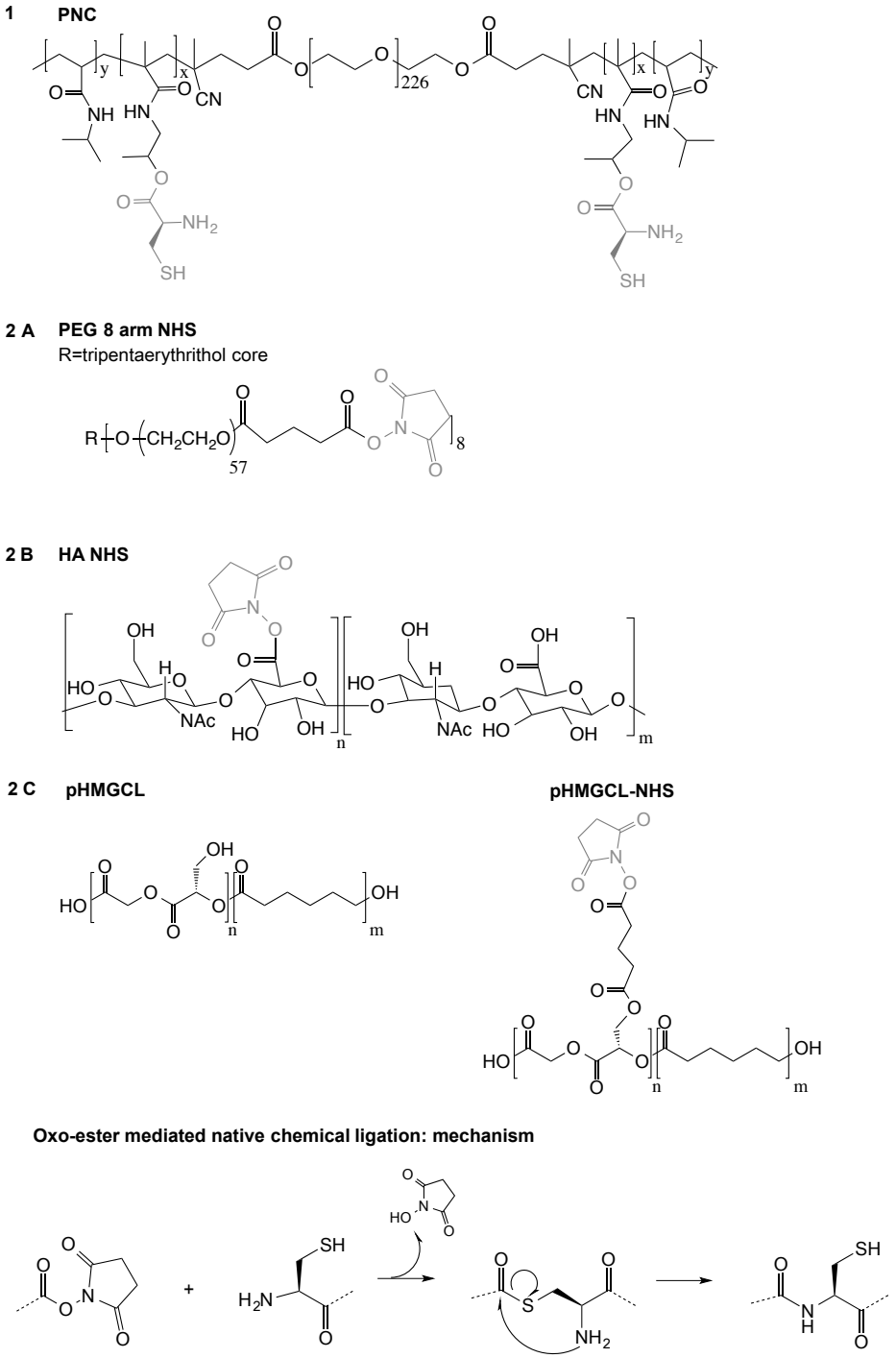

Figure 6.1. Overview of chemical structures of polymers used in this study and chemical cross-linking mechanism (oxo-ester mediated native chemical ligation).

Therefore, hydrogel concentrations of 7.5 wt% PNC mixed with 3.8 wt% PEG-NHS (total polymer conc. 11.3 wt%) or 7.5 wt% PNC mixed with 1.6 wt% HA-NHS (total polymer conc. 9.1 wt%), both corresponding to a 1:1 functional group ratio, were chosen for creating structures with both good shape fidelity as well as maintaining filament extrusion. These concentrations were significantly lower than the concentrations needed for 3D-printing of similar thermosensitive hydrogels without partial pre-cross-linking (≥25 wt%).[14,16] Furthermore, pre-crosslinking times were significantly shorter than previously reported for partially cross-linked hydrogels when extrusion was performed after 2 hours, as a result of the efficient chemical cross-linking using oxo-ester mediated native chemical ligation.[24]

An anatomically relevant model of a femoral condyle was created and printed using PNC-PEG hydrogel formulations (Figure 6.2). Three dimensional structures were created by depositing multiple layers while retaining the shape of the hydrogel (Figure 6.2C and D). The 3D-printed PNC-PEG hydrogels exhibited an average porosity of 47.9 ± 2.3 %. Creating porous networks is extremely important for facilitating nutrient diffusion, tissue contact and tissue ingrowth.[15,40] The shape maintaining properties of these hydrogel filaments were further illustrated by the creation of a hollow cone model (Figure 6.2E). Filaments were deposited onto constructs with an angle of approximately 45°, thereby creating overhang geometries without the necessity of an external support material. Furthermore, porous grid-like constructs of PNC-HA hydrogels were created (Figure 6.2G and H), showing the possibility to create specific internal gaps that can enhance the diffusion of nutrients through the construct.

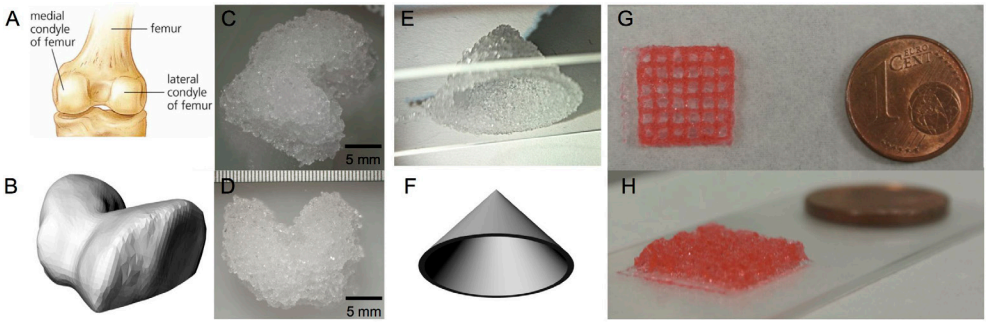

Figure 6.2. A) Schematic display of femoral condyles, adapted from the American Heritage Dictionary.[41] B) CAD model of femoral condyle. C) and D) 3D-printing of PNC-PEG NHS hydrogels in a condyle shape. E) Hollow cone shape, showing the possibility to create overhangs without support. F) CAD model of hollow cone. G) and H) 3D-printing of PNC-HA NHS hydrogels in porous grid shapes.

Overall, there were no clear differences in the possibility to extrude PNC-PEG and PNC-HA hydrogels. However, as a result of the fast cross-linking kinetics of PNC-HA hydrogels it was important to quickly transfer the solutions to the syringe, while still ensuring homogeneous mixing of the two components and avoiding the presence of air bubbles in the mixture, since this hampers the extrusion of continuous, cohesive filaments.
Interestingly, the 3D-printing window, defined as the time frame when it was possible to print the polymer solutions, was not as narrow as previously described for partially cross-linked two-component materials.[1,24] Even after two hours of pre-crosslinking in the syringe, the hydrogels could still be extruded and deposited with the same shape fidelity. Extrusion was possible by increasing the pressure from 3 to 4 bar over time, and continuous extrusion was achieved for the fabrication of a construct of approximately 20 cm^3 during 1 hour. Alternatively, these hydrogels may be attractive for printing with a dual extrusion nozzle. The use of a dual syringe printing head can eliminate the change in viscosity during 3D-printing, since the two components will only be mixed shortly prior to deposition. However, besides the difficulties to allow proper mixing, very fast gelation needs to be ensured to allow the formation of constructs with high shape fidelity. Therefore, this approach may be less feasible for 3D-printing of hydrogels with a relatively low polymer content.

The mechanical and flow properties of the gels were evaluated by rheology experiments, since control over flow properties is one of the major characteristics for successful translation into a 3D-printed construct.[1] In our strategy, four relevant steps of 3D-printing were identified. In the first step, the hydrogels are left in the syringe at room temperature, allowing them to partially cross-link. This step was imitated during rheology experiments by using limited oscillation of 1% strain and 1 Hz frequency at 20 °C and analyzing the evaluation of storage and loss moduli (G' and G") in time. In the second step, the hydrogel is extruded through the nozzle, which was characterized as a shear rate ramp. In the third and fourth step, the partially cross-linked hydrogel is deposited on a 37 °C plate and subsequently allowed to further harden in time. This last part was imitated by increasing the temperature during rheology measurements to 37 °C and again applying minimal oscillation. As depicted in Figure 6.3A and B, G' and G" were measured for 30 minutes at 20 °C, followed by 3 hours at 37 °C. At room temperature, the PNC-PEG aqueous systems showed an increase in G' resulting in a higher value of G' compared to G" after 10 minutes (SI-Figure 6.1), thereby going from fluid-like (viscous) to viscoelastic behavior. In contrast, the PNC-HA mixtures already showed this transition immediately upon starting the rheological measurement. The more rapid gelation of PNC-HA can be ascribed to the higher amount of NHS functionalities per HA chain in comparison to PEG and is in line with previous work.[34] To explain, with a DS of 38% and a molecular weight of 33 kDa, HA had on average 32 NHS moieties

per chain, compared to only 7.4 NHS moieties on PEG. After 30 minutes of cross-linking PNC-PEG reached a storage modulus of 0.7 kPa, while PNC-HA reached a G' of 2.1 kPa.

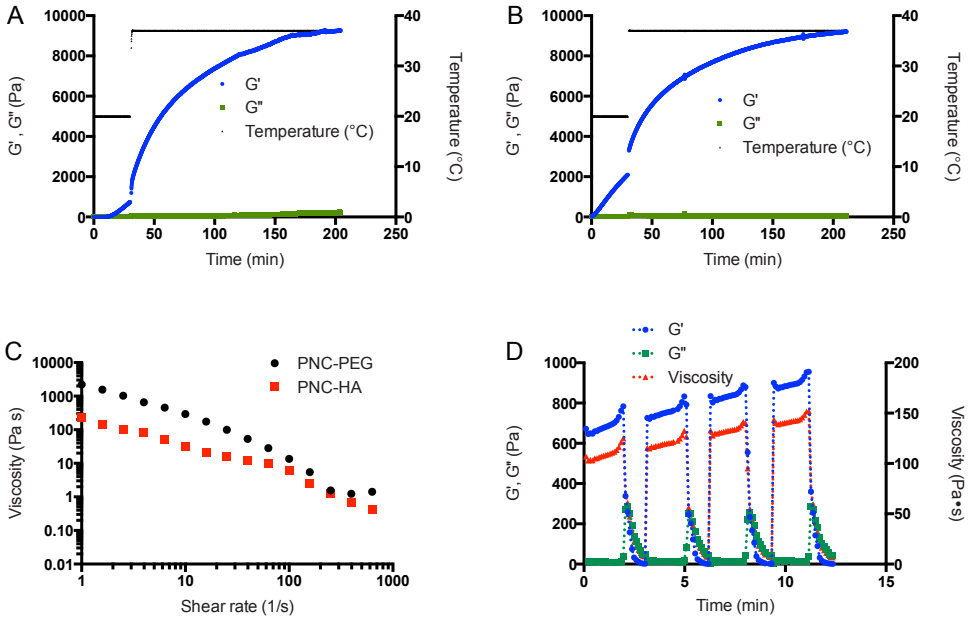

Figure 6.3. Rheological and flow characteristics of hydrogels imitating the hydrogel plotting process. A) PNC-PEG 7.5-3.8 wt%, 30 min pre-crosslinking at 20 °C, 3 h measuring at 37 °C. B) PNC-HA 7.5-1.6 wt%, 30 min 20 °C, 3 h 37 °C. C) PNC-PEG and PNC-HA shear rate flow sweep, applied after 30 min at 20 ºC. D) Four oscillation strain ramps on PNC-PEG 7.5-3.8 wt% after 30 min at 20 ºC to test hydrogel recovery. Strain rate was increased logarithmically from 0.001 to 1000 s^{-1} during 3 minutes.

Subsequently, the temperature was increased to 37 °C, mimicking the temperature change during deposition on a heated plate. The storage moduli increased immediately to 1.2 kPa and 3.3 kPa for PNC-PEG and PNC-HA, respectively, as a result of the thermoresponsive properties of the polymers. The ~1.6 fold increase in G' resulted in an immediate extra stabilization of the hydrogel network. Rheology measurements also showed a more rapid increase in G' after raising the temperature likely as a result of the increased kinetics of the OMNCL reaction at 37 °C. After an additional 3 hours of network formation, both formulations reached a storage modulus of approximately 9 kPa. A similar storage modulus for both formulations was expected based on a comparable polymer concentration in both hydrogel formulations and an equal functional group content. Furthermore, the flow properties of the hydrogels as experienced during the actual extrusion through the

nozzle were studied by rheology. After increasing the shear rate (Figure 6.3C), a decrease in viscosity was observed, similar to the shear-thinning or pseudoplastic behavior that is often encountered for polymeric solutions.[42] Importantly, as depicted in Figure 6.3D, the process of increasing and decreasing strain that was applied on the hydrogel could be repeated several times, thereby proving that the hydrogel structure remained intact and recovered rapidly. At each step, the storage modulus and viscosity at low shear increased compared to the previous step, showing that the cross-linking continued in time. Based on the used needle diameter (d) of 0.25 mm and a printing velocity ($\boldsymbol{\nu}$) of 5 mm/s, the estimated shear rate ($\dot{\boldsymbol{\gamma}}$) in the needle was calculated using the equation:

$$\dot{\gamma} = \frac{8\nu}{d} \tag{6.3}$$

which corresponded to 160 s^{-1}.[35] Here, we assumed that the printing velocity matches the velocity in the needle. At this shear rate, the partially cross-linked hydrogels had a low viscosity of 5.4 Pa•s for PNC-PEG and 2.5 Pa•s for PNC-HA (Figure 6.3C). Additionally, the hydrogels showed a sudden collapse in viscosity at a strain rate of approximately 12 s^{-1} (SI-Figure 6.3C). These viscosity profiles confirm that with our 3D-printing approach the hydrogels were moldable, thereby making it possible for the gels to be extruded through a small needle. It must be noted that during extrusion, shear forces exerted on the hydrogel are maximal near the wall instead of homogenously as during the rheology experiments, hence minimally influencing the hydrogel structure in the middle of the nozzle. Rutz *et al.*[24] previously suggested that extrusion of partially cross-linked hydrogels was likely facilitated by the localized rupture of the gel at the wall of the nozzle, thereby facilitating the extrusion of continuous cohesive filaments.

6.3.3 Reinforced hydrogel-thermoplastic constructs

To increase the mechanical strength of the 3D-printed hydrogels, multi-material constructs were formed by combining the hydrogel with a thermoplastic polyester. To this end, an NHS-functionalized thermoplastic polymer, abbreviated as pHMGCL-NHS was successfully synthesized and characterized to enable the formation of covalent grafting with the hydrogel, thereby allowing optimal material integration.

The thermoplastic polymer pHMGCL contained 8% HMG groups, defined as the molar ratio HMG/CL. The OH groups of HMG were fully functionalized with NHS groups in a two-step reaction. Successful functionalization is shown by ^{1}H NMR spectroscopy (Figure 6.4). The polymers are abbreviated as pHMGCL and pHMGCL-NHS for the polymers with and without NHS functionalities respectively, and the polymer characteristics are listed in Table 6.1.

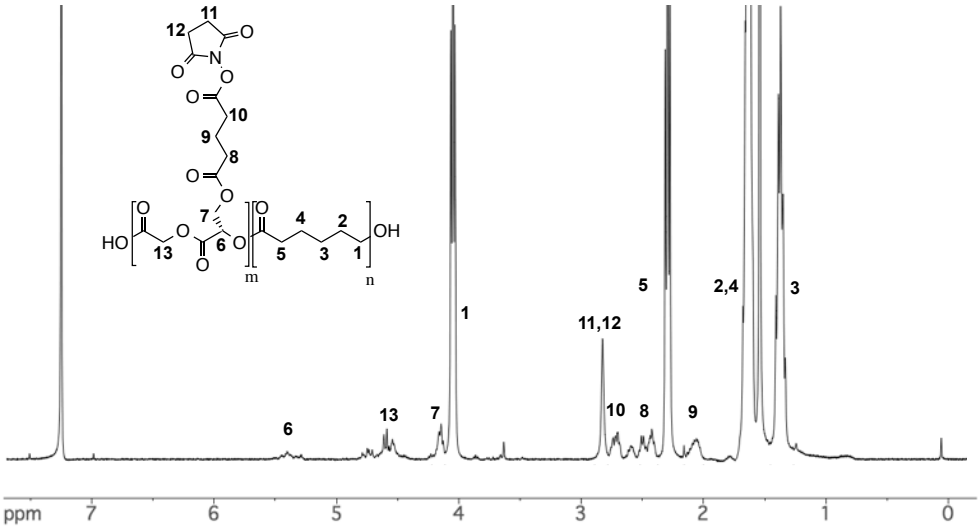

Figure 6.4. Chemical structure and ^{1}H NMR of NHS-functionalized thermoplastic pHMGCL-NHS in $CDCl_3$. Ratio NHS/CL=8/92.

Table 6.1. pHMGCL and pHMGCL-NHS characteristics.

	Ratio HMG/CL	Ratio NHS/CL	T_m (°C)	T_g (°C)	ΔH_f (J/g)	M_n (kDa)	M_w (kDa)	PDI
pHMGCL	8/92	-	49	-47	65	16.3	22.4	1.4
pHMGCL-NHS	-	8/92	50	-38	53	17.9	23.0	1.3

Analysis of the number average molecular weight (M_n) by GPC showed a slight increase from 16.3 to 17.9 kDa after functionalization with NHS groups, indicating that neither premature cross-linking nor chain scission had occurred during the synthesis. Additionally, the thermal properties of the obtained polymers were evaluated with DSC. Both pHMGCL and pHMGCL-NHS displayed semi-crystalline thermoplastic behavior with a low T_g of -47 and -38 °C respectively and a melting temperature (T_m) around 50 °C. The increase in T_g after NHS functionalization was ascribed to the lower mobility of the polymer chains as a result of the bulky NHS groups.

Reinforced thermoplast-hydrogel constructs were fabricated as depicted in Figure 6.5 from a cylindrical porous scaffold. Pores filled with hydrogel were created with a size of 1.1 ± 0.4 mm, which is in good agreement with the 1.5 mm strand spacing of the

designed model. The Young's modulus increased from 17 ± 1 kPa for only hydrogel based constructs to 645 ± 12 kPa for reinforced hydrogels, a 38 fold increase (Figure 6.5C). Importantly, the mechanical strength of the reinforced construct was similar to the thermoplastic construct alone (814 ± 75 kPa), thereby primarily dependent on the thermoplastic properties. Therefore, it is expected that the mechanical strength of the reinforced constructs can be further tailored by altering the construct geometries, such as fiber distance and fiber diameter.[45]

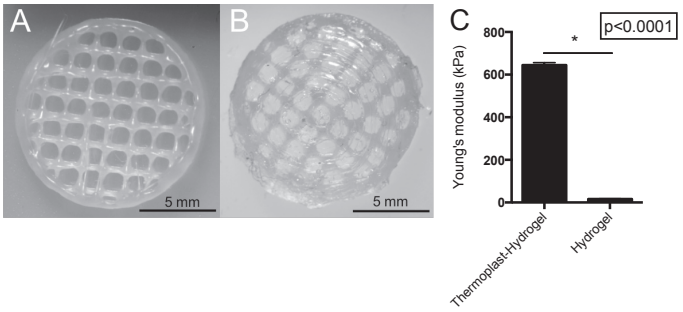

Figure 6.5. Reinforced thermoplast-hydrogel constructs. A) pHMGCL-NHS 3D-printed network. B) pHMGCL-NHS – PNC-PEGNHS thermoplast-hydrogel construct. C) Young's modulus as measured by DMA of PNC-PEG NHS hydrogel and reinforced thermoplast-hydrogel constructs.

To get insight whether the hydrogel is indeed covalently grafted to the thermoplastic support material, the functional group ratio of NHS:cysteine at the thermoplast-hydrogel interface was calculated. To this end, the amount of functional groups per volume was calculated where we assumed that all functional groups were equally distributed over the materials (*i.e.* same density of functional groups at interface and bulk). The amount of functional groups per volume present on the thermoplastic polymer was estimated using the mass percentage of functional groups in the thermoplastic polymer and the density of the polymer. This was compared to the number of available cysteine groups, using the polymer concentration in the hydrogel. On average, the thermoplastic polymer pHMGCL-NHS has 22 times more functional groups per volume (and thus also at the interface) compared to the number of cysteine moieties in the used hydrogel. Therefore, it can be expected that there are plenty NHS groups on the thermoplastic polymer available for cross-linking with the cysteine moieties in the hydrogel. This material integration was tested in a creep-recovery experiment by applying friction at the material interface (Figure 6.6). For this, a cysteine:NHS functional group ratio of 2:1 was used in the hydrogel to ensure that remaining cysteines were available for cross-linking with the thermoplastic. In a creep-recovery experiment, a stepwise increased torque force, followed by a 1-minute recovery, was applied on top of the thermoplastic. The moment that the thermoplastic was disintegrated from the hydrogel was characterized by high strain

values and a lack of strain recovery. The corresponding torque force was assigned as the point of construct failure. As shown in figure 6.6C, PNC-PEG hydrogels combined with pHMGCL-NHS exhibited a significantly 1.6 fold higher resistance against rotational friction compared to hydrogels combined with the thermoplastic without NHS groups (pHMGCL). Therefore, it can be concluded that the functional NHS groups in the thermoplastic contributed to a higher material integration, similarly to what has been found previously for photopolymerized constructs.[33] Although the measurements were already performed after 3 hours to limit water evaporation, it is expected that this integration will further increase in time, since it was previously shown that the chemical cross-linking was not completed after 3 hours.[22]

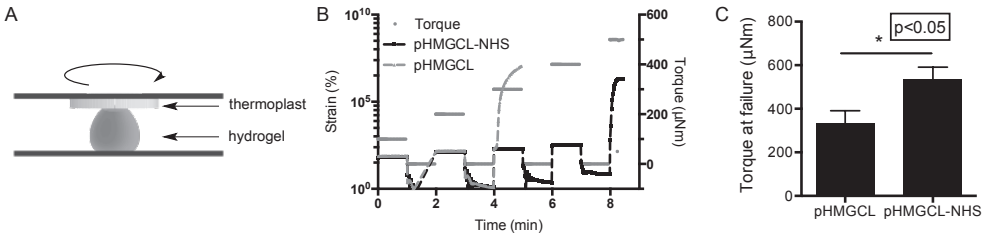

Figure 6.6. Evaluation of hydrogel-thermoplastic integration in creep-recovery tests. A) schematic display of experimental set-up. B) Representative rheology measurement of creep-recovery between thermoplastic and PNC-PEG hydrogel. C) Torque at failure for PEG-pHMGCL and PEG-pHMGCL-NHS constructs (n=3). P<0.05 was considered as significantly different.

Chondrocytes were embedded in the reinforced thermoplast-hydrogel construct to investigate the cytocompatibility of the cells in the hydrogel. Since the polymer solutions had a low viscosity prior to mixing of the two components, chondrocytes were easily and homogeneously mixed with the PNC solution and then added to the PEG or HA solution. Cell viability was analyzed after 1.5 hours for a reinforced pHMGCL-NHS network covalently grafted to a hydrogel containing PNC-PEG or PNC-HA (Figure 6.7A and B) to analyze the effect of initial cross-linking on cell viability. Since there were no clear differences in chondrocyte cell viability in the hydrogels after 4 hours or 7 days of culture (SI-Figure 6.2), an early time point of 1.5 h was used to analyze the differences in cell viability between PNC-PEG and PNC-HA reinforced constructs. The reinforcing thermoplastic fibers are shown in white, with hydrogel containing chondrocytes homogeneously distributed in the pores. Cell viability was significantly higher for the constructs containing hyaluronic acid (90 ± 9 %) compared to constructs containing PEG (43 ± 23 %), as was expected since PEG is a biologically inert material and lacks adhesion sites. Several studies have shown the potential of hyaluronic acid to induce matrix formation by embedded

cells, thereby making it an attractive biomaterial.[46-49] The same viability results were obtained for the hydrogels as such, proving that the thermoplastic network did not adversely affect the viability of the entrapped cells.
The cell distribution was analyzed by histology using a hematoxylin and eosin (H&E) staining. Cells were homogeneously distributed in the PNC-PEG hydrogel (Figure 6.7C and D). Importantly, histological analysis showed that cells were also located near the thermoplastic fibers, thereby showing no deleterious effects on the presence of the thermoplastic polymer strands, in line with previous studies.[33] Similar results of cell distribution were obtained for the PNC-HA reinforced constructs (data not shown). Taken together, these results showed that chondrocytes can be easily and homogeneously incorporated in the reinforced constructs and showed a favorable cell viability in the constructs containing hyaluronic acid.

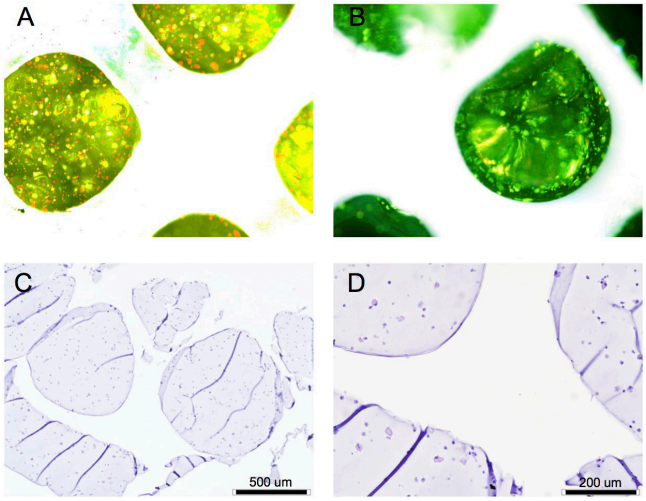

Figure 6.7. Chondrocyte-laden hydrogels reinforced with thermoplastic pHMGCL-NHS network. A) Representative live (green) and dead (red) staining of reinforced PNC-PEG hydrogels and B) reinforced PNC-HA hydrogels. The thermoplastic network is shown in white, with the chondrocyte-laden hydrogels in the pores. C) and D) Hematoxylin and eosin staining of PNC-PEG hydrogels showing homogeneous cell distribution near reinforced thermoplastic network.

6.4 Conclusion

This study describes the development of a novel bioink from a partially cross-linked, yet extrudable and self-supporting hydrogel. The hydrogels were chemically cross-linked by oxo-ester mediated native chemical ligation and physically cross-linked after deposition on a 37 °C printing plate as a result of their thermoresponsive properties. Further, mechanical strength was greatly enhanced after covalent grafting to a thermoplastic polymer scaffold. The bioinks described in this study provide new possibilities for biofabrication, given its versatility in mechanical properties, high construct integrity and controllable 3D-printing as supported by rheology.

Acknowledgements
This work was supported by a grant from the Dutch government to the Netherlands Institute for Regenerative Medicine (NIRM, grant No. FES0908) and the Dutch Arthritis Foundation. Part of the research leading to these results has received funding from the European Union Seventh Framework Programme (FP7/2007-2013) under grant agreement n° 309962 (HydroZones) and from the European Research Council under grant agreement n°647426 (3D-JOINT).

Supporting Information

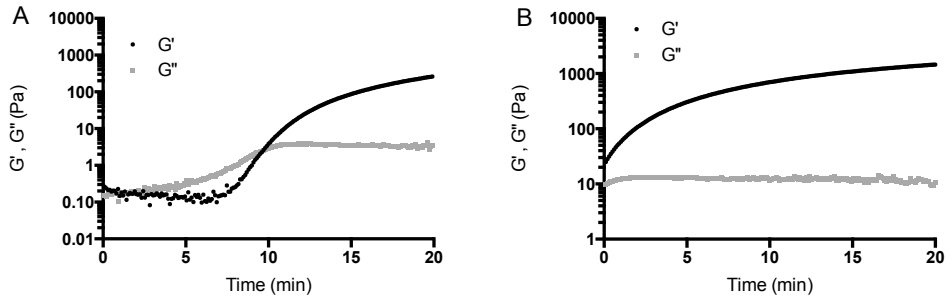

SI-Figure 6.1. Evaluation of storage modulus (G') and loss modulus (G") during the first 20 minutes of pre-cross-linking at 20 °C of A) PNC-PEGNHS (7.5-3.8 wt%) and B) PNC-HANHS (7.5-1.6 wt%).

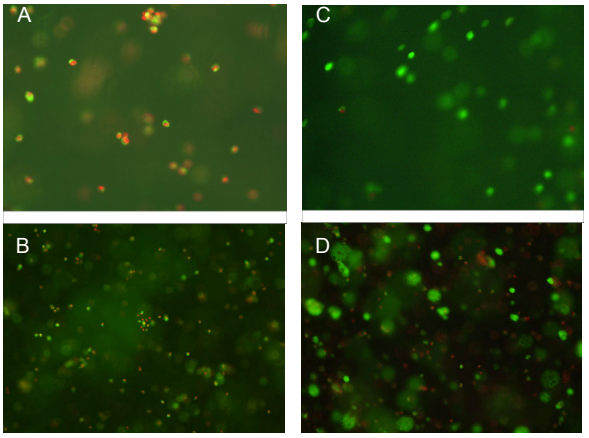

SI-Figure 6.2. Live Dead chondrocyte viability of PNC-PEG (7.5-3.8 wt%) after A) 4 hours and B) 7 days. Chondrocyte viability of PNC-HA (7.5-1.6 wt%) after C) 4 hours and D) 7 days.

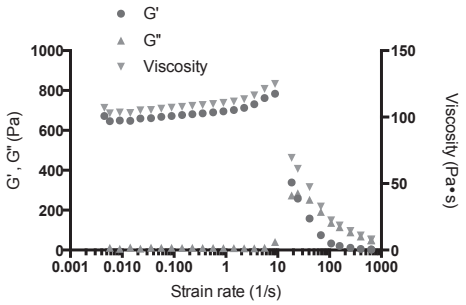

SI-Figure 6.3. Effect of increasing strain rate on storage modulus (G′), loss modulus (G″) and viscosity of PNC-PEG (7.5-3.8 wt%) as measured by rheology.

References

1. J. Malda, J. Visser, F. P. Melchels, T. Jüngst, W. E. Hennink, W. J. A. Dhert, J. Groll and D. W. Hutmacher, *Adv. Mater.*, 2013, **25**, 5011-5028.
2. A. Skardal and A. Atala, *Ann. Biomed. Eng.*, 2015, **43**, 730-746.
3. F. P. Melchels, J. Feijen and D. W. Grijpma, *Biomaterials*, 2010, **31**, 6121-6130.
4. F. P. W. Melchels, M. A. N. Domingos, T. J. Klein, J. Malda, P. J. Bartolo and D. W. Hutmacher, *Prog. Polym. Sci.*, 2012, **37**, 1079-1104.
5. N. E. Fedorovich, J. Alblas, J. R. de Wijn, W. E. Hennink, A. J. Verbout and W. J. A. Dhert, *Tissue Eng.*, 2007, **13**, 1905-1925.
6. B. Derby, *Science*, 2012, **338**, 921-926.
7. D. B. Kolesky, R. L. Truby, A. Gladman, T. A. Busbee, K. A. Homan and J. A. Lewis, *Adv. Mater.*, 2014, **26**, 3124-3130.

8. T. J. Klein, S. C. Rizzi, J. C. Reichert, N. Georgi, J. Malda, W. Schuurman, R. W. Crawford and D. W. Hutmacher, *Macromol. Biosci.*, 2009, **9**, 1049-1058.
9. S. J. Buwalda, K. W. M. Boere, P. J. Dijkstra, J. Feijen, T. Vermonden and W. E. Hennink, *J. Controlled Release*, 2014, **190**, 254-273.
10. N. A. Peppas, J. Z. Hilt, A. Khademhosseini and R. Langer, *Adv. Mater.*, 2006, **18**, 1345-1360.
11. D. Seliktar, *Science*, 2012, **336**, 1124-1128.
12. T. Billiet, M. Vandenhaute, J. Schelfhout, S. Van Vlierberghe and P. Dubruel, *Biomaterials*, 2012, **33**, 6020-6041.
13. M. Kesti, M. Müller, J. Becher, M. Schnabelrauch, M. D'Este, D. Eglin and M. Zenobi-Wong, *Acta Biomater.*, 2015, **11**, 162-172.
14. R. Censi, W. Schuurman, J. Malda, G. Di Dato, P. E. Burgisser, W. J. A. Dhert, C. F. Van Nostrum, P. Di Martino, T. Vermonden and W. E. Hennink, *Adv. Funct. Mater.*, 2011, **21**, 1833-1842.
15. F. P. W. Melchels, W. J. A. Dhert, D. W. Hutmacher and J. Malda, *J. Mater. Chem. B*, 2014, **2**, 2282-2289.
16. N. E. Fedorovich, I. Swennen, J. Girones, L. Moroni, C. A. Van Blitterswijk, E. Schacht, J. Alblas and W. J. A. Dhert, *Biomacromolecules*, 2009, **10**, 1689-1696.
17. D. E. Discher, P. Janmey and Y.-l. Wang, *Science*, 2005, **310**, 1139-1143.
18. I. Mironi-Harpaz, D. Y. Wang, S. Venkatraman and D. Seliktar, *Acta Biomater.*, 2012, **8**, 1838-1848.
19. Y. Jiang, J. Chen, C. Deng, E. J. Suuronen and Z. Zhong, *Biomaterials*, 2014, **35**, 4969-4985.
20. Q. Wan, J. Chen, Y. Yuan and S. J. Danishefsky, *J. Am. Chem. Soc.*, 2008, **130**, 15814-15816.
21. I. Strehin, D. Gourevitch, Y. Zhang, E. Heber-Katz and P. B. Messersmith, *Biomaterials Sci.*, 2013, **1**, 603-613.
22. K. W. M. Boere, J. v. d. Dikkenberg, Y. Gao, J. Visser, W. E. Hennink and T. Vermonden, Biomacromolecules, 2015, DOI: 10.1021/acs.biomac.5b00802.
23. A. Skardal, J. Zhang, L. McCoard, S. Oottamasathien and G. D. Prestwich, Adv. Mater., 2010, 22, 4736-4740.
24. A. L. Rutz, K. E. Hyland, A. E. Jakus, W. R. Burghardt and R. N. Shah, *Adv. Mater.*, 2015, **27**, 1607-1614.
25. A. Skardal, J. Zhang, L. McCoard, X. Xu, S. Oottamasathien and G. D. Prestwich, *Tissue Eng., Part A*, 2010, **16**, 2675-2685.
26. W. Schuurman, V. Khristov, M. W. Pot, P. R. Van Weeren, W. J. A. Dhert and J. Malda, *Biofabrication*, 2011, **3**, 021001.
27. J. Visser, B. Peters, T. J. Burger, J. Boomstra, W. J. A. Dhert, F. P. W. Melchels and J. Malda, *Biofabrication*, 2013, **5**, 035007.
28. J. Visser, F. P. W. Melchels, J. E. Jeon, E. M. van Bussel, L. S. Kimpton, H. M. Byrne, W. J. A. Dhert, P. D. Dalton, D. W. Hutmacher and J. Malda, *Nat. Commun.*, 2015, **6**, 6933.
29. M. A. Woodruff and D. W. Hutmacher, *Prog. Polym. Sci.*, 2010, **35**, 1217-1256.
30. H. Seyednejad, T. Vermonden, N. E. Fedorovich, R. van Eijk, M. J. van Steenbergen, W. J. A. Dhert, C. F. van Nostrum and W. E. Hennink, *Biomacromolecules*, 2009, **10**, 3048-3054.
31. H. Seyednejad, D. Gawlitta, R. V. Kuiper, A. de Bruin, C. F. van Nostrum, T. Vermonden, W. J. Dhert and W. E. Hennink, *Biomaterials*, 2012, **33**, 4309-4318.
32. H. Seyednejad, D. Gawlitta, W. J. A. Dhert, C. F. Van Nostrum, T. Vermonden and W. E. Hennink, *Acta Biomater.*, 2011, **7**, 1999-2006.

33. K. W. M. Boere, J. Visser, H. Seyednejad, S. Rahimian, D. Gawlitta, M. J. van Steenbergen, W. J. A. Dhert, W. E. Hennink, T. Vermonden and J. Malda, *Acta Biomater.*, 2014, **10**, 2602-2611.
34. K. W. M. Boere, B. G. Soliman, D. T. S. Rijkers, W. E. Hennink and T. Vermonden, *Macromolecules*, 2014, **47**, 2430-2438.
35. B.-H. Hu, J. Su and P. B. Messersmith, *Biomacromolecules*, 2009, **10**, 2194-2200.
36. D. Neradovic, C. F. van Nostrum and W. E. Hennink, *Macromolecules*, 2001, **34**, 7589-7591.
37. J. S. Moore and S. I. Stupp, *Macromolecules*, 1990, **23**, 65-70.
38. C. Y. Chang, A. T. Chan, P. A. Armstrong, H.-C. Luo, T. Higuchi, I. A. Strehin, S. Vakrou, X. Lin, S. N. Brown and B. O'Rourke, *Biomaterials*, 2012, **33**, 8026-8033.
39. J. Visser, P. A. Levett, N. C. R. te Moller, J. Besems, K. W. M. Boere, M. H. P. Van Rijen, J. C. de Grauw, W. J. A. Dhert, R. van Weeren and J. Malda, *Tissue Eng.*, 2015, **21**, 1195-1206.
40. S. J. Hollister, *Nat. Mater.*, 2005, **4**, 518-524.
41. *The American Heritage® Dictionary of the English Language*, Houghton Mifflin Harcourt Publishing Company, Fifth edn., 2015.
42. M. Guvendiren, H. D. Lu and J. A. Burdick, *Soft Matter*, 2012, **8**, 260-272.
43. R. Darby, *Chemical Engineering Fluid Mechanics*, Taylor & Francis, 2nd edition edn., 2001.
44. W. D. Callister and D. G. Rethwisch, *Materials Science and Engineering*, Wiley, SI Version, 8th edn., 2010.
45. L. Moroni, J. R. De Wijn and C. A. Van Blitterswijk, *Biomaterials*, 2006, **27**, 974-985.
46. H. S. Yoo, E. A. Lee, J. J. Yoon and T. G. Park, *Biomaterials*, 2005, **26**, 1925-1933.
47. J. Baier Leach, K. A. Bivens, C. W. Patrick Jr and C. E. Schmidt, *Biotechnol. Bioeng.*, 2003, **82**, 578-589.
48. M. N. Collins and C. Birkinshaw, *Carbohydr. Polym.*, 2013, **92**, 1262-1279.
49. P. A. Levett, F. P. Melchels, K. Schrobback, D. W. Hutmacher, J. Malda and T. J. Klein, *Acta Biomater.*, 2014, **10**, 214-223.

CHAPTER 7

SUMMARY AND PERSPECTIVES

7.1 Summary

The research described in this thesis was part of the Netherlands Institute of Regenerative Medicine (NIRM) program. NIRM aims to make fundamental contributions to new strategies for regenerative medicine by using novel genetic, stem cell and biomaterial approaches including hydrogel materials.[1] The progress in hydrogel development over the past decades has contributed to the transition of hydrogels from simple water absorbing materials to multifunctional platforms for a range of biomedical applications. Nevertheless, some shortcomings in the hydrogel properties remain, limiting widespread translation to the clinic. This thesis aimed to address some limitations of hydrogels in the design of new hydrogel-based biomaterials. Hydrogel formation under physiological conditions in the presence of living cells or bioactive compounds requires suitable polymer cross-linking strategies. Furthermore, control over the hydrogel properties, such as mechanical strength and degradation behavior is necessary to obtain reproducible and tunable biomaterials towards specific needs. Lastly, hydrogels are soft materials and therefore do not fulfill the mechanical requirements for some regenerative medicine applications. The work described in this thesis focuses on the development of the next generation of hydrogel biomaterials taking into account the above mentioned issues.

In **Chapter 1,** the main applications of hydrogels in the biomedical field, i.e. for the sustained delivery of drugs and facilitating regeneration of tissues are discussed. Furthermore, a variety of polymers that can form the hydrogel building blocks are categorized based on their source (natural or synthetic) and their cross-linking mechanism. Particular attention is given to thermoresponsive self-assembly, photopolymerization and chemoselective reactions as promising cross-linking strategies that are employed in this thesis. Finally, advanced methods to obtain hydrogels by injection or 3D-printing are described. While injectable hydrogels offer a minimally invasive administration route of formulations to a patient, 3D-printing enables the formation of complex constructs through a layer-by-layer hydrogel deposition.

Chapter 2 reviews the hydrogel developments over the past 50 years, starting from the landmark paper of Wichterle and Lim that described the fabrication of soft contact lenses from 2-hydroxyethyl methacrylate (HEMA) polymeric networks.[2] Initially, hydrogels were formed from water soluble monomers or simple hydrophilic synthetic polymers such as poly(vinyl alcohol) (PVA) and poly(ethylene glycol) (PEG) or semi-synthetic hydrogels based on cellulose derivatives. Subsequently, stimuli-sensitive hydrogels that respond to external triggers were developed, which offered new opportunities in hydrogel administration as *in situ* forming formulations.

Particularly interesting were the developments in temperature-sensitive hydrogels, such as PEG-polyester block copolymers and poly(*N*-isopropylacrylamide) (pNIPAAm). In the decennia following these discoveries, more complex systems e.g. stereocomplexed hydrogels, cyclodextrin- and peptide-based hydrogels were designed. New insights resulted in the formation of hydrogels that consisted of covalent cross-links between the polymeric building blocks with complementary functional groups. Novel chemistries such as copper free click chemistry and native chemical ligation allowed hydrogel formation under physiological conditions without the use of toxic reagents or catalysts.[3,4] A special class consisted of dual responsive hydrogels that are both cross-linked by temperature-induced physical interactions and covalent bonds. These formulations are attractive as injectable systems because of their rapid thermogelation and subsequent stabilization through covalent cross-linking of polymers. Alternatively, composite hydrogels were introduced that contained for example ceramic or degradable polymeric particles, carbon nanotubes or thermoplastic fibers to enhance their mechanical strength or to tune drug release. The development of even more complex systems is expected in the future. However, limiting the material complexity to facilitate clinical translation and commercialization should be taken into consideration.

In **Chapter 3**, the development of a novel hydrogel is described that was formed by a dual gelation mechanism.[5] A cysteine-functionalized thermoresponsive triblock copolymer was synthesized from the novel monomer *N*-(2-hydroxypropyl) methacrylamide-cysteine (HPMA-Cys) and *N*-isopropylacrylamide (NIPAAm). This polymer consisted of a poly(ethylene glycol) (PEG) mid block, flanked by random blocks of HPMA-Cys and NIPAAm monomers. When this polymer was mixed with thioester-functionalized cross-linkers based on either PEG or hyaluronic acid (HA), cysteine and thioester moieties reacted under physiological conditions (pH 7.4, 37°C), yielding a native peptide bond. Quick network formation at 37 °C was ensured through temperature-induced physical gelation, while covalent bonds that stabilized the hydrogel structure were formed by native chemical ligation (NCL). To demonstrate the versatility of this hydrogel, a collagen mimicking peptide was covalently ligated to the hydrogel building block by NCL, as was proven by Nuclear Magnetic Resonance (NMR) spectroscopy and Gel Permeation Chromatography (GPC).

Based on the results obtained in this chapter and new literature findings, the characteristics of these hydrogels were further investigated and these hydrogels were further developed. In **Chapter 4**, thermoresponsive hydrogels cross-linked by NCL were compared with a recently described variation termed oxo-ester mediated native chemical ligation (OMNCL). While NCL involves a reaction between cysteine

and a thioester, in OMNCL cysteine reacts with an activated oxo-ester, such as *N*-hydroxysuccinimide (NHS), which was used in this study. Therefore, cross-linkers were synthesized based on linear or 8-arm poly(ethylene glycol) with thioester or NHS functionalities that could react with the previously described cysteine functionalized thermoresponsive polymer. Gelation kinetics, mechanical strength, chondrocyte cytocompatibility and release of the model protein lysozyme were investigated. Rheological measurements revealed that hydrogels using OMNCL chemistry were formed more rapidly and showed a higher mechanical strength. Also, using 8-arm PEG instead of linear PEG cross-linkers resulted in a 5-fold increase in mechanical strength of the hydrogels. Stiffness of these OMNCL covalently cross-linked hydrogels was more than 100 times higher than those containing only thermal physical cross-links. Additionally, endothelial cell viability was significantly higher for hydrogels obtained by OMNCL cross-linking. Incubation of lysozyme with the individual hydrogel components showed ligation of lysozyme to the NHS-functionalized PEG building block. However, when this protein was loaded in the hydrogel network during its formation it was released for more than 90%. This result showed that the cross-linking reaction was indeed rather chemoselective. Furthermore, the tunability of degradation rates of these hydrogels was investigated. To this end, the monomer dimethyl-γ-butyrolactone (DBA), that contained a hydrolysable lactone ring, was incorporated in the thermoresponsive polymer. Hydrolysis resulted in an increased lower critical solution temperature (LCST) over time and increased water uptake in the hydrogels. By varying the DBA content in the thermoresponsive building block, degradation rates were tailored from 12 days up to 6 months.

Although it was possible to tune the hydrogel stiffness to some extent, hydrogels in general remain mechanically weak materials, which could potentially hamper an application in load-bearing tissues. To increase the mechanical strength, hydrogels can be supported with a thermoplastic polymer material. In **Chapter 5**, the fabrication of a 3D-printed construct consisting of alternating layers of thermoplastic material and hydrogel was investigated, with the goal to covalently graft the thermoplastic material and hydrogel layers to obtain a mechanically integrated construct.[6] Gelatin was studied as a model hydrogel since it has been frequently demonstrated to have high potential for cartilage regeneration.[7,8] Poly(hydroxymethylglycolide-co-ε-caprolactone) (pHMGCL), a hydroxyl derivatized poly-ε-caprolactone, was chosen as thermoplastic polymer because this polymer was reported with favorable biodegradation and cell attachment compared to the commercially available poly-ε-caprolactone (PCL).[9,10] Hydroxyl moieties of this thermoplastic polyester were partially converted into methacryl groups, yielding a novel methacrylate functionalized PCL. Also gelatin was functionalized with methacrylate groups, thereby enabling the formation of covalent bonds in the materials through photopolymerization using

UV irradiation. The potential of grafting the hydrogel and thermoplastic material at the material interface was assessed by mechanical tests. The grafting at the hydrogel-thermoplastic interface resulted in at least 5-fold higher mechanical resistance after applied shear forces. Furthermore, this thermoplastic polymer was 3D-printed in an anatomically relevant model of a condyle shape of which the pores were infused with a methacrylated gelatin hydrogel. To study the potential of the obtained hydrogel-thermoplastic constructs for cartilage regeneration, chondrocytes were embedded in the gelatin hydrogel and differentiation was assessed. Extracellular matrix formation specific for cartilage tissue was shown *in vitro* by considerable glycosaminoglycan and collagen type II production. Similar results were obtained *in vivo* when the constructs were subcutaneously implanted in rats, showing the potential of these constructs in regenerative medicine.

The 3D-printing of hydrogel-based materials was further investigated in **Chapter 6** using the developed two component hydrogels of Chapter 4. Based on the rapid gel formation and rheological and cytocompatibility characteristics, the OMNCL cross-linked hydrogel was selected as component of 3D-printed construct. NHS-functionalized cross-linkers were developed from 8-arm PEG and hyaluronic acid. These polymer solutions were partially cross-linked before plotting to ensure a high shape fidelity of the construct. In this way, relatively low polymer concentrations of approximately 10 wt% were used and the resulting gels were deposited without collapse of the construct. Rheological assessment of the polymer solutions and hydrogels confirmed the expected flow properties as was achieved during 3D-printing and showed a quick recovery of the hydrogels after applied shear forces. Encouraged by the results obtained in Chapter 5, the reinforcement of these hydrogels with a newly developed thermoplastic polymer was investigated. This thermoplastic polymer was synthesized from poly(hydroxymethylglycolide-co-ε-caprolactone) in which *N*-hydroxysuccinimide moieties were coupled to the hydroxyl groups. Reinforced constructs that contained covalent bonds between the hydrogel and thermoplastic material again showed a higher mechanical integrity after application of shear and consequently improved interface-binding strength compared to constructs without covalent bonds between the hydrogel and thermoplastic material. Chondrocytes were encapsulated in the reinforced constructs and showed a good viability in the constructs that contained hyaluronic acid, underlining its potential in biomedical applications.

7.2 Perspectives

This thesis describes novel promising hydrogel systems for use as biomaterials. Nevertheless, further optimizations and research is necessary to take the next steps for their clinical translation. Optimizations can be categorized in further design of the polymers, investigations into the biomedical applications and further improvements in biofabrication technologies.

7.2.1 Polymer design

Photopolymerization is a highly efficient cross-linking method, but it requires additional equipment and the use of UV light that can potentially be harmful for cells.[11,12] In this thesis, promising alternatives for UV-induced polymer cross-linking were proposed with the introduction of chemoselective conjugations via native chemical ligation (NCL) and oxo-ester mediated native chemical ligation (OMNCL). A side reaction that cysteine-functionalized polymers can undergo is disulfide bond formation between thiol moieties. Chapter 3 demonstrated that this reaction occurs with much slower kinetics than NCL and OMNCL as proven by rheology experiments.[5] This finding is in agreement with the studies of Messersmith *et al.* who investigated the kinetics of both reactions with NMR.[13] Nevertheless, after cross-linking thiol moieties remain present in the network that could form additional cross-links. It has been suggested by the group of Messersmith that these additional cross-links further stabilize the hydrogel structure and prevent swelling of the hydrogel, so disulfide formation as such is not necessarily unfavorable.[13] Controlling the reaction kinetics is however important to determine the final product. Additional research into the quantification of the NCL and OMNCL conversion in time and the extent and kinetics of disulfide formation can give more insight into the hydrogel formation, hence obtaining a better control in the eventual hydrogel properties. Kinetics of NCL and OMNCL reaction can for example be adjusted by incorporation of different amino acids preceding the cysteine moiety.[4]

One important concern of the native chemical ligation reaction that remains is the formation of a byproduct. As described in Chapter 5, using oxo-ester mediated native chemical ligation is a good alternative, since no toxic thiol byproducts are released after cross-linking. However, an alcohol byproduct remains, in this case *N*-hydroxysuccinimide. Additionally, oxo-esters are susceptible for hydrolysis, which would result in a decrease in pH due to the formation of carboxylic acid residues. A promising alternative approach was suggested by Messsersmith *et al.* with the introduction of a cyclic thioester precursor.[14] When an *N*-terminal cysteine reacts with this cyclic thioester, it causes a ring opening and after the *N*-to-*S* acyl shift the thiol remains attached to the polymer (Figure 7.1). They reported successful

hydrogel formation using a 5-membered ring (thiolactone). We applied this method to introduce thiolactone functionalities in our hydrogel building blocks. However, substantial hydrolysis of this cyclic thioester occurred before reaction with cysteine took place, most likely as a result of the ring strain. In a preliminary study, we investigated the use of a 6-membered cyclic thioester. Although PEG cross-linkers functionalized with this cyclic thioester were readily synthesized and these thioesters were much less susceptible for hydrolysis, a reaction with cysteine did not occur under physiological conditions. An explanation for this lack of reactivity is most likely the high stability of the 6-membered ring. A 7-membered ring is expected to be a better choice, also based on the successes that are booked in e.g. caprolactone ring opening polymerizations.[15,16] However, a drawback here is the multiple step and complicated synthesis of this precursor, thereby limiting potential commercialization.
Since the majority of the monomers used for the synthesis of the hydrogel building blocks in this study is commercially available, scaling up of the polymers will be feasible. Nevertheless, optimizations need to be investigated to enable good manufacturing practice (GMP) production of the developed monomers and polymers.

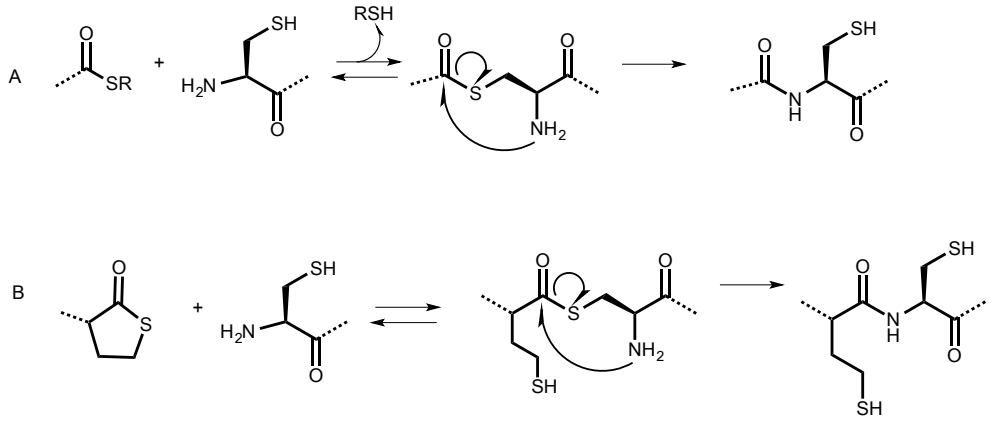

Figure 7.1. Native chemical ligation (NCL) reaction scheme utilizing A) a linear thioester and B) a cyclic thioester.

7.2.2 Biomedical applications

The studies described in this thesis mainly focused on the polymer design, characterization and scaffold fabrication. However, great progress can still be made in further developing these hydrogels for successful biomedical applications. As shown in this thesis, especially the combination of natural polymer based materials and synthetic materials formed promising constructs for regenerative medicine. This can be explained by the inherent interactions of natural polymer based materials with cells. In the studies described in this thesis, preliminary studies towards the

regeneration of cartilage tissues were performed. Extensive differentiation studies towards new tissue formation both *in vitro* and *in vivo* need to be carried out to further evaluate the potential of the studied materials for regenerative medicine. Potential adverse effects of the hydrogels after injection or implantation need to be investigated *in vivo* as well as their degradation times *in vivo*, which may not necessarily match degradation rates found *in vitro*. Herein, optimizations can be considered such as polymer composition, polymer concentration, glycosaminoglycan content and peptide grafting. Future research may investigate additional combinations of synthetic and natural polymers as a continuation of the results described in this thesis. Functional peptides can be grafted to the NHS functionalized thermoplastic polymer, which can be easily accomplished using peptides containing an *N*-terminal cysteine. Furthermore, gelatin may be incorporated in the OMNCL cross-linked hydrogels through NHS or cysteine functionalization of the lysine moieties of gelatin. Other possible applications of these hydrogels may be as *in vitro* screening models,[17] which would particularly be interesting for 3D-printed constructs since they can resemble human tissues to a higher extent. This covers for example the possibility to screen for drug toxicity or model diseased tissues.

7.2.3 Technological perspectives

With the emerging progress in additive manufacturing technologies, we are on the footstep of an exciting era where tremendous new possibilities are opened for the fabrication of complex constructs. Although 3D-printing by filament deposition yields large and stable constructs, it does not achieve the resolution of for example electrospinning or stereolithography. Electrospinning uses electrostatic forces that allow the production of nanostructured scaffolds. A drawback of electrospinning is however the low control over the spatial deposition of the fibers.[18] A recently introduced variation termed 'direct write electrospinning' provides a promising approach of controlling the spatial deposition and organization of thin fibers.[19] Combination of this electrospinning method with a gelatin hydrogel showed successful reinforced constructs that closely approached the mechanical properties of natural tissues.[20] It is expected that the mechanical properties can be even further improved when the hydrogel is covalently grafted to the thermoplastic electrospun fibers, similarly to what was demonstrated in Chapters 5 and 6 of this thesis. However, currently the success of melt write electrospinning is limited to some thermoplastic materials and therefore improvements in electrospinning equipment and further developments of other materials are necessary before employing this strategy. Alternatively, 3D-printing can also be combined with electrospinning.[21] Herein, alternating layers of organized microfibers and nanofiber webs are deposited from melt deposition and electrospinning printing heads. Park *et al*. demonstrated an improved cell adhesion and proliferation as a result of these inserted nanofiber

matrices.[22] Additionally, Xu *et al*. reported enhanced mechanical properties of the resulting constructs through combination of hydrogel printing and electrospinning.[23] Another interesting strategy uses coaxial printing heads for the extrusion of hollow or multi-material filaments. Cornock *et al*. reported the fabrication of hollow multi-layered co-fibers consisting of alginate and poly-ε-caprolactone by coaxial melt extrusion.[24] Hollow printed fibers were subsequently infused with hydrogel or cells. In this way, microchannels can be fabricated that form vascular-like structures.[25] This new method may be implemented using the materials reported in this thesis. In this way, hollow fibers of thermoplastic material infused with hydrogel can be created that have a covalently linked material interface. Scaffolds based on the thermoplastic polyester used in our studies were previously fabricated using coaxial electrospinning,[26] therefore the aforementioned strategies are likely feasible for creating multi-material constructs with the materials as described in this thesis.

Additionally, further investigations are necessary for the 3D-printing of two component hydrogels. These hydrogels form attractive biomaterials for bioprinting, given the tailorable mechanical properties, mild reaction conditions and stabilization of the structure without the requirement of post treatment. However fabrication of large-sized constructs by means of 3D-printing remains challenging. As an alternative strategy to partial pre-crosslinking, 3D-printing of two component hydrogels can potentially be achieved using a dual syringe consisting of two reservoirs that are combined towards a static mixer before the nozzle.[27] Hereby, the viscosity of the precursor solutions will not be altered during printing and shear forces to which the cells are exposed are lower compared to pre-crosslinked hydrogels as used in Chapter 6 in this thesis. Yet, this strategy has the disadvantage that it requires very rapid cross-linking kinetics since the solution viscosity should quickly increase after extrusion to allow fabrication of constructs with high shape fidelity. The PNC – HA-NHS hydrogel described in Chapter 6 may be a good candidate for this approach since cross-linking occurred rapidly for this hydrogel formulation. However, thorough developments in this printing setup are needed that ensure good mixing of the precursors without blocking the nozzle, while at the same time creating constructs with high shape fidelity. This can be especially challenging when using two solutions that differ substantially in viscosity. Therefore, selection of appropriate hydrogel building blocks may be more crucial in this approach than for pre-crosslinked hydrogels.

7.3 Conclusions

In conclusion, this thesis describes the development of novel dual cross-linked hydrogels by temperature-induced physical cross-linking and chemoselective ligation. The formation of mechanically strong hybrid 3D-printed constructs was demonstrated that consisted of covalently grafted hydrogel and thermoplastic layers. These hydrogel-based materials have favorable and tunable characteristics as injectable and 3D-printable systems for further investigations in biomedical applications. Besides tissue engineering applications, the developed hydrogels are expected to be also attractive candidates as injectable depots for sustained drug release or as *in vitro* screening models. Further optimizations and development of these polymers can underscore the encouraging features of these new biomaterials.

References

1. http://www.nirmresearch.nl, (accessed June 25, 2015).
2. S. J. Buwalda, K. W. M. Boere, P. J. Dijkstra, J. Feijen, T. Vermonden and W. E. Hennink, *J. Controlled Release*, 2014, **190**, 254-273.
3. J. Xu, T. M. Filion, F. Prifti and J. Song, *Chem. Asian J.*, 2011, **6**, 2730-2737.
4. B.-H. Hu, J. Su and P. B. Messersmith, *Biomacromolecules*, 2009, **10**, 2194-2200.
5. K. W. M. Boere, B. G. Soliman, D. T. S. Rijkers, W. E. Hennink and T. Vermonden, *Macromolecules*, 2014, **47**, 2430-2438.
6. K. W. M. Boere, J. Visser, H. Seyednejad, S. Rahimian, D. Gawlitta, M. J. van Steenbergen, W. J. A. Dhert, W. E. Hennink, T. Vermonden and J. Malda, *Acta Biomater.*, 2014, **10**, 2602-2611.
7. M. S. Ponticiello, R. M. Schinagl, S. Kadiyala and F. P. Barry, *J. Biomed. Mater. Res.*, 2000, **52**, 246-255.
8. W. Schuurman, P. A. Levett, M. W. Pot, P. R. van Weeren, W. J. Dhert, D. W. Hutmacher, F. P. Melchels, T. J. Klein and J. Malda, *Macromol. Biosci.*, 2013, **13**, 551-561.
9. H. Seyednejad, T. Vermonden, N. E. Fedorovich, R. van Eijk, M. J. van Steenbergen, W. J. A. Dhert, C. F. van Nostrum and W. E. Hennink, *Biomacromolecules*, 2009, **10**, 3048-3054.
10. H. Seyednejad, D. Gawlitta, R. V. Kuiper, A. de Bruin, C. F. van Nostrum, T. Vermonden, W. J. Dhert and W. E. Hennink, *Biomaterials*, 2012, **33**, 4309-4318.
11. B. Baroli, *J. Chem. Technol. Biotechnol.*, 2006, **81**, 491-499.
12. N. E. Fedorovich, M. H. Oudshoorn, D. van Geemen, W. E. Hennink, J. Alblas and W. J. Dhert, *Biomaterials*, 2009, **30**, 344-353.
13. I. Strehin, D. Gourevitch, Y. Zhang, E. Heber-Katz and P. B. Messersmith, *Biomater. Sci.*, 2013, **1**, 603-613.
14. P. B. Messersmith, J. Su and B.-H. Hu, 2011.
15. H. Seyednejad, A. H. Ghassemi, C. F. van Nostrum, T. Vermonden and W. E. Hennink, *J. Controlled Release*, 2011, **152**, 168-176.
16. N. E. Kamber, W. Jeong, R. M. Waymouth, R. C. Pratt, B. G. Lohmeijer and J. L. Hedrick, *Chem. Rev.*, 2007, **107**, 5813-5840.
17. N. T. Elliott and F. Yuan, *J. Pharm. Sci.*, 2011, **100**, 59-74.

18. Z.-M. Huang, Y.-Z. Zhang, M. Kotaki and S. Ramakrishna, *Compos. Sci. Technol.*, 2003, **63**, 2223-2253.
19. T. D. Brown, P. D. Dalton and D. W. Hutmacher, *Adv. Mater.*, 2011, **23**, 5651-5657.
20. J. Visser, F. P. W. Melchels, J. E. Jeon, E. M. van Bussel, L. S. Kimpton, H. M. Byrne, W. J. A. Dhert, P. D. Dalton, D. W. Hutmacher and J. Malda, *Nat. Commun.*, 2015, **6**, 6933.
21. G. Kim, J. Son, S. Park and W. Kim, *Macromol. Rapid Commun.*, 2008, **29**, 1577-1581.
22. S. H. Park, T. G. Kim, H. C. Kim, D.-Y. Yang and T. G. Park, *Acta Biomater.*, 2008, **4**, 1198-1207.
23. X. Tao, W. B. Kyle, Z. A. Mohammad, D. Dennis, Z. Weixin, J. Y. James and A. Anthony, *Biofabrication*, 2013, **5**, 015001.
24. R. Cornock, S. Beirne, B. Thompson and G. G. Wallace, *Biofabrication*, 2014, **6**, 025002.
25. Q. Gao, Y. He, J.-z. Fu, A. Liu and L. Ma, *Biomaterials*, 2015, **61**, 203-215.26.
H. Seyednejad, W. Ji, F. Yang, C. F. van Nostrum, T. Vermonden, J. J. J. P. van den Beucken, W. J. A. Dhert, W. E. Hennink and J. A. Jansen, *Biomacromolecules*, 2012, **13**, 3650-3660.
27. J. Malda, J. Visser, F. P. Melchels, T. Jüngst, W. E. Hennink, W. J. A. Dhert, J. Groll and D. W. Hutmacher, *Adv. Mater.*, 2013, **25**, 5011-5028.

APPENDICES

NEDERLANDSE SAMENVATTING

Samenvatting

Het onderzoek beschreven in dit proefschrift focust zich op de ontwikkeling van nieuwe hydrogelen voor biomedische toepassingen. Hydrogelen bestaan uit gecrosslinkte en hydrofiele polymeernetwerken die daardoor veel water kunnen absorberen en worden onder andere gebruikt in contactlenzen en medische implantaten. Doordat hydrogelen veel water bevatten vertonen ze veel overeenkomsten met het menselijk weefsel en zijn hierdoor aantrekkelijke materialen voor onder andere de lokale afgifte van farmaca en herstel van beschadigd weefsel. Weefselherstel is met name cruciaal in weefsels die geen of weinig eigen bloeddoorstroming hebben, zoals (hyalien) kraakbeen. Voor deze toepassing kan een hydrogel beladen worden met cellen en/of groeifactoren om de regeneratie van het weefsel te bevorderen. De algemene eigenschappen van hydrogelen zijn beschreven in **Hoofdstuk 1**. Hydrogelen zijn opgebouwd uit hydrofiele polymeernetwerken die vernet zijn door ofwel fysische (niet-covalente) of chemische (covalente) bindingen. Een speciale klasse van fysische bindingen wordt gevormd als gevolg van een externe verandering, zoals door de verhoging van de temperatuur wat ook wel thermosensitief gedrag wordt genoemd. Wanneer gebruik gemaakt wordt van thermosensitieve polymeren in combinatie met chemische bindingen kunnen aantrekkelijke injecteerbare formuleringen gemaakt worden. Na injectie zorgen de thermosensitieve eigenschappen tot snelle netwerkvorming, waarna dit netwerk gestabiliseerd wordt door de covalente bindingen tussen de polymeerketens. Het voordeel van een injecteerbare formulering is dat dit een relatief patiëntvriendelijke toediening betreft en onregelmatige beschadigingen in het weefsel volledig opgevuld kunnen worden. Als alternatief kunnen hydrogelconstructen ook vervaardigd worden met behulp van een 3D-printer. Dit geeft de mogelijkheid tot het vormen van poreuze constructen, wat de uitwisseling van voedingsstoffen met het omliggende weefsel en de ingroei van nieuw weefsel bevordert.

Ondanks deze veelbelovende eigenschappen hebben hydrogelen ook bepaalde tekortkomingen voor biomedische toepassingen. Om hydrogelen geschikt te maken als injecteerbare formuleringen moeten de juiste chemische reacties voor crosslinking van de polymeren worden gebruikt die geen negatieve invloed hebben op cellen in het polymeernetwerk of op het omliggend weefsel. Verder zijn hydrogelen zeer zachte materialen, wat problemen kan opleveren wanneer ze geplaatst worden in lichaamsdelen die veel mechanische druk ondervinden, zoals in bot en kraakbeengewrichten. Uiteindelijk is het noodzakelijk om de eigenschappen van de hydrogelen, zoals degradatiesnelheid en mechanische sterkte, te kunnen controleren en waar nodig aan te passen aan de uiteindelijke toepassing. **Hoofdstuk 2** geeft een overzicht van de ontwikkeling van hydrogelen gedurende de afgelopen 50 jaar. Dit hoofdstuk laat een duidelijke progressie zien in het onderzoek naar hydrogelen

van simpele polymeernetwerken tot aan complexe systemen met als doel om betere en controleerbaardere eigenschappen te verkrijgen voor biomedische toepassingen, zoals hogere mechanische stabiliteit en gereguleerde afgifte van farmaca.

Ontwikkeling van nieuwe injecteerbare hydrogelen

In **Hoofdstuk 3** wordt een nieuwe hydrogel beschreven die toegepast kan worden als injecteerbare formulering. Deze hydrogel bestaat uit polymeren die zowel fysisch als chemisch vernet zijn. De fysische netwerkverbindingen worden gevormd door het assembleren van polymeerketens na verhoging van de temperatuur boven de 31°C. Hierdoor gedraagt de polymeeroplossing zich als een vloeistof bij kamertemperatuur en neemt de viscositeit snel toe na verhoging van de temperatuur tot lichaamstemperatuur. De chemische reactie die tot stabilisatie van het netwerk leidt, wordt 'native chemical ligation' (NCL) genoemd. Deze chemisch selectieve reactie vindt plaats onder fysiologische omstandigheden (pH 7.4 en 37°C). De chemische selectiviteit zorgt ervoor dat de netwerkvorming niet of nauwelijks invloed heeft op biologische componenten in het hydrogel-netwerk of in omliggend weefsel. De beschreven hydrogel is opgebouwd uit twee polymeercomponenten in water, namelijk een thermosensitief blokcopolymeer met cysteine functionaliteiten en een crosslinker met thioester groepen. Er zijn twee verschillende crosslinkers gebruikt; de eerste is een polyethyleenglycol (PEG) derivaat en de tweede een hyaluronzuur (HA) derivaat. Hyaluronzuur heeft hierbij als voordeel dat dit een lichaamseigen polymeer betreft en daarom goede eigenschappen heeft voor biomedische toepassingen. De chemische NCL reactie vindt plaats wanneer deze twee componenten met elkaar gemengd worden. Wanneer dit systeem geïnjecteerd in het lichaam wordt, vindt snelle netwerkvorming plaats door de temperatuurverandering en daaropvolgend wordt het netwerk gestabiliseerd door de chemische reactie tussen de twee componenten. Aansluitend is een collageen-achtig peptide aan het thermosensitieve polymeer covalent gekoppeld en op deze manier in de hydrogel geïntroduceerd.

Deze hydrogel is verder ontwikkeld met als doel om meer inzicht te krijgen in de materiaalsterkte, degradeerbaarheid en cytotoxiciteit zoals beschreven in **Hoofdstuk 4**. Hierbij is de NCL reactie van Hoofdstuk 3 vergeleken met een variant genaamd 'oxo-ester mediated native chemical ligation' (OMNCL). Het verschil tussen deze twee reactiemechanismen is dat NCL een thioester functionaliteit gebruikt en OMNCL een oxo-ester functionaliteit om te laten reageren met cysteine groepen gekoppeld aan het thermosensitief polymeer. De crosslinker is ofwel opgebouwd uit een lineaire PEG of een 8-armige PEG. Onderzoek naar de materiaalsterkte van de hydrogelen liet duidelijk zien dat sterkere gelen verkregen kunnen worden met het OMNCL reactiemechanisme en wanneer gebruik wordt gemaakt van de 8-armige

PEG crosslinker. Eveneens zorgde het gebruik van de OMNCL reactie voor een betere cytocompatibiliteit, waardoor deze hydrogelen interessant zijn voor toepassingen in combinatie met cellen. De resultaten lieten zien dat deze hydrogelen geschikt zijn voor de afgifte van het modeleiwit lysozym. Bovendien liet het onderzoek in dit hoofdstuk zien dat de degradatiesnelheid van deze hydrogelen gevarieerd kan worden door het inbouwen van het monomeer DBA in de polymeerstructuur en het gehalte hiervan te variëren. Dit monomeer bevat een lacton ring die gedurende de tijd gehydrolyseerd wordt, wat zorgt voor versnelde degradatie van de hydrogel. Door de mogelijkheid om de eigenschappen zoals materiaalsterkte en degradatiesnelheid van deze hydrogelen aan te passen, kunnen ze voor verscheidene toepassingen gebruikt worden.

Ontwikkeling van nieuwe 3D-printbare biomaterialen

In **Hoofdstuk 5** wordt beschreven hoe hydrogelen vervaardigd kunnen worden in sterke 3D-printbare constructen voor kraakbeenregeneratie. Om dit te bewerkstelligen is de hydrogel gecombineerd met een thermoplast. Deze thermoplast is veel sterker dan de hydrogel en blijft daardoor beter intact wanneer mechanische krachten op het construct worden uitgeoefend. De hydrogel is daarentegen een geschikt materiaal om cellen in te verwerken. Als hydrogel is hier voor gelatine gekozen, aangezien dit eiwit veelvuldig is onderzocht voor kraakbeenregeneratie. Met behulp van een 3D-printer kunnen zijdelings lagen van hydrogel en thermoplast tegen elkaar aan worden gelegd, waarna een drie-dimensionaal construct opgebouwd wordt. Om te voorkomen dat dit construct uit elkaar valt na blootstelling aan externe krachten, zijn de hydrogel en thermoplast lagen covalent aan elkaar gebonden. Hiertoe zijn beide materialen gemodificeerd met methacrylgroepen. Deze methacrylgroepen kunnen met elkaar reageren na bestraling met UV licht. Inderdaad lieten mechanische testen, zoals afschuifexperimenten, zien dat de bindingssterkte op het grensvlak sterk verhoogd was en de constructen grotere krachten konden weerstaan. Eveneens is gedemonstreerd dat deze constructen geschikt zijn voor kraakbeenregeneratie. Hiervoor zijn kraakbeencellen (chondrocyten) in de hydrogel gemengd en in het 3D-construct opgenomen. *In vitro* studies en implantatie van de constructen onder de huid van ratten lieten zien dat nieuwe kraakbeenspecifieke matrix geproduceerd werd.

De mogelijkheden van het 3D-printen van hydrogelen is verder onderzocht en beschreven in **Hoofdstuk 6**. Hiervoor zijn de twee componenten hydrogelen die beschreven staan in hoofdstuk 4 gebruikt. Eveneens zijn hier crosslinkers gebruikt die zijn opgebouwd uit ofwel PEG of hyaluronzuur. Door de twee componenten (temperatuurgevoelig polymeer en crosslinker) eerst voor een half uur in de voeder

van de 3D-printer te mengen, kunnen complexe hydrogelconstructen geprint worden die bestaan uit materialen met een relatief lage polymeerconcentratie. Door het gedeeltelijk vormen van een netwerk in de voeder wordt al een zekere stijfheid van de hydrogelfilamenten verkregen. Opeenvolgend neemt deze stijfheid toe door de filamenten af te zetten op een verwarmde plaat als een gevolg van de thermosensitieve eigenschappen van deze hydrogelen. Vervolgens neemt de stijfheid verder toe na het printen van het construct tot mechanisch stabiele materialen. Om deze stijfheid nog verder te verhogen werd de hydrogel opnieuw gecombineerd met een thermoplastisch materiaal, vergelijkbaar met de resultaten in hoofdstuk 5. De binding tussen de hydrogel en thermoplast lagen in de 3D-print vond hier plaats door de OMNCL reactie. Uiteindelijk zijn chondrocyten in deze verstevigde constructen gemengd, die het fabricatieproces goed doorstaan in de constructen die hyaluronzuur bevatten.

Conclusies

Dit proefschrift beschrijft de ontwikkeling van nieuwe dubbel gecrosslinkte hydrogelen als interessante materialen voor injecteerbare formuleringen en voor het vervaardigen van 3D-printconstructen. De variabele mechanische sterkte en degradatiesnelheid bieden veelbelovende mogelijkheden van deze hydrogelen voor biomedische toepassingen.

APPENDICES

CURRICULUM VITAE AND LIST OF PUBLICATIONS

Curriculum Vitae

Kristel Boere was born on May 26, 1988 in Raamsdonksveer, the Netherlands. After finishing her pre-university education at Dongemond College in Raamsdonksveer, she started her bachelor's programme in chemistry at Utrecht University in 2006. During her master's programme Drug Innovation, she performed a 9 months internship at the department of Pharmaceutics, Utrecht University, investigating flower-like micelles. After this, she did a 6 months internship at the department of Bioengineering at Rice University in Houston (USA) developing novel injectable hydrogels in the research group of prof. dr. A.G. Mikos. In September 2011 she started her PhD research project at the department of Pharmaceutics under the supervision of prof. dr. ir. W.E. Hennink and dr. ir. T. Vermonden. This project focused on the development of hybrid dual cross-linked hydrogels as injectable and 3D-printable biomaterials and the results of this project are presented in this thesis. Kristel continued her career in September 2015 as a material research engineer at the R&D department of Ultimaker working on material development for 3D-printing.

Publications from this thesis

K.W.M. Boere, B.G. Soliman, D.T.S. Rijkers, W.E. Hennink, T. Vermonden. Thermoresponsive injectable hydrogels cross-linked by native chemical ligation, Macromolecules, 47 (2014) 2430-2438.

K.W.M. Boere*, J. Visser*, H. Seyednejad, S. Rahimian, D. Gawlitta, M.J. van Steenbergen, W.J.A. Dhert, W.E. Hennink, T. Vermonden, J. Malda. Covalent attachment of a three-dimensionally printed thermoplast to a gelatin hydrogel for mechanically enhanced cartilage constructs, Acta biomaterialia, 10 (2014) 2602-2611. *Both authors contributed equally.

S.J. Buwalda*, K.W.M. Boere*, P.J. Dijkstra, J. Feijen, T. Vermonden, W.E. Hennink. Hydrogels in a historical perspective: from simple networks to smart materials, Journal of controlled release, 190 (2014) 254-273. Review. *Both authors contributed equally.

K.W.M. Boere, J. van den Dikkenberg, Y. Gao, J. Visser, W.E. Hennink. Thermogelling and chemoselectively cross-linked hydrogels with controlled mechanical properties and degradation behavior, Biomacromolecules, 16 (2015) 2840-2851

K.W.M. Boere, M.M. Blokzijl, J. Visser, J.E.A. Linssen, J. Malda, W.E. Hennink, T. Vermonden. Biofabrication of reinforced 3D-scaffolds using two-component hydrogels, Journal of Materials Chemistry B, (2015) DOI: 10.1039/C5TB01645B.

Other publications

A.J. de Graaf*, K.W.M. Boere*, J. Kemmink, R.G. Fokkink, C.F. van Nostrum, D.T.S. Rijkers, J. van der Gucht, H. Wienk, M. Baldus, E. Mastrobattista. Looped structure of flowerlike micelles revealed by ^{1}H NMR relaxometry and light scattering, Langmuir, 27 (2011) 9843-9848. *Both authors contributed equally.

A.K. Ekenseair, K.W.M. Boere, S.N. Tzouanas, T.N. Vo, F.K. Kasper, A.G. Mikos. Synthesis and characterization of thermally and chemically gelling injectable hydrogels for tissue engineering, Biomacromolecules, 13 (2012) 1908-1915.

A.K. Ekenseair, K.W.M. Boere, S.N. Tzouanas, T.N. Vo, F.K. Kasper, A.G. Mikos. Structure–property evaluation of thermally and chemically gelling injectable hydrogels for tissue engineering, Biomacromolecules, 13 (2012) 2821-2830.

S. van Berkum, P.D. Biewenga, S.P. Verkleij, J.B. van Zon, K.W.M. Boere, A. Pal, A.P. Philipse, B.H. Erné. Swelling enhanced remanent magnetization of hydrogels crosslinked with magnetic nanoparticles, Langmuir, 31 (2014) 442-450.

J. Visser, P.A. Levett, N.C.R. te Moller, J. Besems, K.W.M. Boere, M.H. Van Rijen, J.C. de Grauw, W. Dhert, R. van Weeren, J. Malda. Crosslinkable hydrogels derived from cartilage, meniscus and tendon tissue, Tissue Engineering Part A, 21 (2015) 1195-1206.

Patent

A.G. Mikos, K.F. Kasper, A.K. Ekenseair, T.N. Vo, K.W.M. Boere, T.J. Touchet. Injectable hydrogels, US Patent 20150079020 A1 (2014).

Selection of podium presentations

K.W.M. Boere, J. Visser, H. Seyednejad, W.J.A. Dhert, W.E. Hennink, J. Malda, T. Vermonden, Strong cartilage constructs by crosslinking a 3D-fabricated thermoplastic network to a cell-laden hydrogel. *International Society for Biomedical Polymers and Polymeric Biomaterials, Washington D.C., 09-07-2014*

K.W.M. Boere, B.G. Soliman, D.T.S. Rijkers, W.E. Hennink, T. Vermonden, In situ forming hydrogels by thermogelation and native chemical ligation, *Dutch Polymer Days 17-03-2014 (Best presentation award Biomedical workshop)*

K.W.M. Boere, B.G. Soliman, D.T.S. Rijkers, W.E. Hennink, T. Vermonden, Native chemical ligation as a tool to form peptide-functionalized in situ crosslinkable thermosensitive hydrogels, *Netherlands Society for Biomaterials and Tissue Engineering 29-11-2013*

K.W.M. Boere, J. Visser, H. Seyednejad, M.J. van Steenbergen, W.J.A. Dhert, W.E. Hennink, J. Malda, T. Vermonden, Can hydrogels match mechanical properties of articular cartilage?, *Dutch Polymer Days 19-03-2013, Plenary Session*

APPENDICES

DANKWOORD

Dat was het dan. Het klinkt cliché, maar de 4 jaar promotie zijn inderdaad omgevlogen. Deze zowel gezellige als leerzame tijd was natuurlijk nooit zo snel verlopen zonder alle betrokkenen in dit project.

Tina, bedankt dat je altijd voor me klaar stond als co-promotor. Je was altijd beschikbaar om me weer op het juiste pad te zetten. Je team is gigantisch gegroeid de afgelopen jaren en dat zegt natuurlijk al genoeg.

Beste Wim, als promotor was het natuurlijk je taak om strict en kritisch te zijn. Maar zonder jouw kritische en snelle feedback op artikelen had ik het niet zo snel voor elkaar kunnen krijgen. De ongenuanceerde grappen en gezelligheid tijdens de vrijdagmiddag borrel maakten dit geheel compleet.

Mies, luide stem en muziek, eigen gebrouwen bier en altijd bereid om te helpen. Volgens mij zijn dit de eigenschappen die een analist moet hebben om het lab draaiende te houden. Joep, Louis en Roel, bedankt voor alle extra ondersteuning in het lab. Barbara, fijn dat je zo betrokken bent en ik altijd bij je binnen kon lopen.

Many thanks to my students. Laura, it was a great start having you as such a motivated student, I think I learned at least as much from you as you learned from me. Bram, jouw belangrijke bijdrage in hoofdstuk 3 heeft het artikel zeker opgefraaid, leuk dat je nog altijd langs komt voor een praatje. Yuan, thanks for all your input during your hard-working time in the lab. Gruson en Ali, ook jullie bedankt voor jullie bijdrage.

Zoals het met een promotie periode gaat heb ik natuurlijk collega's zien komen en gaan. Mijn periode bij biofarmacie begon onder supervisie van Albert. Voor die leuke en leerzame stage bij jou had ik het nog niet eens overwogen om zelf te gaan promoveren. Mijn eerste twee jaren waren lang niet zo leuk geweest zonder het gezelschap van Markus, Roy en Isil. Markus, altijd fijne discussies tijdens borrels en bokbierfestivals, geweldig hoe jij en Claire het naar jullie zin hebben in jullie USA avontuur. Roy, jouw hulpvaardigheid en gezelligheid lijkt geen grenzen te kennen, succes in Canada! Isil, thanks for being always optimistic and smiling.

Ook de twee laatste jaren heb ik veel leuke mensen leren kennen. The great UMC lunch group has changed over the years, but was always a pleasant break from work. Jeffrey, Jan Jaap, Lies, Amr, Karina and Maria, thanks for all the nice conversations. Erik, bedankt voor alle gezelligheid op vrijdagmiddagen en daarbuiten en natuurlijk dat je mijn paranimf wil zijn.

Werken aan hydrogelen en tissue engineering projecten werd een stuk leuker wanneer er met collega's overlegd kon worden. Hajar, thanks for the early collaboration. Anna, Maarten and Marzieh, I enjoyed all our discussions and look forward to receive your

theses. Maarten, bedankt voor alle hulp bij de 3D-printer en dat je mijn paranimf wil zijn.

Thanks to all other colleagues I met during my PhD. Having colleagues from so many different countries was a big cultural experience on itself. Sima, thanks for all your jokes and effort to learn Dutch. Merel, bedankt dat ik zo nu en dan mijn ei bij je kwijt kon. Yang, it was always great to discuss science with you.

I had the pleasure to be involved in different collaborations during my PhD. Anne (UCL) and Geralda/Pavel (MRI), thanks for the interesting projects. Dirk, bedankt voor de extra chemiekennis die altijd weer snel uit de mouw werd geschud. Maar met name wil ik natuurlijk de orthopedie in het UMC bedanken. Jetze, jij (mede met je studenten) stond altijd weer direct voor me klaar en het maakte je niet uit met wat voor stinkend of visceus goedje ik dan weer aan kwam. Ik ben benieuwd waar jouw efficiënte en positieve manier van werken je nog allemaal gaat brengen. Jos Malda, bedankt voor de fijne samenwerking.

Het open David de Wiedgebouw leent zich uitstekend om in de gaten gehouden te worden, maar ook om aan te schuiven bij elkaars borrels. Niet te vergeten de mannen van Medchem, met name Peter en Paul, bedankt voor de vloeibaar stikstof en de biertjes.

Gelukkig was er nog tijd voor afleiding met vrienden buiten het lab. Christine, Freddy, Remco en Tamara, het was altijd fijn om verhalen op te rakelen en te filosoferen over de wetenschap tijdens onze etentjes. Inge, Claudia en Melissa, de middelbare school is weer een tijd geleden, maar mooi dat we elkaar niet uit het oog zijn verloren. Chantal, bedankt voor alle leuke momenten door de jaren heen.

Pa en ma, bedankt voor alle steun en begrip waardoor alles mogelijk leek te zijn. Het zal wel deze steun zijn geweest dat we geen van allen voor de makkelijke weg hebben gekozen. Diana, Luc (en de kleine Amber), als echte bèta's begrepen jullie goed waar ik mee bezig was en het was fijn dit soms kort door te spreken. Esther, in hetzelfde schuitje door allebei te promoveren, maar jouw onuitputtelijke doorzettingsvermogen is altijd een goed voorbeeld voor mij geweest. Geniet van je tijd in Wenen samen met Michaël. Familie van den Reijen, ik heb me altijd goed welkom gevoeld bij jullie thuis.

Tot slot natuurlijk Jeroen. Jouw steun heeft hier en daar zijn duidelijke sporen nagelaten in mijn hoofdstukken, maar ook bedankt voor alle ontspanning en leuke momenten.

Kristel